UNIVERSITY OF CAPE TOWN

FACULTY OF ENGINEERING AND THE BUILT ENVIRONMENT

DEPARTMENT OF CIVIL ENGINEERING

Geotechnical Engineering Design of a Tunnel Support System - A Case Study of Karuma (600MW) Hydropower Project

Geotechnical Engineering Group

Student: **Ongodia Joan Evelyn**

Supervised by
Dr. Denis Kalumba

A thesis submitted in partial fulfilment of the requirement for award of the degree of Master of Science in Civil Engineering specializing in Geotechnical Engineering at the University of Cape Town

[April 2017]

PLAGIARISM DECLARATION

1. I know the meaning of plagiarism and declare that all the work in the document, save for that which is properly acknowledged, is my own. This thesis/dissertation has been submitted to the Turnitin module (or equivalent similarity and originality checking software) and I confirm that my supervisor has seen my report and any concerns revealed by such have been resolved with my supervisor.
2. I have used the UCT Author-date-referencing-guide 2016 based on the Harvard convention for citation and referencing. Each significant contribution to and quotation in this dissertation from the work or works of the other people has been attributed and has been cited and referenced.
3. This dissertation is my own work.
4. I have not allowed and will not allow anyone to copy my work with the intention of passing it as his or her own.

Signature: …… Signed …… Date…April 5th 2017……

Student Name: … Ongodia Joan Evelyn …….

DEDICATION

to the

Almighty God

ACKNOWLEDGEMENTS

At the end of the tunnel, the light of this achievement so shines brightly!

I am grateful to my family, supervisor, colleagues and friends for their support and inquiries on my work. They have in different ways contributed to the completion of this study.

I am greatly indebted to my supervisor, Dr. Denis Kalumba, for sourcing my financial aid, his countless support, guidance, patience and encouragement. His constructive criticism and feedback improved the quality of this research.

My sincere gratitude also goes to Julian Baring Scholarship Fund (JBSF) for their financial support. Also, the processing of the JBSF funding was facilitated by Ms. Mary Hilton, the communications and marketing manager of Engineering and the Built Environment faculty at the University of Cape Town (UCT). I appreciate her support.

I would also like to thank the Uganda Electricity Generation Company Limited (UEGCL), especially Dr. Eng. Harrison E. Mutikanga, the Chief Executive Officer and Mrs. Chiria Drakua Eunice who offered constructive suggestions, encouragement and scholarly resources for this study. I also appreciate the geological and project insights given by Mr. Ojha Brajesh and Mr. Raju S. of Energy Infratech Pvt Limited (India) and Mr. Lucky Nene of AECOM (South Africa) shared insight on tunneling.

Much appreciation goes to Dr. Tannant Dwayne of the University of British Columbia Okanagan for his invaluable insights on geological and practical aspects which shaped the final outcome.

The support by Avril Courie, Sophia Pan, Douglas Twinamatsiko, Okhala Muacanhia, Fardiah Chemisto, Zainab Babalola, Andrew Zwiers, Ednah Veterai, Ruth Nekura, Babalwa Ontjies, Abby Chwadi, Athini Kenke, Sharon Chipeperuka, David Davies, Christian L Polorigni, Mercy Dada, Engr. Rachel S Ugye, civil engineering staff, colleagues and friends is appreciated.

Spiritual and moral support extended by my church families at Makerere Full Gospel Church (Uganda) and His People Baxter Church (South Africa) congregations was invaluable. Inspiring phone calls and follow-ups by Pastor and Mrs. Agnes Zziwa of Seeta Full Gospel Church (Uganda) were much needed. *Taata ne Maama mwebale nnyo.*

Special gratitude goes to Eng. Mudali and Mrs. Mudali (Uncle Emma and Auntie Sarah) of Pitch-Build (Uganda) Limited for their guidance, advise and encouragement. *Mwanyala nnabi*. To my beloved family: Dad - Simon Peter Ongodia, Mom - Salome Nyadoi Ongodia, Ann Elizabeth Okotha, Frances Petronella Ongodia, Santhosh Joseph, Simon Peter Ongodia Jr., Pheona Veronica Ongodia, Daniella Blessed Mukisa, Alicia Mirembe Thanzan, Theo Avilash Santhosh, Uncle Fr. John Peter and Grandpa Alenyo for the phone calls, messages, emails, voice notes and early morning wake-up calls– *Eyalama noi:* a*fwoyo swa. You are each a true legend and blessing.*

Above all, GOD who is ever true and faithful. Eyalama noi, Papa Edeke Lokasuban!!!

ABSTRACT

Tunnels have been built since 2180 B.C., through the stone age. They became popular worldwide since the eighteenth century, as transportation, military, mining, conveyance, storage and flood control structures. Due to the increasing world population, urbanization and industrialization, the construction of underground tunnel structures are preferred as they limit interferences with existing surface uses of the land and water bodies.

Although underground tunnels are a common flexible construction alternative, they are high hazard risk structures. The risks are mostly related to ground conditions. Tunnels buried at depth disturb in-situ conditions, cause ground instability and ultimately failure. Widespread tunnel failures, though not publicly advertised because of their adverse implications, have claimed human lives, cleared cities, cost 100 million United States dollars' worth in financial losses and year-long project delays. As such, stability of the structures is crucial to prevent the catastrophes thereby reducing societal outcries.

Permanency of underground structures is ensured by provision of adequate resistance to any impeding failure of the ground surrounding deep underground excavations. The effectiveness of the ground-support interaction depends on geology, material properties, geotechnical parameters, loads of the surrounding ground mass and mechanism of the interaction.

Using actual project information, the factors influencing stability, structural resistance as well as methods to select the required support are explored in this dissertation. The study used typical geological data of an underground tunnel component of Karuma, a proposed 600MW hydropower project in Uganda. It doubles as the largest hydropower project and first underground construction, to date. The project is located along the River Nile in a sensitive ecosystem neighboring both a major national park and the Great Rift Valley system in East Africa.

The instability problem at Karuma was assessed using scientific and universal tunneling practice. Typical site data formed input for the geotechnical engineering design of the tunnel support based on analytical, observational and empirical methods. The study demonstrated that all methods were independent and dissimilar for the same geotechnical engineering challenge of the underground structure. The most comprehensive method was the one based on geotechnical engineering principles and rock mechanics theory.

The outcomes of the different approaches in this study were unique functions of their underlying scientific philosophies. The study proposes that in designing adequate support systems to resist forces causing failure of underground tunnels, excavations buried in the ground should encompass several methods. The most conservative design should be chosen to ensure permanency.

TABLE OF CONTENTS

LIST OF FIGURES

LIST OF TABLES

LIST OF EQUATIONS

NOTATIONS AND ABBREVIATIONS

General abbreviation	Description
ASTM	American Society for Testing and Materials
B.C.	Before Christ
ESR	Excavation Support Ratio
FEM	Finite Element Model
GIs	Geotechnical Investigations
GSI	Geological Strength Index
HPP	Hydropower Plant / Project
ISRM	International Society of Rock Mechanics
RMR	Rock Mass Rating
RQD	Rock Quality Designation
RS	Rock and Soil
TBM	Tunnel Boring Machine
UCS	Unconfined Compressive Strength
USACE	United States Army Corps of Engineers

Scientific abbreviation	Description
cm	Centimeter
m^3/s	Cubic meters per second
GPa	Giga Pascal
km	Kilometer
kN	Kilo newton
kPa	Kilo Pascal
m	Meter
mm	Millimeter
MPa	Mega Pascal
MW	Mega Watt

Scientific notation	Description	Unit
c	Cohesion	kPa
º	Degrees	-
ϕ	Angle of internal friction	º
σ	Stress	kPa
$\leq$	Less than or equal to	-
$\geq$	Greater than or equal to	-
ν	Poisson's ratio	-
∂	Displacement	mm
γ	Unit weight of material	kN/m^3
$\approx$	Approximately equal to	-
$<$	Less than	-
σ_c	Ultimate compressive strength (UCS)	kPa

STUDY TERMINOLOGY

Arch: Continuous basic geometry of the tunnel crown
Block size: Average diameter of a typical rock block measured by observing an exposed rock face at the surface or underground, or rock core obtained by drilling, or from a pile of muck after blasting
Cavern: Hollow opening in the ground such as a tunnel excavation
Crown: Top of the tunnel, also known as the tunnel roof
Dip: The vertical angle of the line of maximum inclination, measured from a horizontal plane
Dip direction: The orientation of the horizontal projection of the line of maximum inclination, measured clockwise from the North
Elastic behaviour: This occurs when stress induced is directly proportional to the strain in a material
Heading: It is the crown portion of an underground tunnel excavation
Invert: Bottom of the tunnel, also known as the tunnel floor
Overbreak: Unwanted rock removal which is beyond the specified maximum excavation perimeter therefore it is a line outside the pay line. It is also called the B-line.
Plastic zone: Extent of failure zone resulting from high ground stresses surrounding an excavation and comprising loose unstable rock blocks or wedges
Plunge: Orientation of the tunnel axis to the horizontal, when looking from the opening of the excavation. For instance, horizontal excavations have a zero-degree plunge
Rockburst: Failure of a significant volume of rock mass which involves sudden collapse of wedges from the tunnel side walls, crown or floor. It is also known as popping.
Sequential excavation: Tunnel construction method involving removal of earth in stages including the top heading, bench and invert
Shaft: Vertical excavation built to provide heading or as a starting point for horizontal tunnel excavation. It is also used to analyse the rock profile
Shotcrete: Also known as gunite, is a mixture of cement, sand, aggregate, water and accelerators in correct proportions, with maximum size of aggregate less than 10mm projected at high velocity from a spray nozzle on a surface to form a layer of pneumatically applied concrete on that surface.
Spalling: Term for rock bursts from the tunnel side walls
Span of a tunnel: The distance between the excavated face and the nearest support
Stand-up time: Duration for which an excavated surface may be left unsupported before it breaks down. It is also called the bridge-action period
Strike of the plane: Direction of the line of intersection of the plane and a horizontal surface
Underbreak: Unwanted rock removal that is less than the specified minimum excavation perimeter. It is also called the A-line.
Wall: Vertical side of a tunnel, which is also called a side wall
Wedge: Triangular rock block created in isolation by intersection of structural discontinuity sets such as fault lines and/or joints but are a part of the fractured soft rock blocky mass

1 INTRODUCTION

1.0 Background

Clean energy relates to two of the United Nations Foundation Millennium Development Goals (MDGs) on global sustainability and socio-economic development. Hydropower is a preferred form of clean energy where water resources are abundant (Tshering, 2012). Yet, hydropower requires massive land to build because its component structures operate sequentially and are thus spread out (IEA, 2014; Chatzivasileiadis et al., 2013).

Increased strain on land, urbanization and the need for improved service delivery favor underground construction as a flexible alternative construction solution (Ghimire & Reddy, 2013; Spackova, 2012; Road Tunnel Manual (RTM), 2009; Lance et al., 2007). Underground structures range from caves, basements, entire buildings to passage way structures. Tunnels are passageways which can be built to serve different purposes including mobility of people and traffic, underground storage, military fortification and conveyance (Sousa, 2010). In hydropower construction projects, hydro tunnels are used to convey water for electricity generation purposes. In either scenario, the structures are similar whether conveying water to or away from the turbine pit where electricity is generated because the loads imposed externally and internally are the same in both segments (CIRIA C683, 2006).

Despite underground structures having advantages such as earthquake tolerance, they are complex capital intensive high hazard risk structures which ought to be handled with care (Sousa, 2010; United States Army Corps of Engineers (USACE), 1997). This is the reason that when the magnitude of loads imposed exceeds the capacity of the tunnel infrastructure to resist them, instability occurs ultimately causing failure (USACE, 1997).

More often, information on tunnel collapse is seldom publicized because of the high legal and environmental implications especially in critical environments such as populated cities, sensitive ecosystems and urbanized areas (Mohammed, 2015; Spackova, 2012; Lance et al., 2007). Afflicted societies have cried out for the problem to be eliminated (Sousa, 2010). In response, increasing efforts are made to address underground instability challenges (Mohammed, 2015).

Failure of structures built underground is multifaceted because it is much harder to predict and more detrimental than surface structures where impeding failure can be observed and mitigated timely. Tunnel failures cause surface and subsurface impacts, massive property damage and loss, high rehabilitation costs and loss of human lives (Konstantis et al., 2016; CEDD, 2015; RTM, 2009). Sousa (2010) found that up to 100 million United States dollars in financial losses have been attributed to tunnel failures including periods of six months to years of project time lost to investigate and remedy the scenarios. Figure 1-1 illustrates one among several tunnel tragedies around the world.

Figure 1-1: Sasago tunnel collapse in Tokyo, 2012 (a) aerial view and (b) inside the tunnel
Source: CNN (2012)

1.1 Problem statement

Failed tunnel structures have resulted in societal outcries to eliminate the problem (Sousa, 2010; Lance et al., 2007). The failures mostly result from ground conditions, construction method, workability issues and contractor experience (Konstantis et al., 2016; Sousa, 2010; Blake, 1989). Fifty-three percent of global tunnel failures are related to ground conditions (Lance et al., 2007). Therefore, correctness of geotechnical and geological ground conditions, herein after referred to as the ground, is critical to ensure safe and stable tunnel establishment (Mohammed, 2015; Spackova, 2012).

Problematic ground varies comprising hard, abrasive, weak, squeezing and swelling material, rock bursts and discontinuities such as faults[1], fissures[2] and jointing; most of which can only be accurately assessed when the ground is exposed during excavation. Additionally, rock is naturally very diverse and impossible to generalise its properties, behaviour, design and suitable construction methods (Palmström, 1995). Notwithstanding, the technical industry has the professional obligation and is under a lot of pressure to provide adequate and safe infrastructure, during and after construction. Similarly, insurers are under pressure to cap subsurface risk appropriately (Konstantis et al., 2016; Sousa, 2010). The challenge is imperative especially in the current age where construction must expand vertically downwards to cope with increasing strain on land arising from population growths and multiple diverse uses.

It was against this background of the aggravated need for development of underground tunnels through adequate and safe tunnel designs that this study was undertaken. The study aimed to provide insight to the most significant factor causing tunnel failure - the ground. It is based on the fact that structural stability and safety of tunnel structures can be provided by adequate ground-support. Support is provided by structural members installed in the ground where they are anchored to mobilize support by resisting the stresses causing deformation or displacement. The effectiveness of the ground-support interaction mechanism depends on a good understanding

[1] A shear fracture in a rock mass along which movement has taken place
[2] Small cracks

of existing conditions and resisting forces. This can be realized through geotechnical engineering aspects pertinent for the design of tunnel support systems which was the focus of this study.

1.2 Justification of the study

To date, the topic of underground works including tunneling is largely unknown thereby generally abstract (Sousa, 2010). Establishment and assessment of ground conditions, material classification, selection of necessary supports and tunnel construction methods are predominantly based on experience (Sousa, 2010; Hoek et al., 1995; Blake, 1989). However, experience and individual judgement is subjective and could be faulted. In addition, whereas collective centralized experiences could benefit the field of tunneling, hardly any information on the subject has been collated despite tunnel construction dating 2180 B.C. (Mohammed, 2015; Sousa, 2010). Some country-specific technical manuals, guidelines and classification systems which are used to streamline tunneling include the United Kingdom's Tunnel Lining Design Guide (2004), the New Australian Tunneling Method (NATM), the Chinese HC standard for tunneling, the Indian tunneling standard and the adapted Czech NATM (Spackova, 2012; Sousa, 2010; PRC, 2008).

Presently, methods borrowed from engineering geology are mostly applied. These include visual observation, mapping, quick assessment using hand-held tools and charts (Hoek et al., 1995). Although widely recognized, the methods are rather subjective. Specifically, a single chart or classification system cannot exhaust major factors relevant to establish tunnel support. Therefore, it is common practice to use a combination of charts to design tunnel support systems. Besides, charts give a range of estimated parameters making it impossible to calculate a single value of the resisting force which corresponds to the necessary support capacity. In engineering terms, the value would correspond to a unit factor of safety thereby the necessary ground support. In other words, the ground-support interaction is equivalent to the load-resistance equilibrium.

The reliance and dependence on geological methods including their adoption in tunneling by geotechnical engineers amongst other stakeholders can perhaps be explained by the lack of an understanding of ground-support interactions. For this reason, the mechanism of structural support of the surrounding rock mass and the geotechnical engineering design of tunnels are explored herein.

1.3 Objective of the study

The objective of this study was to present a geotechnical engineering analysis and to check the stability of the rock mass surrounding a tunnel structure in order to design adequate tunnel support systems for stability.

To achieve this objective;

1. Factors affecting stability of underground tunnels in rock were explored.
2. Current methods used to design tunnel support systems were examined.

3. Analysis of factors influencing rock tunnel loads at depth and thereby the minimum adequate support was undertaken.

This study considered a hydro tunnel in Karuma, which upon completion will convey water for purposes of generating electricity. The typical geology that was representative of the project site was investigated.

1.4 Scope and limitations of the study

The design presented in this study was limited to relevant literature related to tunneling, principles of rock mechanics and geotechnical engineering theory, software used, current field practices and the case study's record of geotechnical investigations.

Three methods comprising the analytical, finite element and conventional methods were explored. Geological conditions of the case study site were used to investigate an adequate tunnel support system. Mainly, geotechnical engineering factors influencing tunnel stability were considered including a highlight of key simplifying assumptions. Other aspects pertaining to design of tunnel supports such as the structural integrity of the rock bolts, shotcrete and concrete lining were outside the scope of this work.

The analytical method comprised rock mechanics principles, theory and equations to calculate loads of the surrounding rock mass. Support for the corresponding ultimate load was selected from a design table. The Finite Element Method (FEM) used the Rocscience RS^3 software package to design the support system. The conventional method involved mainly geological charts and the handy tools which were used during the site visit.

1.5 Outline of the study

The write-up herein comprises five chapters.

- Chapter 1 introduces the study, justifies the relevance of the study, highlights the study objective and defines the scope.
- Literature relevant to this study is reviewed in Chapter 2 and 3 to establish a basis for accomplishing the objectives of this study.
    - Chapter 2 covers tunnels, their history, types, construction and previous experiences from other tunnels.
    - Chapter 3 discusses key geotechnical considerations for tunneling including geology, geological rock properties, geotechnical rock parameters, tunnel stability, rock loads and the rock-support mechanism.
- Chapter 4 explains the study methodology. It introduces the case study for which a suitable tunnel support system is designed using the conventional chart method, finite element method and analytical method based on solution of rock equations.
- Chapter 5 concludes this effort and makes further recommendations.

2 TUNNELS

2.0 Introduction

Tunnels are horizontal civil or mining engineering structures whose lengths are either longer than twice the diameter of the structure or the sum of both the diameter and height of the structure (Mohammed, 2015; Yavuz, 2006). They are usually underground structures constructed by excavating through the ground in places where surface construction is restricted, but could also be built on the surface or submerged (Beaver, 1972). Restrictions to surface construction can be due to natural barriers, legal requirements, populated cities, existing infrastructure or other existing land uses. Underground tunnels reduce the demand for land and can be distinguished by the material and/or structure overlying it. A tunnel overlain by a road or railway may be called a subway, but when it passes underneath a canal it may be referred to as an underpass, aqueduct or a subaqueous tunnel (Sousa, 2010).

This chapter comprises five sections. The first section presents the history of tunnels in detail to elaborate on the origin of modern tunneling methods. The chapter further provides an explanation of the terms, genealogy and criteria followed in choosing tunnel types and excavation methods. Common tunnel cross-sections are discussed and their method of construction is explained; including the process, methods and monitoring during construction. Finally, tunnel failure incidents are recounted with key lessons to be learnt to avoid similar catastrophes.

2.1 History of tunnels

Although the actual origin of tunnels is uncertain, Europe and North America started tunneling actively in the eighteenth century (Prior, 2016; Sousa, 2010; Blake, 1989; Beaver, 1972). The stone age man, Caucasians, Siberians, Babylonians, Egyptians, ancient Greeks, Persians and Romans built tunnels for shelter, mining, conveying water and to fortify kingdoms from siege, accessing tombs and transportation prior to the recorded works in Europe and North America (Sousa, 2010; Marie, 1998; Beaver, 1972). Figure 2-1 illustrates the evolution of the tunneling shields from (a) Brunel to (b) Barlow and eventually to (c) Greathead shield.

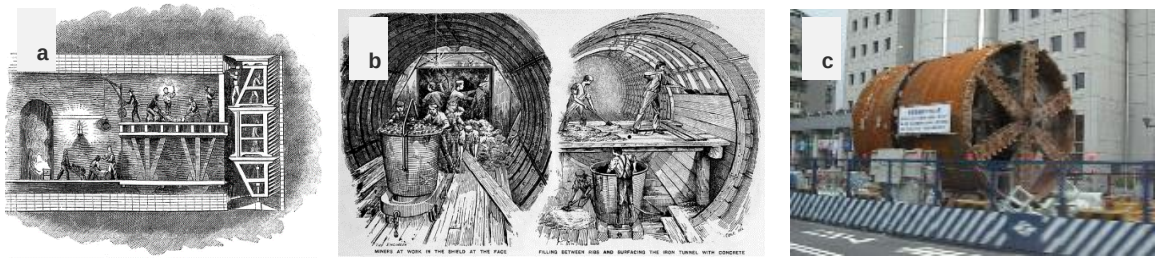

Figure 2-1: Evolution of the shield
Source: TRRL (1973)

Tunnels are built for different purposes which include mining, military, utilities, transportation, access, storage, irrigation and passages of wind, wildlife or water conveyance (Sousa, 2010; Yi, 2006). Over centuries, tunnel purposes are generally similar. Siberians built tunnels for mining, Romans built tunnels for military purposes to fortify cities, Babylonians built tunnels for water conveyance and storage while the English built tunnels for transportation mainly in the wake of industrialisation (Sousa, 2010). Present day tunnels are built for transportation, flood control, water storage and conveyance for hydropower generation, among other reasons.

2.1.1 Evolution of the tunneling shield

The eighteenth century's need for alternative less congested traffic routes in London led to the idea to tunnel under the navigable River Thames waterway. Initial attempts to manually excavate were futile due to difficult ground conditions, constrained workspace and inundation (Beaver, 1972). Later the first tunneling shield was invented by Brunel in 1825 (Prior, 2016; Beaver, 1972; Patey, 1972). Brunel's rectangular-shaped tunneling shield (Figure 2-2) provided structural support to the excavation and magnified the working space. It did not however alleviate inundation and its use was laborious and uneconomical. The invention was birthed from observation of the shipworm whose scientific name is *Teredo navalis* also known as *T. navalis*. The elongated worm-like bivalve mollusc bores the tunnel using its pair of triangular calcareous plate valves and lines the hole with mollusc extruded chalky material (Rowley, 2005). Figure 2-3 illustrates the tunneling behaviour of a shipworm, also known as the sea termite, a destructive pest for submerged timber, piles and piers especially in tropical climates with no known treatment (Elam, 2009; Werme et al., 2010).

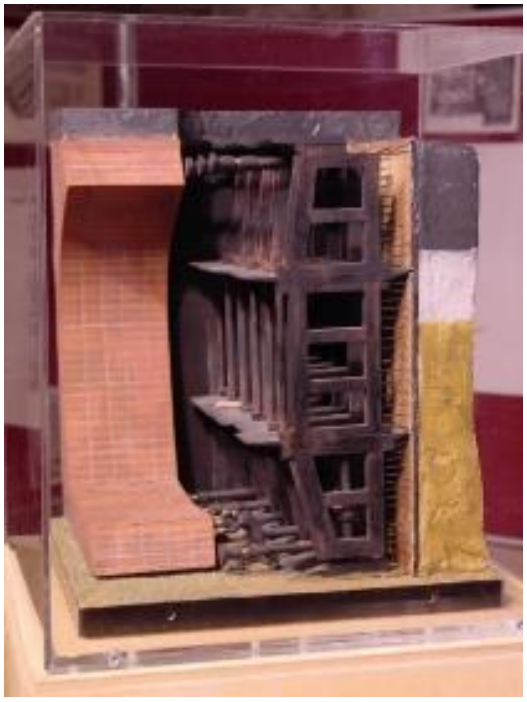

Figure 2-2: Brunel' s tunneling shield
Source: Kimball (2007)

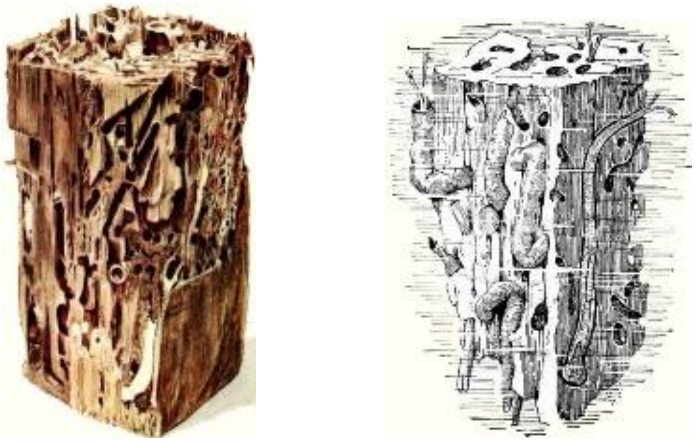

Figure 2-3:Timber infested by shipworm
Source: Kent (1860)

Around 1864 a more superior circular shield, known as the price excavator, was invented by Barlow (Beaver, 1972). The invention was developed from the realization that horizontally driven iron cylinders could tunnel through most ground and the circular shield was used to construct the Gotthard Tunnel where it registered a fast rate of tunneling progress. The tunnel was lined with prefabricated cast-iron assembled and bolted in directly with the tail end of the shield. Although some literary sources such as Sousa (2010) and Blake (1989) suggest that the circular shield was a modification of the first shield, both Brunel's and Barlow's inventions were unique and each was patented (Beaver, 1972).

During the Gotthard project, Greathead significantly modified the circular shield (Sousa, 2010; Beaver 1972). No specific details of the modifications were put forth but its final design incorporated Haskin's compressed-air idea to hold back soft ground at the excavation face and injection of high pressure grout to fill the void between the lining and excavation (Beaver, 1972). Greathead's shield (Figure 2-4) was first tested in the construction of the London railway (TRRL, 1973). Its use in the project was assessed as simple, fast and economical earmarking modern tunneling shields. After a period of challenges and military opposition towards development of tunneling technologies, Robbins Company in 1953 invented the military mole which marked the advent of rotary tunneling machinery (Sousa, 2010).

Although the earliest shield was developed by Brunel in 1825, the most significant cutting edge locomotive power-driven Tunnel Boring Machine (TBM) called the "Mountain Slicer" was built in 1846 by Henri-Joseph Maus (Hapgood, 2004). It was a large, complex machine with over 100 percussion drills set in shafts, gears and springs which was first tested in 1875 during the construction of the English Channel and used to dig the Fréjus rail tunnel through the Alpsand (Beaver, 1972). Figure 2-5 shows examples of TBM varieties. TBMs reduce construction risks by supporting and balancing the weight of the surrounding ground and hydrostatic pressures hence they are suitable for soft and water-logged conditions (Hoek et al., 1995). They also give faster tunneling progress rates and lower costs in hard ground (Blake, 1989).

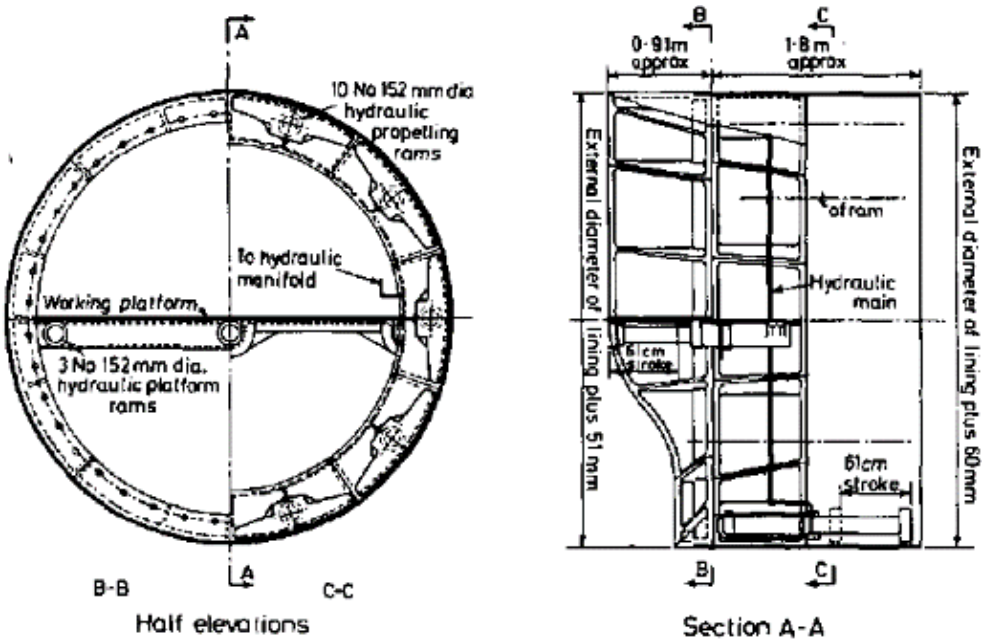

Figure 2-4: The Greathead tunnel shield design
Source: TRRL (1973)

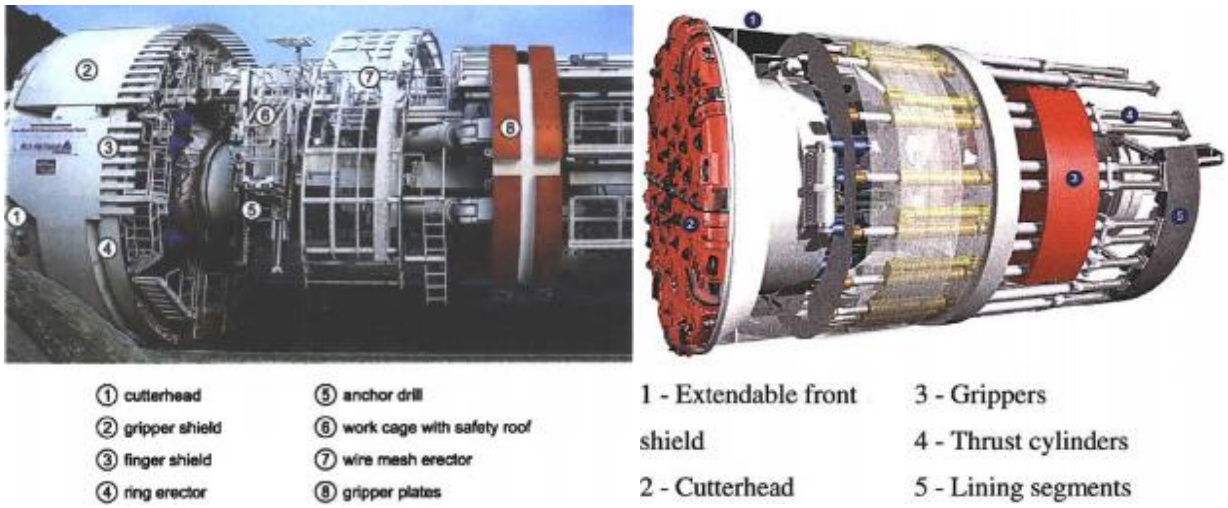

Figure 2-5: Examples of TBMs
Source: Sousa (2010)

2.1.2 Drilling age

After the use of Haskin's compressed air to hold up excavations had failed, a pressurized rotary water-driven hydraulic rock drill was invented by Brandt in 1876 during construction of the Simplon tunnel. Although the drill increased the rate of tunneling progress, it was superseded later in 1970 by hydraulic oil percussive drills which marked the onset of modern drilling (Beaver, 1972; West, 2005).

The Drill and Blast (D&B) method usually involves staged construction. This is because the material is soft and should be handled carefully. The blasting procedure involves 1) marking the

tunnel profile, 2) setting up the blasting array, 3) drilling small diameter holes about 2-4 m deep into the ground, 4) loading and 5) detonating explosives to break the ground. After blasting, the tunnel is first allowed to aerate in order to eliminate toxic gases. Then the excavation is checked, scaled, mucked and supported. Figure 2-6 is an example of (a) a modern twin drill jumbo and (b) a blasting array (highlighted in red are the detonating cords and holes in which explosives are placed) for a D&B rock excavation.

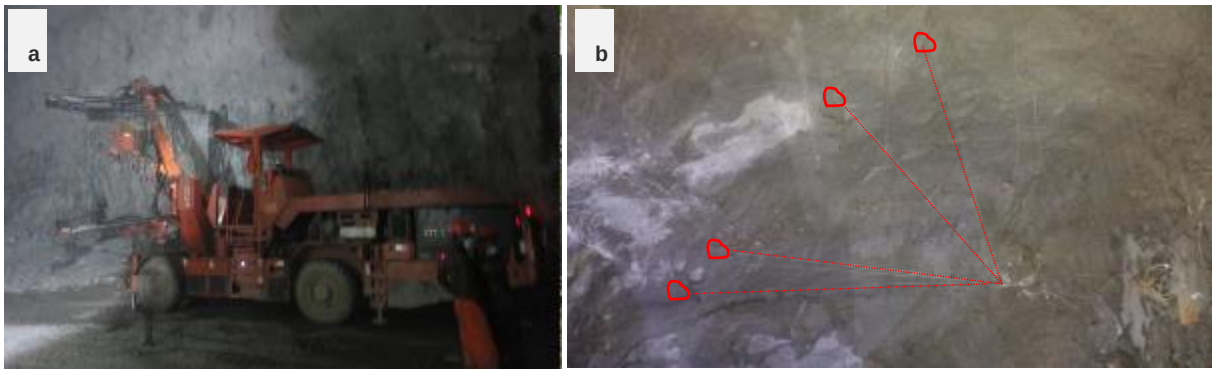

Figure 2-6: (a) Twin-drill jumbo and (b) Blasting array

2.2 Terminology and types of tunnels

The tunneling terms, types and methods used in this century are similar to earlier nomenclature. For example, Siberians mined wet ground in low temperatures; Babylonians used the present day cut and cover method to construct tunnels; Egyptians used a combination of abrasive-coated copper saws and hollow reed drills to excavate soft rock; ancient Greeks tunnelled from two opposite headings and generally excavations were supported with timber struts (Sousa, 2010; Beaver, 1972). However, supports have gradually evolved from timber to steel, shotcrete, rock bolts and their different combinations.

Most common terms stem from the intended purpose, construction method, material, geometry, and support such that a tunnel name concisely describes it. Based on construction method tunnels can be 1) mined or bored at great depth, 2) cut-and-covered at shallow depths, 3) immersed / submerged in waterways, 4) jacked when existing surface services such as roads/rails should not be interrupted and 5) inverted arch tunnels.

Based on materials out of which they are constructed, tunnel types vary from soft ground, rock and mixed-face. The different tunnel types can be constructed in different shapes (discussed in section 2.2.4) and uniquely supported depending on the purpose. A tunnel can be lined or unlined depending on ground material properties, service function and design life (see Figure 2-7). For instance, temporary construction accesses excavated in hard competent rock may be left unlined without compromising the safety and integrity of the structure. For permanent structures, tunnels exposed to severe factors and loading or excavated in weak rock may require lining to improve their overall stability and ensure functionality. The design life of tunnel structures is usually 100 to 150 years and they must be able to withstand earthquakes of 7.5 magnitude (Sousa, 2010).

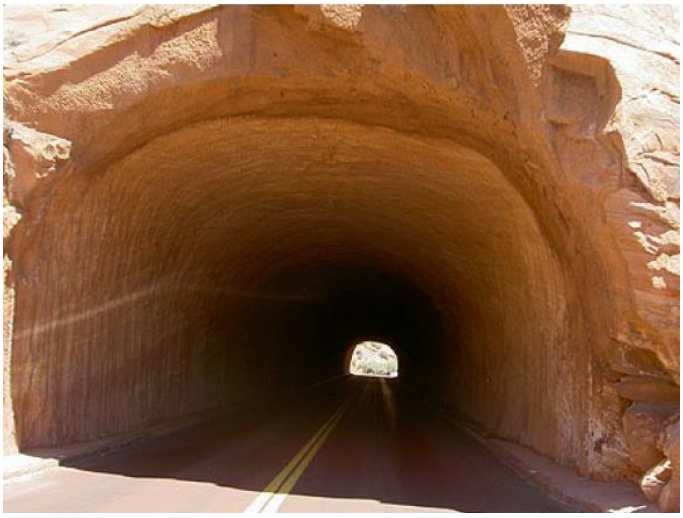

Figure 2-7: Unlined tunnel in Utah
Source: RTM (2009)

2.2.1 Purposes of tunnels

Tunnel structures are built for 1) construction access, 2) vehicular and pedestrian transportation purposes, 3) storage, 4) military fortification, 5) mining, 6) flood control and 5) conveyance of wildlife, wind, sewage, gas and water. Except for transportation tunnels, the other types of tunnels are built as hollow structures to hold or transmit materials. In addition to the main portals, emergency exits are usually provided where the tunnel lengths are significant, in order to ensure safety (Mohammed, 2015). Figure 2-8 shows some examples of road tunnels.

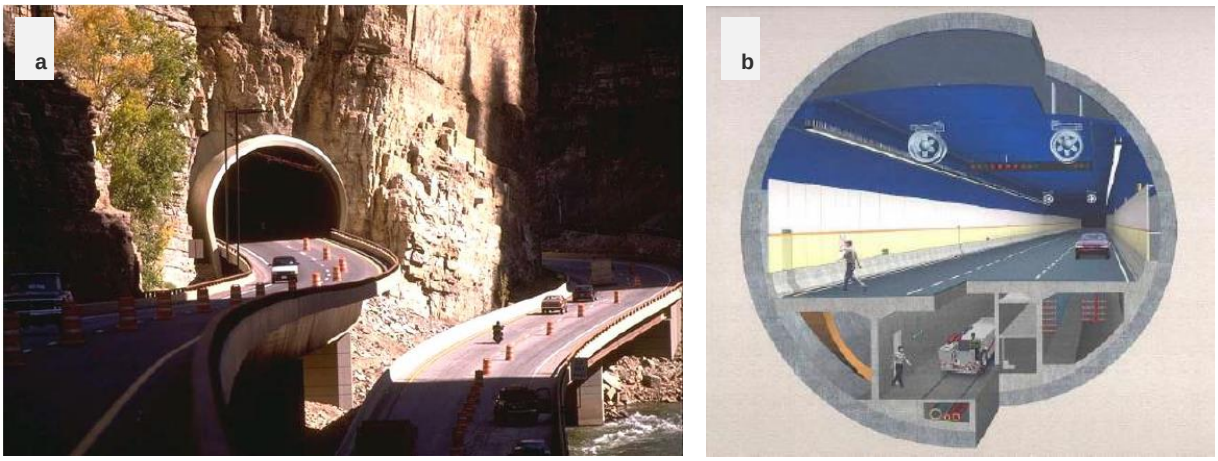

Figure 2-8: Transportation tunnels in a) Colorado and b) Shanghai
Source: RTM (2009)

2.2.2 Tunnels types based on construction method

2.2.2.1. Mined or bored tunnels

Early tunneling methods involved the use of miner gangs who dug out the ground by hand. This method was used until the advent of the tunneling shield which mechanically bore the ground. The excavation is buried at depth without unearthing the ground above such that the tunnel is invisible at the surface. The ground material is the main factor controlling the excavation. It can be soil, rock, mixed face or water. Mixed face refers to a combination of different types of material boundaries traversed which make construction difficult (Mohammed, 2015).

2.2.2.2. Cut-and-Cover tunnels

In ground conditions which can be excavated and backfilled easily, cut-and-cover tunnels are built. A trench is excavated at shallow depth and precast or cast in-situ tunnel elements are built with a strong overhead roof support system and backfilled. Most of London's established underground transport networks were cut-and-covered. However, the surface disruptions favoured boring for tunnel construction at the end of the 19th century. Furthermore, where shallow tunnels are required under water immersed tunnels are more suitable. The cut and cover method can take a top-down or bottom-up construction approach, although the latter causes more surface disruptions (RTM, 2009).

2.2.2.2.1. Top-Down method

Permanent structural tunnel support walls and capping beams are constructed first from the ground surface using slurry walls, secant pile walls or contiguous bored piling. The tunnel roof, tied into the support walls, is then cast in-situ or built using precast beams. The surface is reinstated while further construction is continued below, protected by the roof. Thus, the down time of surface services is reduced and interruptions minimized. Once subsurface excavation is completed, the tunnel floor is constructed similar to the roof. Secondary walls are installed, final finishes made and additional structural piles are provided to limit the span in wider tunnels (Mohammed, 2015). Figure 2-9 illustrates the steps taken to construct top-bottom cut-and-cover tunnels.

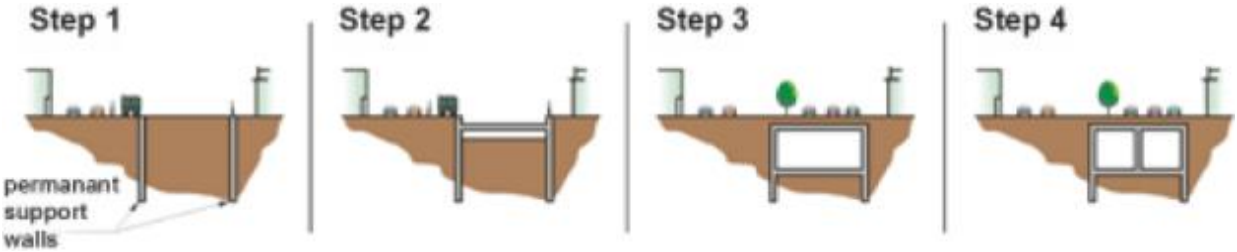

Figure 2-9: Top-bottom cut-and-cover tunnel construction steps
Source: Mohammed (2015)

2.2.2.2.2. Bottom-Up method

Where it is not critical to limit surface disruptions, bottom-up cut-and-cover tunnels are built (Mohammed, 2015; RTM, 2009). Lateral earth supports which may be temporal structures in relation to the overall construction are installed to brace[3] the ground. A trench is then excavated with muck piled at the surface. The tunnel is constructed in-situ or using precast concrete, arches or corrugated steel inside the trench. After tunnel construction, the trench is backfilled and the surface reinstated. Figure 2-10 illustrates the steps taken for construction according to RTM (2009).

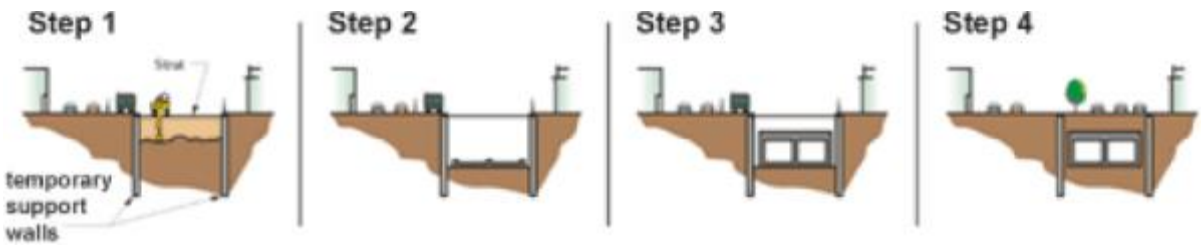

Figure 2-10: Bottom-up cut-and-cover tunnel construction steps
Source: Mohammed (2015)

2.2.2.3. Immersed / Submerged tunnels

The method of construction involves immersion or submersion of the tunnel elements in water. Water provides support to the tunnels and they facilitate crossing sea water bodies. These types of tunnels were first built in 1893 as sewage lines in Boston and in 1910 as railroad under the Detroit River (de Wit & van Putten, 2012; Sousa, 2010). Tunnel elements are constructed from prefabricated structural steel (Figure 2-11a), reinforced concrete or concrete-filled steel elements on shipways, dry docks (Figure 2-11b) or improvised floodable basins (Sousa, 2010; Ingerslev, 2003). After element construction, they are floated and carefully installed in a dredged trench, connected to other types of tunnels such as cut-and-cover tunnels (Figure 2-11c) and linked to the surface via depressed open approaches or artificial landfalls. Finally, they are covered with backfill which makes them to be surrounded with soil pressure and nearly static waters thus they are protected from anchors and sinking ships. Immersed concrete tunnels are cheaper hence more popular than the steel types which include double-shell, single-shell and sandwich. Figure 2-12 shows locations of immersed tunnels around the world. Notably, none exists in the African continent, possibly because most immersed tunnel projects were achieved through inter-governmental collaborations supported by the need for inter-trade (Beaver, 1972).

[3] Lateral support provided for the vertical side-walls of an excavation.

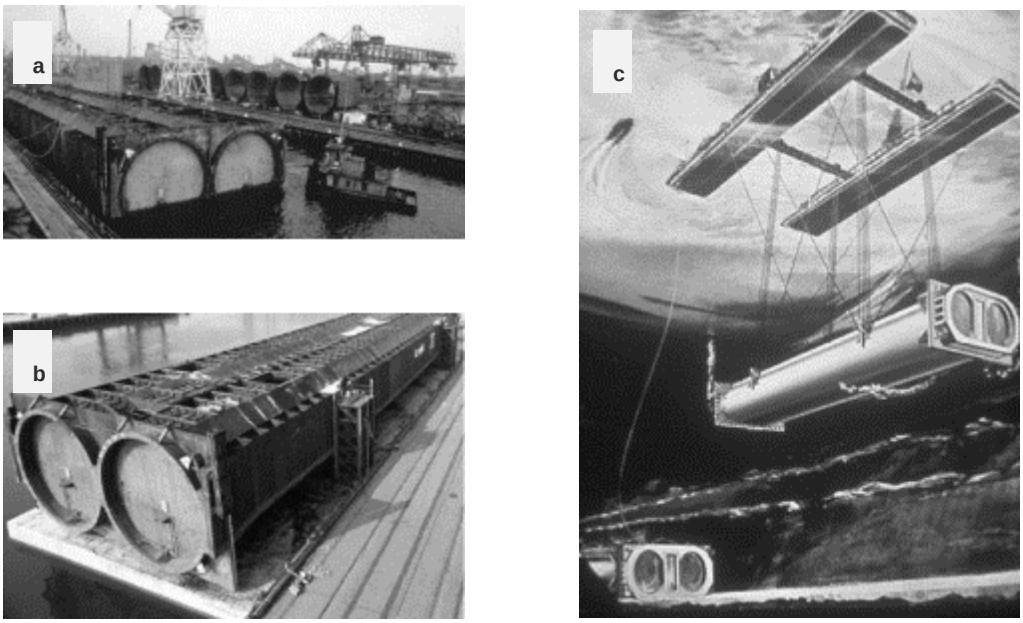

Figure 2-11: Immersed tunnel construction
Source: Ingerslev (2003)

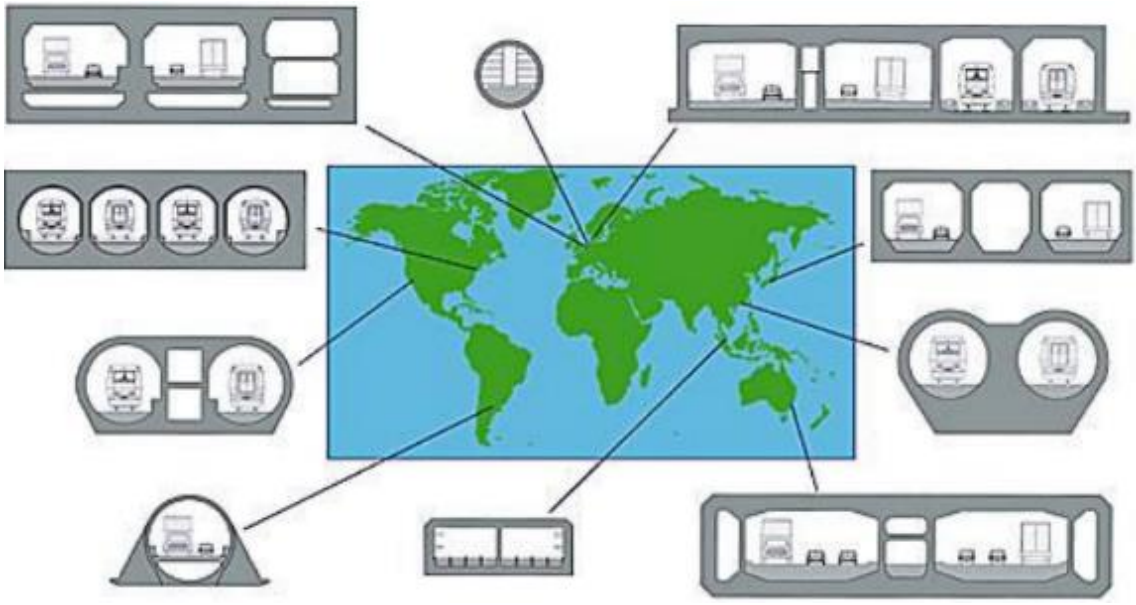

Figure 2-12: Locations of immersed tunnels
Source: de Wit & van Putten (2012)

Benefits of immersed tunnels include; ability to traverse soft ground including riverine alluvial deposits at shallower depths below bed level, a flexible overhead clearance with limited visual intrusion of water scenery, suitability for earthquake-prone zones, wide highways, horizontal and vertical rail/road alignments, shorter crossings and a well-regulated construction process (Ingerslev, 2003). Element construction, dredging and tunnel installation activities can be carried out in tandem unlike boring with uncertainties (de Wit & van Putten, 2012). However, design and construction of immersed tunnels has significant environmental impacts such as water bed

disturbance mainly from trenching, impact on water quality and interruptions to the aquatic marine ecosystem species, especially their breeding grounds.

A variation of immersed tunnels used for crossings at deeper locations where there is ship traffic and shallow locations where short approaches are expected is Submerged Floating Tunnels (SFTs) also known as suspended tunnels or Archimedes bridge (Ingerslev, 2003). They are supported to float within the water column above the sea bed by their buoyancy, anchored on piers, hung from pontoons or supported at the ends. Fatigue and corrosion are critical design considerations for SFTs because they are reversible, supported at discrete intervals and exposed to water currents and wave pressures. Although SFTs have been researched and model designs developed in the USA, Norway and China, none have been constructed yet (Ingerslev, 2010; Sousa, 2010).

2.2.2.4. Jacked box tunnels

For jacked box tunnels, a large precast reinforced concrete box protected with a shield fitted at its front is jacked horizontally through the ground at very shallow depth beneath an existing service such as a runway or railroad that must not be interrupted. In the process, the enclosed earth prism is either excavated or a flocculating agent is used to dissolve the material faster before supporting the excavation (Viggiani, 2012). Common applications include storm drains, instrumentation monitoring portals[4], utility services, pedestrian underpasses, subways and fauna undercrossing. The method allows fast and economical construction with hardly any interference on the surface including uninterrupted traffic flows and it is not affected by wet ground conditions (Lynn, 2006). Figure 2-13 illustrates the process of constructing jacked box tunnels: (a) shows a launch slab along which the jacked box is driven into the ground and (b) shows a completed jacked box tunnel.

Figure 2-13: Launch slab along which box is driven in and completed jacked box tunnel
Source: Lynn (2006)

2.2.2.5. Inverted arch tunnels

These are variations of tunnels in which the tunnel floor is slightly curved downward rather than flattened. The arched invert is only constructed after excavation is completed with the provision

[4] An opening of the tunnel, also known as the entrance or exit.

of roof support to limit deformation and optimise curvature at the bottom of the tunnel. Although not much is known including theoretical approaches to inverted arch tunnel design for dynamic loading, inverting the arch increases a tunnel's structural load-bearing capacity (Zhongming, 2015). This is due to formation of a ring structure which causes the bending moment to be altered into an axial compressive force (Kawata et al., 2014).

2.2.3 Tunnels types based on construction material

2.2.3.1. Soft ground tunnels

Soft ground tunneling presents several challenges (Ongodia et al., 2016). The challenges range from face collapse, loose material such as quick sand or large silt deposits encountered and very limited stand-up times. Therefore, great precaution is required from the onset. Common methods used to excavate tunnels in soil include mining, using shields or the pressurized face TBM which prevents the ground from collapsing (Blake, 1989). Mining is usually done in stages according to any of the typical Sequential Excavation Method (SEM) arrangements illustrated in Figure 2-14. A suitable sequence is chosen depending on the stand-up time of the unsupported excavation.

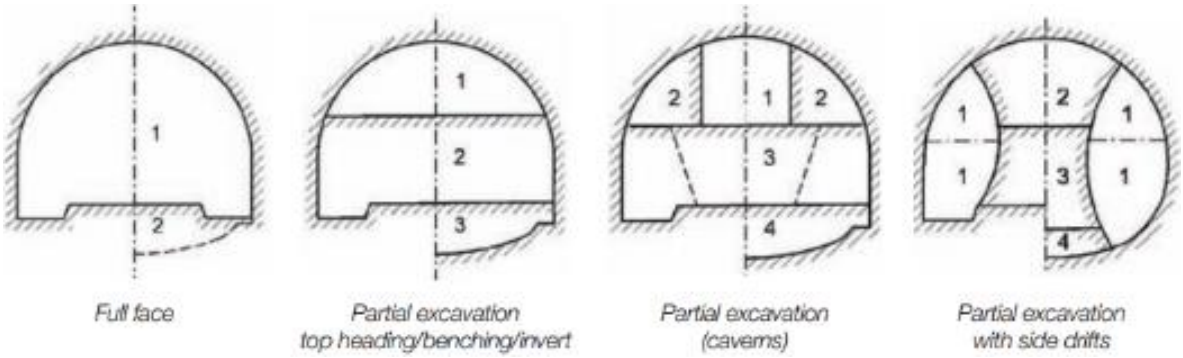

Figure 2-14: Typical excavation sequences for conventional tunneling
Source: ITA (2009)

2.2.3.2. Rock tunnels

Depending on the rock strength and hardness, different methods are used to construct rock tunnels. Further on for this study, the term tunnel refers to a hydro tunnel built in rock. Mechanized excavators are suitable to excavate softer rock while the TBM, SEM and D&B methods are suitable for hard rock. The TBM is very popular due to faster and controlled tunneling ability although it has a high capital cost. A TBM is a high technology machine usually comprising a cutter head, gripper, shield, thrust cylinder, conveyor and rock reinforcement equipment and it excavates by applying enormous rotating and crushing pressure on the rock face, chipping it with several disc cutters mounted on the cutter head (Mohammed, 2015). Cutters shown in Figure 2-15 are replaced in variation of the rock hardness, strength, jointing, strain and abrasive material properties to minimize the effective breaking energy (Blake, 1989). For very hard intact rocks, cutters with grinding ability are suitable. For hard rocks, cutters with less teeth are suitable to break the rock. The hard-jointed rocks require smoother cutters to limit the

crushing effect that would otherwise worsen the rock condition. For soft rocks, fixed chisel pick cutters are most suitable. Figure 2-15 a, b and c show the cutters with grinding ability, less teeth and smoother cutters, respectively.

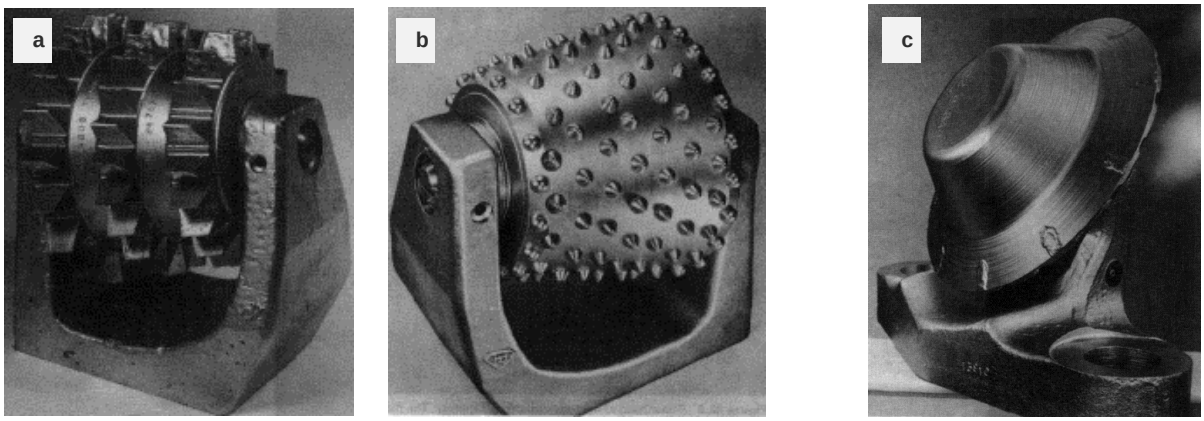

Figure 2-15: Rock tunneling machine cutters
Source: Blake (1989)

2.2.4 Tunnel cross-sections and shapes

Tunnels are also identified according to their cross-section and shape. The choice of shapes mainly depends on purpose and the need for a working platform and minimal stress concentrations. Traditionally early day tunnels were mostly square or rectangular. Circular shapes became common with the invention of Barlow's shield and eventually with more research and field applications, several tunnel cross-sections were developed with better advantages (Figure 2-16). The most common shapes used are discussed below.

1. Square and rectangular shaped sections (Figure 2-16 a and b) are regular in shape and have flat bottoms hence they are suitable for jacked box construction and transportation purposes.
2. Horse-shoe shaped sections (Figure 2-16c) have a semi-circular roof, arched sides and a curved invert. The curved edges have minimal stress concentration corners and its fairly flat floor provides a good working platform for construction. Tunnel roofs are curved to provide stability against collapse because the rock at the center of a roof span is most susceptible to collapse (Marie, 1998). Horse-shoe shapes are suitable for unlined rock, soft ground transportation tunnels and lined hydraulic soft rock tunnels. Although, they are difficult to construct, they deform less than elliptical sections thereby requiring less support which makes them an economical option (Hoek et al., 1995).
3. Elliptical sections (Figure 2-16d) have a narrow floor hence unsuitable for traffic but they can be used as sewerage tunnels. They are suitable to construct in soft ground rather than rock and present construction difficulties. Their fairly curved walls resist external and internal pressure and they maintain a self-cleansing velocity only second to egg-shaped sections.
4. Circular cross-sections (Figure 2-16e) offer greater resistances to external pressure than elliptical sections. They are suitable in lined soft ground conditions such as soft clay or cohesion-less soil to convey water and sewerage (Luwalaga, 2013). They are unsuitable for

traffic because of the need to backfill which makes it difficult to provide a fairly flat surface desirable for vehicles.

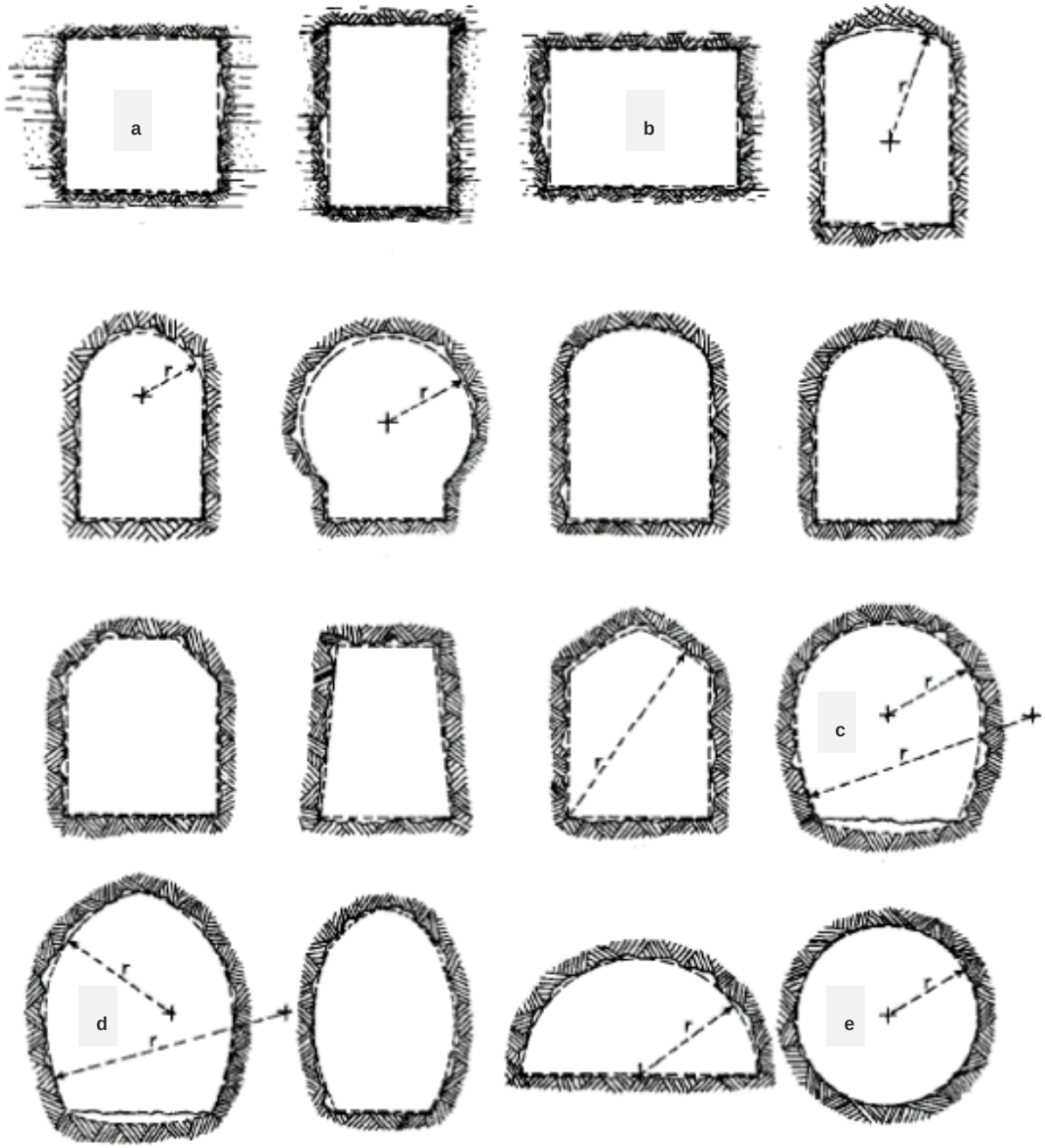

Figure 2-16: Tunnel cross-sections
Source: Wahlstrom (1973)

2.3 Tunnel construction

2.3.1 Processes

Tunnel construction is generally characterised by uncertainties. Each project is unique although project lifecycle stages are similar. Uncertainties can be broadly clustered as human and organizational factors (Spackova, 2012). Recently probabilistic prediction models have been developed to alleviate the issue of time, cost and geological uncertainty (Spackova, 2012; Sousa, 2010). However, use of such models for projects is yet to be understood and adopted by the majority of project stakeholders.

Tunnel design processes are extensive and should be comprehensive to minimize the likely risks (Marie, 1998). Tunnel project stages include routing, costing, detailed geotechnical investigations and selection of the construction method depending on existing land uses, restrictions, available contractor expertise and risks (Blake, 1989). Figure 2-17 summarizes the lifecycle of a tunneling project and geotechnical engineering expertise is required throughout all stages. Various alignment options are considered initially and the most technically feasible tunnel route with least complexity is chosen. Costing is based on unique tunnel features, type, geometry, necessary ground improvement, hydrogeological conditions, excavation support, construction access, method, equipment, estimated rate of tunneling progress and contractor rates.

The most viable option considered for development is based on a Cost Benefit Analysis (CBA), Multi-Criteria Analysis (MCA) and the Levelized Cost of Capital (LCC) (Spackova, 2012). Geotechnical investigations are done along the tunnel route to establish technical feasibility for construction based on site geological conditions. The method depends on material strength and contractor expertise to avoid unnecessary damage and further weakening of the surrounding material (Hoek et al., 1995). Basically, the main excavation axis should be aligned away from weaker areas non-parallel to the orientation of discontinuities (Kanji, 2014; Hoek et al., 1995) to limit overbreak.

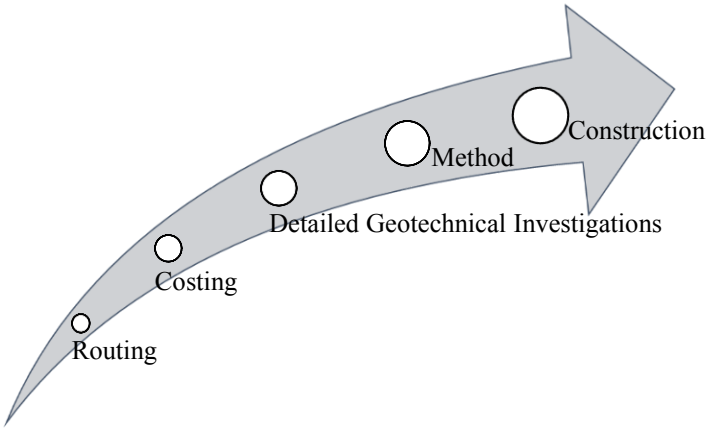

Figure 2-17: Tunneling project life cycle
Source: *Adapted from* Blake (1989)

2.3.2 Establishing site geology for construction

Feasibility geological investigations to characterize the rock mass condition along the tunnel route involve surface and subsurface geological surveys using intrusive methods, geophysics, remote sensing, aerial photography, satellite imagery and visual observation (Jones, 1989). Geological outcrops, landforms, faults, folds, hydrology comprising rivers, streams, springs and vegetation are identified from surface surveys. Subsurface surveys identify cavities, buried geological structures, ground water hydrogeology, stratification, material embedment depths, synclines and anticlines. From preliminary surface assessments, trial boring is done to procure laboratory test samples, log borehole profiles and perform resistivity measurements which indicate the variable site geology based on resistance measurements that are then compared on a scale to identify the rocks present (Jones, 2017). Finally, a comprehensive geological map, 2 or 3D geological logs and model of the site conditions is drawn showing all details.

Rock mass characterization properties include area topography, location of suitable rock formation boundaries, structural features, hydrogeological properties, rock type, rock weathering[5] conditions, deformability properties, failure criterion, in-situ stresses, loading conditions, geomechanical and geometric properties of discontinuities (Marie, 1998; Jones, 1989). Diagrammatic representations of tunnel orientation with respect to geology and geological features are included in Appendix A.

2.3.3 Tunneling methods

Tunnel construction methods broadly classified as conventional and machine excavation include cutting with mechanical means, fire-setting (rapid heating and cooling), D&B, tunneling with machinery and/or combinations depending on ground conditions and contractor competence (ITA, 2009; Jones, 1989). The conventional method, also referred to as the New Austrian Tunneling Method (NATM), is preferred for most projects because it is flexible and suitable for variable ground conditions and tunnel shapes (Spackova, 2012; ITA, 2009). However, nomenclature associated with the NATM is still controversial and it is also referred to as SEM, Sprayed Concrete Lining (SCL) and defined as either a technique or design philosophy (Sousa, 2010). The disparity in nomenclature and definition by practitioners is not unique to tunneling but is common because of further specialization within broader fields which causes an overlap among cross-cutting principles and/or disciplines. Spackova (2012) explained that this variation is a result of differences in local experience and specific geology.

2.3.3.1. Conventional tunneling (New Austrian Tunneling Method)

Conventional tunneling involves selection of an excavation method, sequence, primary support and auxiliary construction measures (Mohammed, 2015; ITA, 2009). The excavation methods are either D&B for hard rock or mechanically supported excavation for weak rock and soft ground on the full-face or partial excavation of the tunnel cross-section. Full-face is suitable for

[5] The weathering process involves physical disintegration and chemical decomposition of the parent material to form new rock materials with different properties and characteristics.

smaller sections while partial excavation is ideal for wider sections and difficult ground (ITA, 2009). The excavation is stabilized using initial primary support until the final lining is installed.

2.3.3.2. Machine excavation

Machines have a relatively high capital cost and are mostly used to excavate hard rock by mechanical means using teeth, picks or disks (Spackova, 2012). Other rock excavation techniques include D&B, tunneling with machines, cutting and fire-setting (rapid heating and cooling) either the full-face, single or multiple drifts[6] comprising a top heading and benches.

Machines include the TBM, the earth pressure balance machine (EPBM), mix-shield TBM and slurry shields, usually using bentonite fluid. The EPBM balances pressure behind the face and the atmospheric pressure and is suitable for mixed face conditions in open, semi-closed and closed operation modes. Figure 2-18 illustrates the scientific principles by which the EPBM machine operates to balance pressures behind and in front of its face. The mix-shield TBM uses an air-slurry pressure combination to compensate irregularities in the bentonite feeding circuitry and minimize settlement risks. The cutting head of the slurry shield revolves in a sealed pressurized chamber to balance the pressure along the full height of the face and transport muck (see Figure 2-19) especially in open-textured soft cohesion-less soil conditions (Jones, 1989). The bentonite shield was used to excavate the London transport fleet line (TRRL, 1973; Patey, 1972).

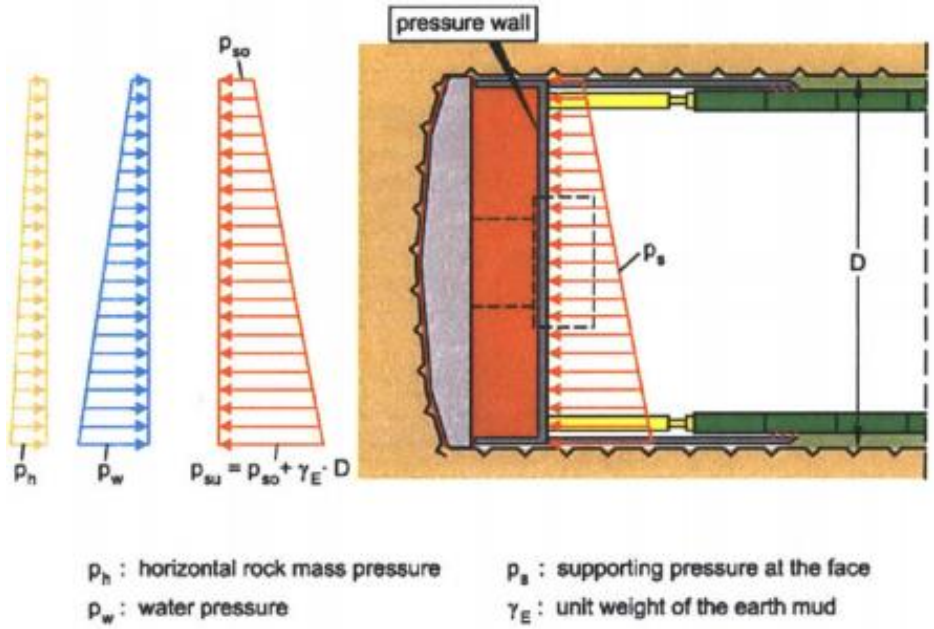

Figure 2-18: EPBM scientific principles of operation
Source: Sousa (2010) after Wittke et al. (2007)

[6] Horizontal excavation

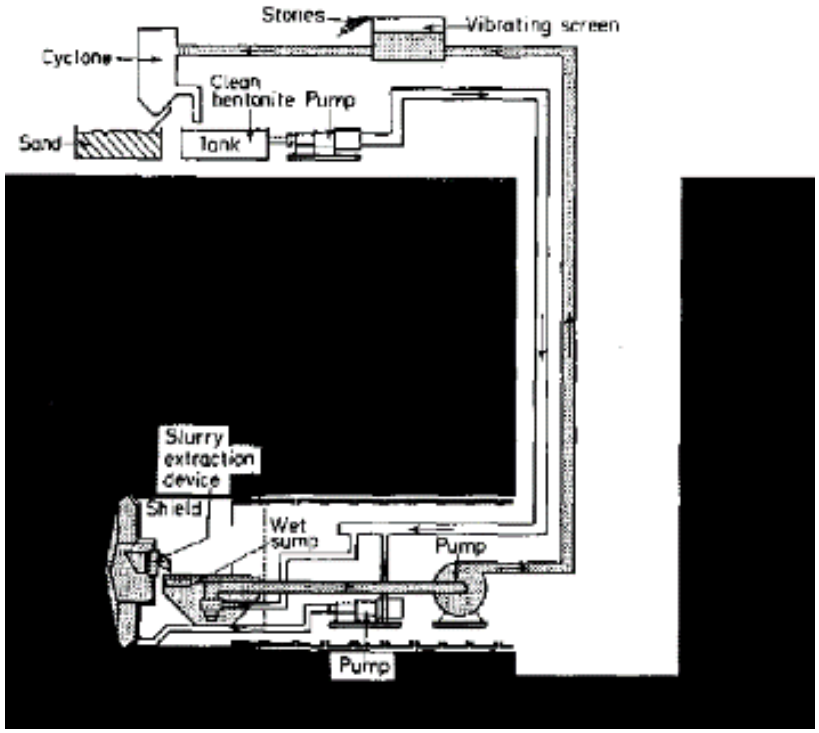

Figure 2-19: Bentonite shield
Source: Blake (1989)

2.3.4 Monitoring the construction process

Tunnel uncertainties are managed by monitoring and observation throughout the construction process (Jones, 1989). This is done in order to control local and global stability for safe construction and service delivery. According to Spackova (2012), geotechnical monitored parameters include ground deformations (strains, changes in inclination or curvature), stresses and stress re-distributions, piezometric levels, temperature and surface displacements. Quick identification of undesirable behaviour, verification and provision of appropriate mitigation measures are important to optimize project design and construction processes (Sousa, 2010). Installed instrumentation is monitored to identify the behaviour of the structures. Type, methods and locations of instruments depends on site geology, environmental conditions and construction methods. Figure 2-20 illustrates the parameters measured during the construction process. The data collected was used to verify earlier assumed geotechnical parameters thus reducing uncertainties, to adapt the support design to local ground conditions (Sousa, 2010). Verification is also essential to develop an economical optimum design that satisfies ultimate and serviceability limit states (Spackova, 2012; Bond & Harris, 2008).

Monitoring is done before, during and after the construction stages of the project lifecycle (Blake, 1989). Before construction, environmental baseline conditions are established to serve as benchmarks. During construction, deviations are observed and efforts made to limit them within acceptable limits. Main components of geotechnical engineering monitoring during construction include face mapping, positional surveying, convergence, extensometer, inclinometer, stress,

vibration, water level and piezometric measurements (Jones, 1989). After construction, the behaviour of the tunnel lining is controlled, and deterioration phenomena are observed by visual inspection and readings of installed instrumentation.

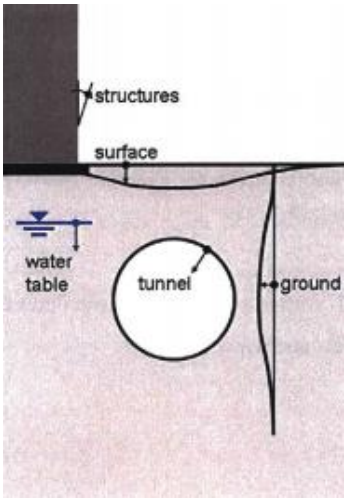

Figure 2-20: Parameters monitored during construction
Source: Sousa (2010) *after* Kovari & Ramoni (2006)

2.4 Experiential lessons from other tunnels

The challenges, high risk associated with underground works and a general lack of exhaustive information such as established standards makes lessons from previous experiences invaluable. This section discusses Hoek's experiences and collated incidents, causes, consequences and remedial measures taken where tunnels have previously failed. Hoek has vast experience and exposure in tunneling and rock mechanics in general including his contribution on a geotechnical engineering software package. Information on tunnel incidents is scarce, generally not available and non-comprehensive because of legal restrictions to publicize and disseminate such details (Sousa, 2010; Mohammed, 2015). Data in Sousa's comprehensive database and insurance investigations reveal similar and related information on tunnel failures all over the world (Spackova, 2012; Konstantis & Spyridis, 2016). Thus, relating stories is necessary to minimize the risk of tunnel failures and losses.

2.4.1 Experiences from Hoek

Field experiences by Hoek (2000) are highlighted in Table 2-1. Typical problems, critical parameters, analysis methods and acceptability criteria associated with underground tunnels are discussed. The problems underscore construction challenges arising from ground conditions and application methods. Critical parameters emphasize specific aspects related to the purpose, positioning and expected loading conditions while analysis methods describe the design and construction processes. Acceptability criteria which suggest limits and approximate ranges of factors of safety that were successfully applied in previous works, are also included.

Table 2-1: Experiential notes on underground tunnels (after Hoek, 2000)

Structure	Typical problems	Critical parameters	Analysis methods	Acceptability criteria
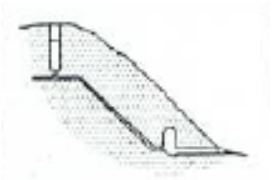 Pressurized hydropower tunnels	Excessive leakage from unlined or concrete lined tunnels. Rupture or buckling of steel lining due to rock deformation or external pressure.	Ratio of maximum hydraulic pressure in tunnel to minimum principal stress in the surrounding rock. Length, thickness and effectiveness of grouted steel lining. Water pressure distribution in the rock mass.	Determination of minimum cover depths along pressure tunnel route from precise topographic maps. Stress analyses of sections along and across tunnel axis. Comparison between minimum principal stresses and maximum dynamic hydraulic pressure to determine steel lining lengths.	Steel lining is required where the minimum principal stress in the rock is less than 1.3 times the maximum static head for hydropower operations or 1.15 for low dynamic pressures operations. Hydraulic pressure testing in boreholes at the calculated ends of the steel lining is essential to check design assumptions.
 Soft rock tunnels	Rock failure where induced stresses exceed strength. Swelling, squeezing or excessive closure when support is inadequate	Strength of rock mass and of individual structural features Swelling potential, particularly sedimentary rocks Capacity and installation sequence of support systems	Stress analyses using numerical methods to determine extent of failure zones and probable displacements in the rock mass. Rock support interaction analyses using closed-form or numerical methods to determine capacity and installation sequence for support and to estimate displacements in the rock mass.	Capacity of installed support should be sufficient to stabilize the rock mass and to limit closure to an acceptable level. Tunneling machines and internal structures must be designed for closure of the tunnel as a result of swelling or time-dependent deformation. Monitoring deformations is an important aspect of construction control.
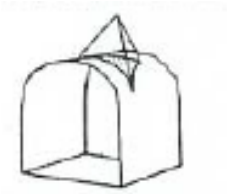 Shallow tunnels in jointed rock	Gravity driven falling or sliding wedges or blocks defined by intersecting structural features. Unravelling of inadequately supported surface material	Orientation, inclination and shear strength of structural features in rock mass Shape and orientation of excavation. Quality of drilling and blasting during excavation. Capacity and installation sequence of support systems.	Spherical projection techniques or analytical methods are used for the determination and visualization of all potential wedges in the rock mass surrounding the tunnel. Limit equilibrium analyses of critical wedges used to study critical parameters for a mode of failure, factor of safety and support requirements.	Factor of safety (equivalent strength factor), including the effects of reinforcement, should exceed 1.5 for sliding and 2.0 for falling wedges / blocks. Support installation sequence is critical and wedges / blocks should be identified and supported prior to exposure by excavation. Displacement monitoring is of little importance.

Table 2-1 continued: Experiential notes on underground tunnels (after Hoek, 2000)

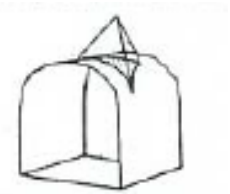 Shallow tunnels in jointed rock	Gravity driven falling or sliding wedges or blocks defined by intersecting structural features. Unravelling of inadequately supported surface material	Orientation, inclination and shear strength of structural features in the rock mass Shape and orientation of excavation Quality of drilling and blasting during excavation Capacity and installation sequence of support systems	Spherical projection techniques or analytical methods are used for the determination and visualisation of all potential wedges in the rock mass surrounding the tunnel. Limit equilibrium analyses of critical wedges are used for parametric studies on the mode of failure, factor of safety and support requirements.	Factor of safety, including the effects of reinforcement, should exceed 1.5 for sliding and 2.0 for falling wedges / blocks. Support installation sequence is critical and wedges or blocks should be identified and supported before they are fully exposed by excavation. Displacement monitoring is of little value.
 Large caverns in jointed rock	Gravity driven falling or sliding wedges or tensile and shear failure of rock mass, depending upon spacing of structural features and magnitude of in-situ stresses.	Orientation, inclination and shear strength of structural features in the rock mass In-situ stresses in the rock mass Shape and orientation of cavern Excavation and support sequence and quality of drilling and blasting	Spherical projection techniques or analytical methods are used for determination and visualisation of all potential wedges in the rock mass. Stresses and displacements induced by each stage of cavern excavation are determined by numerical analyses and are used to estimate support requirements for the cavern roof and walls.	An acceptable design is achieved when numerical models indicate that the extent of failure has been controlled by installed support. The support is not overstressed and displacements in the rock mass stabilize. Monitoring of displacements is essential to confirm design predictions.
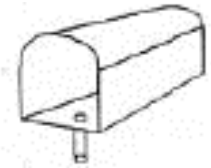 Underground nuclear waste disposal	Stress and/or thermally induced spalling of the rock surrounding the excavations resulting in increased permeability and higher probability of radioactive leakage.	Orientation, inclination, permeability and shear strength of structural features in the rock mass In-situ and thermal stresses in the rock surrounding the excavations Groundwater distribution in the rock mass	Numerical analysis methods are used to calculate stresses and displacements induced by excavation and by thermal loading from waste canisters as well as groundwater flow patterns and velocities through blast damaged zones and fissures in the rock and shaft seals.	Acceptable design requires extremely low rates of groundwater movement through the waste canister containment area in order to limit transport of radioactive material. Shafts, tunnels and canister holes must remain stable for about 50 years to permit retrieval of waste if necessary.

2.4.2 Tunnel failure incidents, causes, consequences and mitigation

Statistics on tunnel failures were summarized geographically, based on tunnel type and construction method by Sousa (2010). Deductions from the study included, 1) Europe registered the highest tunnel failure occurrences mostly attributed to hydraulic NATM tunnels, 2) damage caused was twice as much in urban environments than in rural settings, 3) hydro tunnel case failures resulted from collapse, large water inflows, rock fall, slope slide, flooding and difficult ground conditions, 4) most cases occurred in soil, and 5) few cases were rock transportation tunnels built using the NATM.

Most tunnel failures are attributed to ground instability but other causes include inappropriate construction and inadequate structural support, environmental factors and human error (Mohammed, 2015; Sousa, 2010). Sousa broadly classified the causes as external and internal. External factors relate to the ground and environmental conditions whereas internal factors relate to human error hence can be rectified more easily. Usually combinations of the factors collectively culminate into a disaster event after sometime or sudden failure occurs. Figure 2-21 summaries the causes of tunnel failure including specific cases examples in parentheses. Further details of factors causing tunnel failures are also discussed.

Planning and design errors included 1) lack of surveying and geotechnical studies and/or inadequate evaluation of the geotechnical information available, 2) inadequate competent overburden, 3) inadequate excavation process and/or ground support system, 4) inadequate or faulty ground classification system leading to inappropriate support, 5) wrong choice of construction method, 6) inadequate planning for emergency measures and 7) inadequate lining repair specifications (Sousa, 2010).

Calculation and numerical errors either during the design or construction phase arose from data collection and/or processing of measured parameters from investigations or field monitoring, respectively. Common causes included 1) adoption of incorrect geomechanical design parameters, 2) use of inappropriate models which neglected the effect of water and 3D effects such as existing tunnels, 3) errors in collection of monitoring data, 4) data processing, 5) delayed delivery of monitoring data, 6) unrealistic trigger indicators, incorrect estimation and simulation of stresses exerted on the tunneling profile (Konstantis et al., 2016; Sousa, 2010).

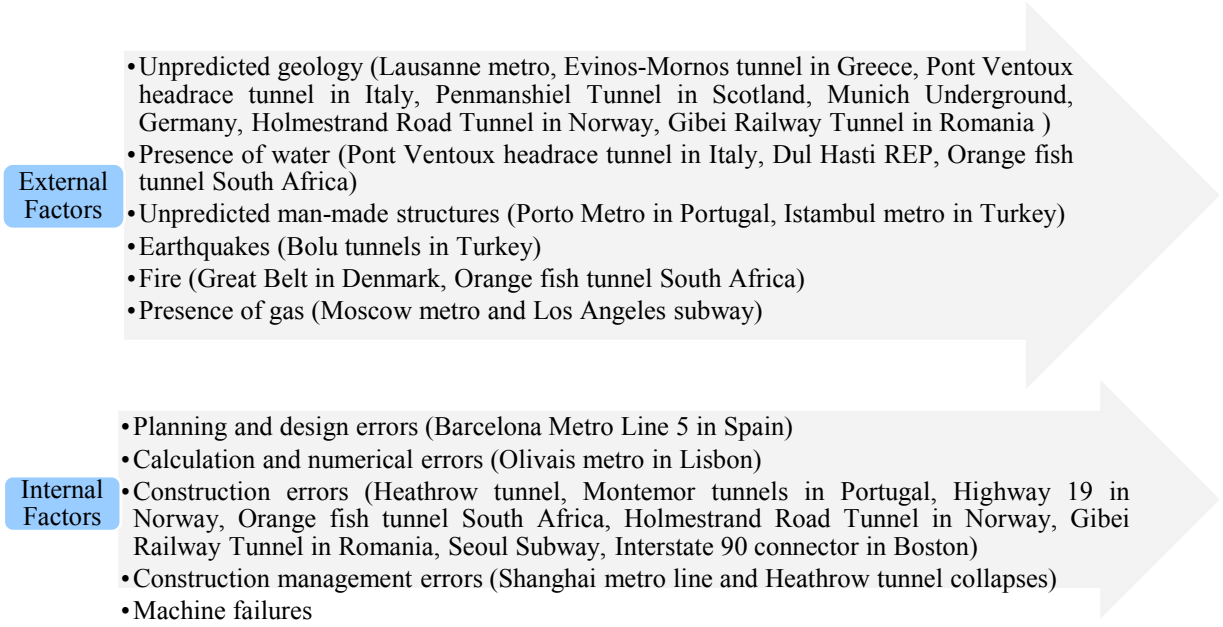

Figure 2-21: Main causes and examples of tunnel failures
Source: Adapted from Sousa (2010)

Construction errors resulted from 1) the use of substandard materials such as an epoxy anchor adhesive with poor creep resistance incapable of sustaining long-term loads (NTSB, 2007), 2) non-adherence to design specification requirements, 3) wrong wall and invert profiling, 3) over-flat invert, 4) defective invert construction arising from shotcrete rebound, 5) defective joint construction arising from poor design detailing, 6) incorrect lining thickness, 7) wrongly installed rock anchors, 8) bolts and (lattice) steel arches, 8) ground freezing pipes, 9) faulty dewatering system, 10) badly executed lining repairs, 11) preliminary investigation carried out without drilling, 12) no probe drilling performed during tunneling, 13) un-stabilized swelling clay prior to blasting, 14) no tunnel face stability analysis, 15) blasting effects close to weathered zone with shallow cover neglected (CEDD, 2015). Face instability was highlighted by most authors including Konstantis et al. (2016), CEDD (2015) and Sousa (2010).

Construction management errors included 1) insufficient specialist staffing, 2) poor communication between project parties, 3) poor sequencing in construction, 4) non-adherence to method statements, 5) bad timing of invert repairs, 6) no integration in planning construction activities, 7) compensation grouting over tunnel, 8) lack of awareness of instrumentation data warning of impending failure, 9) allowing the construction of a parallel tunnel and lack of a vigilant monitoring program (Konstantis et al., 2016; Sousa, 2010).

Common consequences of tunnel failures are summarized in Table 2-2 while Figure 2-22 illustrates an analysis of the consequences from an insurance perspective. The consequences are generally severe, uneconomical and insurance premiums increase linearly when construction works must be stopped for investigations, forensic studies and remedial works after a failure incident occurs (Konstantis et al., 2016).

Table 2-2: Consequences of tunnel failures during construction

Inside the tunnel	At the tunnel surface and surrounding environment
• Loss of human life and equipment • Stoppage of work • Reconstruction of damaged tunnel section • Intervention through remedial measures	• Loss of human life and equipment • Creates sudden state of insurgency and unrest • Disruption of surface activities such as traffic flows and livelihoods • Damage to existing surface structures

Source: Sousa (2010)

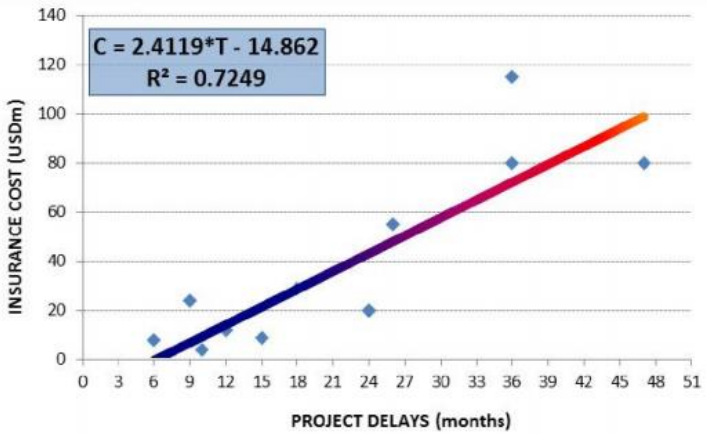

Figure 2-22: Insurance premium cost-time relationship
Source: Konstantis et al. (2012)

2.6 Summary

To sum-up, this chapter presented the history of tunnels; including evolution of the construction methods from hand boring to use of more efficient machine technologies such as the common TBM. Different tunnel types were described. Types were categorised according to purpose for which they are built, the ground material used for construction, method of construction, the support category and shape.

Accordingly, tunnels are built for transport, access, storage, military, mining, passages of wildlife, wind and water. This study considered a Karuma tunnel which will be used to convey water.

Tunnels can be constructed in soil, rock, mixed-faces or water. Thus, soil has been fairly explored in this chapter; including established theory and analysis equations to design and construct with it more specifically on rock tunnels.

Based on construction, tunnels can be mined or bored, cut and covered, jacked and inverted arches. They can also be either lined or unlined and of various shapes. Circular and horse-shoe shapes are most common although the latter is preferred for hydro tunnels as explained in this chapter. Lastly, practical insights, causes of previous tunnel catastrophes, related consequences and remedial measures were given.

Geotechnical engineering considerations involved in the detailed investigation process for tunneling are discussed in the next chapter.

3 GEOTECHNICAL CONSIDERATIONS FOR TUNNELING

3.0 Introduction

This chapter establishes key geotechnical engineering factors relevant for tunneling through rock to understand stability factors and influences for underground excavations in relation to supporting engineering loads. The subject relates to the fact that more tunnels are being constructed below the soil embedment depth in rock (Ghimire & Reddy, 2013). Furthermore, the chapter explores rock which has been researched far less than soil as an engineering construction material (Thomas-Lepine, 2012). Researchers including Mohammed (2015), Greer (2012) and Sousa (2010) indicate that current knowledge on geotechnical engineering analysis methods to design and construct rock tunnels is limited. Mostly geological methods are used. However, geology and geotechnical engineering are distinct. Geology highlights lithological properties assessed visually and by hand whereas geotechnical engineering emphasizes overall mechanical strength measured by testing materials. Strength is a function of overall material properties and it is important to support engineering loads. According to Marie (1998), rock strength for tunneling purposes is its resistance to deformation. Soil[7] is completely degenerated rock. Therefore, current civil engineering rock applications borrow established soil mechanics theories, principles and methods for handling and testing because the rate of underground construction is fast compared to the rate at which engineering theories and practice evolve. Understanding the properties is important to assess factors for tunneling. Rock loads, structural stability, modes of failure and applicable theoretical failure criterion used in analysis of underground tunnels, structural supports to maintain stability of the tunnel structure and the rock-support interactions are discussed.

3.1 Geology

The main aspects of geology are covered in this subsection. They include formation, crustal provinces and physical identification of materials all of which determine the material type, mineral compounds, type of bonding, fabric, structure, behavior and properties (NEH, 2012). Formation explains the origin of earth materials which lays a foundation of the earmarked crustal provinces. Differentiating between earth materials is usually by physical identification.

3.1.1 Formation

Formation dictates the varieties and quantities of available minerals hence the material characteristics which affect geomechanical properties. The three main types of rocks, which include igneous, sedimentary and metamorphic, are indistinct in that they change from one form and type to another depending on the mode of formation and environmental factors (Dunning, 2005; Sepp, 2000). The rock on the earth crust are formed from molten material

[7] Soil can be defined as a loose unconsolidated inorganic material, which has been altered and disintegrated completely such that it has a different structure and reduced strength, on the earth's crust overlaying rock (Venkatramaiah, 2012; Palmström, 1995).

called magma found in the mantle- the innermost part of the earth (McDonough, 1995). Igneous rocks are formed from solidification and crystallization of intrusive magma (beneath the ground surface) or extrusive volcanic rock (above the ground surface) and they are classified according to texture and grain size (Weller, 2015). Sedimentary rocks form from physical deposition of sediments and diatomaceous earth in previous geological ages and they are broadly categorized as clastic, chemical or biological (Dunning, 2005). Metamorphic rocks are formed when igneous and sedimentary rocks are altered by heat and pressure through random processes of cementation, transportation and/or deposition and they are broadly classified as foliated or non-foliated textures (Soil Manual, 1993). A good description of earth materials specifies its mineralogical composition, consistency, color, structure, texture, appearance, mode of transport, important unique features like quartz dykes, striation and strike (Weller, 2015).

Weathering is an external or internal factor which results in formation of new rock types whose origin and behavior can be traced from the constituents (Soil Manual, 1993). Surface weathering and hydrothermal alteration processes cause mechanical disintegration and chemical decomposition thus changing the rock structure and behaviour (Dunning, 2005). Alterations result in material deformation and reduced mechanical structural properties whereas mechanical disintegration involves joint separation, joint formation by rock fracture and the opening up of grain boundaries and fracture or cleavage of mineral grains (Weller, 2015). Disintegration increases the number of joints and affects material coherence without changing composition except where minerals are lost during transportation (Short, 1999). On the other hand, chemical decomposition causes rock decolourization, breakdown of complex silicate minerals and mineral leaching (Smyth & McCormick, 1995). Decomposition results in new chemical and mineralogical compositions and influences both the joint condition and rock material (Sepp, 2000; Soil Manual, 1993). Rock classifications showing the broader relationships are summarized in Figure 3-1. The rock cycle illustrating the interactions between rock types is given in Figure 3-2.

3.1.2 Crustal provinces

Crustal geological provinces are zonal extents of predominant geological types and formations covering the earth's crust (McDonough, 1995). Six structural geological provinces exist: shield (igneous rock), platform (sedimentary rock), orogen (foreland basin system), structural basins, Large Igneous Province (LIP) and extended thin crust (Short, 1999). Shield such as the Canadian shield and Baltic shield, is a large area of exposed basement Precambrian rock in the earth's crust with a gentle convex surface surrounded by sediment covered platforms. Platform is part of the stable earth's crust covered by flat-lying or gently tilted strata underlain by consolidated basement rocks at varying depths. Orogen (island arc, continental arc and forearc) systems fold or deform during an orogenic cycle to form mountain ranges, volcanic features and accretionary wedges. Structural (cratonic and foredeep) basins are low crustal areas of tectonic origin comprising synclines or deposited sediments. They are often sources of coal, petroleum and groundwater. LIP comprising Large Volcanic Provinces (LVP) and Large Plutonic Provinces (LPP) are an extremely large accumulation of igneous rocks resulting from

mantle plumes, tectonic plate processes or flood basalt depending on geological factors including latitude and continental configuration (Dunning, 2005). Extended thin crust comprises the rifted/continental margin and rift. The continental margin such as the North American basin range, is the ocean floor between the shore line and the abyssal ocean floor including the continental shelf, continental borderland, continental slope and continental rise. The rift such as the Great Rift Valley system is a long narrow continental trough bordered by normal faults marking a zone of lithosphere rupture under tension. Figure 3-3 illustrates the provinces compiled from seismic refraction data by the United States Geological Survey (2016). From the figure, the African continent is predominated by the continental shield and platform; extended thin crust exists along the coastal areas with some LIP closer to the equator, scattered basin and limited Orogen in parts of northern and southern Africa. Figure 3-4 is a world stress map which shows seismicity and tectonic plate boundaries and major discontinuities on a global scale.

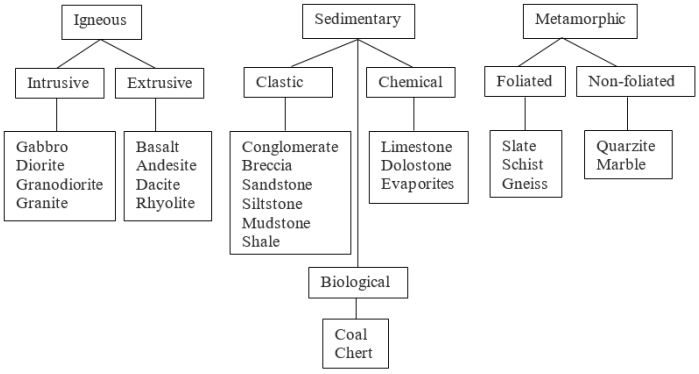

Figure 3-1: Rock classification tree
Source: A*dapted from* Short (1999)

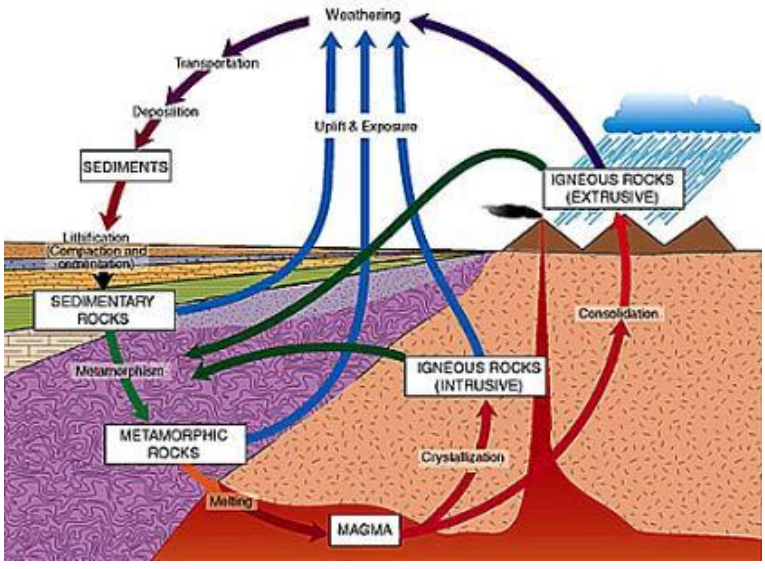

Figure 3-2: Rock cycle
Source: Short (1999)

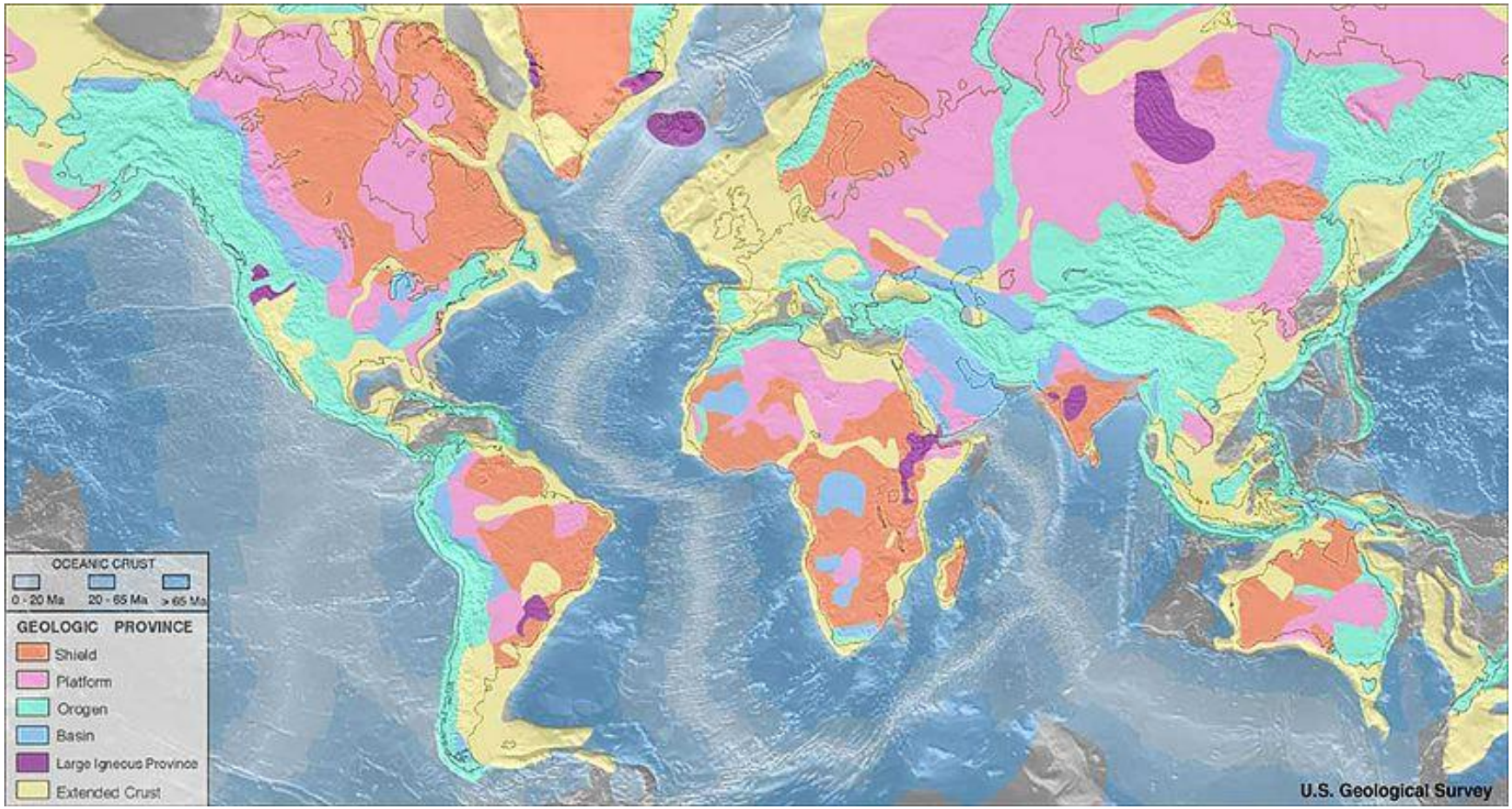

Figure 3-3: Global geological provinces
Source: United States Geological Survey (2016)

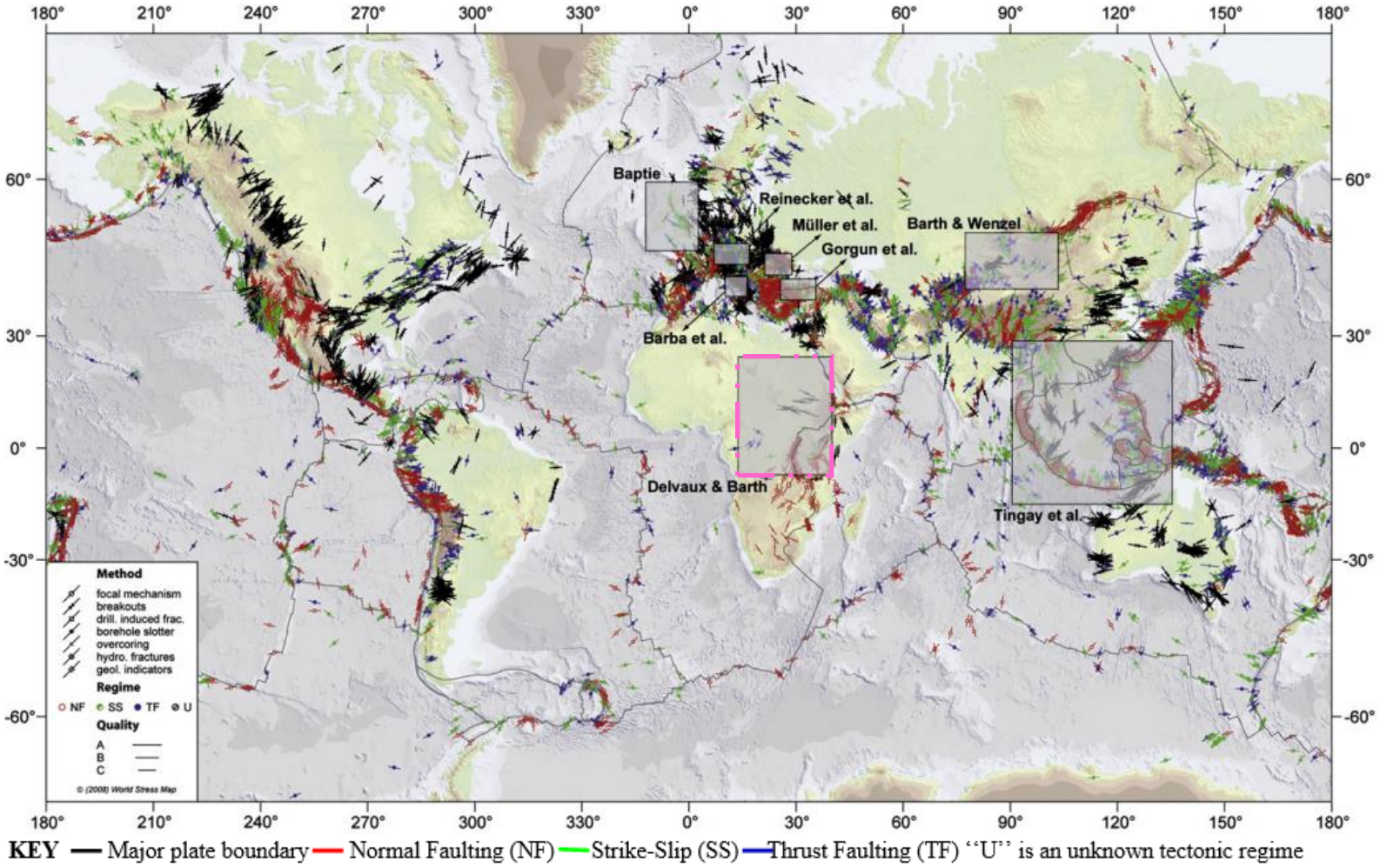

Figure 3-4: World stress map
Source: Heidbach et al. (2010)

3.1.3 Physical identification of materials

The handy geological engineering tools are important to accurately collect and record field data objectively (Weller, 2015). Geological engineering tools comprise charts, a dictionary, atlas and fieldwork journals which are employed to describe, classify, distinguish between different rock categories and evaluate the materials encountered at the project site. Insights can also be borrowed from reputable practicing geologists such as Weller (2015)'s journal and field collection. Table 3-2, Table 3-3 and Table 3-4 present Weller's geological notes including some chemical formulae which give material descriptions including information on texture, color, reaction/behavior with water, odour and actual appearances are illustrated with photographic imagery. As much information as possible is gathered to identify material origins, behavior and unique characteristics which influence geo-mechanical properties and ability of the rock to support engineering loads (Brown et al, 1983). Other aids to identify properties of rocks and minerals are included Appendix B.

Rock properties are measurable or describable lithologic characteristics which can be observed, evaluated qualitatively and classified by hand and/or tested in the laboratory (Palmström, 1995). Lithological characteristics include solid constituents/petrology, texture, mineral composition, color, cementation, formation age and processes (Brown et al, 1983). Generally, observed and qualitative properties are geological whereas tested properties are geotechnical because the strength parameter must be quantified.

3.2 Geological properties of rock

Although rock is naturally stable or slowly changes its chemical composition only under extreme conditions, its material properties influence strength, deformability, permeability and stability of rock masses (Stegner, 1971; Palmström, 1995). Material properties of a rock determines whether it is suitable for construction or not and the precautions required when using it. It is therefore important to understand rock mineralogy, structure and fabric, discontinuities/discontinuity sets, hydrogeology, squeezing and swelling problematic material behavior (Panthi, 2006; Sepp, 2000). Table 3-1 shows the specific material properties which influence discontinuous rock parameters.

Table 3-1: Rock parameters

Parameter	Specific material properties
Rock mass structure	Type, strength, degree of weathering of rock, in-situ stress magnitudes and direction
Rock mass description	Interlocking / wedge spacing, block size and shape, discontinuity sets and persistence
Discontinuities	Type, orientation, roughness, aperture / width, infilling material type
Construction	Excavation method and support sequence
Hydrogeology and voids	Groundwater, seepage / permeability, pore pressures

Source: Sabatini et al. (2002) and Jones (1989)

Table 3-2: Igneous rocks

Rock type	Description	Appearance
Glassy texture		
Obsidian	Volcanic glass without gas bubbles. Color: usually black or dark brown but can be white to light gray (snowflake obsidian). Breaks with a conchoidal (shell-like) fracture and has very sharp edges. Varieties: (a) Pitchstone (variation of obsidian which is beginning to devitrify) (b) Perlite [light-colored volcanic glass that has an abundance of curved fractures with Apache tears (dark, solid nodules of obsidian)]	  a  b
Pumice	Very light-weight volcanic glass/glass foam filled with gas bubble holes (vesicles). Floats on water. Color: mostly gray but varies.	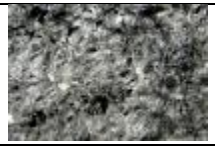 
Aphanitic texture (fine-grained)		
Rhyolite	Pastel-colored, high-silica, fine-grained rock with occasional sprinkling of small crystals. Mineral grains invisible with the naked eye. Colors: gray, light brown, tan, pale yellow, pink and other earth colors. Same chemical and mineral content as granite. Using food terms, it resembles baloney. Varieties: (a) Lithophysa/thundereggs either large hollow, bubble like structures or small spherulites with radial structures filled with agate material or hollow (geodes). It can also be found in rhyolites	  a
Andesite	Fine-grained rock intermediate in color and mineral composition between rhyolite and basalt. Color: gray or some shade of medium brown. Usually have a porphyritic texture. Are larger visible crystals surrounded by the gray or brown andesite.	 

Source: Adapted from Weller (2015a)

Table 3-2 continued: Igneous rocks

Rock type	Description	Appearance
Basalt	Fine-grained rock rich in iron that gives it a black to brown color which may oxidize to red. Varieties: Vesicular or scoria (basalt with large number of gas bubble holes). Hawaiian fluid lava flows produce basalt. Minerals: Primarily pyroxene and calcium-rich plagioclase [$NaAlSi_3O_8$-$CaAl_2Si_2O_8$] feldspar, magnetite is almost always present. Varieties: (a) Diabase: well-shaped visible plagioclase feldspar crystals embedded in a thick, dark mass of pyroxene. (b) Pyroxenite: Medium to coarse textured pure pyroxene mineral which metamorphoses into serpentine.	
Rare types	(a) Trachyte: Fine-grained volcanic rock with a mineral composition same as syenite. (b) Tuff: Rock made up of compacted, small volcanic fragments.	
Phaneritic (coarse-grained) texture		
Granite (or simply grain-rock)	Coarse-grained rock with a pink to reddish color. Mineral composition: Mainly small crystals of orthoclase [$(K,Na)AlSi_3O_8$] feldspar (pink or reddish color), quartz (usually gray), albite/sanidine (or white sodium feldspar) and either muscovite/white mica [$KAl_2(AlSi_3O_{10})(OH)_2$] or biotite/black mica [$K(FeMg)_3AlSi_3O_{10}(OH)_2$]. It weathers and crumbles into loose grains. (Note: If albite cooled rapidly, nepheline would be formed.) Varieties: (a) Albite, (b) Aplite is of fine-grained granitic composition often found as dykes within a granite.	
Diorite	Coarse-grained rock intermediate in composition between granite and gabbro. Minerals: White albite feldspar and iron rich minerals. Color: Nearly white to quite dark, depending on quantities of iron rich minerals present. Has the same mineral content as andesite. Varieties: (a) Monzonite: Has equal amounts of plagioclase and orthoclase feldspars. Its intermediate between syenite and diorite.	

Table 3-2 continued: Igneous rocks

Rock type	Description	Appearance
Gabbro	Dark coarse-grained rock. Has the same mineral content as basalt, but its grains are visible to the naked eye. Mineral: Labradorite (plagioclase feldspar) which causes flashes of color. Varieties: (a) Anorthosite composed almost entirely of plagioclase feldspar with mostly calcium.	   a
Rare types	(a) Dunite: Also called a peridotite and consists almost entirely of the mineral olivine. (a1) Kimberlite: Peridotite with phlogopite mica. (Diamonds are often associated with kimberlites.) (a2) Peridotite: Purely olivene composition. (b) Granodiorite: Intermediate composition between diorite and granite. (c) Syenite: Comprises mostly potassium feldspar (orthoclase, microcline, or perthite) with hornblende or biotite.	 a  a1  a2 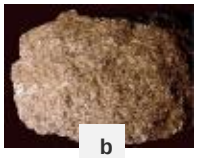 b 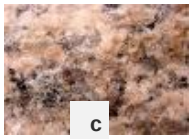 c
Mixed grain sizes (large and small)		
Porphyry	Porphyry simply refers to the two distinctly different grain sizes present in an igneous rock. The larger crystals are called phenocrysts (often feldspar or hornblende crystals) and the finer crystals are the groundmass or matrix. The groundmass can be rhyolite, andesite, or basalt and even, rarely, granite. Varieties: (a) Dacite with same mineral composition as a quartz diorite, contains plagioclase, quartz, pyroxene or hornblende and sometimes biotite and sanidine (a variety of orthoclase feldspar).	   a
Very large grain size (crystals larger than ½ inch)		
Pegmatite	Very coarsely crystallized. Has the same mineral composition of granites with large crystals of mica and feldspar. Some of the largest crystals in the world have been found in pegmatites. For example, gem minerals such as tourmaline and beryl are found in pegmatites.	 

Source: Adapted from Weller (2015a)

Table 3-3: Sedimentary rocks

Rock type	Description	Appearance
Clastic (fragmental) sedimentary rocks		
Conglomerate (Traditionally known as "puddin' stone")	Rounded or semi-rounded pea-sized and larger rock fragments cemented together, transported over long distances, deposited along shorelines or channels.	
Breccia	Angular pea-sized and larger rock fragments cemented together. Transported over short distances, common along fault zones. Takes on varied colors.	 
Sandstone	Coarse to fine grained sand cemented together. Distinguishable with the naked eye. Variable: Mature or quartz (light-colored, rounded, well-sorted grains), immature or graywackes (angular grains of several different minerals), Arkoses (contain feldspar grains). Colors: White, gray, pink, red, brown, or black. Gritty feel on a fresh broken surface. Minerals: Silica (quartz) and lime (calcite). Quartz is by far the most common. Varieties: (a) Oolite: Tiny round calcite or hematite grains formed from layers of mineral-coated sand grains. (An ool is an individual grain with a pearl-like structure).	   a
Siltstone	Cemented silt-sized particles, intermediate between sandstone and shale. Individual grains are not visible, slightly feel on surface. Varied wide range of colors.	 

Source: Adapted from Weller (2015b)

Table 3-3 continued: Sedimentary rocks

Rock type	Description	Appearance
Shale	Clay-sized particles or clay minerals compressed by rock overburden and cemented together. Accumulated clay at ocean or lake bottoms. It is fissile (ability to split in layers of fairly flat fragments) and the split surface is irregular and bumpier than slate. Colors: Black, gray, brown, red or gray, depending on iron oxides and carbon content. Often a good source of fossils.	 
Chemical sedimentary rocks		
Limestone	Has a calcite ($CaCO_3$) mineral composition consisting of limey mud or entirely fossil shells or any mixture in between. Bubbles freely when in contact with strong hydrochloric acid (HCl) because of the acid-carbonate reaction. Color: light gray or brown to dark gray or brown. Varieties include Coquina, Fossiliferous, Lithographic, Encrinal and Travertine (porous precipitate of ground and surface water).	 
Dolomite*	Chemically altered limestone by replacement of calcium minerals with magnesium to form $CaMg(CO_3)_2$ It fizzes (produces bubbles) when in contact with HCl at a much slower rate than $CaCO_3$.	 
Gypsum*	Chemical composition $CaSO_4.2H_2O$. Softer than human fingernails, can be scratched or bruised easily, does not taste like salt and does not fizz when in contact with HCl because it is a very stable compound. Color: Usually white or pale reddish-brown when stained by iron oxide. Chemical structure loses water molecules at high temperatures. Crushes into very fine powder when dry. The rock can be referred to as gypstone. Varieties: (a) Anhydrite ($CaSO_4$) which is gypsum that has since lost its water content.	   a
Salt	Mineral: Halite/sodium chloride (NaCl) with a cubical cleavage. Color: Usually white or colorless but can be lightly colored with iron oxide or clay inclusions. Dissolves in water creating a melted-looking surface when washed off with water. Has a salty taste. (Note: It is not recommended to lick strange rocks.) The rock can be referred to as rock salt or saltstone.	

Source: Adapted from Weller (2015b)

Table 3-3 continued: Sedimentary rocks

Rock type	Description	Appearance
Chert	Chemically deposited cryptocrystalline (very fine-grained) quartz, SiO_2. Commonly found as nodules embedded in limestone and exposed when limestone is dissolved by rainwater. Color: Usually dull gray or brown. Varieties: (a) Flint (can be chipped into sharp implements such as arrowheads and has a shiny surface.) (b) Jasper (chert that is strongly colored red, orange, yellow, green, brown, reddish or brown resulting from iron compounds.) (c) Taconite (iron-rich chert formed by the replacement of earlier minerals by silica and iron oxides.)	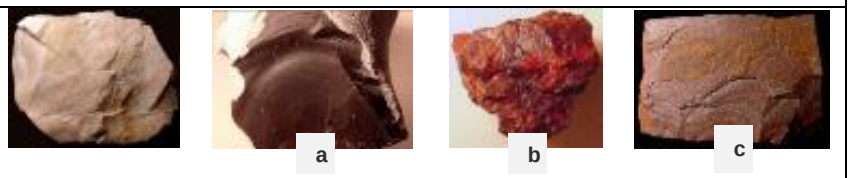
Biological sedimentary rocks		
Coal	Formed from accumulated decomposed organic materials and debris that have been altered and compacted. Varieties: Peat (slightly altered materials), lignite (soft, brown coal), bituminous coal (black, and waxy-looking) and anthracite (most altered hard, black coal with highest carbon). Coal is less dense than normal rocks.	
Amber	Ancient, hardened tree sap, natural light-weight plastic. Much lighter in weight than a typical stone. Unworked amber has a dull surface marked by a myriad of minute fractures. The clear, inner amber can only be exposed by chipping off its corner or grinding the surface. Color: Creamy yellow to transparent yellow or red to a dark brown. Used for preserving trapped insects for millions of years.	

*Denotes same mineral and rock name

Source: Adapted from Weller (2015b)

Table 3-4: Metamorphic rocks

Rock type	Parent rock	Description	Appearance
Foliated (layered)			
Slate	Shale	Unlike shale, it breaks into very flat, thin sheets and produces a ringing sound like ceramic when struck with a blunt object. Shale produces a dull thud. Color: Dark-gray or red.	
Phyllite	Slate	The cleavage surface of phyllite is not flat like slate, but is commonly rippled. Its surface has an undulating pattern and silky sheen appearance due to the presence of tiny mica crystals.	
Schist	Phyllite	Texture: Medium to fine grained. Foliated due to flat mica minerals. Large mica crystals give a sparkly appearance and it has a bumpy surface.	
Gneiss	Schist	Same mineral composition as granite although distinguished by the presence of mineral layers or minerals aligned in one direction (lineation) or crumpled in layers (foliation). Has feldspar lenses between mica layers. Gneiss is a very common metamorphic rock.	
Rare types		(a) Mylonite: Sheared rocks (b) Argillite: Product of metamorphosed siltstone or shale but before slate is formed. (c) Jaspilite: Common in Precambrian banded iron deposits consisting of alternating layers of red jasper and iron oxides.	
Non-Foliated			
Marble	Limestone	Formed during regional or contact metamorphism where the limestone may be brecciated and then re-cemented. Color results from organic and iron compounds such as graphite gray streaks, white, pink, brown or black. Bubbles in hydrochloric acid because of the acid-carbonate reaction.	

Source: Adapted from Weller (2015c)

Table 3-4 continued: Metamorphic rocks

Rock type	Parent rock	Description	Appearance
Quartzite	Sandstone	Closely cemented sand grains such that breaking cuts through individual grains, closer to quartz-cemented sandstone.	
Serpentine*	Olivine [$(MgFe)_2SiO_4$] and Pyroxene	The term serpentine refers both to hydrous magnesium silicate (antigorite and chrysotile) minerals and metamorphic rocks consisting of these minerals. Texture: Veins, fractures. Color: Light to dark green	
Hornfels	Basalt, Shale or Siltstones	Fine-grained baked rock. Color: Light gray to dark black.	
Rare types		(a) Amphibolite: Comprises amphibole and plagioclase feldspars with little or no quartz. (b) Ecologite: Granular rock comprising garnet and pyroxene. (c) Epidote Granite (Unakite): Altered granite containing epidote, has a distinct salmon-pink orthoclase vs. yellow-green epidote. (d) Metconglomerates are metamorphosed conglomerates. (e) Jade pebble (f) Ophiolite (or greenstone) is a metamorphosed basalt or gabbro that now contains chlorite, serpentine, epidote and albite. (g) Skarn is a mining term for limestones and dolomites which have metamorphosed into silicate, iron, magnesium and aluminum minerals. (h) Ptygmatic folds	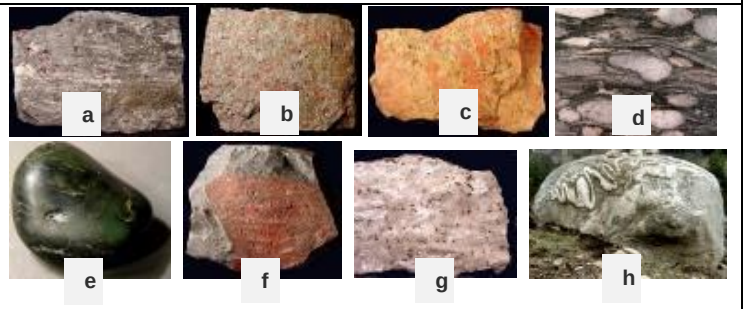

*Denotes same mineral and rock name

Source: Adapted from Weller (2015c)

3.2.1 Mineralogy, structure and fabric

Rock mineralogy, structure and fabric are each functions of its origin, formation processes and the environment (Sepp, 2000; Barla, 1974). Individual rock mineralogy (composition), structure (texture) and fabric (mineral size) are related to the material properties as illustrated in Figure 3-5. It is important to understand the basic formation and variations in compounds because the final types of compound as well as any possible transitions determine the overall behaviour of the rock as construction material (Panthi, 2006; Palmström, 1995). Important characteristics include hardness, suitable methods and materials for tunneling (Sepp, 2000).

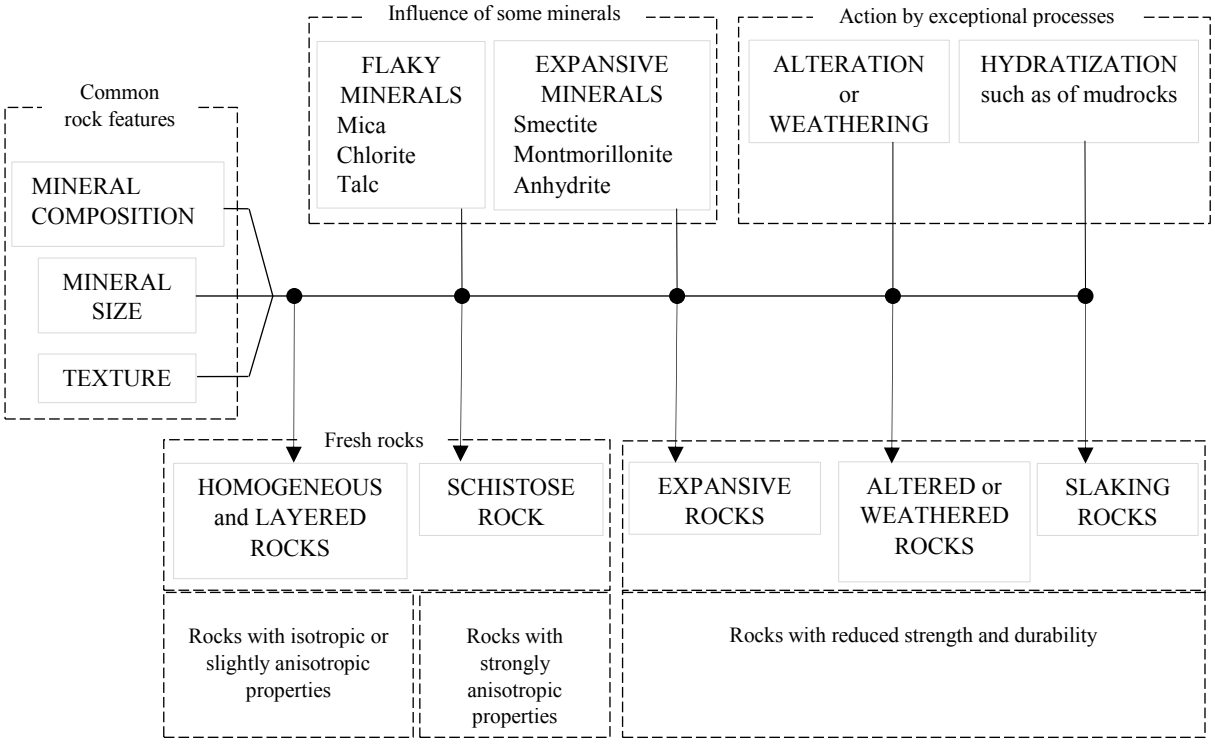

Figure 3-5: Mineralogy, structure and fabric factors influencing rock properties
Source: Palmström (1995)

According to Smyth & McCormick (1995), mineralogy provides a background to understand the physics and chemistry of rock and Ghobadi et al., (2016) further explain that mineralogical compositions affect the groundwater quality and can cause deterioration of concrete materials in tunnels.

Structure refers to physical appearance of the rock, the texture and its unique features such as faults, joints, spacing of joints, outcrops and dykes. The actual morphology and physical form of the rock structure influences surface properties and behaviour hence tunnel function (Hochella et al., 1989).

Rock fabric also called foliation, refers to spatial and geometric configuration of its constituents, its appearance associated with folding during rock formation and its structural and textural occurrence (Waldron, 2009). Bedding, banding, dense interlocking, heterogeneous

fabric, anhydrite layers or veins, void spaces and microscopic structures such as grain boundaries, sizes and structure are examples of fabric (Waldron, 2009; Archanjo et al., 2008). Microscopic fabric structures influence mucking and cutting ability of the excavator (Hemphill, 2012). This is because fabric structures provide local stability of the tunnel excavation by swelling when the threshold stress of micro-crack initiation is exceeded (Amann et al., 2014). Specifically, veins can prevent disintegration of the surrounding rock mass by arresting growing fractures (Panthi, 2006). Depending on the rock type, temperature of the environment and humidity conditions; rocks may slake, disintegrate or swell (Hochella et al., 1989). Slaking is the most adverse situation and presents the greatest challenge to tunneling (Blake, 1989). Slaking is the separation of rock fragments along their crystal lattices into flakes or small particles by hydration/swelling and oxidation processes especially at higher clay contents (Dunning, 2005). Understanding material properties such as slaking helps in selecting the best tunnel approach and rate of driving so that the excavation does not worsen the rock condition (Barla, 1974). For instance, it is common practice to tunnel perpendicular to schisoticity and bedding planes to avoid further damage to the rock condition (Zia, 2016).

Geological studies of the earth's crust revealed that igneous rocks are most abundant rock type (NGS, 2015). Igneous rocks are also the most suitable material for tunnel construction because they have a dense interlocking and minor directional differences in rock mechanical properties hence they present few challenges to tunnel driving (Blake, 1989). Sedimentary rocks are softer than igneous rocks, have bedding planes and laminations of weaker assemblages cemented together with inter-granular material and exhibit significant anisotropy in their physical properties. This wide variation in structure, strength and behavior causes the greatest difficulty for tunnel construction as compared to igneous and metamorphic rocks. In addition, sedimentary rock types such as mudrocks which are susceptible to slaking and swelling are not stable in the long term (Hochella et al., 1989). On the other hand, metamorphic rocks are generally hard, have high strength, a varied structure, composition, properties, orientations of the platy minerals and considerable anisotropy. As such, metamorphic rocks especially micaceous and chloritic schists cause intermediate difficulty for tunnel construction (Palmström, 1995).

Igneous rocks comprise predominantly granite, gabbro and basalt formations (NGS, 2015). The arrangement of the earth's strata is such that less dense materials overlie denser layers at the bottom. Of the three igneous varieties, granite is the least dense rock and it forms the largest composition of continental crust (Hemphill, 2012). This rock has abundantly been broken down, transported, deposited and lithified to form sedimentary rocks of varying thicknesses. As such, derivatives of granitic rocks are the most common rock encountered during construction. Characteristics of granitic rocks include anisotropy, homogeneity, imperviousness, strong weathering resistance, temperature indifference and high melting temperatures above 650 ºC (Archanjo et al., 2008; Sydney, 2006). The thickness of granitic layers determines the overall rock mass strength especially for hard rock which has been amalgamated (Sydney, 2006). The strength of the rock determines the capacity of a road header required and excavation rates. Stronger rocks resist penetration hence slow excavation rates

(Hemphill, 2012). In this state, a machine with a higher mechanical energy is required to break the crystal bonds in rock compared to the effort required to break decomposed softer rock (Hochella et al., 1989).

The main chemical composition of the earth is a single mineral group of silicate compounds also known as tectosilicates (Marshall & Fairbridge, 1999). Silicates constitute about 95% of igneous rocks, 75% of metamorphic rocks and more than 60% of sedimentary rock constituents. Both Dunning (2005) and Gargaud (2011) explain that silicate minerals contain a fundamental $[SiO_4]^{-4}$ structure and the final space distribution of the four oxygen (O_2) atoms around the central silicium (Si^{4+}) atom is used to classify them. The positively charged Si atom is surrounded by four O_2 atoms to form the silicate molecule (Figure 3-6) which is fairly stable. Generally, atoms form molecules then minerals and finally rocks and rock masses (Dunning, 2005). Aggregated silicate minerals form granitic rock of various types, compositions and properties depending on the earth elements present in its structure (Sydney, 2006). A mineral is a natural chemically stable solid network of crystal lattices comprising jointed segments of bonded molecules. For example, Figure 3-7 shows the structure of quartz ($[SiO_2]$). Common granitic varieties include plagioclase feldspar ($[CaAl_2Si_2O_8]$), potassium feldspar ($[KAlSi_3O_8]$), sodium feldspar ($[NaAlSi_3O_8]$), mica ($[K_2(Al,Mg,Fe)_{4\text{-}6}(Al,Si)_8O_{20}(OH,F)_4]$) and amphibole ($[Na(Na,Zn,Li,Ca,Mn,Fe^{2+},Mg)_2(Mg,Fe^{2+},Mn,Al,Fe^{3+},Ti,Zn,Cr)_5(Si,Al,Ti)_8O_{22}(OH,F,Cl)_2]$). The different granitic varieties are products of the stable earth element which may replace Si or get replaced by the subsequent stable element in the chemical reactivity series (Rudnick & Gao, 2003; McDonough, 1995). The charts in Figure 3-8 show (a) the composition of granite and (b) a triangulated classification based on its constituent quantities of quartz, plagioclase feldspar, potassium feldspar or sodium feldspar. Both charts are used as handy tools in the field to identify, name and establish rock properties for engineering design assessment and construction.

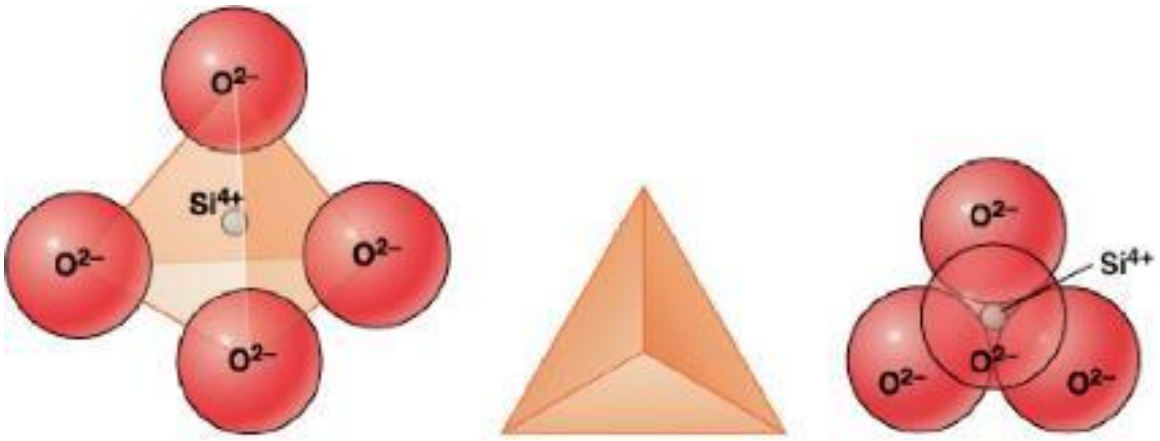

Figure 3-6: Structure of a silicate mineral
Source: Dunning (2005)

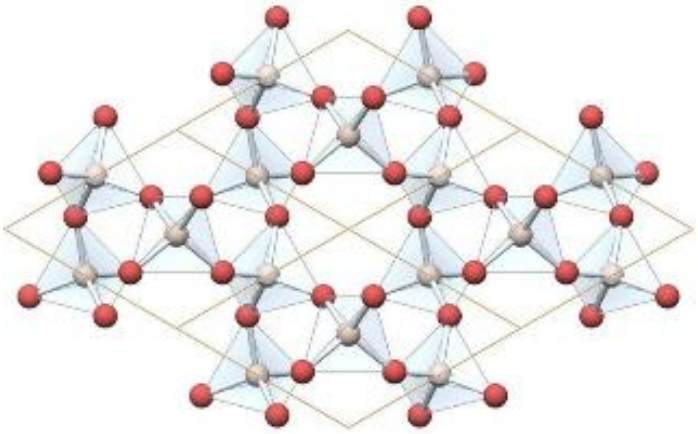

Figure 3-7: Network of SiO_4 crystal lattices forming quartz
Source: Redd (2012)

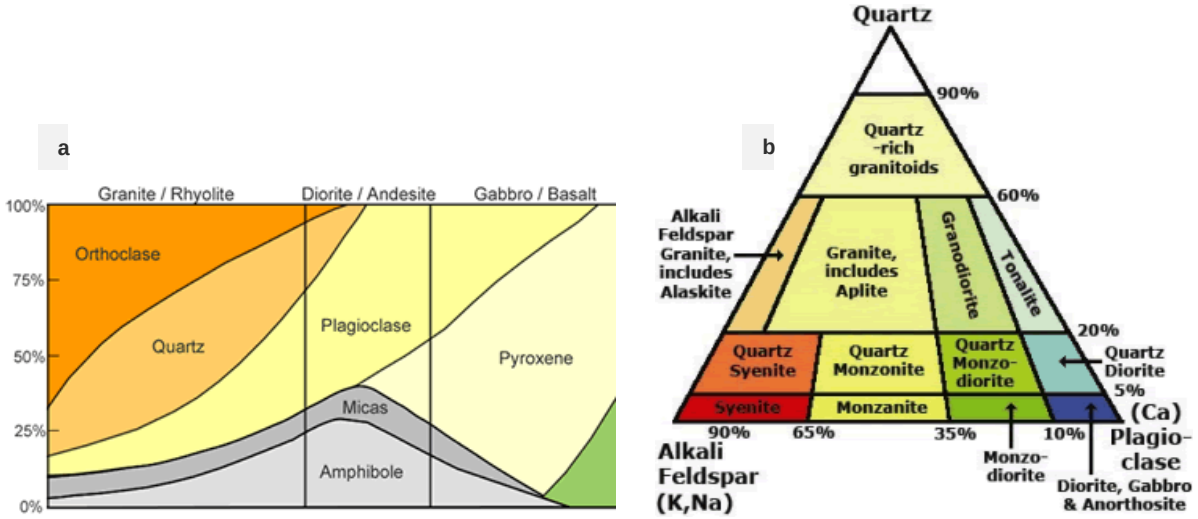

Figure 3-8: (a) Granite composition and (b) Classification
Courtesy: Geology.com (2015)

As a result of varying granitic rock structures from the earth elements, compositions have different surface properties, behaviour and strength depending on the predominant element (Sydney, 2006; McDonough, 1995; Hochella et al., 1989). These properties determine the suitable geological rock materials, methods and tools such as cutters which are selected for tunneling (Hoek et al., 1995; Blake 1989). The following situations are important to evaluate,

1. Mineral strength: Excavating strong minerals such as quartz is difficult and can inflate project costs as consumable machine parts including drill bits and cutters are replaced frequently (Blake, 1989).
2. Material infilling: Physico-mechanical rock strength is reduced when the weak planes of sedimentary and metamorphic rocks are filled with flaky elastic and anisotropic minerals such as mica, chlorite, amphiboles and pyroxenes (Wahlstrom, 1973). Alteration products of weathered basalts and anhydrite rock varieties or fine clay minerals such as montmorillonite shales, infilling joint seams or faults (Wahlstrom, 1973). Infillings of

mica schists and phyllites reduce the strength of the rock because they have strong anisotropic mechanical properties (Palmström, 1995).

3. Sheet minerals such as serpentine, talc and graphite: These easily slide along cleavage surfaces thereby reducing rock strength (Palmström, 1995).
4. Presence of montmorillonite clay minerals: Moisture causes swelling/squeezing of the mineral structure and associated construction difficulty such as mudflows and face collapses (He, 2014; Kanji, 2014; Jean et al., 2003; Hoek et al., 1995).
5. Clay varieties present: The magnitude of joint roughness weakening, core softening and reduction of both strength and wedge interlocking varies for different clays (He, 2014; Kanji, 2014). Also, the ultimate effect causes rock falls and slides in underground caverns and cuttings (Hoek et al., 1995; Palmström, 1995).

3.2.2 Discontinuities / discontinuity sets

Discontinuities are distinct structural breaks and geological interruptions in the intact homogeneous rock mass which convert it into a discontinuous assemblage of discrete wedges whose shape and size are defined by their boundary margins (Zhao, 2015; NEH, 2012). Stream cobbles, talus and glacial boulders are natural factors which widen discontinuities in certain situations depending on the environment (Hochella et al., 1989). Discontinuities influence engineering characteristics by controlling the overall rock mass strength, behavior, permeability, pore pressures, stability, effort required to excavate, stresses and deformations (NEH, 2012; Eberhardt, 2012). Table 3-5 describes the major discontinuities present in a rock mass. The origin, nature and propagation of faults dictates the level of flexibility and positioning of underground project components (Hemphill, 2012; Wahlstrom, 1973). The main features which define rock wedges include faults, fractures, shear zones, bedding planes, folding/bedding planes, dykes, joints, joint infilling, foliation, void spaces, degree of saturation, tension cracks, broken/jointed rock (Franki, 2008). Figure 3-9 shows seven main types of discontinuities which directly influence deformation of the rock mass, joints and weak zones according to Palmström (1995). Figure 3-10 illustrates joint features which are useful deciding factors during construction. The features are used to identify and name discontinuities as shown in Figure 3-11.

Discontinuities are characterised by low strengths and deformation therefore, they aid material separations by allowing water ingress (Zhao, 2015; Spang, 2004; Hochella et al., 1989). This ability makes them favourable for tunneling although only in very limited cases (Piteau, 1972). Structurally, discontinuities intersect to create triangular or irregular separations with isolated rock wedges[8] or rock blocks, respectively (Palmström, 1995). The separations along discontinuity lines usually coincide with localized shear zones and bedding planes (Zhao, 2015). It is favourable to tunnel in the dip direction and perpendicular to the strike direction (Headland et al., 2008). Also, tunneling in medium hard rock is favourable in that an average excavation effort is required and the advance rate is usually fast compared to hard rock (Piteau, 1972). Discontinuities favour construction depending on their cause, age, direction, location

[8] In this study the term wedge refers to rock wedges, rock blocks or both.

and history of development (Hochella et al., 1989). Specifically, the susceptibility to groundwater flow, filling, roughness, nature of contacts, degree and nature of weathering, type and amount of gouge are important factors for tunneling (Palmström, 1995).

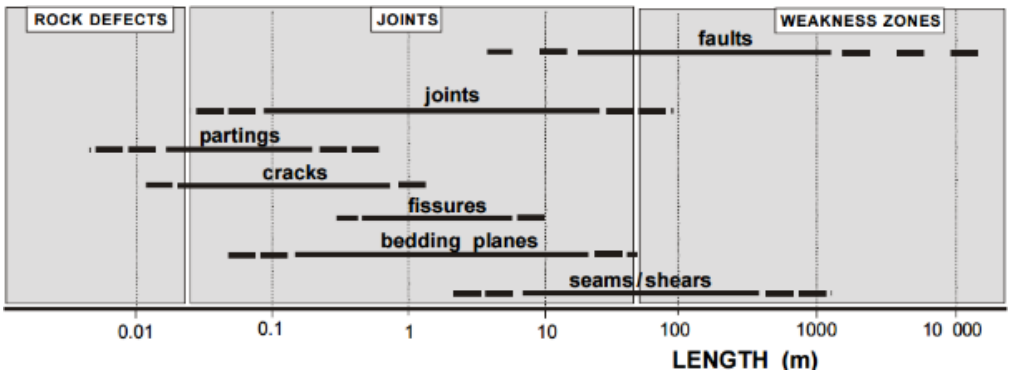

Figure 3-9: Main discontinuities influencing rock mass properties
Source: Palmström (1995)

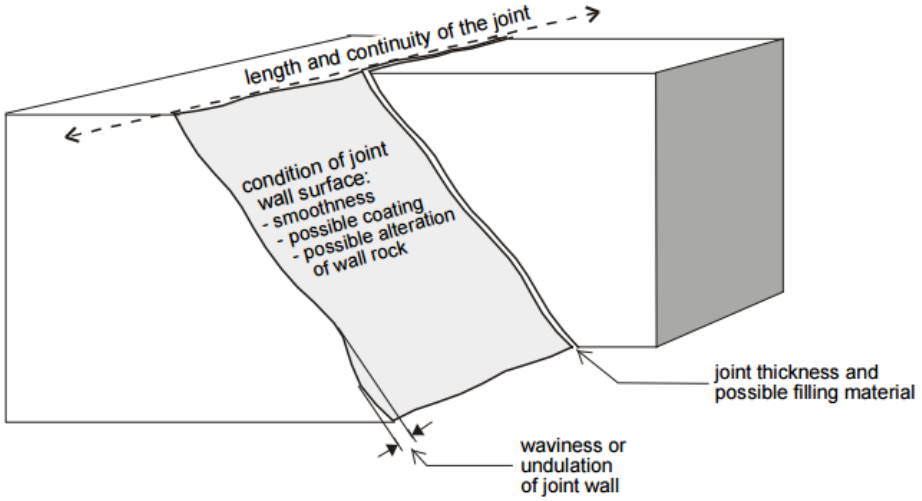

Figure 3-10: Joint features
Source: Palmström (1995)

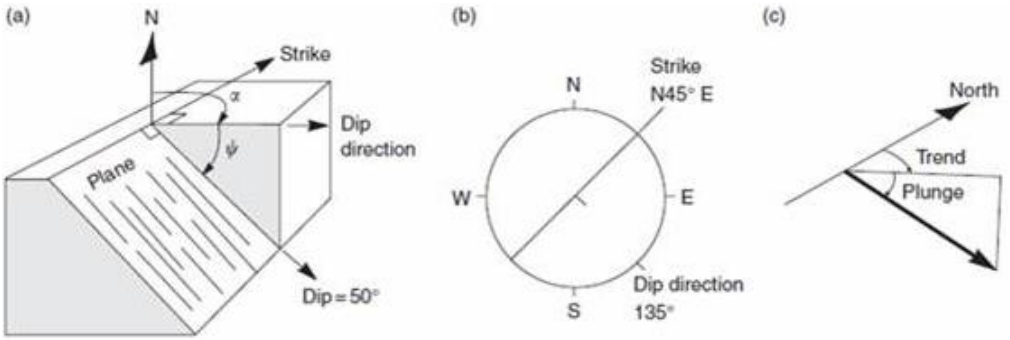

Figure 3-11: Naming discontinuities based on plane orientation
(a)Isometric view (b) Planar view (c) Isometric view of plunge and trend lines
Source: Varanasi (2009)

Table 3-5: Major discontinuities present in a rock mass

Rock type	Discontinuity	Physical properties	Geotechnical aspects
Igneous (predictable and random features)	Cooling joints	Systematic sets of hexagonal joints perpendicular to cooling surfaces are found in lavas and sills. Larger spaced intrusions typified by doming and cross joints.	Easier to deal with columnar joints because they have regular patterns. Other joints are usually widely with variable orientation and nature
Sedimentary (features identified by geological mapping)	Bedding planes/ bedding joints	Parallel to original deposition surface mostly horizontal in unfolded rocks	Flat and persistent over long distances Likely changes in lithology, strength and permeability. Mostly close, tight with cohesion but opens due to weathering and unloading
	Salty cleavage	Close parallel discontinuities formed in mudstones during diagenesis and resulting in fissility.	
	Random fissures	Important mass feature, common in recently consolidated sediments.	Greatly influences strength and permeability for many clays.
Metamorphic (mapping and unique trends)	Salty cleavage	Close spaced, parallel and persistent planar integral discontinuities in fine-grained strong rock.	High cohesion where intact but persistent planar integral discontinuities in fine-grained strong rock.
All (features identified variably including mapping, interpolation and extrapolation)	Tectonic joints	Persistent fractures from tectonic stresses. Joints occur as sets with regional stress fields.	Tectonic joints classified as shear or tensile depending on origin. Shear joints are smoother. Impersistence and high strength resulting from laterally dead joints.
	Faults	Fractures of variable aperture in zones of sheared rock	Low shear strength mostly in slicken-sided or gouge areas associated with high groundwater flow or act as barriers to flow. Deep weathering zones occur along faults. Recent faults may be seismically active.
	Sheeting joints	Rough widely spaced fractures parallel to the ground surface, formed from unloading under good quality tension.	Mostly adverse (parallel to slopes) and may be persistent.
	Lithological boundaries	Varied rock type boundaries depending on geological history.	Weathering rock concentrations often mark distinct changes in properties such as strength, jointing and permeability. Often form barriers to groundwater flow.

Source: (NEH, 2012)

3.2.3 Hydrogeology

The interactions between geological features and subsurface groundwater properties and its role in geological processes, environments, recovery, contamination and utilization are covered under hydrogeology (Sharp, 2007). Groundwater significantly affects geological properties such that the material properties are modified especially where expansive clay minerals are present. Expansive clays are sensitive to water which results in them swelling or expanding. Recharge sources including precipitation, surface runoff, percolation and nearby wells affect the degree of saturation, hydrostatic head of water and pore water pressures. Likewise, the degree of saturation influences humidity, percentage of saturated voids and pore pressure build up (Dunning, 2005). Water bearing slightly-filled fault zones, aquicludes, joints and aquifers significantly affect tunneling, thus it is important to understand the ground hydrological processes and their impact on tunnel structures (Bondarchuk et al., 2012; Jean et al., 2003; Blake, 1989). The evaluation of inter-relationships between properties of the solid rock and water as well as external influences from the excavation process are vital (Sepp, 2000; Hochella et al., 1989). Figure 3-12 illustrates the main factors and sub-interactions between the rock, hydrogeology, ground stresses and construction. Flowing water widens any discontinuities present in the rock mass causing physical degredation because the porewater pressure induces stresses. The induced stresses and widened discontinuities are responsible for collapse and sliding failure thereby guiding selection of excavation geometry, purpose and support requirements (Bondarchuk et al., 2012). As such, provision of adequate drainage is important.

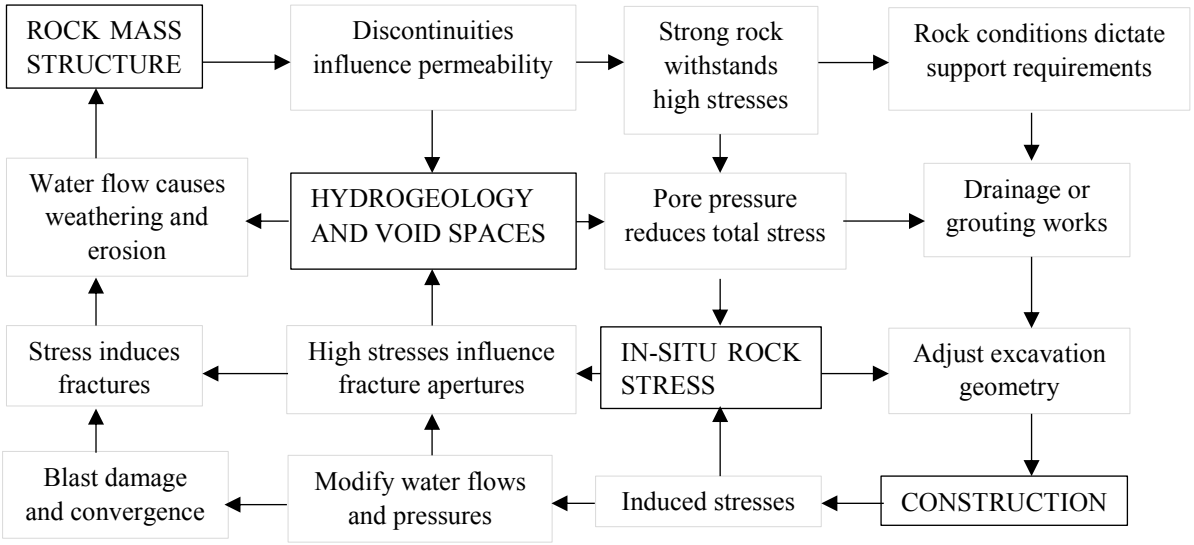

Figure 3-12: Interactions between ground factors
Source: Redrawn after Jones (1989)

The relevance of drainage, avoidance of hydrostatic pressure build-up and redirecting groundwater flows are important in tunneling (RTM, 2009; Jones, 1989). High hydrostatic heads and water velocities cause deterioration of the tunnel surface and instability issues especially arising from rock squeezing and swelling (Mokhtari et al., 2013). Provision of adequate drainage is therefore important to safeguard tunnels and it depends on proper sizing and suitable provisions (Ghobadi et al., 2016). Sizing is based on accurate model prediction of

the flow zones and flow rates for the design and construction of tunnels which should incorporate the sources of groundwater, its flows and tunnel seepage (UC&T, 2014; Hemphill, 2012). Groundwater inflow is variable and it results from precipitation, surface percolation, subsurface leakages and infiltration. Seepage of water through the structure can undermine stability causing eventual failure.

According to Mohammed (2015), drainage in tunnels is usually provided for using sumps and pumps of adequate capacities which match the duty cycle of discharge pumps and fitted with debris traps (sand filters, oil and fuel separators) at the portals and low points to collect flowing water. Smooth bends are necessary to avoid internal pressure build-ups and high stress concentrations in the surrounding ground and potential breakages or bursts (Hoek et al., 1995; Blake, 1989). Sump and pump provisions should comprise non-combustible drain inlets, pipes and ventilation ducts at potential leakage points and intersections behind the lining and a gentle downward slope for gravitational flow (Bondarchuk et al., 2012). Alternatively, tunnel membranes can be sprayed to prevent water ingress and egress (Ghobadi et al., 2016; Barton & Grimstad, 2014). Figure 3-13 shows details of a robust drainage system.

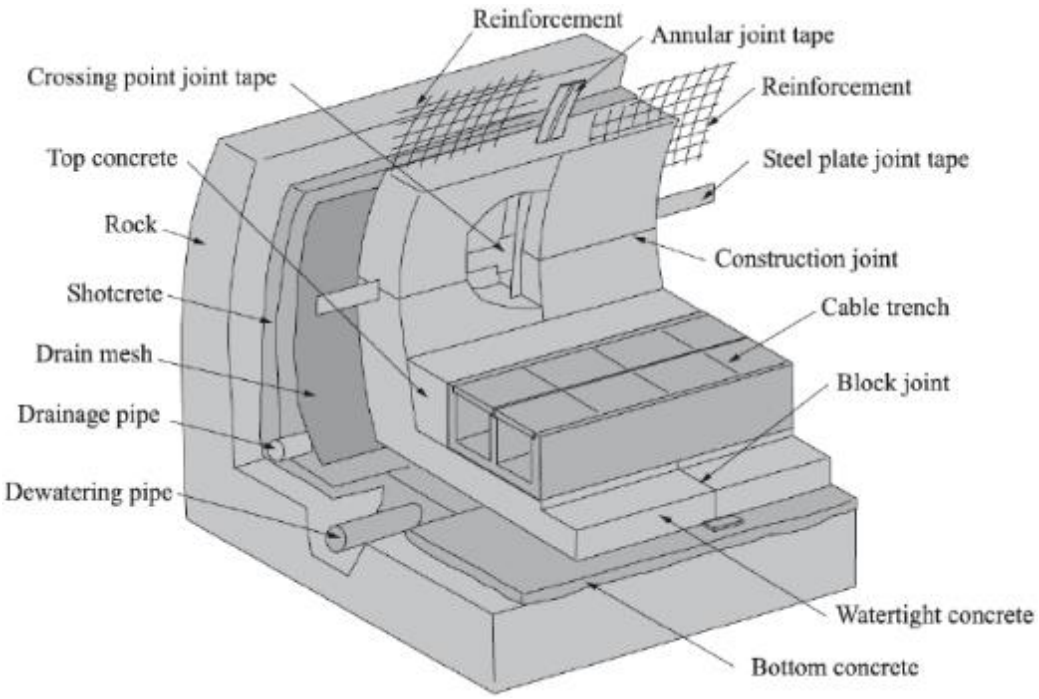

Figure 3-13: Typical drainage of a tunnel
Source: Mohammed (2015)

3.2.4 Squeezing and swelling

Common rock behaviour encountered in tunneling include rock bursts in form of spalling (sliding of sidewall wedges) and popping (collapse of roof wedges), heaving of bottom floor wedges, squeezing and swelling (Viggiani, 2012; Kang & Lu 1991). From the list of common rock behaviour, squeezing and swelling resulting from water ingress and drainage, are most problematic and challenging because they are difficult to predict and mitigate (Mokhtari et al.,

2013; Steiner, 2000). Squeezing and swelling behaviour which are comparable to shrink and swell behaviour in soils, cause significant stability challenges during construction (Franki, 2008; Craig, 2004). Squeezing and swelling are contrasting rock behaviour mostly associated with weak discontinuous rock conditions and are undesirable properties for tunneling (Steiner, 2000; Kang & Lu 1991). Research by Sousa (2010) revealed that the most common tunnel failures caused by severe face instability resulted from squeezing.

Squeezing in rock tunnels occurs in the plastic zone due to shearing of the surrounding rock mass when its in-situ unconfined compressive strength (UCS) is too low to resist the inward movement of the excavation and the ratio of rock mass strength, τ_{rock} to in situ stress, $\sigma_{in\text{-}situ}$ falls below 0.2 (Mohammed, 2015; Hoek, 2001; Steiner, 2000). Mathematically, $(\tau_{rock}/\sigma_{in\text{-}situ}) < 0.2$. Also, field research by Solak & Schubert (2004) and Hoek's (1999) tunneling experience showed that tunnel deformations increase with decreasing block size so that UCS (σ_{ci}) is inversely proportinal to wedge sizes (d). Equation 3-1 illustrates this relationship. Factors influencing ground squeezing include initial state of the in-situ stress, ground strength and deformations, structure orientations, groundwater conditions, construction and lining procedures and methods.

$$\sigma_{ci} = \sigma_{c50}(50/d)^{0.18}$$ **Equation 3-1**

where σ_{c50} is the UCS for a 50mm diameter sample

Swelling on the other hand may occur without the plastic zone. It is associated with montmorillonite clay minerals of the smectite group such as exist in shale and slate rock discontinuities (Mokhtari et al., 2013; Hoek, 2001). The clay structure has a very high affinity for water causing it to imbibe water and expand when saturated through aggregation and flocculation of the clay fabric (Murck et al., 1997). Figure 3-14 shows how montmorillonite clay infillings in discontinuous rock expand by physicochemical effects. Expansive behaviour depends on initial water content, groundwater conditions, void ratio, mineral composition, internal structure and confining pressure (Mokhtari et al., 2013; Williams et al., 1985).

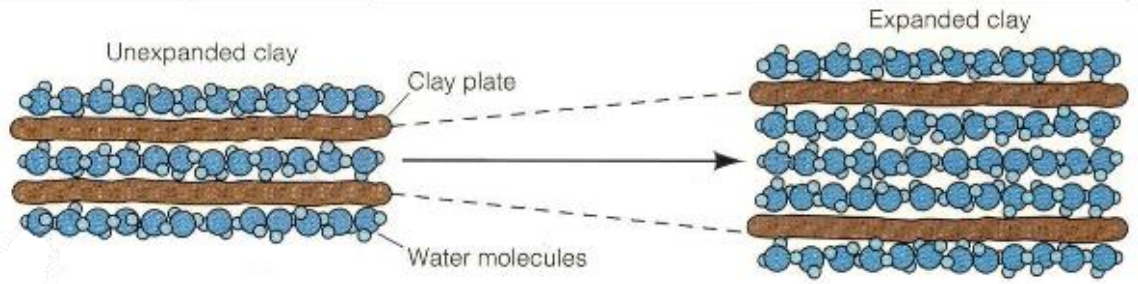

Figure 3-14: Expansive mechanism
Source: Murck et al. (1997)

3.3 Geotechnical rock parameters

This section discusses rock strength and necessary tests for establishment of rock parameters, including rock squeezing behavior and geological prediction during excavation. The chapter

further presents the rocks mass classification systems in two sections under quantitative and qualitative categories.

3.3.1 Rock strength

Rock physio-mechanical strength properties vary depending on mineralogy, type of bonding, structure and fabric (Palmström, 1995; Wahlstrom, 1973). Likewise, rock mass strength depends on its overall properties but where various discontinuities are present, strength mainly depends on individual material properties (Thomas-Lepine, 2012). Discontinuities are particularly important for fresh igneous rocks because they are intact and of generally high strength having discontinuities which control rock mass properties (Panthi, 2006). On the other hand, material properties are significant for sedimentary and metamorphic rocks where discontinuities are many because of their formation history (Dunning, 2005). Figure 3-15 shows geometric rock mass properties which are important for engineering purposes. In the figure, 1) two discontinuity sets are shown, 2) the wall strength also represents its roughness, 3) the orientation is given in terms of the dip and dip direction, 4) the spacing shown is the apparent spacing rather than the actual spacing, and 5) when a ground penetrating radar is used, it traverses along the borehole length (Zhao, 2015). According to Torres (2008), actual spacing is the perpendicular distance measured between the discontinuity sets whereas the apparent spacing is measured horizontally.

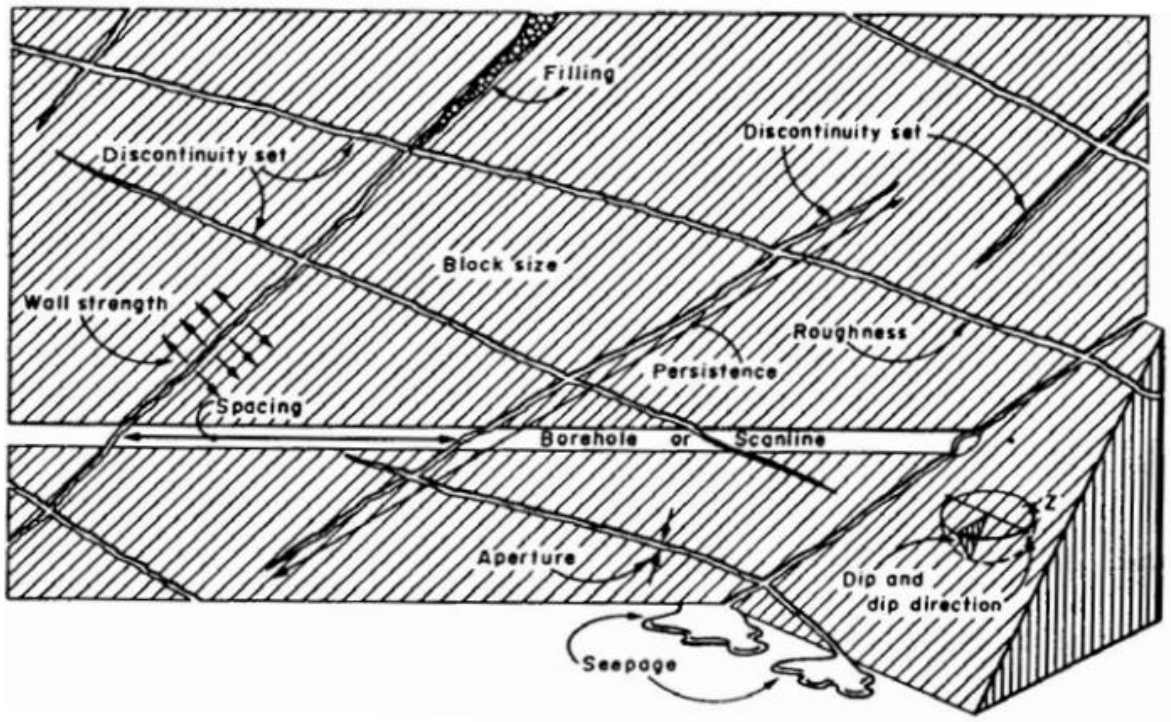

Figure 3-15: Main geometric properties influencing rock strength
Source: Zhao (2015)

Based on mechanical strength and ability to support engineering loads, rocks are either hard or soft (He, 2014; Hemphill, 2012). Hard rock strength is greater than 25 MPa which corresponds to the upper limit of strength for soft rock and the latter approximates soil at its lower limit

(Ongodia et al., 2016). For this study, soft rock is considered to have a maximum strength of 25 MPa. However, the requirements of rock strength are different for both mining and civil engineering (Hustrulid, 2000; Brown et al., 1983). Rock strength is more critical for mining because of the steeper slopes and greater excavation depths compared to civil engineering works (Hoek, 2001). Table 3-6 shows the rock categories which are based on the minimum unconfined compressive strength (UCS) developed as part of the guidelines for soils and rock logging in South Africa (2001). The table highlights the difference between definitions of rock strength in civil engineering and mining terms.

Table 3-6: Engineering rock categories based on UCS

Application	Civil engineering rock		Mining rock
Unconfined Compressive Strength (UCS)	1-3 MPa	Very soft	Soft rock
	3-10 MPa	Soft	
	10-25 MPa	Medium hard	
	25-70 MPa	Hard	Hard
	70-200 MPa	Very hard	
	>200 MPa	Extremely hard	
Reference	Guidelines for soils and rock logging in South Africa (2001)		Kanji (2014) and Marinos (2014)

Usually, soft rock has undesirable engineering properties including various discontinuities, low porosity, highly weathered weak unconsolidated rock mass with loose sediments and requires either advance or immediate support when excavated (Marinos, 2014; Luwalaga, 2013; Hoek, 2001). Soft rock tunnel widths are therefore restricted to shorter stand-up times and mandatory immediate support compared to hard rocks (Bieniawski, 1992). Consequently, hard rock is preferred for engineering purposes because of its strength, higher bearing capacity and fairly intact rock mass structure with fewer discontinuities (Ongodia et al., 2016). In addition to rock strength, other important parameters include stratigraphy, cavities, groundwater, engineering and index material properties and its visual classification along the longitudinal profile (Panthi, 2006; Brown et al., 1983).

3.3.2 Tests to establish rock parameters

The extent of tests performed depends on the scale of the project, its requirements, design and construction parameters (Hemphill, 2012). This section discusses the main rock parameters which influence tunneling. The parameters include: rock strength, squeezing and unknown geological conditions ahead of the tunnel advance face. Besides, methods to assess and evaluate strength and squeezing potential are discussed as well as those that are used to predict geology ahead of a tunnel advance face. Also, standards to assess different rock parameters are given.

Appropriate guidelines and standards are followed to test and establish parameters which are analyzed and from which conclusions are drawn. Common standard guidelines for testing include the International Society of Rock Mechanics (ISRM) and American Society for Testing and Materials (ASTM). The standards enable concise and consistent documentation (Sabatini

et al., 2002). This is especially important to streamline tunneling information and data gathered for future reference. For example, Figure 3-16 shows a range of shear strength parameters for soft weathered granitic rock with interlocking blocks published by Hoek & Bray (1974). From the figure, soft blocky granite has a cohesion ranging about 0.05 to 0.2 MPa and angle of internal friction ranging between 31° to 45°. Cohesion in rock is insignificant and only a measure of the surface roughness is important (Mohammed, 2015; Thomas-Lepine, 2012). Material parameters can be estimated easily by positioning them on the chart. However, such estimates are only helpful during initial early project stages. According to Hoek et al. (1995), field stresses are the same for a radial extent of about 50 km. Therefore, values can be adopted from sources of published literature within the same geographic region. Other common charts that can be used to roughly estimate preliminary rock parameters are included in Appendix B of this report.

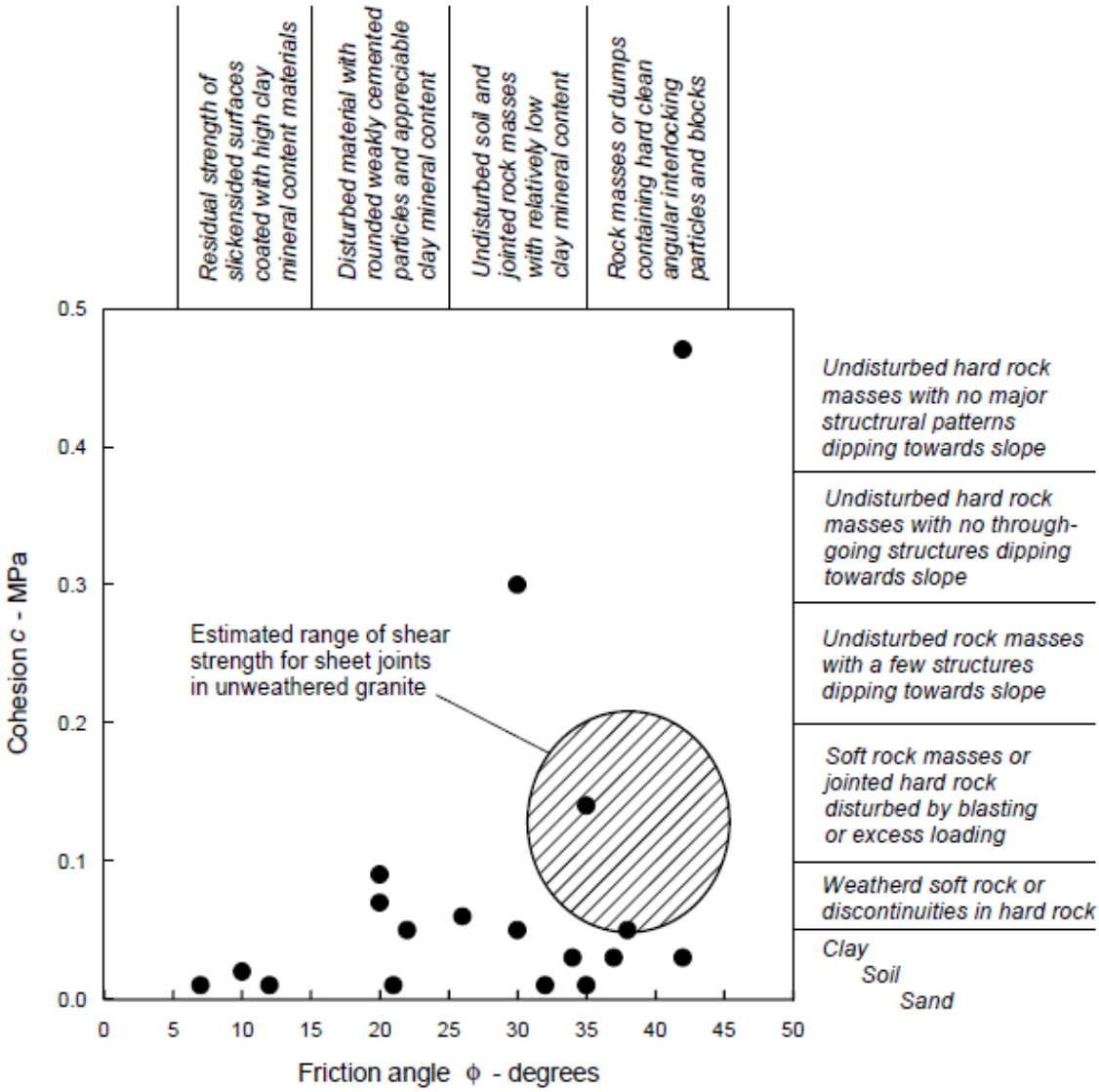

Figure 3-16: Shear strength of soft blocky granite
Source: Hoek & Bray (1974)

Other conventional ways to evaluate geotechnical engineering materials include observation, quick preliminary tests, sampling, boring, in-situ testing, laboratory methods and geophysical investigations (Mohammed, 2015). Early parameter estimations are useful for planning and decision making. Quick preliminary tests are used for initial assessment of some parameters like rock hardness in the field using handy tools. Tools used to estimate hardness include a knife, copper penny, pictures and charts (FHA, 1991). Actual laboratory or in-situ tests to assess various important rock parameters for all rock types according to the ASTM standard are listed in Table 3-7. Although laboratory tests are easier to perform, because the test environment is controlled, the tested sample does not account for the influence of discontinuities and boundary conditions of the rock mass (NEH, 2012). For that reason, in-situ field tests on rock are more accurate and preferable. Hoek et al. (1995) observed that hydraulic fracturing and over-coring methods gave more accurate values of in-situ field stresses at depth compared to strength values obtained from laboratory shear box and triaxial tests. Instead of performing a complex UCS test, a much simpler point load test which requires less expertise can be performed in the laboratory. The value of the point load index is then used with the chart shown in Figure 3-17 to estimate the corresponding UCS value for rock strength. Alternatively, a special triaxial cell (Figure 3-18) can be used for field measurements in place of laboratory triaxial tests.

Table 3-7: Tests for rock properties (ASTM)

Test	Parameter	Reference
Uniaxial compression	UCS of intact rock	D2938
Direct shear	Direct shear strength	D5607
Brazilian Tensile Strength (BTS)	Strength and roughness	D3967
Strength-Deformation	Compressive strength and elastic moduli	D7012
Acoustic velocities	Competency and subsurface condition	D5777
Cerchar Abrasivity Index (CAI)	Resistance to wear	D7625
Tabor abrasion test	Abrasiveness (also indicates cut and wear)	D1044
Schmidt hammer hardness	Soundness and hardness	D5873
Point Load (PL) index test	Strength value	D5731
Slake durability index	Disintegration resistance	D4644
Rock classification	Mineral identification	C 856
Moisture content	Moisture content by rock mass	D2216
Permeability	Hydraulic conductivity	D4525
Thermal needle probe procedure	Thermal conductivity of soft rock	D5334
Guidelines for identification of further rock parameters and condition		
Rock Quality Designation (RQD)	Rock mass classification and strength	D5878
Seismic refraction	Subsurface condition using geophysical methods	D5777
Geophysical methods	Selection of surface geophysical methods	D6429

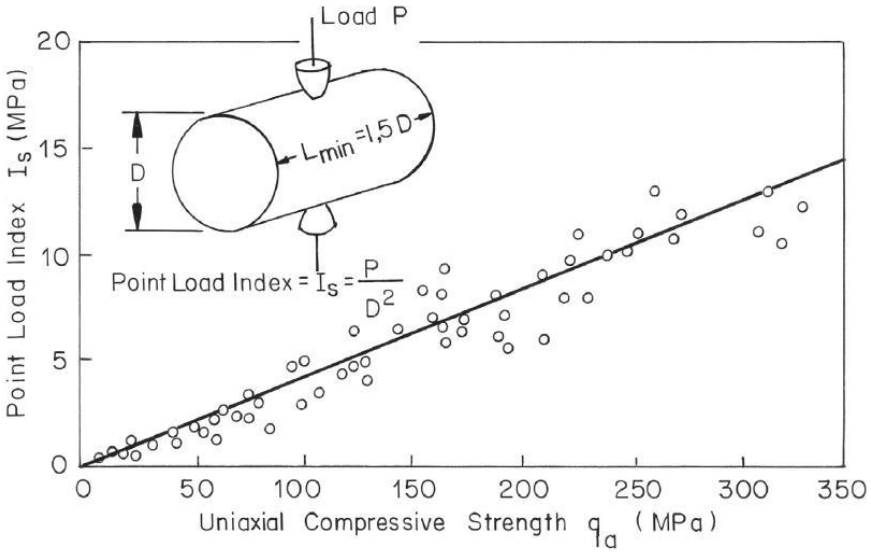

Figure 3-17: Rock strength correlations from point load test
Source: Bieniawski (1973)

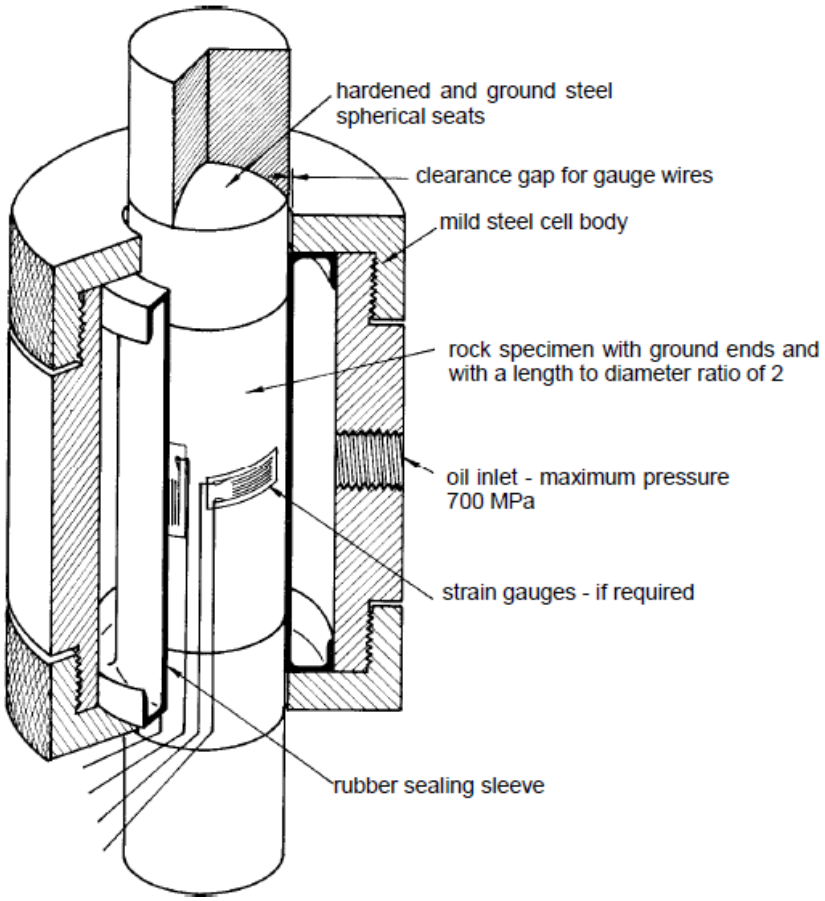

Figure 3-18: Specialized field triaxial cell for testing rock
Source: Hoek et al. (1995)

Tests to identify squeezing/swelling potential in rock are borrowed from related soil tests. Mohammed (2015) explains that the measured laboratory swell pressure should be applied to

the rock to induce stability by arresting swelling. The tests include the soil expansion potential, coefficient of linear extensibility, double oedometer test, van der Merwe's method, empirical relationships and mathematical heave prediction using the soil water characteristic curve (Badenhorst et al., 2015, Williams et al., 1985). The tests to determine the potential squeezing or swelling ability of rock are generally complex, delicate and their results are not usually easy to interpret. Therefore, the chart in Figure 3-19 can be used to predict squeezing behaviour. It was developed to predict squeezing problems based on strains of an unsupported excavation. From the figure, when calculated strains from finite element analysis reach 2.7% severe squeezing is expected and support is necessary commensurate with the instability (Mohammed, 2015; TLDG, 2004). In extreme cases, squeezing can lead to conversion of a horse-shoe shaped tunnel section if constructed into a circular section (Barla, 1974).

In addition to testing rock strength and its squeezing potential, it is essential to predict ground conditions ahead of tunnel advance during the excavation process (Panthi, 2006). Testing ground conditions ahead of the tunnel face is important as it helps to minimise unexpected failure events arising from sudden problematic ground conditions during construction. Geological prediction of the full excavation profile is performed after using percussion drilled probes or pneumatic machines. Figure 3-20 illustrates geological prediction using probes. The drilling penetration rate, return water flow and core recovery of the probes serve as early indications of probable ground conditions a few meters from the exposed face. Pneumatic machines record performance parameters which indicate geology ahead of the face (Sousa, 2010).

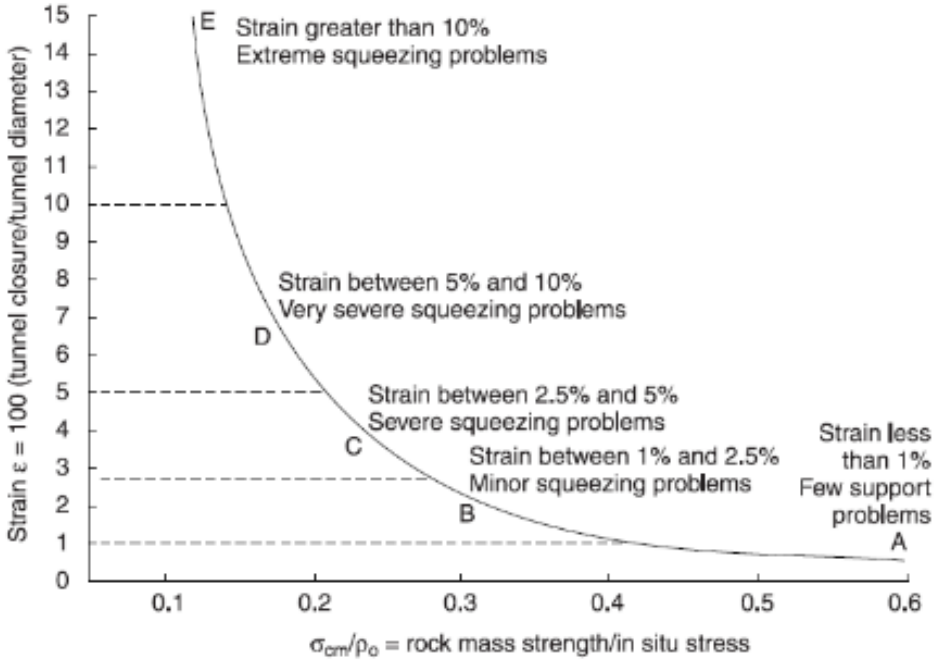

Figure 3-19: Tunneling strain and squeezing
Source: TLDG (2004) after Hoek et al. (1995)

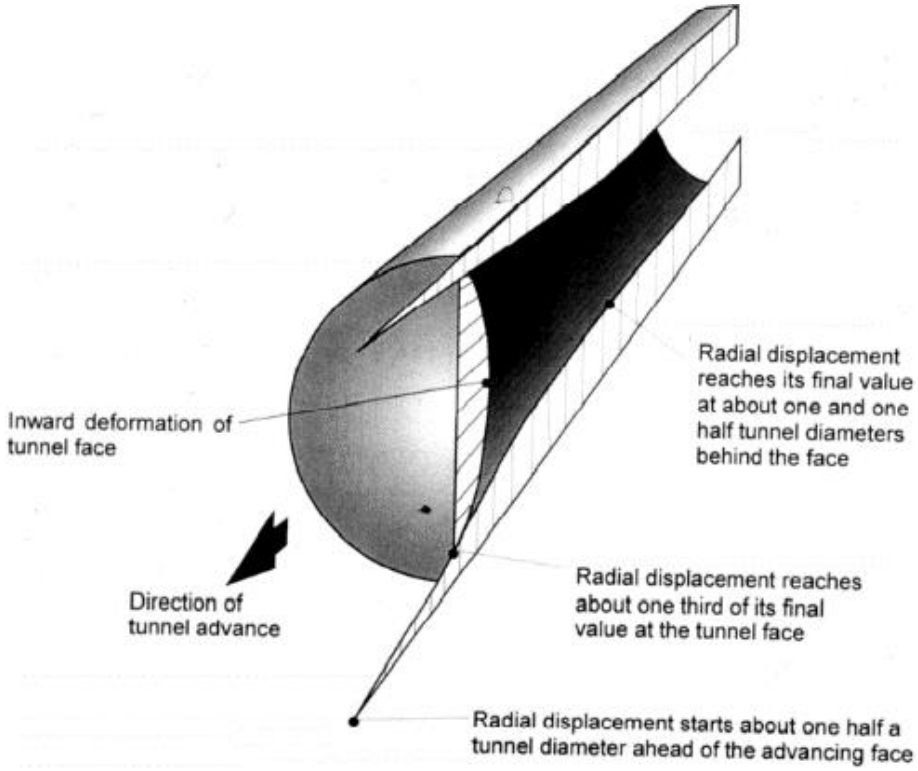

Figure 3-20: Geological prediction ahead of tunnel advance, using probes
Source: Hoek et al. (1995)

3.3.3 Rock mass classification systems

Rock mass classification systems are used to simultaneously classify unique rock material and indicate suitable design of the necessary support because they are based on relationships between rock mass parameters and case histories of engineering construction. According to Jean et al. (2003), classification systems estimate necessary stability requirements from rock mass conditions and their influencing factors. The factors include ground water, seismic activity and physico-mechanical properties (Hoek et al., 1995). Classification generally comprises description of material parameters (strength, type, geological name, competency, alteration, weathering), degree of jointing (spacing, block size, RQD), in-situ stresses, jointing (sets, conditions, pattern), excavation (method, purpose, orientation, dimension), block shape, faults, zones of weakness, orientation and inclination of dominant discontinuities.

Palmström (1995) highlights the most important quantitative and qualitative systems rock mass classification and design systems with application in tunneling. Quantitative systems include RMR, Q-system, RQD, RMR and Q-system extensions. The rock competency and alteration are also categorized as quantitative methods to classify rock. Qualitative systems comprise the Terzaghi rock load, Lauffer's stand-up time, Rock Structural Rating (RSR), size-strength, Basic Geotechnical Description (BGD) and Unified Rock Classification System (URCS). Generally, the traditional methods differ from recent research most of which suggests five rock categories.

3.3.3.1. Quantitative rock mass classification systems- rock mass rating, Q system, rock quality designation and the GSI Chart

The quality of tunneling depends on the extent of weathering. Five rock classes are known based on the degree of weathering (Hoek et al., 1995). The classes in order of increasing degree of weathering and decreasing strength comprise of Class I, II, III, IV and V. Rock Mass Rating (RMR), Q and Rock Quality Designation (RQD) classify the rock according to the extent of weathering and individual properties. The three methods give an indication of the level of deformation, thus the support requirement for tunnel excavations. Tunnel route selection, methods, ground treatment, timing and type of the support are each considered in relation to the degree and grade of rock weathering. Therefore, understanding application of the systems to classify rock based on the degree of weathering is important. The RMR and Q system are the most widely used standard geomechanical rock classification systems which classify rock according to strength depending on the degree of weathering although they give more superior design and construction estimations (Kanji, 2014; Jean et al., 2003; Deree & Deree, 1989). On the other hand, the RQD is mostly used to calculate the RMR and Q-value.

The Rock Quality Designation (RQD) is a measure of the degree of jointing or fracture in rock. It represents the in-situ rock mass quality as a percentage of intact rock cores longer than 10 cm for the total length of rock recovered from a drilled borehole. Alternatively, where drilled core samples are not available the RQD is calculated using Equation 3-2 where J_v is the volumetric joint count (Hoek et al., 1995). J_v by definition is the number of joints per unit length for all discontinuity sets per unit volume. The joints counted are those which are visible from surfaces that are not filled with clay. According to Wahlstrom (1973), the RQD value is mostly used to calculate RMR and Q-values as well as rate the rock competency and quality at depth based on core recovery from exploratory drilled samples. Studies about the Discontinuous Deformation Analysis (DDA) method by Tsesarsky & Hatzor (2005) revealed that correlation with RQD is problematic and unreliable especially for rock masses comprised of horizontal layers with vertical joints. RQD cannot be used alone for engineering design and construction.

$$\mathrm{RQD} = 115 - 3.3\mathrm{J_v} \qquad \textbf{Equation 3-2}$$

The RMR[9] method is important in tunneling and was developed by Bieniawski (1973) based on an extensive study of tunnels whereby discontinuities governed the ground response. It gives the geomechanical classification as a sum of the independent RMR ratings of each of the structural disparities within the rock mass and positioning the structure with respect to tunnel driving is unique to the RMR system (Kanji, 2014). Structural disparities include 1) UCS, 2) RQD, 3) groundwater conditions, 4) condition of discontinuities, 5) spacing of discontinuities and 6) orientation of discontinuities. Based on this method, the direction of tunnel excavation is positioned away from discontinuities to avoid widening along the discontinuities. The RMR method limits excavation and support options (Jean et al., 2003). RMR values range between

[9] For mining purposes, the term used is 'mining rock mass rating' abbreviated as MRMR and it includes in-situ and induced stresses, stress changes, the effects of blasting and weathering (Hoek et al., 1995).

0 to 90 and values below 20 indicate poor rock mass (Thomas-Lepine, 2012). Further details on rock mass classification including examples are given in Appendix C.

Barton et al. (1974) developed the Q-system, also known as the Q-value or the tunneling quality index from a study of 1000 Scandinavian tunnels excavated by drill and blast method. The system gives a quantitative indication of adequate tunnel support to ensure stability and estimates rock mass parameters (Mohammed, 2015; Hoek et al., 1995). According to Barton & Grimstad (2014), application of the Q-system generally incorporates the holistic rock mass geology. Specifically, though the Q-system considers the tunnel quality in terms of material properties including joint surface characteristics, strength, infillings, pressure, excavation dimensions, a stress parameter and an index Excavation Support Ratio (ESR[10]) (Jean et al., 2003). ESR is an indication of the factor of safety and depends on the purpose and stability requirement of the excavation thereby the Q-index is useful to select suitable reinforcement support for civil engineering works where rock falls are common or expected. Hoek et al. (1995) state that an ESR value of 1.6 is acceptable for hydro tunnels. The Q-index and the equivalent dimension[11], D_e of the excavation can be calculated using Equation 3-3 and Equation 3-4, respectively. Joint surface characteristics measured along the exposed surface of a joint after excavation of the rock mass, include the joint set number (J_n), joint roughness number (J_r), joint alteration number (J_a), joint water-reduction factor (J_w), and stress reduction factor (SRF). Mohammed (2015) classified the quotients RQD/J_n, J_r/J_a and J_w/SRF as measures of block size, joint friction and joint stress, respectively. Furthermore, Jn/Jr is used to estimate overbreak (Barton & Grimstad, 2014). Joint strength can be calculated using Equation 3-5. Classification of individual rock parameters to estimate the Q-index are given in Appendix C. Typical Q-values range between 10^{-3} to 10^{3} on a logarithmic scale (Barton & Grimstad, 2014; Hoek et al., 1995).

$$Q = \left(\frac{RQD}{J_n}\right) \times \left(\frac{J_r}{J_a}\right) \times \left(\frac{J_w}{SRF}\right) \quad \textbf{Equation 3-3}$$

$$D_e = \frac{\text{Excavation span, diameter or height (m)}}{\text{Excavation Support Ratio (ESR)}} \quad \textbf{Equation 3-4}$$

$$\tau = \sigma_n \tan\left(\phi + JRC \log_{10}\left(\frac{JCS}{\sigma_n}\right)\right) \quad \textbf{Equation 3-5}$$

where σ_n is the normal stress on the plane of failure, ϕ is the angle of internal friction, JRC is the joint roughness coefficient and JCS is the joint wall compressive strength

RMR and Q systems consider the UCS, RQD, joint frequency, roughness, infilling and hydrostatic pressure. RMR and Q systems are related by Equation 3-6 and Equation 3-7.

[10] ESR depends on the purpose and stability requirement of an excavation and indicates the factor of safety. It is usually 1.6 for hydropower tunnels.

[11] The ratio of excavation dimensions to excavation support ratio for underground works.

$$RMR = 9\ln(Q) + 44 \quad \textbf{(TLDG, 2004)} \quad \textbf{Equation 3-6}$$

$$Q = 10^{\frac{RMR-50}{15}} \quad \textbf{(RTM, 2009)} \quad \textbf{Equation 3-7}$$

A further description of both systems is given in Table 3-8. The table highlights main differences between the RMR and Q system in terms of characterisation, project purpose and empirical relations. Independent application of each of the RMR and Q system methods limits the parameters that can be obtained and assessed. The challenges and practical limitations which exist in each method highlight the need to use more than one single method to classify the site.

Table 3-8: RMR and Q rock classification systems

Parameter	RMR	Q system
Characterisation	Jointing patterns described except anisotropic rock	Discontinuity mechanical properties In-situ stresses
Project purpose	Orientation with respect to axis structure Bolt lengths are easily determined Stand-up time (conservative) Not helpful to choose excavation method	Not relevant to orientation Bolt length are usually inaccurate Easily choose roof support Helpful to choose excavation method
Empirical relations	RMR, strength and deformability parameters	Q, physical and mechanical parameters

Source: Jean et al. (2003)

The Geological Strength Index (GSI) is another method to classify rock in the field except intact rock, sparsely jointed rock, waste rock, broken or transported material and soils (Hoek, 2016). Similarly, classification based on the GSI is rather subjective. The index considers the intrinsic characteristics of the rock mass (Hoek et al., 1995), incorporates the excavation and condition of jointing characteristics (Kanji, 2014; Marinos, 2014) and in-situ stress conditions, discontinuities and groundwater (Russo et al., 1998). The chart (Figure 3-21) is a handy tool from which a suitable value of undisturbed rock strength can be selected quickly in the field although its use may be imprecise owing to variations in observation, interpretation and blasting effects (Hoek, 1999). For example, the rock mass could be recorded as very blocky or just blocky, with a thin line differentiating the two distinct structures. GSI values range from 10 for extremely poor rock mass to 100 for intact rock (RTM, 2009). GSI values above 25 correspond to good to reasonable rock mass quality and below 25 corresponds to very poor quality rock mass (Hoek et al., 1995). Hoek (2016) gives reference GSI charts (see Appendix C), for benchmarking in the field, which classify different rocks in terms of their GSI rating and a corresponding shear strength envelope for the rocks.

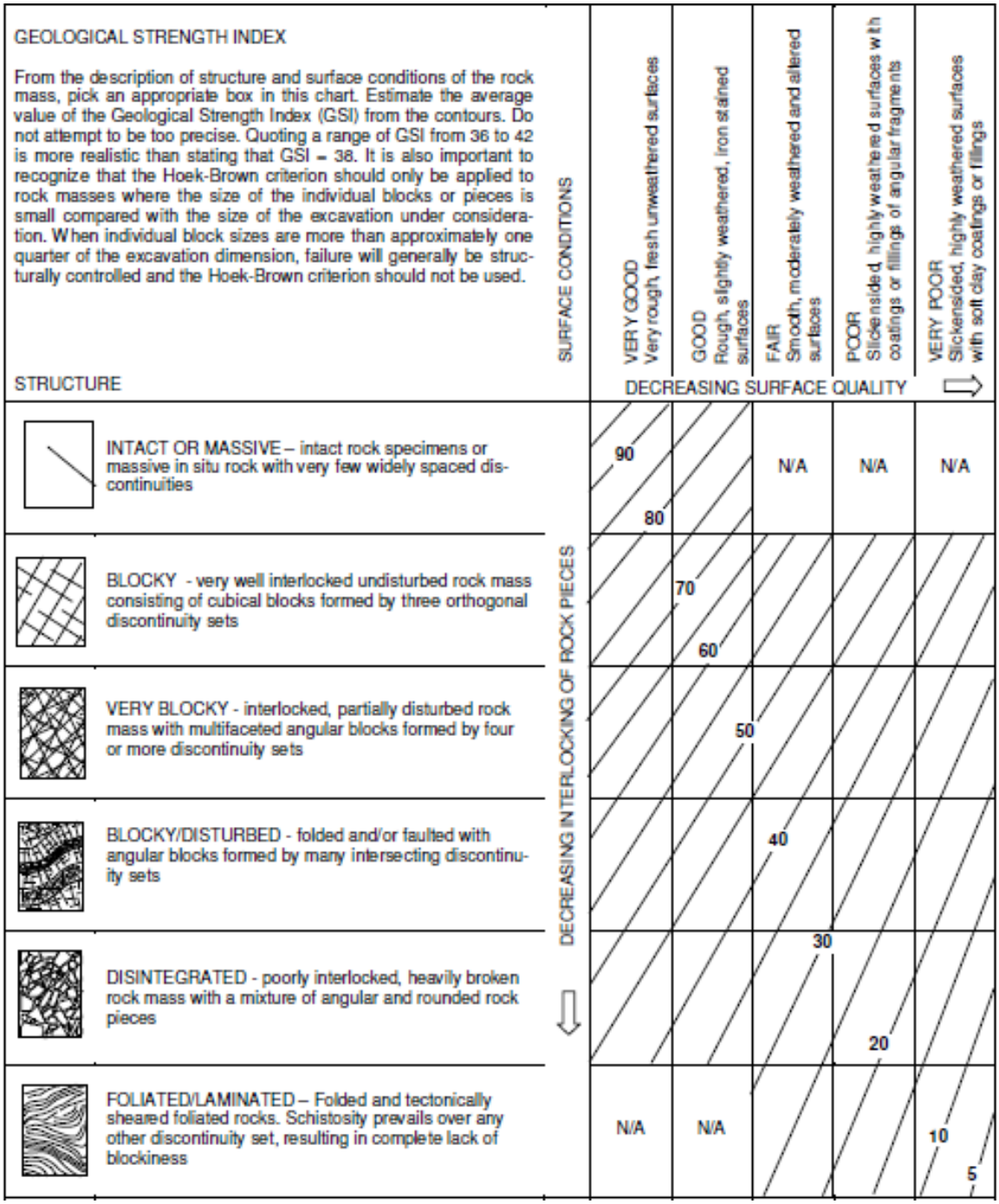

Figure 3-21: Geological Strength Index (GSI) chart
Source: Hoek (1999)

Rock competency and alteration (rock as a continuum material)

The competency factor of the rock mass is the ratio of the magnitude of the compressive strength to its in-situ stress which also indicates the extent of squeezing for the rock mass (Yavuz, 2006). The extent of stress redistribution depends on the UCS of rock and initial state of stress which increases after excavation (Marie, 1998). Therefore, competency directly influences stress redistribution during excavation which affects stability and integrity of the tunneling process. Based on competency, rock conditions are assigned a single value from 1 to

5 corresponding with five natural categories (Wahlstrom, 1973). Conditions range from original or intact, fault zones, joints and rock alterations. The five rock categories corresponding to the numerals 1 to 5 are highly competent, moderately competent, marginal, moderately incompetent and highly incompetent with a scale varying from 1 to 5. The value chosen should be the most representative state of the material and not an average intermediate state.

Rock alteration is an important factor in tunneling because it directly distinguishes between various rock materials in terms of strength, hardness, resistance to cutting and the extent of cavities. At the bottom scale of the continuum, rock is completely degenerated into soil, the material is soft, of low strength, comprises various cavities and has squeezing challenges which makes it is difficult to balance the excavation during tunnel construction. At the top of the continuum where rock is fresh and intact, the ability to support engineering loads is good and important. However, the rate of tunneling and tunnel advance is slow because of the rock hardness which also lead to high wear costs. Therefore, it is important to understand and correctly characterize the rock to plan the costs, limit project escalations as well as to select appropriate tools and construction methods. Rock can be classified ranging from the lowest to the highest in terms of UCS based on the position on a continuum scale (Figure 3-22). The chart generally separates the ground material as soil, soft rock and hard rock with the broken vertical line distinguishing between soft and hard rock (Kanji, 2014). However, the ground varies widely with depth between differing subsoil types to highly fractured weak weathered rock and finally to massive strong rock (TLDG, 2004). Furthermore, the disparities between soil and rock are generally quantitative rather than qualitative.

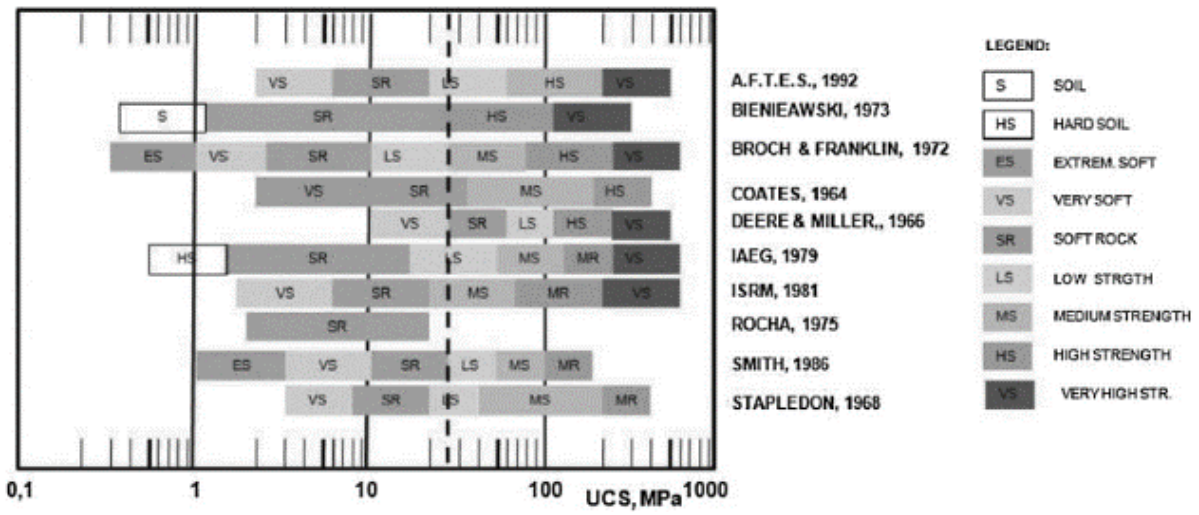

Figure 3-22: Rock continuum scale
Source: Adapted from Kanji (2014)

3.3.3.2. Qualitative rock mass classification systems

Terzaghi's rock load classification method

Traditional classification systems using steel sets mainly highlight provision of support to loads but modern tunneling methods are flexible and emphasize ground-rock interaction systems using mostly shotcrete and rock bolts (RTM, 2009). The load concept is still applied especially in the initial stages of project design but is too general for tunneling applications (Jauch, 2000). The rock mass conditions are classified in nine categories which are more detailed descriptions compared to the five commonly known rock classes. The associated descriptions include: Hard and intact rock (class I), hard stratified rock or schistose (class II), massive moderately jointed rock (class III), moderately blocky and seamy rock (class IV), very blocky and seamy rock (class V), completely crushed but chemically intact sand and gravel rock (class VI), squeezing rock, moderate depth (class VII), squeezing rock, moderate depth (class VIII) and swelling rock (class IX).

Lauffer's stand-up time

In this method, the relationship between stand-up time and unsupported span is not constant but varies depending on orientation of the tunnel axis, tunnel shape, excavation and support method. Seven rock classes in terms of stability are described in this system based on stand-up time as a function of rock mass quality for an unsupported tunnel. Stable (class A), brittle (class B), very brittle (class C), fractured (class D), very fractured (class E), squeezing (class F) and highly squeezing (class G). However, this method is very conservative for modern applications (Jauch, 2000).

Rock structure rating

Rock Structure Rating (RSR) uses a numerical approach to describe the rock mass quality and design support. RSR is the arithmetic sum of their weighted numerical values and range from a minimum of 19 for the worst conditions to a maximum of 100 for the best conditions (Jauch, 2000). It considers two main factors comprising geological and construction parameters. Geological parameters comprise rock type, joint pattern, joint orientations, discontinuity types, major faults, shears, and folds, material properties and weathering/alteration. Construction parameters comprise tunnel dimensions, direction of drive and method of excavation. All factors are clustered into three broader categories A, B and C. Factor A is a general appraisal of the rock structure, B is the effect of discontinuity pattern with respect to the direction of tunnel drive and C is the effect of groundwater inflow. However, according to Jauch (2000) the RSR application involves subjective judgement of these three factors and as a result is imprecise.

Size-Strength

The Size-Strength method is a two-parameter (intact rock strength and spacing of discontinuities) classification procedure based on block sizes on a macroscopic scale. The measured block size is correlated with the point load test measurements on a logarithmic scale to classify the rock. It is mostly applied during planning, subsequent daily designs of

underground excavations and ground control systems. However, the method is seldom used because it ignores the influence of joints (Jauch, 2000).

Basic geotechnical description

The method was developed by the International Society for Rock Mechanics (ISRM) to simplify and standardize rock characterization and classification using agreed intervals, terminology and symbols. Information obtained from observed outcrops, trenches, adits[12] or boreholes is included in the logs, maps and geological sections using standard identification terms and symbols to categorize the rock mass. Some Basic Geotechnical Description (BGD) standard intervals are correlated with numerical values for better practical application and then incorporated within the RMR system. However, the BGD is more a rating of rock material properties than the rock mass itself, therefore, it is not exhaustive (Jauch, 2000).

Unified rock classification system

The unified rock classification system (URCS) method developed rock clusters such that only important parameters are described and the number of symbols are minimized by using four-letter notations. Each letter represents a physical property. The properties include weathering, strength, discontinuities and densities estimated in the field using fingers, hand lens, ball peen hammer, a spring-loaded scale and a bucket of water exhaustive (Jauch, 2000). Each property is divided into five ratings which convey uniform meaning to engineering geologists, design engineers, inspectors and contractors. The notation AAAA indicates the best rock conditions (no support). The notation EEEE indicates the worst rock conditions. Like the BGD, this method only gives a rating of single rock properties but it is also not exhaustive.

3.4 Tunnel stability

Response effects cause strain and further ground stress which result in force redistribution and new surcharge forces. For instance, strains from a finite element analysis result indicate the possible squeezing potential (Mohammed, 2015). Notably, information on geology and ground responses to the loads imposed helps to guide the design of optimal supports for stability (Amadei & Stephansson, 1997).

3.4.1 Factors influencing stability

Stability of tunnel infrastructure depends on the rock conditions, material properties, residual strength, burial depth of the tunnel, and both the disturbance factor and tunnel diameter associated with the excavation process (Hochella et al., 1989). Main properties include Poisson's ratio, Young's modulus, shear modulus and stiffness which influence the magnitude of stresses and deformations (Greer, 2012). Poisson's ratio, ν is related to the coefficient of lateral earth pressure, K_o at rest. K_o defines the initial undisturbed stress conditions of the rock mass at rest along a plane strain as $\nu = K_o/(1+K_o)$. Also, the angle of internal friction, ϕ and K_o

[12] Small sized tunnel constructed specifically to provide access to a main project tunnel and it can be sealed off once access is no longer required.

are related: $K_o = 1-\sin\phi$. At rest, $\phi = 44^o$ hence typical values of K_o and ν are 0.35 and 0.25, respectively (Yavuz, 2006; Kim & Yoo, 2002). At shallow depths, the ground stress is a function of the burial depth such that the horizontal field stress is a product of the overburden mass or unit weight of the material and acceleration due to gravity. In other words, in-situ stresses are related to the cover depth over the tunnel sections (Perri, 2007). In blocky and jointed rock mass, stability problems are associated with gravity falls of wedges from the roof and sidewalls. This is because weak shear planes exist along various rock discontinuities without significant confinement to control crack propagation (Mohammed, 2015). At greater depths, the rock confinement is significant so that the ground stresses contribute towards stability of the structures (Greer, 2012). Figure 3-23 is a schematic illustration of the field stresses surrounding an excavation at depth. In the figure, a rock element is further isolated to indicate the stress orientations on the ground.

Conventionally, compressive stresses are positive and tensile stresses are negative. Three principal ground stresses denoted as σ_1, σ_2 and σ_3, in ascending order of magnitude exist and excavation cause stress redistribution. σ_1 is the major principal stress thereby the largest compressive stress while σ_3 is the minor principal stress thereby the least compressive stress and largest tensile stress (Hoek, 2016). Values of the stresses are determined from a triaxial test and the difference between σ_1 and σ_3 is the deviator stress.

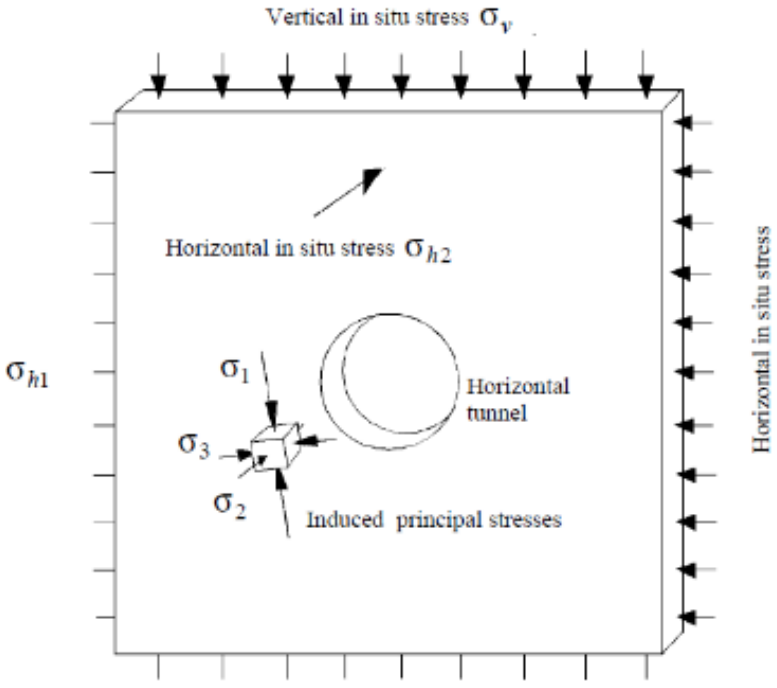

Figure 3-23: Stresses surrounding an excavation
Source: Hoek et al. (1995)

Field stresses at depth confine structures thus provide stability to a certain degree. Figure 3-24 illustrates how burial depth affects stability: (a) The excavation is closer to the surface and has a significant zone of tensile and shear failure, (b) shows a relatively reduced failure zone as the excavation is farther from the surface, and (c) has a significantly small failure zone as it is buried farther inside the ground. At significant burial depths, any resulting failure including

major rock bursts or popping, sliding, spalling and slabbing is induced (Mohammed, 2015; Hoek et al., 1995). Spalling or slabbing are minor forms of induced stress failure in the rock mass whose induced failure potential can be estimated from the Strength Factor (SF). SF against shear failure is = $(\sigma_{1f} - \sigma_3) / (\sigma_1 - \sigma_3)$, where $(\sigma_{1f} - \sigma_3)$ is the strength of the rock mass and $(\sigma_1 - \sigma_3)$ is the induced/deviator stress, σ_1 and σ_3 are major and minor principal stresses, and σ_{1f} is a major principal stress at failure. A SF greater than 1.0 indicates that the rock mass strength is greater than the induced stress, meaning that there is no overstress in the rock mass (Greer, 2012). When SF is less than 1.0, the induced stresses are greater than the rock mass strength; the rock mass is overstressed and likely to behave in the plastic range.

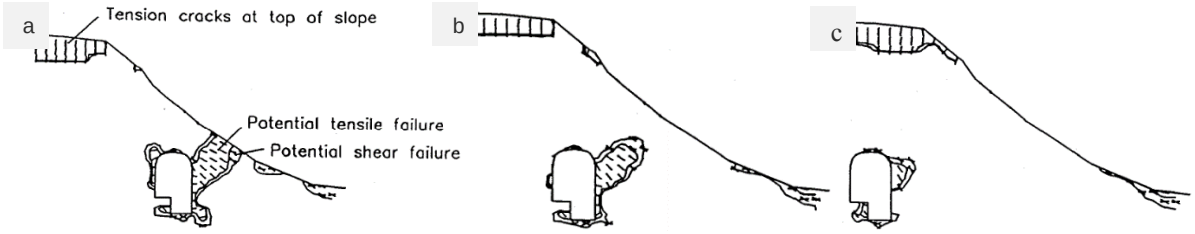

Figure 3-24: Confining stresses at varying depths from the surface
Source: Hoek et al. (1995)

Typically, discontinuities control the stability of rock masses such that even at great depths, if discontinuities are many they can induce failure along the various planes of weaknesses. Figure 3-25 is a diagram which illustrates potential unstable wedges isolated along discontinuities in the surrounding rock mass of a tunnel. Unstable roof wedges usually fail by collapse, sidewall wedges fail by either sliding or displacement and floor wedges fail by bottom heaving (Hemphill, 2012; Hoek et al., 1995; Kang & Lu, 1991). The system of weak planes collectively constitutes the failure mechanism. It is imperative to understand the possible failure mechanisms by determining the number, orientations and conditions of the joints because joints are significant features of a discontinuity system (Mohammed, 2015). Thus, to understand the potential failure mechanisms, the discontinuity system is characterized and its geometric parameters described in detail including a determination of the joint numbers, pattern, spacing, thicknesses, material infilling, roughness, alteration, stress and water condition (Greer, 2012; Palmström, 1995). A good understanding of the failure mechanism and characteristics of the discontinuity system is essential to deal with stability issues in discontinuous rock masses (Mohammed, 2015; Palmström, 1995).

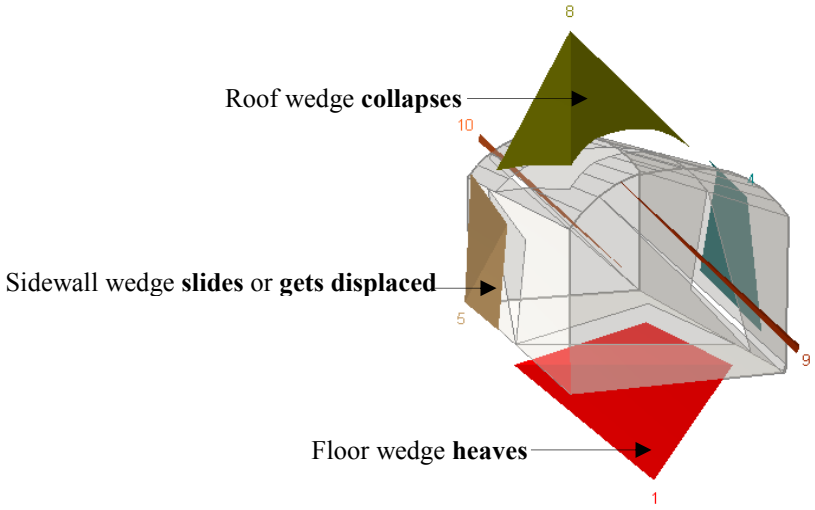

Figure 3-25: Unstable wedges
Source: Rocscience (2016) and Wahlstrom (1973)

3.4.2 Structurally controlled rock mass stability

The overall state of a rock mass is generally controlled by discontinuities (Hoek, 2014; Greer, 2012). The main discontinuous structural features which separate rock masses into discrete but interlocked isolated wedge pieces are bedding planes and joints (Hoek, 2014; Hoek et al., 1995). When a rock mass is excavated a free wedge face is created. The wedge is free from restraint of the surrounding rock. Thus, the confining stress which once contributed towards the stability of the wedge is removed thereby making it susceptible to collapse or sliding. Wedges fail by collapse from the roof (also called gravity falls), they are displaced and caused to slide out of the sidewalls along the weak shear planes of the discontinuities depending on the behavioural properties of the plane (Hochella et al., 1989). The process unravels into further wedges if left unsupported until a natural arching in the rock prevents further propagation of the problem or the cavern is filled with loose wedges (Mohammed, 2015). As wedges fall or slide out of position, the overall restraint and interlocking of the rock mass is reduced hence stability is minimized. Sliding may occur when the free wedge face is exposed and the adjoining faces are free to move because of induced strains (Hoek, 2014). Shear sliding planes are usually separations of adjoining wedge faces along joints. When the joint separation is not decisive, cohesion and friction along the plane are important and the shear strength of the joint is given by Equation 3-8. Other consideration factors include; Groundwater, ground stresses and strains and the methods of loading (Greer, 2012). Methods of loading include: Groundwater, ground stresses and strains, short-time static loading, long-time static loading, repeated loading, dynamic loading and quasi-static loading (Hoek, 1977). Failure occurs when the material properties are too weak to resist the forces causing displacement (Hemphill, 2012; Greer, 2012; Hoek, 1993). Theories such as Hooke's law which is a linear theory of elasticity are applied to check instability associated with sliding (Mohammed, 2015; Hoek, 2014).

$$\tau = \sigma_n \tan\phi + c$$ **Equation 3-8**

where τ is the shear strength, σ_n is the normal stress, ϕ is the angle of internal friction and c is the cohesion.

Analysis of structurally controlled instability begins with modelling the problem. Stereographic plots are drawn indicating the average dip and dip direction of significant discontinuity sets such as joints (Hoek, 1993). The structural data is obtained from borehole logs and pilot tunnel mapping (Hoek, 1977). Figure 3-26 illustrates how a stereo net is developed. The stereo net is an equal area lower hemisphere plot of the three discontinuity sets including a tunnel axis plunge marked with a cross. Using computer software packages such as UNWEDGE by Rocscience (2016), unstable wedges are identified, their properties measured and scaled to represent the field situation. For collapsing wedges, essential properties include the weight, size and actual shape whereas for sliding wedges material behaviour and properties such as the Young's modulus, Poisson's ratio, elasticity and joint infilling are important (Greer, 2012). The wedge parameters are used to calculate the factor of safety against failure. Independent factors of safety are calculated for each wedge in line with the mode of failure. An appropriate reinforcement system is designed for the rock mass considering each unstable wedge comprising the general rock instability issues (Mohammed, 2015; Hoek, 1977).

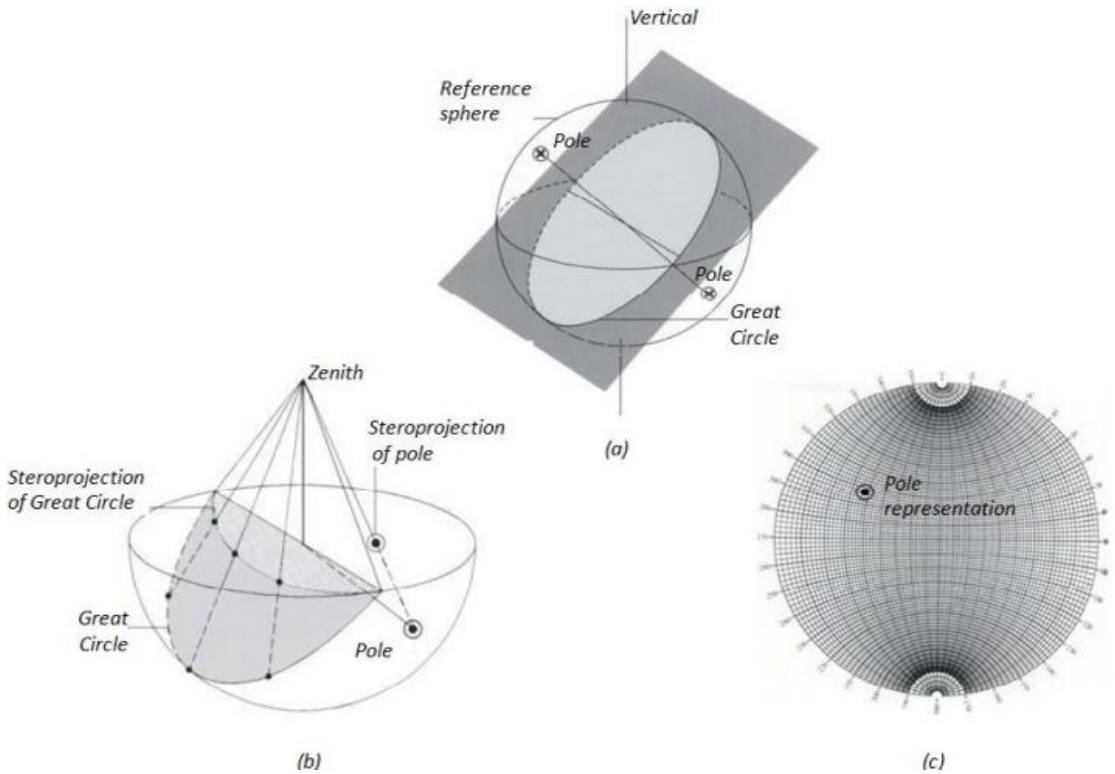

Figure 3-26: Stereographic projection of a pole (a) Reference sphere, (b) Hemispherical projection, (c) Stereo net
Source: Torres (2008) after Brady & Brown (2004)

Near the surface, tunnel instabilities mostly occur during construction (Hemphill, 2012). Mechanical excavation by boring or drilling and blasting produces significant impact in the ground. The resulting tremors and vibrations from the ground beneath are usually felt at the surface. The magnitude of vibration, tremors and impact at the surface depend on the depth of burial. The rock overburden acts as a buffer which dampens the effect of operations in the ground (Hoek, 2014). However, some surface interaction effects from underground excavations are delayed failures. For example, small scale deep-seated movements and hydrostatic pressure build-ups in the overburden eventually cause subsidence at the surface after prolonged periods of escalation and crack propagation (Hustrulid, 2000). Tunnels failures and effects of failure visible at the surface are referred to as daylight collapse (Sousa, 2010). Therefore, precaution should be taken to keep the effect of construction at a minimum to avoid surface interruptions, immediate and delayed failures (Hoek, 1993).

3.4.3 Stability during excavation, the plastic zone and limiting equilibrium

Prior to excavation, the ground is generally stable (Yavuz, 2006; Stegner, 1971). The vertical gravity load is equal to the weight of the overburden rock mass, circumferential stress at the tunnel wall is approximately twice that existing prior to excavating and radial stress equals zero (Bickel et al., 1996). In-situ stresses increase after excavation thereby causing tunnel walls to fail (Hoek, 2014). Excavation removes the restraint thereby loosening the surrounding rock. It also causes stress relaxation, stress redistribution, introduces new fractures and further widens existing ones if not properly controlled thereby influencing instability (Hoek et al., 1995). The extent and height of loosening depends on the ratio between joint spacing and excavation span but it is controlled by the spacing of the joints and material shear strength (Mohammed, 2015; Tsesarsky & Hatzor, 2005). According to ITA (2009) and Hoek et al. (1995), control of the excavation process is best achieved using the Sequential Excavation Method (SEM) or New Austrian Tunneling Method (NATM). The extent and timing of instability depends on geology, stand-up time, critical areas to support and the maximum unsupported span[13] of the tunnel (Hoek, 1993). Figure 3-27 shows approximate stand-up times based on the tunnel roof span and RMR. According to Bieniawski (1992), a 13 m span tunnel has an average rock stand-up time approximately 10^3 hours which is equivalent to about 41 calendar days. The maximum unsupported span can be calculated using Equation 3-9 from the Excavation Support Ratio (ESR) and the Q-index.

$$Maximum\ unsupported\ span = 2\mathrm{ESRQ}^{0.4} \qquad \textbf{Equation 3-9}$$

Tunnel deformations from forces surrounding the plastic zone of the rock mass progressively increase until excavation is completed as illustrated in Figure 3-28 (a) and (b). The stability of excavations is evaluated by limit equilibrium analyses based on failure criterion and related theory. At the point of limiting equilibrium/tunnel failure ($P_i < P_{cr}$) the critical pressure, P_{cr} at which the surrounding rock mass fails with no volume change in the plastic zone is calculated from Equation 3-10 and the corresponding plastic zone radius, r_p and radial plastic

[13] Maximum unsupported span is the distance between the excavated face and the nearest tunnel support.

displacement, u_{ip} of the tunnel side walls are given by Equation 3-11 and Equation 3-12, respectively. For stability ($P_i > P_{cr}$), the surrounding rock mass only undergoes elastic deformation and the inward radial elastic displacement of the tunnel sidewall, u_{ie} is given by Equation 3-13.

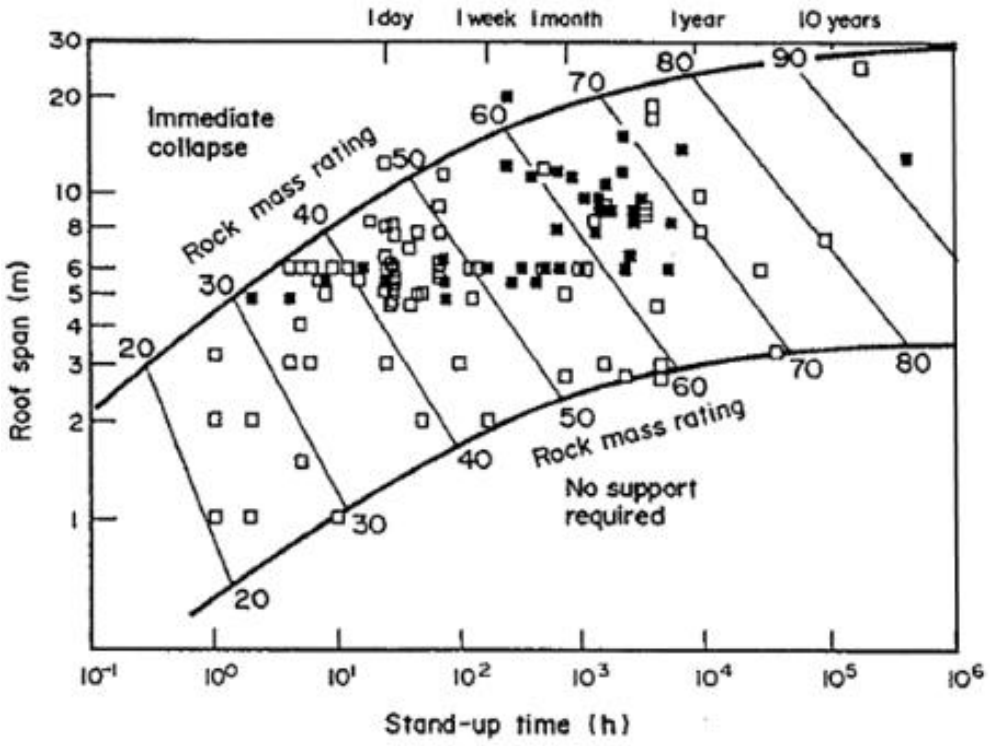

Figure 3-27: Approximate rock stand-up times
Source: Bieniawski (1992)

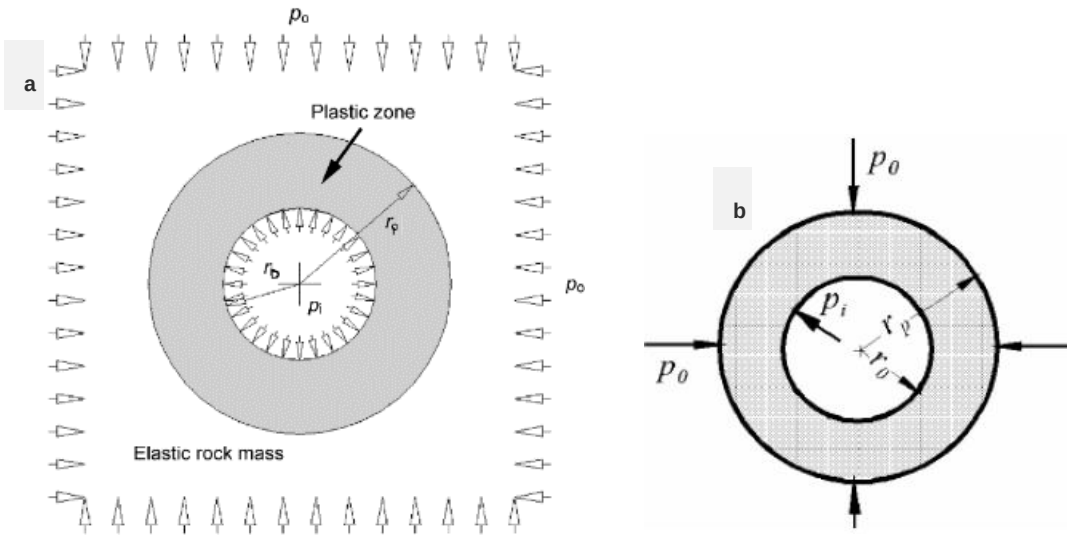

Figure 3-28: (a) Elasto-plastic zone stresses in rock mass and (b) surrounding stresses
Source: (a) Adapted from TLDG (2004) and (b) Mohammed (2015)
where r_o is the circular tunnel radius, r_p is the plastic zone radius, P_i is the support pressure and P_o are the horizontal and vertical stresses considering lithostatic conditions acting at depth

$P_{cr} = (2P_o - \sigma_{cm})/(1 + k)$ *where the coefficient of lateral earth pressure,* $k = \frac{1+\sin\phi}{1-\sin\phi}$

Equation 3-10

and σ_{cm} is the rock mass compressive strength

Equation 3-11

$$r_p = r_o\left[\frac{2(P_o(k-1)+\sigma_{cm})}{(1+k)((k-1)P_i+\sigma_{cm})}\right]^{(1/(k-1))}$$

Equation 3-12

$$u_{ip} = \left(\frac{r_o(1+v)}{\varepsilon_m}\right)\left[2(1-v)(P_o - P_{cr})\left(\frac{r_p}{r_o}\right)^2 - (1-2v)(P_o - P_i)\right]$$

where ε_m is the Young's modulus or deformation modulus and ν is the Poisson's ratio

Equation 3-13

$$u_{ie} = \left[\frac{r_o\,(1+v)}{\varepsilon_m}\right](P_o - P_i)$$

3.5 Rock loads

This section discusses the main loads associated with hydro rock tunnels. According to the Road Tunnel Manual (2009), the ground response to excavation is expressed in terms of measured stresses, deformations and strains. Usually, stresses are most significant and responsible for tunnel failure. Studies of rock bursts by Durrheim et al. (1998) showed that in-situ stresses are very significant and can reach high values of 1.8 for the k-ratios. As such, conservative approaches which assume 0.5 as the k factor with its corresponding overburden are often inaccurate. Rock stresses are usually pressures expressed in kPa units and they can also be called rock loads (Hoek, 1993). Marie (1998) notes that rock loads surrounding a tunnel are generally under triaxial compression. Figure 3-29 shows a line diagram of forces and

Figure 3-30 illustrates how the rock loads are distributed and supported for a tunnel at depth. The weight of rock enclosed in cdd_1c_1 is transferred by the system of rock bolts from the tunnel roof to the floor where it is supported (Terzaghi, 1946).

In addition to the gravitational weight of wedges, tunnel loads include contact grouting pressures, thermal stresses, groundwater pressure and creep. The overburden weight of wedges, grouting and groundwater pressures induces stresses which cause failure by gravity falls. Generally, the overburden weight increases with cavern width (Marston & Anderson, 1913). The weight of rock and water above the tunnel significantly resist deformations whereas the friction effects of overlying natural materials are insignificant. On the other hand, thermal stresses and creep cause deformation and strain in the rock (Hoek, 2014).

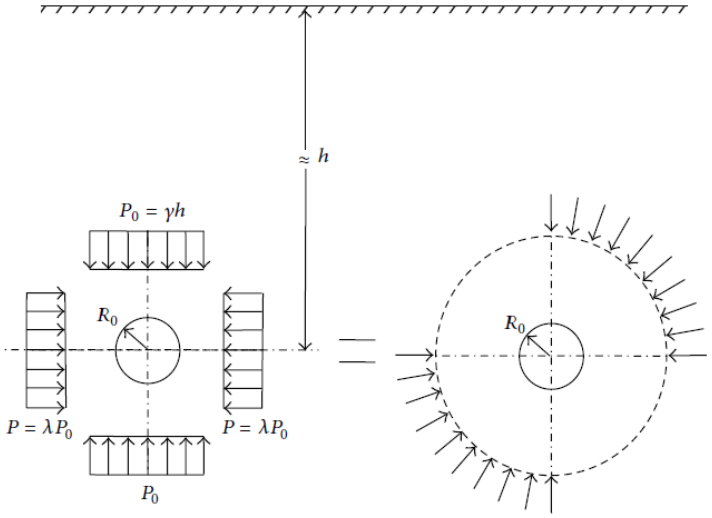

Figure 3-29: Line diagram showing forces on a tunnel at depth
Source: Zhang et al., (2015)

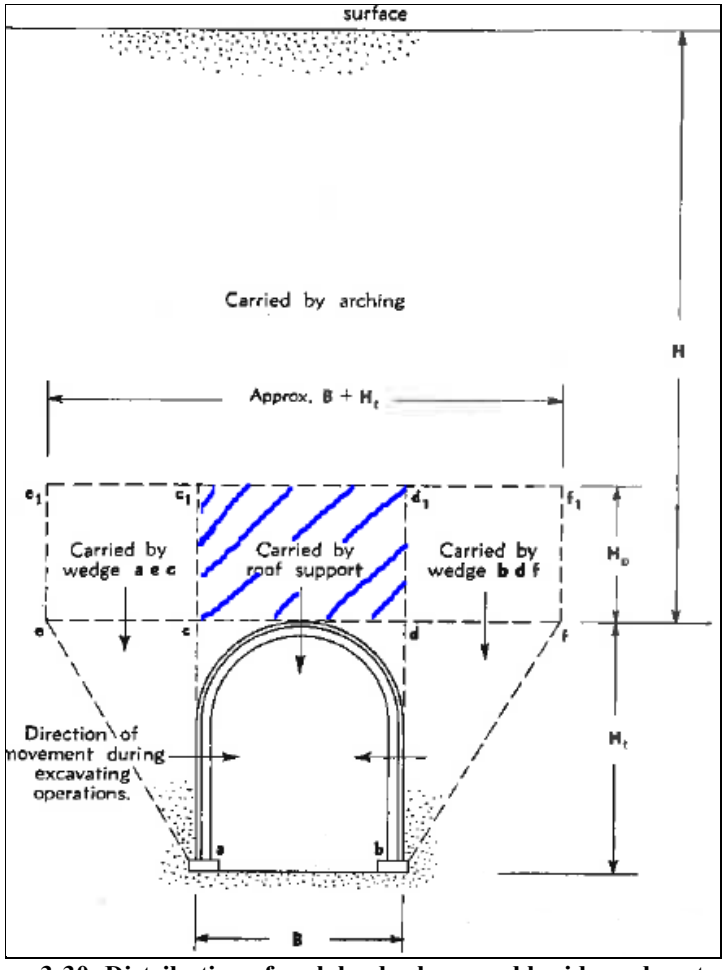

Figure 3-30: Distribution of rock loads above and besides a deep tunnel
Source: Adapted from Terzaghi (1946)

Other forces experienced by the tunnel include the self-weight of materials, upthrust, external pore pressures and an internal pressurized system (Hemphill, 2012; Hoek, 1993). Underground hydro tunnels are generally pressurized gravity tunnels whose flow approximates open channel flows (USACE, 1997). The water is pressurized due to the high velocities necessary to drive the turbines, its flow is aided by gravitational forces and approximates open channel flows because the rate of flow into the tunnel structure is less than the capacity of the open channel. From the open channel river flow, boulder suspensions and other matter cause drag and friction at the tunnel surfaces. Figure 3-31 is a longitudinal schematic illustration by CIRIA C683 (2006) which shows the internal processes and loads that an operational hydropower tunnel is subjected to during its operations.

Variable tunnel loads, that are indispensable in designing the lining, include earthquakes, transient water waves such as the water hammer, blast loads and the hydrostatic pressure (Hoek, 1977). According to RTM (2009), hydrostatic pressure load of water acts normal to the tunnel surface and it is obtained by dividing the load of water by the external hydrostatic pressure. Both the maximum observed level of the groundwater and the level one meter above the 200-year flood level are considered. The maximum groundwater level observed is considered at its normal level.

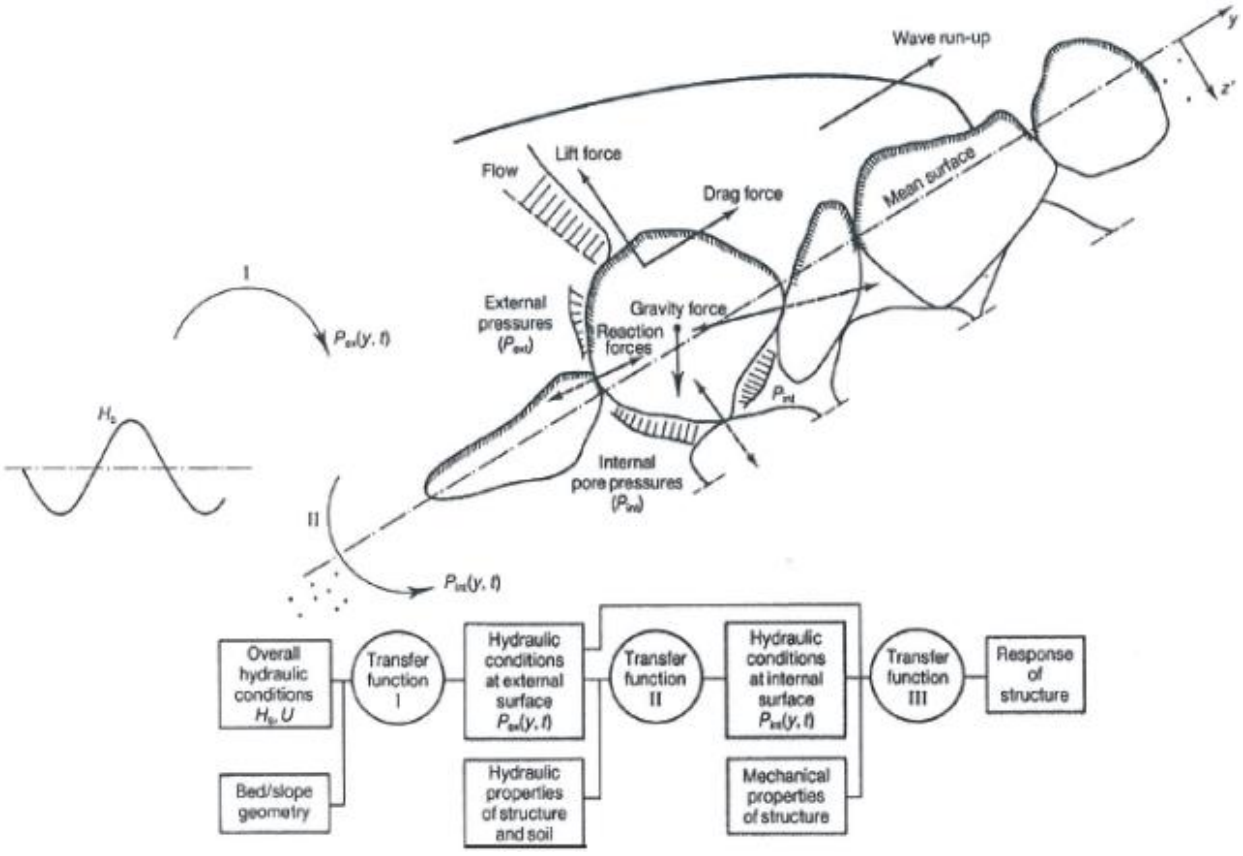

Figure 3-31: Hydraulic and structural responses
Source: CIRIA C683 (2006)

3.5.1 Tunnel failure

Tunnel walls fail in compression when the support system capacities are inadequate to support the loads (Zhang et al., 2015; Marie, 1998). Rock loads significantly influence field stress and its redistribution. Stresses in the plastic zone are considered instead of elastic zone stresses because material bonds are altered and the residual strength is retained which enhances overall stability (Iowa, 2014). However, rocks deform by physical expansion, stress dilatancy and structurally as a result of displacement and collapse of the wedges or blocks along discontinuities (Wang et al, 2014). The magnitude of complex nonlinear rock deformation depends on inherent material properties (He, 2014). According to Yoshinaka & Nishimaki (1981), the extent is indicated by strain softening and nonlinear failure envelopes. Failure occurs because of weak strata, discontinuities, in-situ stress, displacement, unsupported excavation, uncoupling of support systems and deep-seated deformation (Zhang et al., 2015; He, 2014). Rock failure in form of rock bursts, slip or rotation may occur depending on the unique rock features, geological structures and external factors (as illustrated in Table 3-9). Rock bursts, slip and rotation follow wedge, planar and overturning failure mechanisms, respectively (Thomas-Lepine, 2012).

Table 3-9: Ultimate limit state rock failure

Type	Failure mechanism
Collapse	Rock slope instability / wedge failure
Sliding	Wedge failure / displacement
Heaving	Expansion and strain softening
Bearing capacity	Shear
Rock bursts	Shear or splitting
Wall failure and floating	Shear

Source: Ongodia et al. (2016) after Viggiani (2012)

According to Hoek at al. (1995) and Mohammed (2015), wedge collapses and sliding are common but heaving of the bottom wedges is a rare condition. In contrast, other researchers indicate otherwise (Li et al., 2005; Liu & Zhang 2003; Kang & Lu 1991). Yu et al. (2012) stated that at greater depths exceeding the critical depth deformation in the tunnel roof, sidewall and floor increases significantly, especially floor heaving, which occurs in squeezing and swelling ground. Although the term great depth is commonly referred to in tunneling, its actual definition in terms of the distance below the ground surface is imprecise. Perri (2007) defines the shallow depth to be a distance less than b(50/GSI) and deep excavations as a distance greater than b(GSI/5). On the other hand, Terzaghi (1946) suggests that 10,606 m below the existing ground level is a critical burial depth while Marie (1998) suggests that critical depths as that of 600 m and 5800 m for soft and hard rock, respectively. Figure 3-32 (A) illustrates external conditions influencing rock bursts: (a) significant overburden in a deep tunnel, (b) residual stresses, (c) forces causing elastic strain and (d) ground squeezing. Residual stresses are naturally a result of geological processes of formation such as igneous dike intrusion, increase with depth, influence on large deformations and surrounding rock mass failure when

in-situ stress magnitudes are large (Yu et al., 2012). Ground squeezing can be initiated from peripheral cracks associated with blasting operations. Figure 3-32 (B) shows how rock fractures vary from (a) conjugate shear, (b) multiple conjugate shear, (c) longitudinal tension or lateral extension and (d) extension fracture on a small scale when uniaxial stresses are applied. On the other hand, Table 3-10 shows types of failure in different rock masses and stresses.

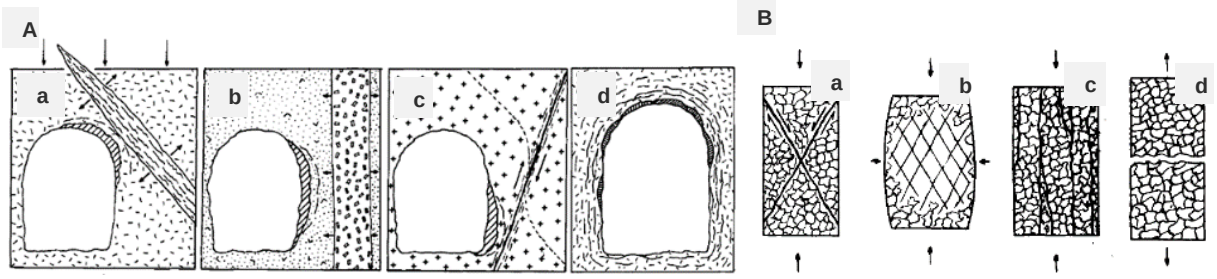

Figure 3-32: (A) Conditions influencing rock bursts (B) Common types of fractures
Source: Wahlstrom (1973)

3.5.2 Failure criterion

The stability of excavations is evaluated by limit equilibrium analyses based on failure criteria and related theory. The common methods are the Mohr-Coulomb and Hoek-Brown failure criteria, a linear and non-linear relationship, respectively (Hoek et al., 1995; Hoek,1993). Generally, the Hoek-Brown method for jointed rock masses is the most preferred for underground engineering applications. The method gives the best approximation of jointed rock material characteristics (Greer, 2012). It is also an empirical method which was developed from theoretical results, model studies, and data from tested rock strength. From its practical application Hoek et al. (1995) observed that the method recorded low strength values for tightly interlocked undisturbed rock masses surrounding tunnels. Thus, it is limited in tunnel applications but suitable for rock mass conditions approximating isotropic behaviour and for significantly large engineering structures. The criterion was generalized (Equation 3-14) to simplify its application in geotechnical analyses (Hoek et al., 1995).

Equation 3-14

$$\sigma_1' = \sigma_3' + \sigma_{ci}\left(m_b\left(\frac{\sigma_3'}{\sigma_{ci}}\right) + s\right)^a$$

where σ_1' and σ_3' are major and minor effective principal stresses at failure, σ_{ci} is the UCS for the intact rock pieces, s and a are rock mass characteristic constants and m_b is the Hoek-Brown rock mass constant

At plastic failure, the major and minor principal stresses are linearly related ($\sigma'_1 = k\sigma'_3 + \sigma_{cm}$), where σ_{cm} is the UCS of the rock mass defined by Equation 3-15 and *k* is the slope of the σ'_1-σ'_3 stress curve defined by Equation 3-16. Shear strength parameters can be obtained from Equation 3-17 when they are not determined directly from the laboratory shear box or triaxial tests. Interrelationships between common laboratory tests and the Hoek-Brown equation were developed to quickly assess rock parameters. Parameters such as shear strength, rock mass UCS, σ_{cm} and deformation modulus, E_m can be obtained from the Hoek-Brown equation solved for corresponding GSI range of values, intact rock UCS (σ_{ci}) and material constant (m_i).

Table 3-10: Typical failure in varying rock mass and stress conditions

	Low stress levels	High stress levels
Massive rock	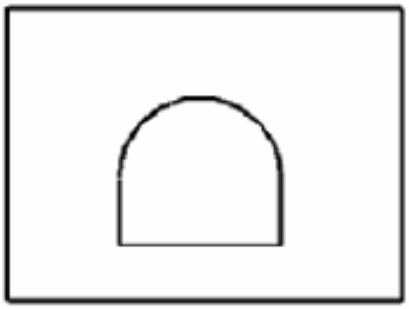 Massive rock subjected to low in-situ stress levels. Linear elastic response with little or no rock failure.	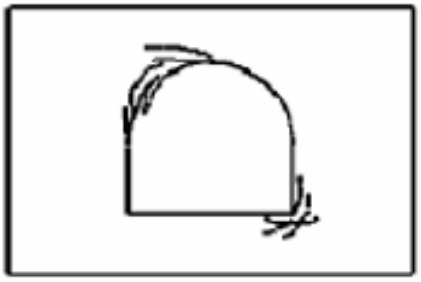 Massive rock subjected to high in-situ stress levels. Spalling, slabbing and crushing initiates at high stress concentration points on the boundary and propagates into the surrounding rock mass.
Jointed rock	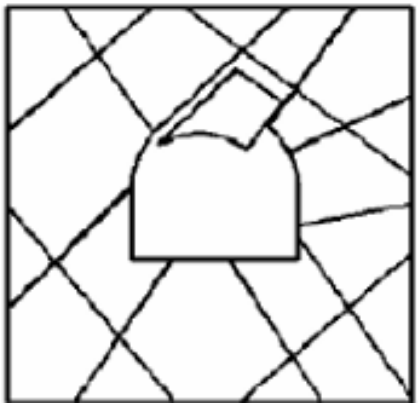 Massive rock, with relatively few discontinuities, subjected to low in-situ stress conditions. Blocks or wedges, released by intersecting discontinuities, fall or slide due to gravity loading.	 Massive rock, with relatively few discontinuities, subjected to high in-situ stress conditions. Failure occurs as a result of sliding on discontinuity surfaces and also by crushing and splitting of rock blocks.
Heavily jointed rock	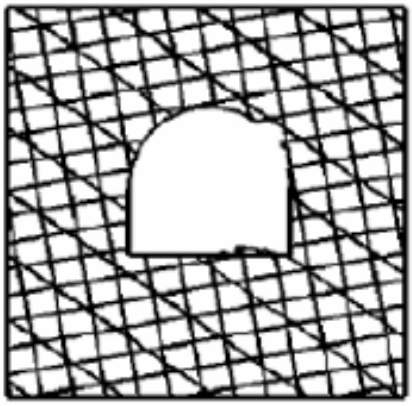 Heavily jointed rock subjected to low in-situ stress conditions. The opening surface fails as a result of unravelling of small interlocking blocks and wedges. Failure can propagate a long way into rock mass if it is not controlled.	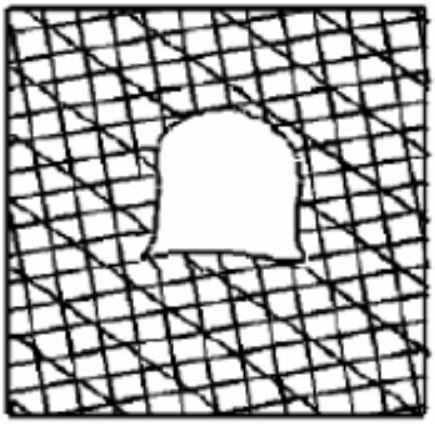 Heavily jointed rock subjected to high in-situ stress conditions. The rock mass surrounding the excavation fails by sliding on discontinuities and crushing of rock pieces. Floor heave and sidewall closure are typical results of this type of failure.

Source: Redrawn after Hoek et al. (1995)

$$\sigma_{cm} = \frac{2c' \cos \phi'}{1 - \sin \phi'}$$ **Equation 3-15**

where c′ and ϕ′ are the effective cohesive strength and angle of friction of the rock

$$k = \frac{1 + \sin\phi}{1 - \sin\phi}$$ **Equation 3-16**

$$\sin \phi' = \frac{k-1}{k+1} \quad \text{and} \quad c' = \frac{\sigma_{cm}(1-\sin\phi')}{2\cos\phi'}$$ **Equation 3-17**

Shear stress and the Hoek-Brown criterion

In the laboratory direct shear test, a normal shear stress is applied to failure but the Hoek-Brown equation uses principal stresses which in turn requires a conversion. For consistency in calculations, Balmer (1952) developed Equation 3-18 and Equation 3-19 to convert the ultimate shear stress at failure into equivalent principal stresses that can be used in the generalized Hoek-Brown equation. Equation 3-20 solves the constant *a* and common fraction in Equation 3-18 and Equation 3-19.

$$\sigma_n' = 0.5(\sigma_1' + \sigma_3') - 0.5(\sigma_1' - \sigma_3')\left(\frac{\frac{\delta\sigma_1'}{\delta\sigma_3'} - 1}{\frac{\delta\sigma_1'}{\delta\sigma_3'} + 1}\right)$$ **Equation 3-18**

where δ = small changes

$$\tau = (\sigma_1' - \sigma_3')\left(\frac{\sqrt{(\delta\sigma_1')/\delta\sigma_3'}}{\delta\sigma_1'/(\delta\sigma_3' + 1)}\right)$$ **Equation 3-19**

$$\textit{where } a = \tfrac{1}{2} + \tfrac{1}{6}(e^{-GSI/15} - e^{-20/3}) \text{ and } \frac{\delta\sigma_1'}{\delta\sigma_3'} = 1 + am_b\left(\frac{m_b\sigma_3'}{\sigma_{ci}+s}\right)^{a-1}$$ **Equation 3-20**

Mohr-Coulomb and Hoek-Brown

The generalized Hoek-Brown equation was translated to an equivalent linear relationship (y = mx + c) for Mohr-Coulomb (Equation 3-21). The relationship was developed from plotting the square of the deviator stress $(\sigma'_1 - \sigma'_3)^2$ on the vertical y-axis against the minor principal stress σ'_3 on the horizontal x-axis, with a slope of $m_i\sigma_{ci}$ and a y-intercept of $s\sigma_{ci}$ (Hoek et al., 1995). The slope and y-intercept of the linear equation correspond with the angle of internal friction, φ' and cohesion, c' respectively. φ' and c' are the rock's shear strength parameters which can be easily used to calculate engineering parameters such as bearing capacity. Triaxial tests performed for minor principal stresses ranging between 0 and $0.5\sigma_{ci}$ can be analysed using Equation 3-22 and Equation 3-23. Figure 3-33 illustrates the Mohr–Coulomb and Hoek–Brown interrelationship.

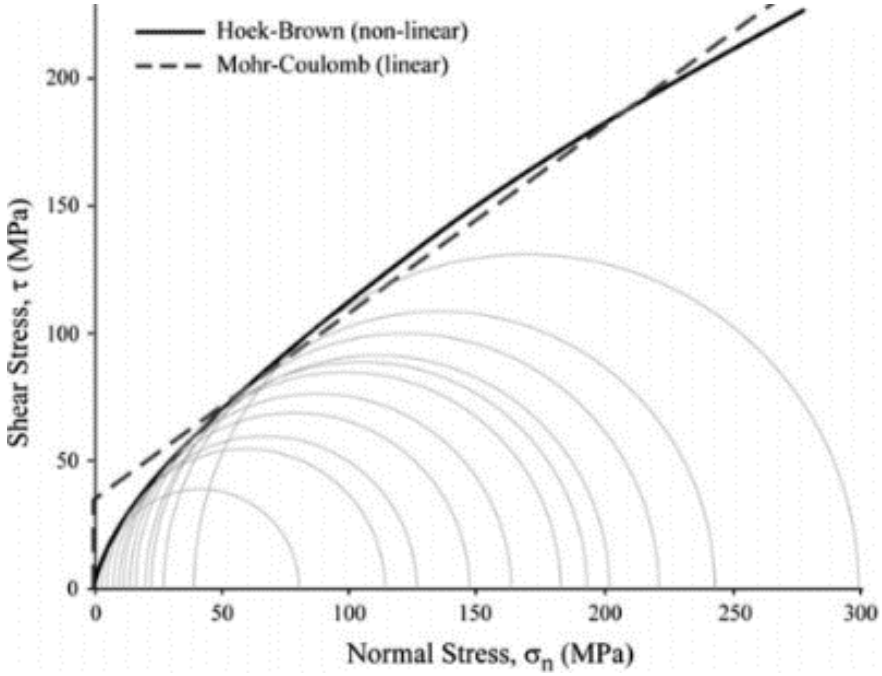

Figure 3-33: Mohr–Coulomb and Hoek–Brown relationship
Source: Eberhardt (2012)

$$y = m_i \sigma_{ci} x + s\sigma_{ci}$$ **Equation 3-21**

where σ_1' and σ_3' are major and minor effective principal stresses at failure, σ_{ci} is the UCS for the intact rock pieces, s and a are rock mass characteristic constants and m_i is the Hoek-Brown rock mass constant for intact rock

$$\sigma_{ci}{}^2 = \left(\frac{\sum y}{n}\right) - \left[\frac{\sum xy - (\sum x \sum y/n)}{\sum x^2 - ((\sum x)^2/n)}\right]\left(\frac{\sum x}{n}\right)$$ **Equation 3-22**

$$m_i = \left(\frac{1}{\sigma_{ci}}\right)\left|\frac{\sum xy - (\sum x \sum y/n)}{\sum x^2 - ((\sum x)^2/n)}\right|$$ **Equation 3-23**

3.6 Rock-Support system structure interactions and mechanisms of support

The surrounding rock mass imposes loads on the tunnel as well as providing its primary support (Bickel et al., 1996). Ground support is provided using individual components which comprise a structural support system to reinforce the ground, prevent deformation of unstable rock wedges and support rock loads (Mohammed, 2015). The appropriate tunnel support method selected depends on the site geomechanical conditions, project contract, contractor expertise, availability of the support members, necessary installation equipment and the cost of the alternatives (Perri, 2007). Rock geology and stand-up time dictate the possible options of temporal or permanent support required to ensure stability of the surrounding rock mass and tunnel structure, either immediately or later. After excavation, sometime is allowed for stress redistribution to occur before highly stiff final support systems are installed to limit the resultant deformations and ensure cost-effectiveness. Inter-relationships between

geomechanical rock properties, applied stresses and necessary support capacities are important and cannot be generalized along the entire tunnel excavation length because rock geology and strength vary (Palmström, 1995). According to Beaver (1972), underestimation of the ground support capacity causes the surrounding rock mass pressures to cave in whereas overestimation forces the excavation outwards thereby crushing the rock mass. Neither of the two scenario is desirable. Therefore, the support capacity should be optimized to avoid buckling when it is underestimated or further fracturing of surrounding rock when the capacity is exaggerated such as hard rock bolts that fail in tension when they are over loaded (Hoek et al., 1995).

The main role and purpose of tunnel support systems is to stabilize the tunnel heading and minimize movements of the surrounding rock mass (Mohammed, 2015). Emphasis is made on the tunnel roof because it generally experiences the peak load (Terzaghi, 1946). The tunnel roof is the most critical area thereby when it cracks, the displacements surrounding the tunnel become much greater so that it becomes an ideal location for installation of most instrumentation (Adhikary & Dyskin, 1997). According to Tsimbaryevitch's theory, loads at the tunnel invert are approximately half of the peak loads experienced at the tunnel roof. In other words, load at the invert = 0.5 $Load_{roof}$ (Nielsen, 2009).

Support systems should be robust and adequate to ensure that the tunnel remains functional, operational and safe in order to minimize impacts and losses from failure (Durrheim et al., 1998; Yu et al, 2012). Thus, the extent of support provided depends on the method of installation and the intended purpose during operations (Zhai et al., 2016). Support on the tunnel can be provided as initial temporary support or final permanent support components. The purpose of initial support is to stabilize the opening to ensure safety before or during construction while permanent support provides structural stability throughout the design life of the structure. Initial support is therefore installed early alongside auxiliary construction measures such as ground improvement, ground reinforcement, dewatering and drainage (Yu et al., 2012). Ground improvement methods include grouting, jet grouting and artificial freezing while ground reinforcement methods use piles, pipe umbrella and face bolts.

Support systems usually comprise rock bolts installed with face plates, wire mesh reinforced shotcrete, steel ribs and lattice girders and a final reinforced concrete lining (Hoek et al., 1995; TLDG, 2004). Either all or some of the components are incorporated depending on the individual unique component's support function. Rock bolts are used for high hazard structures, can be installed prior to excavation where advance support is required as permanent or temporary structures and they experience complex loading mechanisms thus are more susceptible to failure (Hadjigeorgiou, 2016; Zhai et al., 2016). Permanent bolts are installed for periods over two years (Thomas-Lepine, 2012). Figure 3-34 is a schematic representation of a tunnel comprising the different typical tunnel support components. Individual members comprising the tunnel support system are highlighted in the next sub-sections.

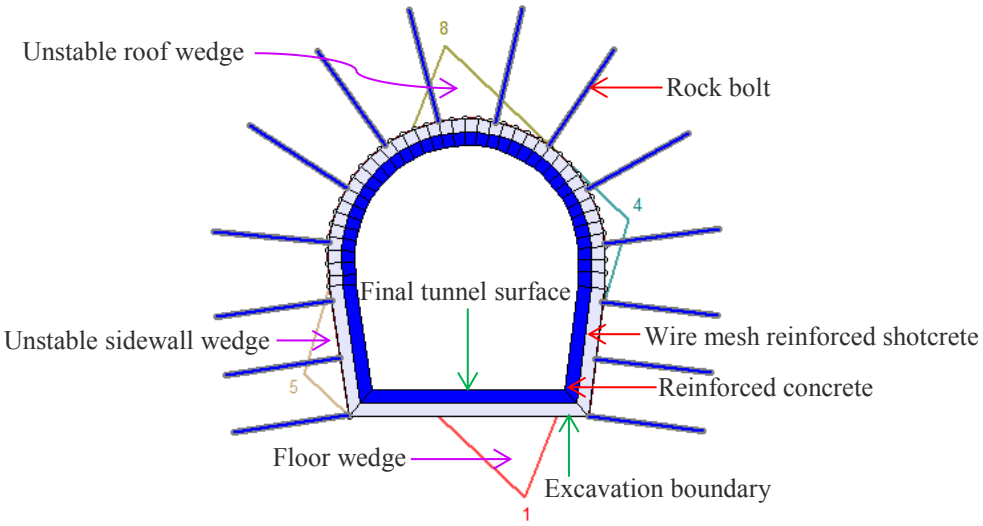

Figure 3-34: Typical tunnel support system components
Source: Adapted from Ongodia et al. (2016)

The mechanism of support is by bolt strengthening alongside the rock-support coupling (He, 2014). The coupling ensures stability by maximizing the bearing capacity and minimizing stiffness of the surrounding rock mass. The mechanism of support is such that the rock bolts limit movement of the wedges within the rock mass and prevent unravelling by pushing the wedges together (Kristjánsson, 2014). The factors influencing the rock-support include stand-up time, bedding characteristics, discontinuities, deformation, in-situ stress, overburden - also called rock load, side fill compaction and installation factor (Kim & Yoo, 2002). These factors are evaluated alongside time-related behaviour, groundwater, effects of ground improvement, type of lining, method of excavation and face support (TLDG, 2004). According to Terzaghi (1946), joints weaken bedding planes when the bending stresses above the tunnel exceed the rock strength. Grouting fills the discontinuities thereby reducing groundwater ingress and deformations leading to an increase in the overall rock strength and stand-up time as a more intact rock mass is created. Thus, a lower capacity of lining will be required than before. However, the actual mechanism of support depends on what happens at the interface between the rock and support structures. Components of the support system which are in direct contact with the rock include bolts, wire mesh, shotcrete and steel ribs. The wire mesh, shotcrete and steel ribs generally overlie the excavated rock surface at an approximately flat smoothened surface. Stresses are distributed to the adjacent support depending on the dynamic span of the support system, geotechnical area and the intermediate loose unstable wedges are supported by the reinforcement steel mesh (Durrheim et al., 1998). The rock-rib and rock-shotcrete bonds between these components and the rock surface are adhesive. According to Mohammed (2015), computer based beam spring models cannot be relied on to explain the interaction because they assume a homogeneous material which is realistically not possible. Therefore, the interaction is simply generalized as an adhesive bond. Attractions between the rock-steel and rock-concrete materials maintain the rock-rib and rock-shotcrete interfaces, respectively. The rock-bolt interaction mechanism is discussed in detail in the next section since they are the main structural support component.

3.6.1 Rock bolts

The terms bolt, anchor or dowel are used interchangeably to mean the same type of support as rock reinforcement (Mohammed, 2015). In this study, the term bolt is that which is used to streamline. However, in cases where required support capacities exceed available rock bolt options, either a bolt-beam combination or cable reinforcement technology is appropriate (Hoek, 2016). Projects where bolt-beam combinations have been used for additional support include the Drakensberg pumped storage project in South Africa, Singkarak hydroelectric project in Indonesia and Thissavros hydroelectric project in Greece (Keyter, 2016).

Rock bolts are reinforcement steel rods having a nut fastened with a face plate at the surface and an end anchor which is driven into the rock perpendicularly or inclined, extending beyond the weak unstable rock mass demarcated by the failure plane (Kristjánsson, 2014). Bolts control movement of structurally isolated rock wedges in an excavated tunnel and they transfer loads from the unstable rock face to the more stable confined interior. During bolt installation either systematically in a pattern or at specific locations called spot bolting, engineers should ensure that the spacing and orientation requirements which give adequate support are provided. Bolt spacing should be less than three times the bolt diameter whereas its length should be approximately twice the spacing between bolts (Hoek, 2016). The installation method chosen depends on geology, Rock Quality Designation (RQD) and the type of excavation. Roof bolts are usually inclined at 15-30 degrees to the roof line and cross discontinuity separation planes along which wedges slide to mobilize the maximum shear resistance against sliding (Hoek et al., 1995). On the other hand, the required capacity and longitudinal extent of bolts depends on rock mass properties, geological features, strength of the rock, excavation geometry and secondary factors such as design of the expansion shell and amount of pre-tensioning for partially grouted steel bars (DSI, 2012). Pull-out tests are used in the field to assess bolt capacities after installation. The tests give an indication of the critical embedment length of rock bolts.

Broad categories and types of bolts include pre-tensioned or un-tensioned, fully grouted, end bearing or tie backs. According to JunLu (1999), combinations and other types of bolts are based on these broad categories except in special cases where ordinary bolts cannot function properly. Special cases include seismic areas, high-risk geological and tectonic hazardous environments and high pressure mining areas (Yavuz, 2006; Hustrulid, 2000). In such cases, alternative support systems include cable bolts, trusses and split sets. End bearing bolts are only grouted at the end of the bolt where it is anchored into the rock while tie back bolts have a plate at the end which is fastened onto the rock to anchor it in and therefore both types only resist failure by bearing on the end. On the other hand, fully grouted (cement or resin) bolts seal joints during the grouting, provide better bolt-rock bond and mobilize resistance to failure by both the shaft friction and end bearing resistance. The focus of this study was on full length grouted bolts because grouting fills the rock voids and discontinuities which is important because groundwater flows and hydrostatic pressures are a main source of instability, failure and geotechnical engineering challenges. Grouting improves the ground conditions, compaction, rock competency, fastens the bolt in the drilled hole and protects it from corrosion

(Hoek, 1999; Wahlstrom, 1973). Furthermore, fully grouted bolts provide the most efficient form of support with cable-like force patterns. A fully grouted bolt is achieved by driving the steel rod into a borehole filled with fast-setting high strength grout. Figure 3-35 illustrates (a) a typical fully grouted rock bolt and b) its related forces which are similar to those of a cable. Important rock-bolt interfaces include 1) at the tunnel surface where the nut is fastened with a faceplate, 2) along the entire skin length of the rod and 3) at the end cone and bail where it is anchored into stable rock. The purpose of a faceplate is to distribute the load from the bolt onto the rock face (Hoek, 2016).

The rock-bolt support mechanism is complex. Figure 3-36 shows typical rock-bolt failure as a result of tension and shear forces. Recent laboratory research by He (2014) developed a new continuous resistance large deformation (CRLD) bolt. The CRLD bolt, although not yet tested in its field application, thickens in tension and remains constant under repeated impact loading therefore its features include a negative Poisson's ratio effect, resistance to large deformation and endurance to impact resistance. According to JunLu (1999), tightening the nut tensions the bolt and the mechanism by which bolts support the rock mass can be explained by suspension, beam building (or stitching) and keying. Either one or a combination of the three basic mechanisms can act based on rock geology and stress regime (Zhai et al., 2016). An additional mechanism by Kristjánsson (2014) to explain the rock-bolt interface is skin control. Overall, suspension and stitching mechanisms coexist.

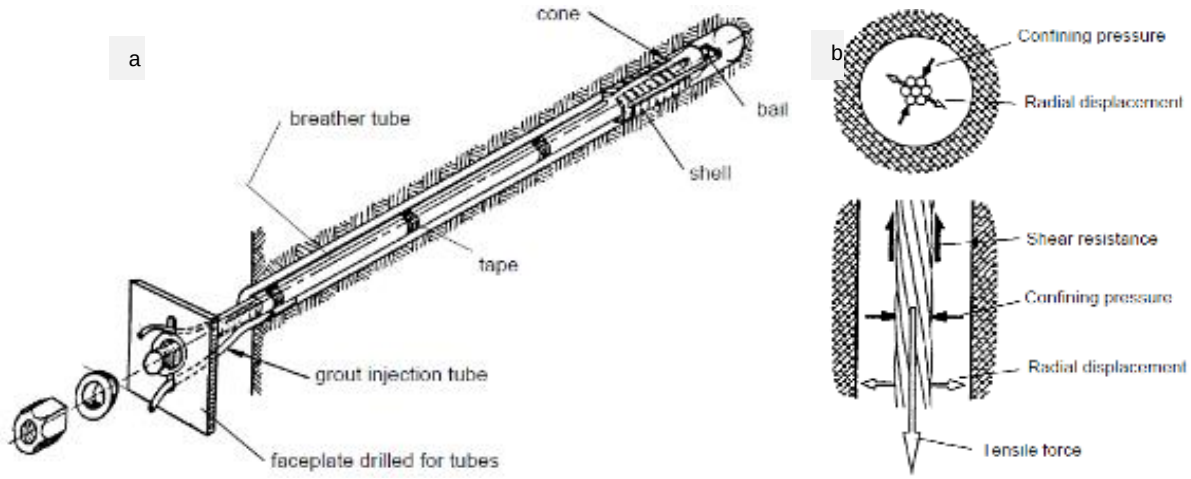

Figure 3-35: (a) Fully grouted rock bolt and (b) forces acting on a bolt
Source: Hoek et al. (1995)

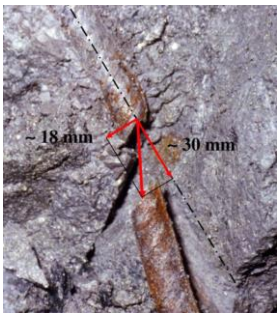

Figure 3-36: Sheared rock bolt
Source: Hadjigeorgiou (2016) after Li (2010)

3.6.1.1. Suspension

Excavation removes the rock mass which previously provided restraint to the overhead mass. Thus, the overhead rock is prone to over break and unravelling if left unsupported for long periods (Terzaghi, 1946). Bolts driven through the tunnel roof are called roof bolts. Roof bolts support loose wedges between the crown of the tunnel and the stable rock at the end anchor. Figure 3-37 shows the phenomenon, capacity and arrangement of roof bolts supporting the rock mass suspended between the crown and the stable rock mass. The rock pressure, P which is equivalent to the bolt capacity can be determined using Equation 3-24 when the unstable rock mass is detached from the adjacent stable mass or otherwise using Equation 3-25 which incorporates the factor of safety, SF (JunLu, 1999). Equation 3-25 can be rearranged to make the axial force, T the subject as shown Equation 3-26.

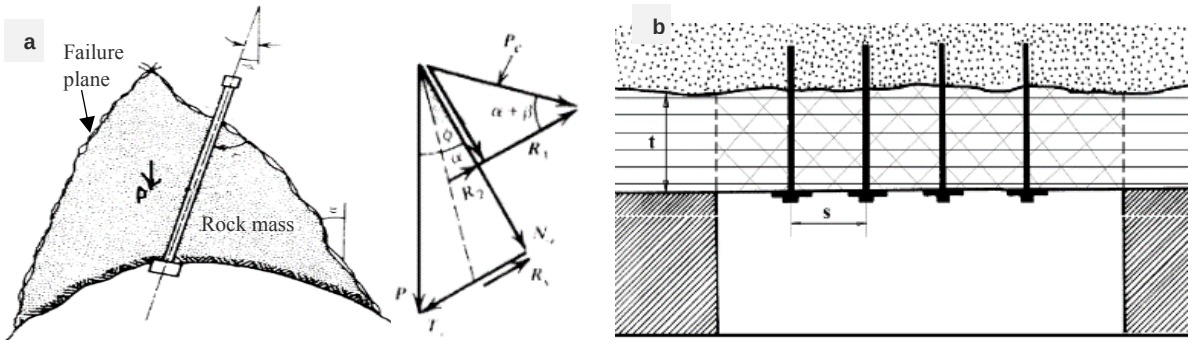

Figure 3-37: (a) Roof bolt support and (b) Array of roof bolts for suspension mechanism
Source: Adapted after JunLu (1999)

Equation 3-24

$$P = \frac{wtBL}{(n_1 + 1)(n_2 + 1)}$$

where w = unit weight of overhead immediate roof, t = thickness of the immediate unstable roof, B = roof span, L = length of immediate roof; n_1 = number of rows of bolts in length L, n_2 = number of bolts per row

Equation 3-25

$$SF = (R_s + R_1 + R_2)/T_\alpha$$

where the friction force, $R_s = P\cos\alpha \tan\beta$, $R_1 = P_c\cos(\alpha+\beta)$, $R_2 = P_c\sin(\alpha+\beta)\tan\phi$, $T_\alpha = P\sin\alpha$, P = dead weight of rock mass, α = angle of the failure plane, β= angle of inclination of the bolt to the vertical, ϕ = Friction angle along the failure plane, T= axial force of bolt

Equation 3-26

$$T = \frac{(SF\,\mathrm{Sin}\propto - \cos\alpha\,\tan\phi)}{\cos(\alpha+\beta)+\sin(\alpha+\beta)\,\tan\phi}$$

3.6.1.2. Beam building (or stitching)

It is not feasible for economical bolt lengths to reach the stable interior rock mass (Zhai et al., 2016). Therefore, bolts provide stability by stitching together bedding planes through axial tension force in the bolts which prevents vertical and horizontal deformation (Kristjánsson, 2014). Tension induces compressive stresses axially and orthogonal to the bolt (Hoek, 1999). Figure 3-38 shows how stitching together overhead bedding planes provides support to the

tunnel roof. Vertical deformation is prevented because the stitched layers act as a stronger fixed-end composite beam. The maximum strain, ε_{max} in the beam is defined by Equation 3-27 when the rock material is assumed to be homogeneous.

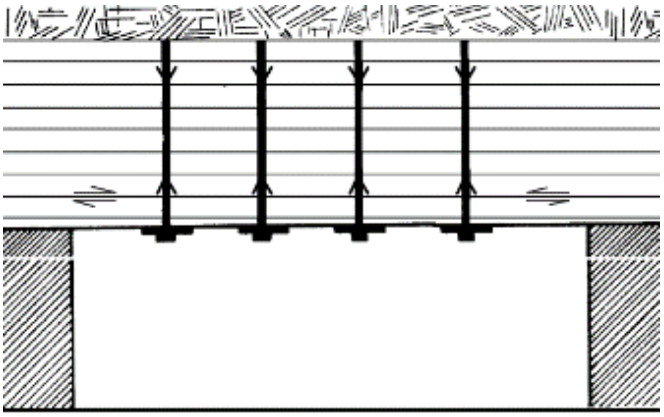

Figure 3-38: Support by stitching overhead bedding planes
Source: JunLu (1999)

Horizontal flat rock beams can be created in sedimentary rock TBM or drill and blast excavations (Bickel et al., 1996). The beam reduces strain but increases bending strength and bending stiffness. Equation 3-28 defines the bending strength of the beam a) without bolts, B and b) with bolts, B_{bolt} whereas Equation 3-29 defines bending stiffness of the beam by c) without bolts, T′ and d) with bolts, T′$_{bolt}$. However, a high bending stiffness increases the loading from top layers thus the whole composite beam may fail by shear and fall out when the shear strength of the composite beam is exceeded by shear forces at either end. In general, stitching is more effective when bedding planes are many, the tunnel span and bolt spacing are small and the tension in the bolt is high (JunLu, 1999).

$$\varepsilon_{max} = wL^2/2\varepsilon t$$ **Equation 3-27**

where w = unit weight of overhead immediate roof, L = length of overhead immediate roof, ε = Young's modulus, t = thickness of the composite beam

$$B = n((bh^2)/6) \quad \text{and} \quad B_{bolt} = b((nh)^2/6)$$ **Equation 3-28**

where n = number of layers, b = length of the beam and h = layer thickness

$$T = n((\varepsilon bh^3)/12) \quad \text{and} \quad T'_{bolt} = \varepsilon b(\frac{nh^3}{12})$$ **Equation 3-29**

3.6.1.3. Keying

The mechanism of keying occurs in highly fractured, blocky and heavily jointed rock mass such that several breaks occur in the support mechanism. Bolts therefore act as keys which link the disjointed smaller systems and in that way act as supplementary support. Figure 3-39 shows

(a) how rock bolts link together the fractured rock mass and (b) the line diagram of forces. The axial stress of the bolt, σ_b required to ensure stability is defined by Equation 3-30. Perpendicular bolts give the maximum support. When $\alpha = \phi$, the rock mass is stable and no bolts are required (JunLu, 1999). However, field conditions and experiential judgement may dictate the need for bolts such as spot bolting when adverse conditions are encountered. The keying effect depends on either active bolt tension or passive tension induced by movement in the rock mass. The effect improves the shear strength but offsets the tensile stresses making it more effective when horizontal stresses are small (Hoek, 1993). The shear strength results from overlapping of the compressive layers which are illustrated by Boussinesq's type distribution cone in Figure 3-40.

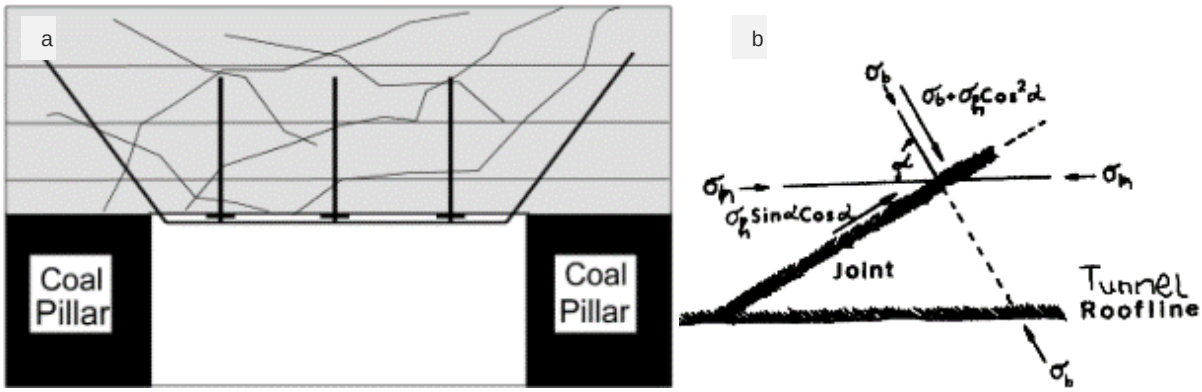

Figure 3-39: (a) Keying mechanism and (b) forces acting in the rock mass
Source: Adapted after Kristjánsson (2014)

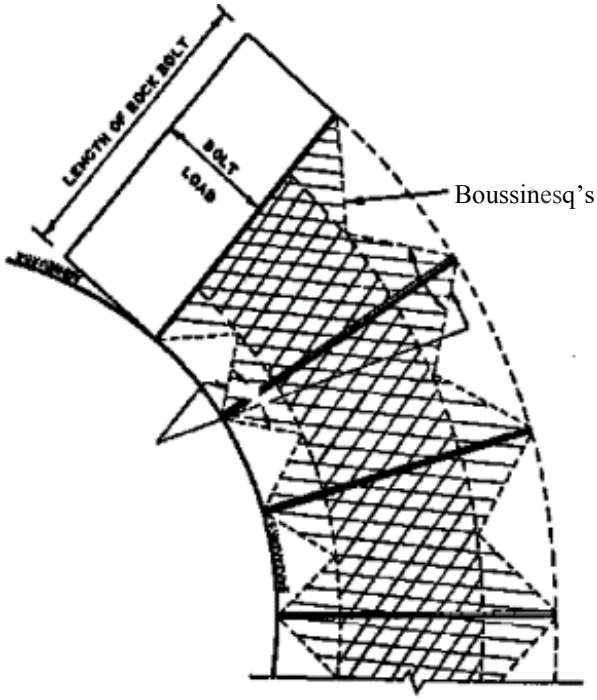

Figure 3-40: Boussinesq's compression zone
Source: JunLu (1999) after Gerrard (1983)

Equation 3-30

$$\sigma_b = (\sigma_h(\sin\alpha\cos\alpha - cos^2\alpha\tan\phi)/\tan\phi)$$

where σ_h = horizontal stress, α = angle between the horizontal plane and normal line drawn to the failure plane, ϕ = friction angle of the failure plane

3.6.1.4. Estimating rock bolt parameters

The full bolt length should be the sum of its length through the longer dimension of the wedge and its anchorage length in the stable rock beyond the overstressed zone of loose rock mass. According to Hoek et al. (1995)'s experience, an anchorage length of about 3 m is sufficient. Usually, bolt lengths range between 3-10 m (Thomas-Lepine, 2012). Analytically, the full bolt length can be calculated using Equation 3-31 where the span and height dimension is used for the roof and sidewall bolt lengths, respectively (Bertuzzi & Pells, 2002). Bolt spacing is particularly important for the beam building effect. For effective support, spacing requirements should satisfy Equation 3-32. For permanent support, bolt capacity in terms of the roof pressure, P_{roof} and the bolt tension, T can be determined using Equation 3-33. According to Hoek et al. (1995), T is usually 1.5 times the uniformly distributed weight of the unstable immediate rock mass about its centroid. A uniform distribution prevents rotating moments which reduce the factor of safety (Hoek et al., 1995). The dead weight of unstable rock wedges is identified using engineering software such as UNWEDGE by Rocscience (2016). Actual weights are calculated based on material properties, composition and configuration.

Length, L **Equation 3-31**

$$L = ((2 + 0.15B)/ESR)$$

where L = full length of rock bolt, B = span length for roof bolts or height dimension for sidewall bolts, ESR = Excavation Support Ratio

Spacing, S **Equation 3-32**

$$S \leq 0.5L, \qquad S = \sqrt{(\frac{T}{P})}$$

where T= axial force and working load of the bolt, P = support pressure

Capacity **Equation 3-33**

$$P_{roof} = \frac{2Q^{1/3}\sqrt{J_n}}{3J_r} \qquad T = 1.5w$$

where P_{roof} = Permanent roof support pressure, Q = rock quality, J_n = joint set number, J_r = Joint roughness, w = weight of unstable immediate rock mass about its centroid

3.6.2 Wire mesh reinforced shotcrete and reinforced concrete linings

After excavation, steel ribs (I or H-beam structural members) and bolts are installed before lining the tunnel along uniform contours. The contours are established using timber blocks and lagging to guide setting out and installation of steel ribs and linings (Wahlstrom, 1973). Steel ribs or arches are used to provide rigid to semi-rigid support thereby reinforcing weaker tunnel sections. Figure 3-41 shows (a) steel ribs and (b) steel arches. Linings comprise wire mesh reinforced shotcrete and concrete linings. Linings are selected depending on the geology and extent of rock fracture. Usually shotcrete is applied as an initial temporal or permanent support to protect workers from falling wedges while concrete is commonly applied as a final permanent lining. When linings are applied over the entire circumferential length of the tunnel

section, they are called support rings. Support rings resist external ground pressures, restrain the surrounding rock mass under seismic conditions and control groundwater ingress and egress into and from the structure (Luwalaga, 2013; TLDG, 2004). Flexibility is given by the modulus ratio (E_g/E_s) which is defined as the ratio of the Young's modulus of the ground, E_g to that of the structure, E_s. According to the TLDG, E_g/E_s is greater than 0.1 for flexible linings, between 0.1-0.01 for ground-support load sharing and less than 0.01 for rigid linings. Flexible and ductile linings are most suitable for tunnels because they are more durable and do not easily crack (Hoek et al., 1995; RTM, 2009).

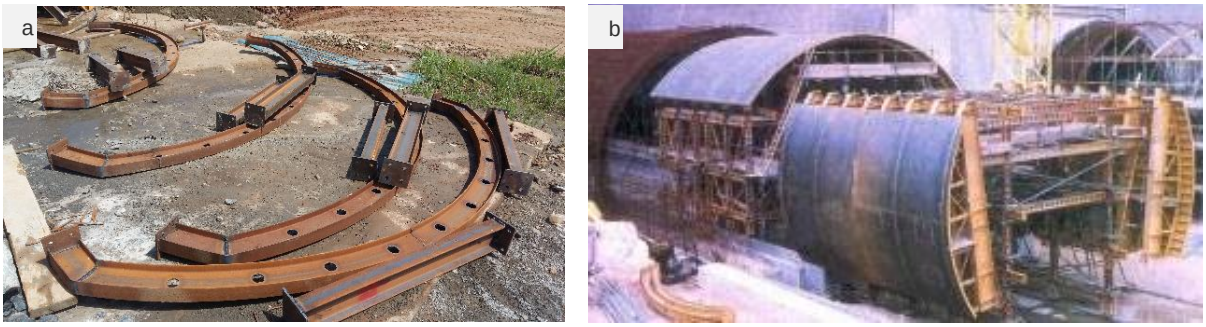

Figure 3-41: (a) Steel ribs and (b) Steel arches
Source: (b) Konstantis et al., (2016)

The surface is scarified to remove loose rock pieces. It is thoroughly cleaned with a compressed air-water jet. This is followed by a steel wire mesh grid securely installed using either rock bolts or short grouted steel pins. Cleaning is important to ensure that an adhesive rock-shotcrete bond is achieved when the shotcrete is sprayed either as a dry or wet mix. The purpose of the mesh is to restrain loose wedges and rock fragments not directly supported by the bolts and to reinforce the shotcrete lining thereby minimizing stiffness of the surrounding rock mass (Wahlstrom, 1973). According to Hoek et al. (1995), a 4 mm diameter wire welded 100 mm x 100 mm grid mesh is adequate reinforcement and shotcrete requirements can be estimated from guidelines (Table 3-11). The table describes the behaviour of a rock mass and gives its support requirements and the estimated shotcrete requirements. Shotcrete is pneumatically applied as either (a) dry or (b) wet mix and dynamically compacted using a high velocity jet as shown in Figure 3-42. It progressively hardens to cement the rock thus making it to act as an intact stable rock mass which cannot be easily disintegrated unless a greater weakening force is mobilised (Hoek et al., 1995). Shotcrete technology is generally practical and tailored to suit site conditions such as quality of the materials, method of application and adequate thickness which covers the rock and is safe from spalling. RTM (2009) recommends shotcrete lining thickness of approximately 200-300 mm. The capacity of shotcrete is determined by crushing cylindrical cores drilled from the tunnel surface to establish 3, 7 and 28 day strengths. Steel lining is then placed over the shotcrete lining. For hydro tunnels, steel lining is required to increase water tightness, avoid leakage and provide additional strength. Hoek et al. (1995) suggest that steel lining should be placed when the minimum principal stress is less than the maximum dynamic water pressure which is approximately 30 % of the

maximum static head of the water in the tunnel. The steel lining is overlain with a final lining of reinforced concrete. High grade concrete of strength ranging from 24-38 MPa 28-day strength with a 127 mm slump, 3-5% air entrainment, a minimum thickness of 250 mm is adequate for cast-in-situ concrete lining (RTM, 2009). Air entrainment is important because tunnel conditions are generally damp to cold and the concrete is specially placed. The high strength steel reinforcement bars and welded wire mesh should conform to ASTM A615 and ASTM A185, respectively. The maximum liner capacities and stiffness can be calculated from Equation 3-34 and Equation 3-35, respectively.

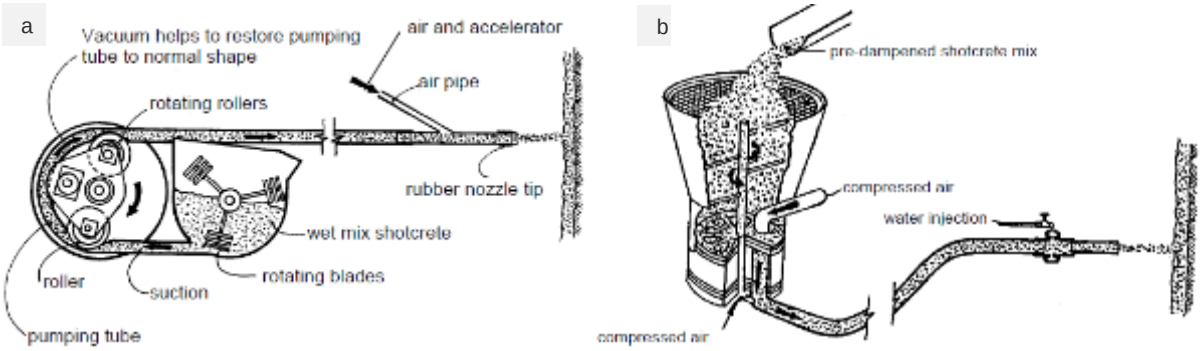

Figure 3-42: Shotcrete mix systems
Source: Hoek et al. (1995)

Maximum support pressure, P_{scmax} **Equation 3-34**

$$P_{scmax} = 0.5\sigma_{cc}[1 - \frac{(r_o - t_c)^2}{r_o^2}]$$

where σ_{cc} = uniaxial compressive strength of concrete or shotcrete (MPa), t_c= thickness of the lining (m), r_o=radius of the tunnel (m)

Stiffness, K_{sc} **Equation 3-35**

$$K_{sc} = \frac{\varepsilon_c(r_o^2-(r_o-t_c)^2)}{2(1-\nu^2)(r_o-t_c)r_o^2}$$

where ε_c = Young's modulus of the concrete or shotcrete (MPa), ν = Poisson's ratio of the concrete or shotcrete, t_c = thickness of the lining (m), r_o = radius of the tunnel (m)

Table 3-11: Guidelines for shotcrete design

Rock mass description	Rock mass behaviour	Support requirements	Shotcrete application
Massive metamorphic or igneous rock with low stress conditions.	No spalling, slabbing or failure	None	None
Massive sedimentary rock. Low stress conditions.	Surfaces of some shales, siltstones, or clay stones may slake because of moisture content change.	Sealing surface to prevent slaking.	Apply 25 mm thickness of plain shotcrete to surface immediately after excavation. Repair any shotcrete damage due to blasting.
Massive rock with single wide fault or shear zone.	Fault gouge may be weak and erodible thus cause in stability in adjacent jointed rock.	Provision of support and surface sealing in vicinity of weak fault or shear zone.	Remove weak material to a depth equal to width of fault or shear zone and grout rebar into adjacent sound rock. Weldmesh used to provide temporary rock fall support. Fill void with plain shotcrete. Extend steel fibre reinforced shotcrete laterally for at least width of gouge zone.
Massive metamorphic or igneous rock. High stress conditions.	Surface slabbing, spalling and possible rock burst damage.	Retention of broken rock and control of rock mass dilation.	Apply 50 mm shotcrete over weldmesh anchored behind bolt faceplates. Alternatively, apply 50 mm of steel fibre reinforced shotcrete on rock and install bolts with faceplates, then apply second shotcrete layer of 25 mm thickness extending along sidewalls as required.
Massive sedimentary rock. High stress conditions.	Surface slabbing, spalling and possible squeezing in shales and soft rocks.	Retention of broken rock and squeezing control.	Apply 75 mm layer of fibre reinforced shotcrete directly on rock surface. Rock bolts or dowels are also needed for additional support.
Metamorphic or igneous rock with a few widely spaced joints. Low stress conditions.	Potential for wedges to fall or slide due to gravity loading.	Provision of support in addition to that available from rock bolts or cables.	Apply 50 mm of steel fibre reinforced shotcrete to rock surfaces on which joint traces are exposed.
Sedimentary rock with a few widely spaced bedding planes and joints. Low stress conditions.	Potential for wedges to fall or slide due to gravity loading. Bedding plane exposures may deteriorate in time.	Sealing of weak bedding plane exposures. Provision of support in addition to that available from rock bolts or cables.	Apply 50 mm of steel fibre reinforced shotcrete on rock surface on which discontinuity traces are exposed, with attention to bedding plane traces.

Table 3-11 continued: Guidelines for shotcrete design

Rock mass description	Rock mass behaviour	Support requirements	Shotcrete application
Jointed metamorphic or igneous rock. High stress conditions.	Combined structural and stress controlled failures around opening boundary.	Retention of broken rock and control of rock mass dilation.	Apply 75 mm plain shotcrete over weldmesh anchored behind bolt faceplates or apply 75 mm of steel fibre reinforced shotcrete on rock, install rock bolts with faceplates and then apply second 25 mm shotcrete layer. Thicker shotcrete layers required at high stress concentrations.
Bedded and jointed weak sedimentary rock. High stress conditions.	Slabbing, spalling and possibly squeezing.	Control of rock mass failure and squeezing.	Apply 75 mm of steel fibre reinforced shotcrete to clean rock surfaces as soon as possible, install rock bolts, with faceplates, through shotcrete, apply second 75 mm shotcrete layer.
Highly jointed metamorphic or igneous rock. Low stress conditions.	Ravelling of small wedges and blocks defined by intersecting joints.	Prevention of progressive ravelling.	Apply 50 mm of steel fibre reinforced shotcrete on clean rock surface in roof of excavation. Rock bolts or dowels may be needed for additional support for large blocks.
Highly jointed and bedded sedimentary rock. Low stress conditions.	Bed separation in wide span excavations and ravelling of bedding traces in inclined faces.	Control of bed separation and ravelling.	Rock bolts or dowels required to control bed separation. Apply 75 mm of fibre reinforced shotcrete to bedding plane traces before bolting.
Heavily jointed metamorphic or igneous rock, conglomerates or cemented rock fill. High stress conditions.	Squeezing and 'plastic' flow of rock mass around opening.	Control of rock mass failure and dilation.	Apply 100 mm of steel fibre reinforced shotcrete immediately and install rock bolts with face-plates. Apply additional 50 mm of shotcrete if required. Extend support down sidewalls as required.
Heavily jointed sedimentary rock with clay coated surfaces. High stress conditions.	Squeezing and 'plastic' flow of rock mass around opening. Clay rich rocks such as containing montmorillonite may swell.	Control of rock mass failure and dilation.	Apply 50 mm of steel fibre reinforced shotcrete immediately, install lattice girders or light steel sets with invert struts as required, then more steel fibre reinforced shotcrete to cover sets or girders. Forepoling or spilling may be required to stabilise face ahead of excavation. Gaps may be left in final shotcrete to allow for movement resulting from squeezing or swelling. Gap should be closed once opening is stable.
Mild rock burst conditions in massive rock subjected to high stress conditions.	Spalling, slabbing and mild rock bursts.	Retention of broken rock and control of failure propagation.	Apply 50 to 100 mm of shotcrete over mesh or cable lacing which is firmly attached to the rock surface by means of yielding rock bolts or cable bolts.

Source: Hoek et al. (1995)

In addition to the support provided by rock bolts and shotcrete, steel ribs and other considerations depending on geological rock classes according to the degree of weathering can be estimated from established guidelines such as indicated in Table 3-12. Empirical, numerical and engineering software methods are also used to design structural supports for underground excavations. Finite Element Methods (FEM) and limiting equilibrium approaches with computer software are used to model tunnel supports and excavation methods based on rock mass ratings.

Table 3-12: Guidelines to design tunnel reinforcement

Rock Class	**RMR**	**Excavation**		**Rock bolts** (20 mm diameter, fully grouted into tunnel roof)		**Shotcrete thickness** (mm)		**Steel ribs** (spacing, m)
		Position/ Advance (m)	Support	Length / Spacing (m)	Placement method	Roof	Sidewalls	
I	81-100	Full face/3	Generally, no support required except spot bolting					
II	61-80	Full face/ 1-1.5	Complete (20 m from face)	3/2.5	Local with wire mesh, occasionally	50	Not Applicable	Not Applicable
III	41-60	Top heading and bench, 1.5-3	Immediate support. Complete- 10 m from face	4/1.5-2	Systematic with wire mesh	50-100	30	Not Applicable
IV	21-40	Top heading and bench, 1.0-1.5	Support alongside excavation. Complete (10 m from face)	4-5/1-1.5	Systematic with wire mesh. Also in sidewalls.	100-150	100	Light to medium (1.5m spots)
V	< 20	Multiple drifts, 0.5-1.5	Support alongside excavation. Immediate shotcreting	5-6/1-1.5	Systematic with wire mesh and Bolt invert. Also in sidewalls.	150-200	150 (and 50 on face)	Medium to heavy (0.75m), with steel lagging and fore poling as required. Close invert.

Source: Bieniawski (1992)

3.7 Summary

This chapter discussed geology, with specific reference to properties of rock materials, rock mass features. The features provide structurally controlled tunnel stability, rock loads, tunnel failure, rock-support components and their associated system interactions. The chapter also provided petrological, structural and rheological knowledge from geology ubiquitous to engineers that is a necessary background for appropriate engineering sampling, testing, design and construction.

The most abundant rock in the earth crust, granite, has a generally stable structure and fabric comprising several silicate crystal lattices (Sydney, 2006). Rock strength and suitability to support engineering loads depends on the intact rock mass or material properties where numerous discontinuities are present. Engineering rock is broadly classified as soft or hard rock with a unconfined compressive strength (UCS) of 25 MPa as a distinct separator. Hard rock with over 25MPa strength is preferred for engineering structures. Rock mass classification systems comprising quantitative and qualitative methods were used to classify the rock in further detail. Quantitative methods include RMR, Q-index, RQD and GSI. Qualitative methods include Terzaghi, Lauffer's stand-up time classification, size-strength, RSR, BGD, URCS and NATM excavation method. The RMR, Q-index and RSR are mostly used.

Rock has several discontinuities and presents varied construction challenges depending on the strength - reliant on material properties and joint interconnectedness. Some of the common problems associated with soft rock are squeezing and swelling. Squeezing results from low strengths which cannot resist the inward movement of an excavation in the plastic zone. Swelling occurs when montmorillonite clay minerals fill the joints and expand when saturated. Therefore, provision of proper and adequate drainage is an important factor in tunneling. Other modes of failure include rock bursts, collapse of the roof wedges, sliding of the sidewall wedges and occasional heaving of the bottom floor wedges. Stability of tunnel structures is fundamental in delivering safe solutions through underground construction to meet human demands and utilize the land resource optimally. The next chapter explains how the geotechnical considerations are applied to design an actual hydro tunnel using a case study.

4 TUNNEL SUPPORT SYSTEM DESIGN – A CASE OF KARUMA

4.0 Introduction

Theory and equations to design of tunnel supports are based on modifications of the Rankine theory for lateral earth pressures although practical experience and engineering judgement are mostly relied on (Hoek et al., 2008; USACE, 1997). According to Mohammed (2015), closed form solutions, numerical analyses and empirical methods emerged through practice. Closed form solutions evaluate failure and load pressures in the plastic zone (RTM, 2009). Numerical analysis considers progressive failure of the surrounding rock mass and its interaction with the support (Thomas-Lepine, 2012). Empirical methods observe tunnel deformation and limit it by installing supports (Bertuzzi & Pells, 2002). In all the different approaches, tunnel support design considers vertical, horizontal and uplift loads acting at the roof, sidewalls and invert, respectively (Mohammed, 2015). Figure 4-1 shows loads surrounding a tunnel. The loads are a function of the geological and geotechnical factors discussed in Chapter 3. Specific factors include: Geomechanical and hydrogeological rock properties, weathering condition, stratification, stand-up time and rock overburden (Marie, 1998). Failure characteristics are unique for specific ground conditions and the adequate support capacity is greater than the rock tensile stresses (Zhang et al., 2015). According to Hadjigeorgiou (2016), failure of support systems occurs when the structure is unstable and fails to meet its functional requirement. As a result, support methods are varied to accommodate stress redistribution after excavation including use of different members comprising a support system (Hoek et al., 1995; Beaver, 1972). Worth noting is that rock strength varies along the entire length of a tunnel excavation. As such, this study considered a tunnel segment of Karuma whose geology was typical therefore representative of the site conditions established from project investigations. Figure 4-2 illustrates a) typical horse-shoe shaped tunnel section and b) the excavated Karuma tunnel.

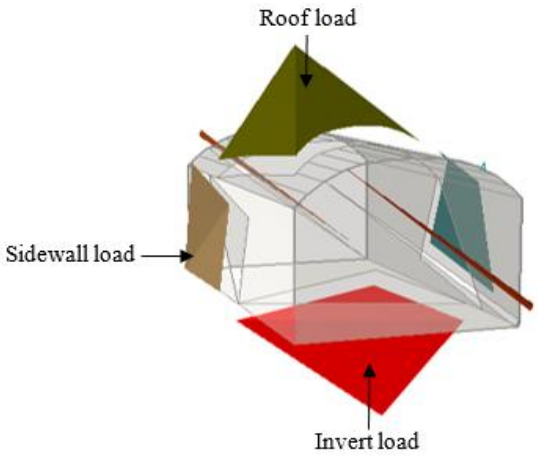

Figure 4-1: Loads surrounding a tunnel

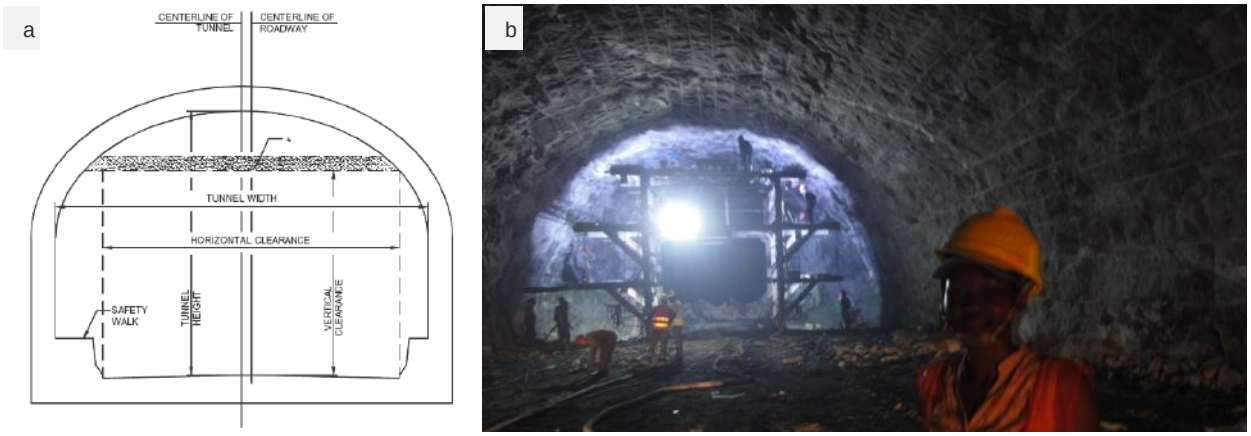

Figure 4-2: a) Typical horse-shoe section (RTM, 2009) and b) the excavated Karuma tunnel

4.1 Case study

The proposed 600MW Karuma Hydropower Project (HPP), herein after referred to as Karuma, is Uganda's largest hydro construction project to date. It is located along the River Nile at 2°14′51″N and 32°16′05″E and the topography consists of a plateau and flat gently sloping (5°) terrain with some undulation (Karuma, 2014). Figure 4-3 shows Uganda's major operational Hydro Power Plants (HP Plant) and projects. Their corresponding electricity generation capacities are 180MW, 200MW, 250MW and 700MW for Nalubaale, Kiira, Bujagali plants and the proposed Ayago project, respectively. The figure also highlights Karuma's geographical location which is close to a sensitive flora-fauna ecosystem comprising the Murchison Falls National Park (MFNP) and wildlife nature reserve. Tunnels were drilled and blasted through rock approximately 70 m below the ground surface on 40 ha of the reserve area. Underground tunnels were the only means to construct a HPP without disrupting the wildlife habitat by limiting surface interferences in the Karuma environment.

The following paragraphs report on Karuma's geological and geotechnical conditions in order to explain both the regional and local geological context of the site. For this study, the regional geology is that of the geographical area comprising Uganda and her neighboring countries; Kenya, Tanzania, Rwanda, the Democratic Republic of the Congo (DRC) and South Sudan. The local geology refers to that in the immediate vicinity of Karuma project site.

According to Kalinga (2016), features which formed because of elevational movement of the peneplain dating from the Miocene Epoch (about 23 to 5.3 million years ago) included; 1) contrasting landforms, highlands, volcanic mountains, plateau, low plains, 2) large lakes, 3) craters, 4) fumaroles, 5) crystalline nepheline-syenite (granular rock of alkalic feldspar, nepheline and other minerals), 6) agglomerates, 7) tuffs and 8) the rift valley system.

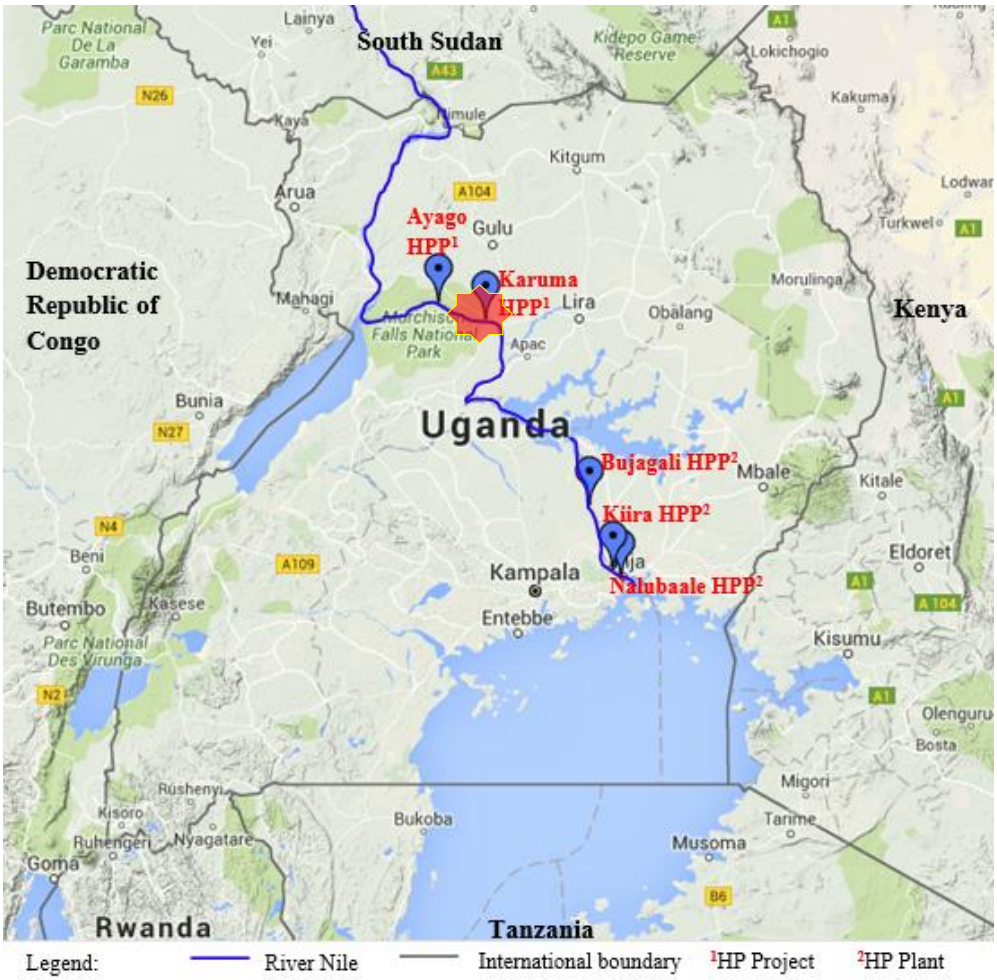

Figure 4-3: Geographical location of Karuma and other major hydropower facilities Uganda's and the
Source: Adapted from Google maps

The rift valley system, which is an elongated low-lying basin of collapsed land bounded by opposed steeply dipping normal faults which drifted apart and extends discontinuously, is the most significant geological and tectonic feature in the region (Wood & Guth, 2015). The earth crust is predicted to separate structurally along the rift to form new tectonic plates (Owor et al., 2016). Figure 4-4a is a Digital Elevation Model (DEM) showing tectonic plate boundaries. The rift system comprises the western and eastern branches extending along the national boundaries as shown in Figure 4-4b. The eastern branch is called the East African Rift System (EARS). Kalinga (2016) and Schlüter (1997) found that regional geological and tectonic features comprise Precambrian, Karoo, Coastal Meso and Cenozoic basement complex and a recent unconsolidated mosaic of lateritic soils, gently dipping and soda-rich lavas overlying sedimentary rock types at river mouths. Studies by Owor et al. (2016) and Schlüter (1997) identified seven geological provinces for Uganda which include largely volcanic igneous, Precambrian craton, Precambrian metasedimentary, Precambrian mobile or orogenic belts, tertiary sedimentary cretaceous, Mesozoic-Paleozoic and unconsolidated sedimentary-type, as shown in Figure 4-5. (Further information on Uganda's geology is included in Appendix D.) The NGS (2015) observed that

the region comprises abundant lateritic reddish brown soils which usually have traces of granite, biotite and amphibolite. According to Heidbach et al. (2010), Uganda's seismicity challenges are minimal because there are no significant stress factors including main tectonic plate boundaries, tectonic regimes or fault lines except surface quartz particles with quartz veins extending in the direction of N70°W.

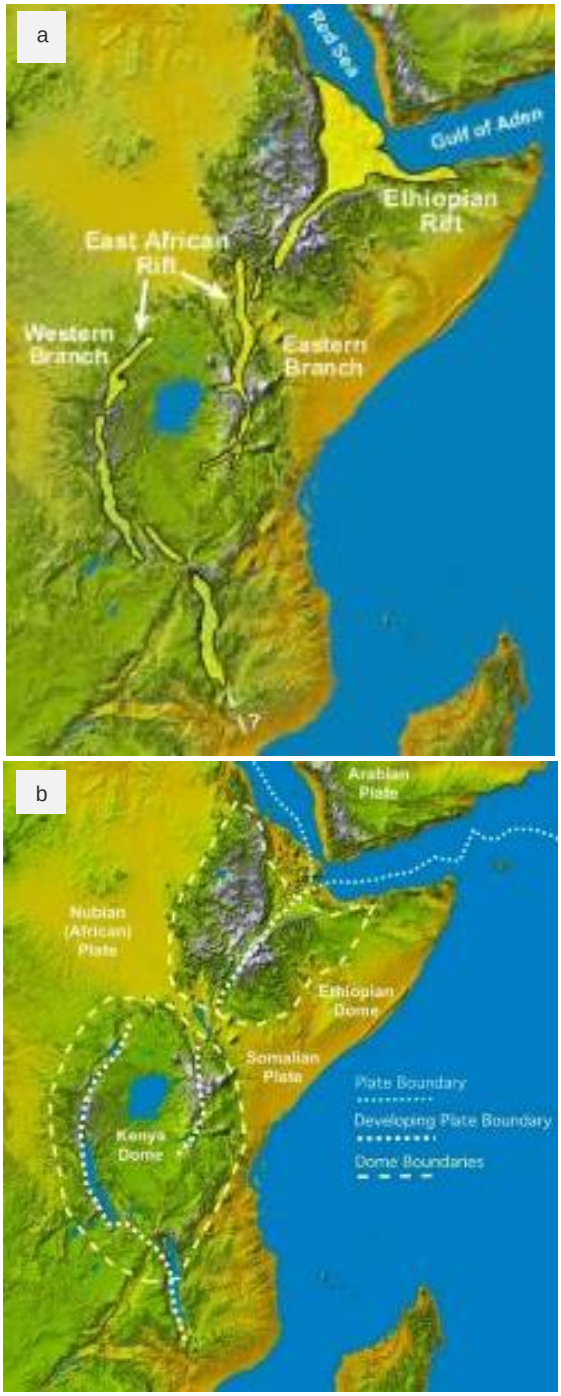

Figure 4-4: Regional structural geology
Source: Wood & Guth (2015) after NASA

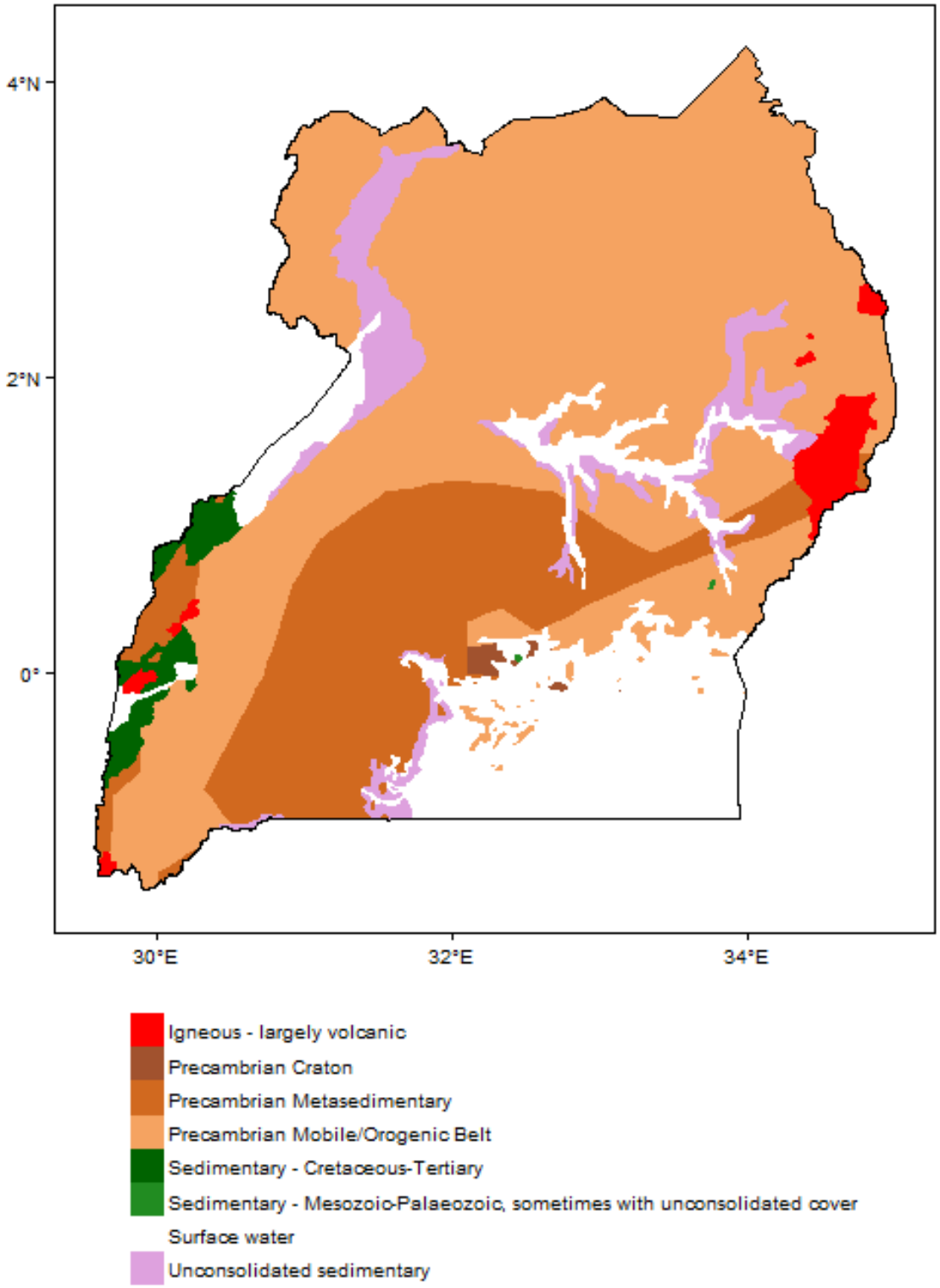

Figure 4-5: Uganda's geological provinces
Source: Owor et al. (2016) after USGS (2016)

Project Geotechnical Investigations (GIs) conducted by the contractor Sinohydro in Uganda comprised of observations, local knowledge of the area, geological mapping, borehole data,

exploration pits, geophysical profiling, in-situ and laboratory testing (Karuma, 2014). From the GIs,

1. Karuma bedrock is igneous gneiss. Figure 4-6 shows the exposed bedrock strata of Precambrian metamorphic rock in scattered places and quaternary residual upper elluvial lateritic soil, locally known as 'murram'.
2. The geosphere lithology comprises Precambrian granitic gneiss, amphibolite gneiss, granite gneiss with mica, biotite granite gneiss and traces of amphibolite as shown in Figure 4-7a. It is characterized by black low strength ferromagnesian minerals, white high strength alternating striation stripes of feldspar quartz minerals containing fine to medium-grained structures with grayish-black specks of thin-interbedded gneissosity.
3. The rock is highly weathered gneiss material. The degree of weathering (Figure 4-7b) varied from completely, highly, moderately and slightly weathered rock located at about 53 m, 57 m, 99 m and greater burial depths, respectively. Rock classification (Table 4-1) indicate approximately 1.45% class II, 86.35% class III, 10.9% class IV and 1.3% class V rock. Further details of the GIs are included in Appendix D. Class IV is the most abundant weak rock therefore critical; thus this study considered it for design.
4. Stratigraphy comprised of Archaean, Proterozoic and Quaternary strata, undifferentiated basement complex granite and Aruan gneiss rocks, older charnockites North of the Albert Nile River; intrusive granite and granite gneiss in the South and distributed Bunyoro sedimentary rocks over the basement complex.
5. From the hydrogeological analysis, no groundwater table was encountered although the ground was generally damp and limited perched water was encountered. Slight permeability of less than 1 Lugeon unit (Lu) in both moderately and slightly weathered rocks, limited dripping pore water prevalent in the Quaternary loose layer and completely weathered rock. Seepage dripping groundwater in Class III and some considerable seepage linear water gushing in Class IV rock. Therefore, drainage including pumping is important.
6. The maximum and minimum horizontal principal stresses, determined by performing hydraulic fracturing tests at the project site, ranged between 3.1-8.9 MPa and 2.6-6.2 MPa, respectively. The direction of the maximum principal stress was N56°E~N60°E.
7. Karuma (2014) investigations found that the area is located in a seismically stable Ugandan craton, on the Victorian plate lying between the Albertine Rift and Aswa shear zone, with few small scale inactive fault lines developed along gneissosity and a seismic intensity of magnitude VII was recorded. Figure 4-8 is a tectonic map of the area (Karuma, 2015).

Figure 4-6: Rock surface (a) Dewatered river bed (b) Granitic gneiss (c) Amphibolite gneiss
Source: Karuma (2015)

Figure 4-7: (a) Lithology and (b) Rock weathering
Courtesy: Sinohydro (2015)

Table 4-1: Rock classification (Karuma, 2015)

Rock Class	Property			Classification		
	Formation	Rock mass condition	Structural planes	RQD %	Q	RMR
II	**A:** Amphibolite, granite gneiss and slightly weathered or fresh amphibolite	Integral to secondly integral	Undeveloped or slightly developed with well closed	80-95	6.6-60	60-80
III	**B**: Lower section of moderately weathered amphibolite and granite gneiss	Secondly integral or frangible	Moderately developed, with pair closed	50-80	0.72-6.6	40-60
	C: Slight traces of biotite and granite gneiss	Relatively integral	Slightly or moderately developed with pair closed			
IV	**D**: Upper section of moderately weathered amphibolite and granite gneiss	Frangible rock mass	Developed with pair closed or poor closed	30-50	0.08-0.72	20-40
	E: Moderately weathered biotite granitic gneiss	Secondly frangible or frangible rock mass	Developed with pair closed or poor closed			
	F: Highly weathered amphibolite and granite, biotite and amphibolite gneiss	Frangible or extremely frangible	Very developed and very poor closed. Fault disturbed zone	0-30	0.08-0.72	20-40
V	G: Completely weathered rock	Disintegrated into sand and soil	Fault zone	0	<0.08	0-20

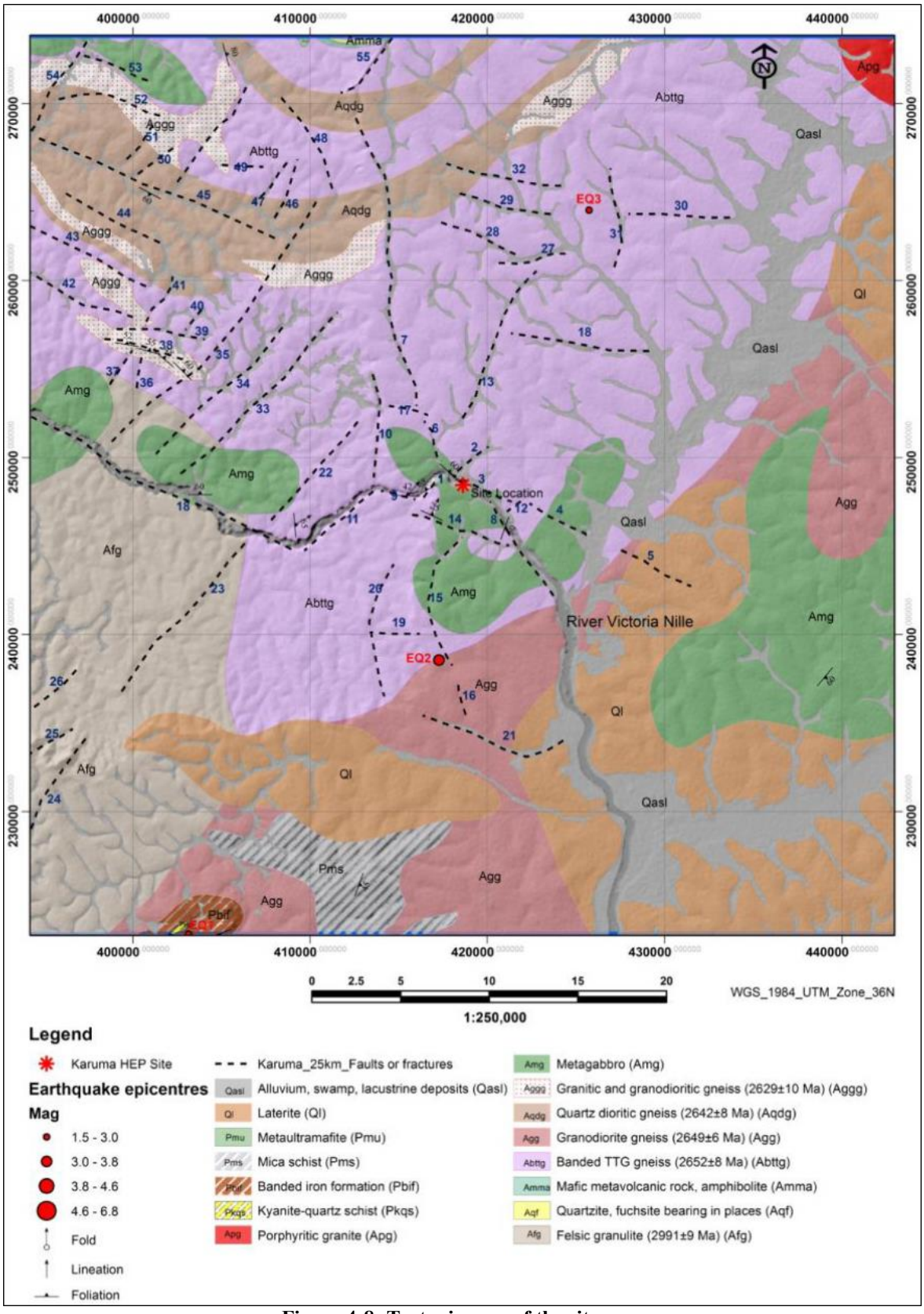

Figure 4-8: Tectonic map of the site area
Source: Karuma (2015)

4.2 Tunnel support estimation

This section explains the design of tunnel support systems using three different approaches: 1) The analytical methods are used to compute rock loads whose support must counteract their weights to ensure stability using equations borrowed from soil mechanics, 2) An empirical method involving Finite Element Modelling (FEM), and 3) The conventional method based on geological systems. According to Bertuzzi and Pells (2002), the precise value of an adequate support parameter is best achieved as a solution to closed-form equations.

4.2.1 Karuma geometry and material parameters

Details of Karuma were used as input to design the tunnel support system. A one-meter wide segment of the tunnel, trending in the S67°W direction from 1075 m elevation upstream at chainage K1+300m to 960m elevation downstream, was studied. The tunnel geometry comprised a flat-bottomed horse-shoe shape with an average cross-section diameter of 12.8 m.

From the project investigations, typical geological conditions at the study location comprised of a highly weathered class IV rock with a unit weight, γ of 27.5kN/m^3, cohesion, *c* of 13.11kPa, angle of internal friction, ϕ of 32°, Young's modulus, E_m = 5000MPa, Poisson's ratio, ν of 0.25, rock mass quality, Q of 0.72, burial depth, *H* of 70 m, height of tunnel of 9 m and span of approximately 13 m, rounded up from 12.8 m (Karuma, 2015). Figure 4-9 shows a cross-section of Karuma hydro tunnel. The section shown was later widened during excavation to almost double the tunnel span.

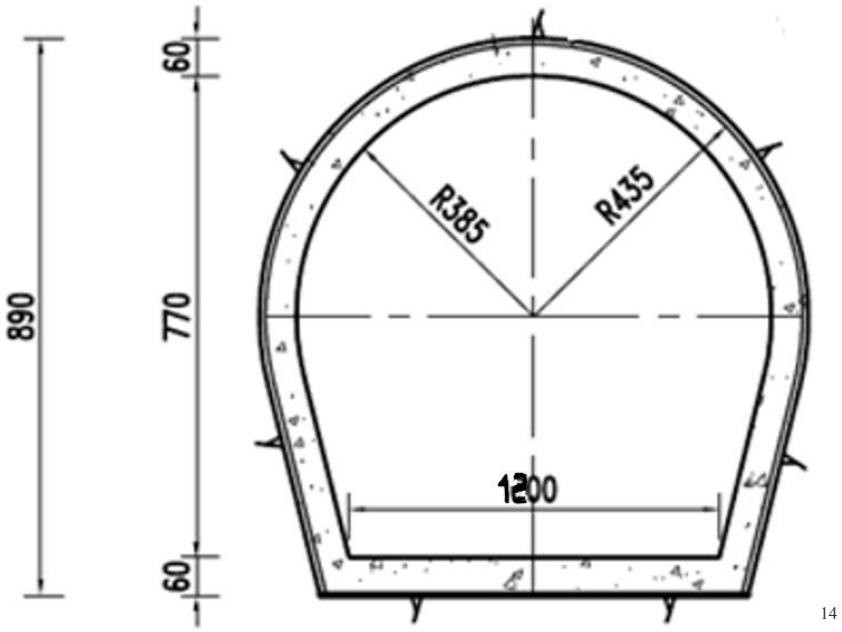

[14]

Figure 4-9: Tunnel geometry
Source: Karuma (2015)

[14] Dimensions are in cm

4.2.2 Simplifying assumptions

Although field-measured parameters are used, the accuracy and correctness of a design is limited to the geometry, construction method, NATM stages and effects, theoretical basis of the solution, interpretation of computed results, support parameters selected and assumptions made. according The main assumption is a hydrostatic in-situ stress field whereby rock loads have a uniform vertical distribution across the tunnel roof and invert thereby preventing bending of the support system (Terzaghi, 1946). Other simplifying assumptions include;

1. A circular cross-section so that support is a uniform internal pressure around the circumference with an elastic-perfectly plastic response (Mohammed, 2015).
2. Isotropic and homogeneous rock mass whereby stability is controlled by main structural discontinuities (Terzaghi, 1946).
3. Symmetry in all cases is ensured by provision of complete support rings such that no bending moments are induced in the structure (RTM, 2009).
4. A permanent support system including steel lining although the minimum principal stress is greater than the maximum dynamic water pressure. This is in consideration of a 60 year design life for the hydopower plant (Karuma, 2015).
5. Constant field stress rather than a gravity force since the tunnel burial depth of 70 meters is relatively deep (Hoek et al, 1995).
6. Based on Hoek et al. (1995), a 50-70% stress reduction and a K_o value less than unity is assumed since the depth to tunnel axis below the ground surface is greater than thrice the tunnel diameter.
7. An Excavation Support Ratio (ESR) of 1.6 for hydropower tunnels (Hoek et al., 1995).
8. An equivalent dimension, D_e of 8 and a factor of safety of 2 for bolt installation challenges and reserve support capacity (Hoek et al., 1995).
9. Good hydraulic properties, negligible hydrostatic presure build-up behind the lining and a leak-proof hydro tunnel (TDLG, 2004).
10. According to Bieniawski (1992), the stand-up time for a 13 m span tunnel is approximately 10^3 hours, an equivalent of about 41 calendar days.

4.2.3 Analytical method

This section presents the analytical design based on numerical relationships. The tunnel support was designed by computing rock loads from geotechnical engineering equations. Geostatic tunnel design methods of adequate support depend on geomechanical material parameters and dimensions of the tunnel excavation as main inputs for the equations (Perri, 2007). The formulae for calculation of loads imposed by the weight of surrounding rock mass have been investigated by several researchers including Prasad (2015), Thomas-Lepine (2012), Nielsen (2009), RTM (2009), Yavuz (2006), Tsesarsky & Hatzor (2005), USACE (1997), Hoek et al. (1995), Barton et al. (1974), Terzaghi (1946) and Marston & Anderson (1913). The articles give formulae and illustrate with sketches the instability problem but no detailed background explanations were included in the text. On the other hand, almost all findings built on the work by Terzaghi (1946)

which focussed on shallow soil tunnels. Barton et al. (1974) rightly suggested that major modifications and further research is necessary to adapt the formulae for deep underground rock tunnels. Furthermore, factoring the loads in the analysis is recommended by Prasad (2015) and USACE (1997).

The analytical design of tunnel support systems involves entering geological parameters as inputs to the equations to obtain a numerical value and either simply selecting a suitable rock bolt from manufacturers' specifications and design tables or using a bolt-beam combination. Manufacturers specially produce specific rock bolt sizes, capacities and material from which designers and tunnel engineers choose to suit their specific requirements. Usually, steel is used. According to Heck et al., (2016) when rock resistances exceed available rock bolt capacities, a bolt-beam combination is economical. The beam is designed on site to allow for bolt pretensioning and rock mass strengthening through stress relaxation to improve stability.

The ultimate rock load is the weight of a collapsing wedge near the bolt and it corresponds to the minimum acceptable support capacity hence its resistance to failure when the factor of safety is unity (Thomas-Lepine, 2012). According to RTM (2009), rock loads are classified as:

1. Earth surcharges
2. Overburden
3. External loads
4. Internal loads
5. Settlement loads.

Prasad (2015) observes that earth surcharges are loads placed above the ground line at the top of a tunnel, and that overburden is the vertical gravity load due to the weight of the surrounding rock mass while external and internal loads include hydrostatic groundwater pressure and the hydrostatic water head and settlement, respectively. This is significant when the combined weight of the structure and backfill exceed the weight of muck excavated.

Prasad (2015) and RTM (2009) found that earth surcharges approximate 4.79 kPa whereas external loads approximate 25% of the full tunnel capacity. According to Perri (2007) all loads are supported radially for deep tunnels at $H > \text{span} * (GSI/5)$ whereas for shallow tunnels at depth $H \leq \text{span} * (50/GSI)$, the rock overburden exerts pressure on the crown and horizontal loads bear on the sidewalls. In addition to rock loads, seismic loading is important in earthquake prone areas and when recommended from investigations. The analytical design is presented in Table 4-2.

Table 4-2: Analytical estimation of rock loads

Material parameters	Highly weathered Class IV rock. Unit weight, γ = 27.5kN/m^3 ; cohesion, c = 13.11kPa ; angle of internal friction, ϕ = 32° ; Young's modulus, ε_m = 5000MPa ; Poisson's ratio, ν = 0.25 ; rock quality, Q = 0.72 ; burial depth, H = 70 m, height of tunnel, h ≈ 9m, span ≈ 13m			
Failure mechanism	**Load description and calculation**	**Output**	**Main reference**	**Remark**
Sliding, overturning and settlement	Due to confining underground stresses acting in all directions, the cavern cannot slide, overturn or settle.	-	Marston & Anderson (1913) and Hoek et al. (1995)	Probability of occurrence increases for shallow caverns but not in deep underground tunnels.
Bearing capacity / support pressures and deformation	Typical modes of failure and they each act in all directions.			Likely expected
Collapse	**Vertical load, P_v on roof = load$_{heading}$** ***Acts at heading***		**Nielsen (2009)**	
	Description: Overburden weight causing geostatic pressure. Bierbäumer's theory Rock mass of height, αH acts on the excavated tunnel, where α = reduction coefficient and the rock mass slides down along conjugate planes inclined at (45° + 0.5ϕ) 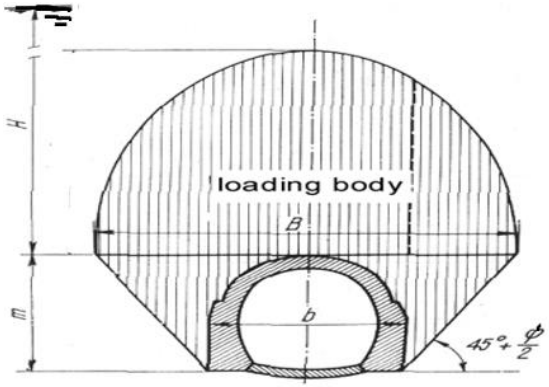 			

Table 4-2 continued: Analytical estimation of rock loads

Failure mechanism	Load description and calculation	Output	Main reference	Remark
	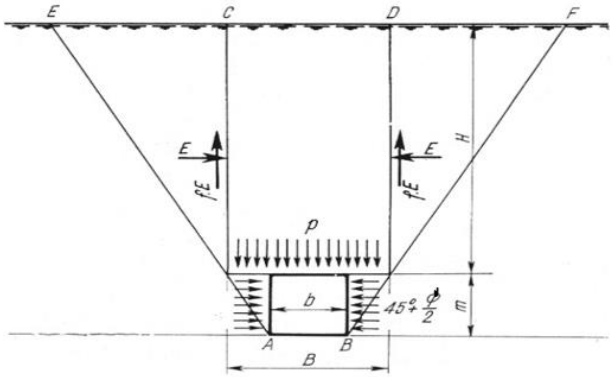 The main sliding rock mass counteracted by friction, S along adjacent vertical sliding planes, above the tunnel is illustrated by the load diagram. Friction is produced by the horizontal earth pressure of the wedges EC and DF acting on the vertical shear planes. Hence the force preventing movement of rock mass, S = *f*.E from Equation 4-1 $S = fE = \tan\phi \tan^2(45^\circ - 0.5\phi)(0.5H^2\gamma)$ **Equation 4-1** S = tan32 tan²(45°-16) (0.5x9²x27.5) = 213.84 Width, B is assumed to be equal to b+2m tan(45-0.5ϕ) as shown in Equation 4-2 $B = b + 2m\tan(45^\circ - 0.5\phi)$ **Equation 4-2** = 13+(2x9) tan 29 = 22.98m Substituting to solve for S as the friction resisting downward movement The roof pressure, P_v on width B is $\alpha_1 Hg$ where α_1 is the reduction coefficient. P_v can be determined using Equation 4-3. And uniformly distributed load, p = P/width……. (i) $P_v = H\gamma B - H^2\gamma\tan^2(45^\circ - 0.5\phi)\tan\phi$ **Equation 4-3**	S=213.84		

Table 4-2 continued: Analytical estimation of rock loads

Failure mechanism	Load description and calculation	Output	Main reference	Remark
	Substituting P into (i) gives Equation 4-4 $p = \frac{P}{B} = H\gamma[1 - \frac{\tan\phi \tan^2(45° - 0.5\phi)H}{B}]$ **Equation 4-4** collecting like terms gives Equation 4-5 $\alpha_1 = 1 - \frac{\tan\phi \tan^2(45° - 0.5\phi)H}{B}$ **Equation 4-5** Therefore, $P_v = \alpha_1 Hg = 799.17kN$ in terms of friction, S the coefficient can be calculated using Equation 4-6 $\alpha_1 = 1 - \frac{0.5SH}{B}$ **Equation 4-6** Note: The friction along the vertical planes reduces the overall geostatic pressure *Values of the reduction coefficient, α_1 corresponding with H and b are read from tables.* For very small overburden depths, $\alpha_1 = 1$ and at great depths where H > 5b, α_1 is independent of depth as shown in Equation 4-7. $\alpha_1 = \tan^4(45° - 0.5\phi)$ **Equation 4-7** For this case, H is > 5b therefore $\alpha_1 = 0.09$ <u>Terzaghi's theory</u> Based on a series of tests where K = 1, the vertical loading P_v relationship is given by Equation 4-8 $P_v = \frac{\gamma B}{2K\tan\phi}$ **Equation 4-8** *where* B, ϕ, and γ are the same as discussed under Bierbäumer's theory For this case, $P_v = ((27.5 \times 22.98) / (2\tan 32)) = 505.67kN$ **Prasad (2015)** $P_v = 0.5b\gamma$ *where* b = span of the tunnel and γ = unit weight of rock $P_v = 0.5 \times 13 \times 27.5 = 178.75kN$	P_v = 799.17kN P_v = 505.67kN P_v = 178.75kN		

Table 4-2 continued: Analytical estimation of rock loads

Failure mechanism	Load description and calculation	Output	Main reference	Remark
	Platts' caving arch theory: *Rock load exerts pressure, P_v on the upper lining* the theory is summarized by Equation 4-9 $P_v = \frac{2a}{3a_1}(3a_1^2 - a^2)$ **Equation 4-9** *where* a_1 is the half arch span of the underground cavern and a is half the bottom width of the underground cavern a = 13 / 2 = 6.5 and a_1 = 31.5 / 2= 15.75 substituting, P_v = ((2 x 6.5) / (3 x15.75)) x ((3 x 15.75 ^ 2) - 6.5^2) = 193.13kN The total vertical pressure, Q in upper tunnel is given by Equation 4-10 $Q = (2\,a_1 H\,\gamma) - (\gamma\,H^2)\tan^2(45° - 0.5\phi)\tan\phi$ **Equation 4-10** Q = (2x15.75x70x27.5) - (27.5x70^2) (tan29)^{2}tan32 = 34,765.98kN	P_h = 193.13 kN P_v = 34,765.98kN		No indication of a usual range of rock loads is documented hence the calculated values are considered absolute. However, 34,756.9kN is ignored since it is out of the range of other calculated values. **Thus, design P_v = 799.17kN**
Inward deformation	**Horizontal load / lateral earth pressures, P_h on side walls** ***Acts on sidewalls***		**Nielsen (2009)**	
	Terzaghi's rough estimate of lateral pressure is given by Equation 4-11 $P_h = 0.3\,\gamma\,(0.5m + h_p)$ **Equation 4-11** *where* h_p = height of loosening core representing the roof load based on Rankine's ratio, and its upper limit is usually 0.56B For this case, assuming the maximum extent, h_p = 0.56B = 12.87m P_h = 0.3 x 27.5 x ((0.5 x 9) +(0.56 x 22.98)) = 143.29kN Whereas for solid rocks, based on Poisson's ratio, ν the lateral pressure can be calculated from Equation 4-12 $P_h = \frac{\nu}{1-\nu}P_v$ **Equation 4-12** P_h = (0.25 / (1 - 0.25)) x 799.17kPa = 266.39kN	P_h = 143.29 kN P_h = 266.39 kN		The result conforms to theory (lateral pressures = ⅓P_v) since it approximates ⅓P_v ≈ 267kN

Table 4 2 continued: Analytical estimation of rock loads

Failure mechanism	Load description and calculation	Output	Main reference	Remark
	OR from Bierbäumer's theory, the horizontal pressure is given by Equation 4-13 $P_h = \gamma H \tan^2(45° - 0.5\phi)$ **Equation 4-13** P_h = 27.5 x 70 x (tan45 - (32 / 2)))^2 = 591.47kN For conservative design, largest P_h is considered thereby the design horizontal pressure is 591.47kN A linear distribution based on the theoretical vertical pressure and not overburden weight should be assumed for lateral pressures (The parabolic distribution indicates a peak load at the centre of the roof).	P_h = 591.47 kN **P_h = 591.47 kN**		For conservative design the highest value of **P_h = 591.47kN**.
Bottom heaving	**Invert load, P_{invert} at bottom ≈ ½load$_{heading}$** ***Acts at the invert***		**Nielsen (2009)**	
	The construction method influences the development, distribution and magnitude of bottom pressures. For closed invert arch tunnels, reactions to the roof pressures mostly act at the bottom and some load is taken up by the surrounding rock masses. Assumption: The active earth pressures displacing a wedge into the excavation are resisted by the passive earth pressures on the ground mass beneath the excavation. The active earth pressure is produced from vertical pressures on lateral parts. 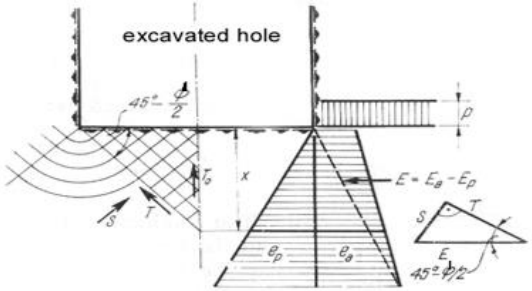		Tsimbaryevitch's theory	

Table 4-2 continued: Analytical estimation of rock loads

Failure mechanism	Load description and calculation	Output	Main reference	Remark
	The active earth-pressure diagram at the perpendicular of the corner point of the excavated cavity is a trapeze. The active earth pressure at depth x is given by Equation 4-14 $e_a = (p + x\gamma)\tan^2(45° - 0.5\phi) - 2c\tan(45° - 0.5\phi)$ **Equation 4-14** At the same time the specific passive earth pressure at depth x is given by Equation 4-15 $e_p = x\gamma\tan^2(45° - 0.5\phi) + 2c\tan(45° - 0.5\phi)$ **Equation 4-15** The depth below the tunnel invert under the influence of uplift pressures, x is obtained by equating Equation 4-14 and Equation 4-15 to give Equation 4-16 $x = \frac{P\tan^2(45° - 0.5\phi) - 2c[\tan(45° + 0.5\phi) + \tan(45° - 0.5\phi)]}{\gamma[\tan^2(45° + 0.5\phi) - \tan^2(45° - 0.5\phi)]}$ **Equation 4-16** where P = (H+m) γ, from the sketch x = {(79 x 27.5) $(\tan29)^2$ - (2 x 13.11) [tan61+ tan29]} / {27.5 x [$(\tan61)^2$ - $(\tan29)^2$]} = 7.47m Also, P contributing to P_{invert} = (H+m) γ = 79 x 27.5 = 2,172.5 kN e_a = (2172.5 + (7.47 x 27.5)) $(\tan 29)^2$ - (2 x 13.11) tan16 = 716.10 kN e_p = (7.47 x 27.5 $(\tan 29)^2$) + (2 x 13.11) tan16 = 745.17 kN E = $\lvert e_a - ep \rvert$ = 29.07kN The associated resultant horizontal force, E = difference in areas of active and passive pressures. The force pushes upwards into the cavern and induces conjugate sliding planes underneath the excavation (see Figure below).	E = 29.07 kN		Resultant horizontal force at tunnel invert which could cause sliding failure.

Table 4-2 continued: Analytical estimation of rock loads

Failure mechanism	Load description and calculation	Output	Main reference	Remark
	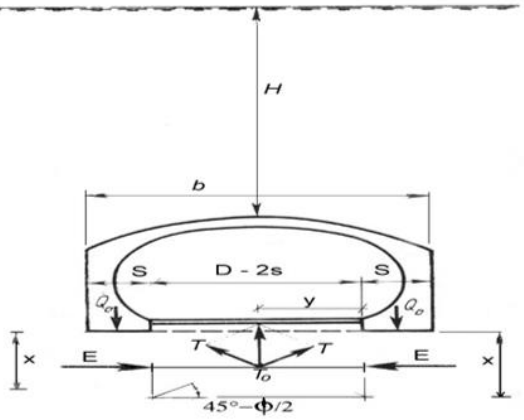 Hence resolving E into parallel and perpendicular components of the plane gives T and S, respectively T = E cos (45º - ϕ/2) = 29.07cos (45-(32/2)) = 25.43kN S = E sin (45º - ϕ/2) = 29.07sin29 = 14.09kN The parallel component tends to displace the rock wedge upward but it is resisted by the frictional component of the normal force, T T = Stanϕ = 213.84tan32 = 133.62kN The resultant uplift vertical pressure acting at the centre line on the bottom plane, resulting from bottom pressures acting at the corners and trigonometric transformations, is given by Equation 4-17 $T_o = 2E\,\frac{\sin^2(45° - 0.5\phi)}{\cos\phi}$ **Equation 4-17** Substituting and solving for T_o gives 16.11kN	To = 16.11kN		Upheaval force is much less than theory suggests as $0.5P_v$ = 399.59kN. Therefore, the larger value is considered hence **To = P_{invert} = 399.59kN**

Table 4-2 continued: Analytical estimation of rock loads

Failure mechanism	Load description and calculation	Output	Main reference	Remark
	Heaving can be prevented using a suitably dimensioned invert arch or by loading the base with a counter weight spread over length, y (Equation 4-18) $y = \frac{x}{\tan(45° - 0.5\phi)}$ **Equation 4-18** For this case, y = 7.47/tan29 = 13.48 m	y = 13.48 m		Breadth across which support is required
	Summary of instability problem In order to simplify a) the solution to the problem, the weights of the unstable wedges in the roof, sidewalls and invert are spread over the corresponding distances to obtain approximate uniformly distributed loads (UDLs) as shown in b) of the figure below. a 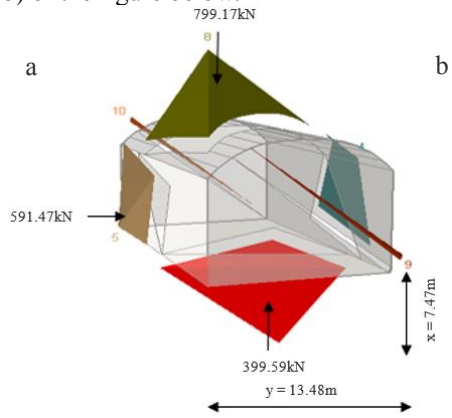 b 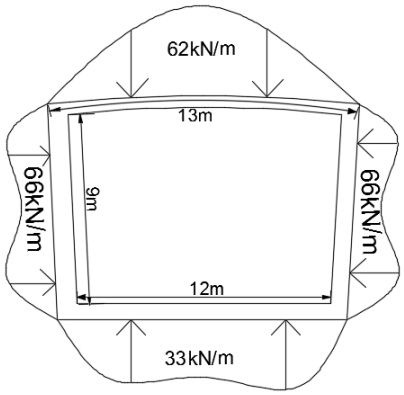			Although some research suggests the floor wedge is usually stable, from the calculations, support is necessary to support the entire surrounding rock mass in order to ensure robustness and safety of the hydro tunnel structure.

From the calculations (Table 4-2) the minimum expected support capacities are 799.17kN, 591.47kN and 399.59kN for the tunnel roof, sidewall and invert and their corresponding UDLs are 62kN/m, 66kN/m and 33kN/m, respectively. Whereas different designs could be considered to suit the variable requirements of the roof, sidewall and invert, for ease of practical application on site, a uniform bolt size corresponding to the highest load was recommended as the minimum capacity to withstand all loads. For this study, an ultimate load of 66kN/m was considered. A corresponding suitable rock bolt capacity is selected from manufacturers' design tables. Various tables are available and can be accessed online. This study used Table 4-3 because it was the manufacturer's option considered for the Karuma project by the contractor. From the table, a 16 mm diameter bolt with an ultimate load carrying capacity of 111kN was suitable.

Table 4-3: Example of rock bolt manufacturer design table

Type	Nominal diameter (mm)	Cross-sectional area (mm^2)	Yield strength (N/mm^2)	Tensile strength (N/mm^2)	Yield load (kN)	Ultimate load (kN)
GEWI® -left-hand thread	**16**	**201**	**500**	**550**	**101**	**111**
	20	314	500	550	157	173
	25	491	500	550	246	270
	28	616	500	550	308	339
	32	804	500	550	402	442
	40	1,257	500	550	628	691
	50	1,963	500	550	982	1,080
GEWI® Plus-right-hand thread	18	254	670	800	170	204
	22	380	670	800	255	304
	25	491	670	800	329	393
	28	616	670	800	413	493
	30	707	670	800	474	565
	35	962	670	800	645	770
	43	1,452	670	800	973	1,162
	57.5	2,597	670	800	1,740	2,077

Source: DSI (2012)

The choice of installation method including the decision to fully grout or not is usually tailored to suit specific geological conditions, the design geotechnical engineer's recommendation and the practical discretion of the contractor. This study recommended;

1. Inclusion of drainage provision behind the support rings. The geotechnical investigations recorded some sections as below the ground water table and some exposed rock surfaces were wet indicating some underground water flows (Karuma, 2015).
2. A pattern of fully grouted rock bolts with face plates installed at 1-1.5 m spacing apart. The bolts are necessary to provide primary support by stitching the rock mass, anchoring loose unstable wedges and resisting the peak loads. Face plates are necessary to cap the bolt and secure it firmly onto the rock surface (Franki, 2008). The closest minimum spacing is suggested to enhance the effect of the beam stitching thereby stability of the tunnel (Kristjánsson, 2014; JunLu, 1999).

3. 200 mm thick wire-mesh reinforced shotcrete lining. The purpose of this support ring will be to protect smaller rock wedges, not directly anchored by the bolts, from spalling (Franki, 2008).
4. A final lining of 400 mm thick reinforced concrete. This support ring provides secondary structural support to the excavation and it provides more permanency than the shotcrete (Hoek et al., 1995).

Contractor discretion and practicality are important in tunneling. Therefore, the design can be adapted accordingly but in consultation with an experienced geotechnical engineering practitioner.

4.2.4 Finite element method

Finite Element Methods (FEMs) comprising numerical approaches are useful for analysis of underground stresses and loading situations. The methods are used to calculate approximate ranges of a solution and generate two-dimensional (2D) or three-dimensional (3D) models (Kim & Yoo, 2002). The software models simulate ground-support interactions including tunnel deformation and construction sequences (RTM, 2009; Mohammed, 2015). This study used Rocscience RS^3 software FEM package because of its ability to replicate existing geomechanical properties, inbuilt tutorials and examples and its suitability to model rock mass of various discontinuous excavated in 13 m wide spans (Crouch & Starfield, 1984). Furthermore, RS^3 is recommended by the British Tunneling Society and the Institution of Civil Engineers and was used by Panda et al. (2014) to investigate the stability of tunnels at an operational hydropower plant in India (Tunnel Lining Design Guide, 2004). RS^3 3D models are solutions for the progressive rock mass failure based on the Mohr-Coulomb failure criterion (Hoek, 2016). Other Rocscience 2016 software packages used included UNWEDGE and RocData. Figure 4-10 shows (a) stereo net and (b) isolated unstable wedges drawn from the Karuma (2015) field-identified dense zone of jointing (foliation- N25~57°E NW(SE)∠70~85°) and steep dip joint sets (N15~33°W NE∠75~85°, N78~88°W NE∠75~85 and N73~82°W SW∠45~65°). Software generated surrounding rock loads using UNWEDGE are higher but within the range of calculated loads, except in the sidewalls. RocData was used to estimate shear strength characteristics, as shown in Figure 4-11, by adjusting the software inbuilt examples.

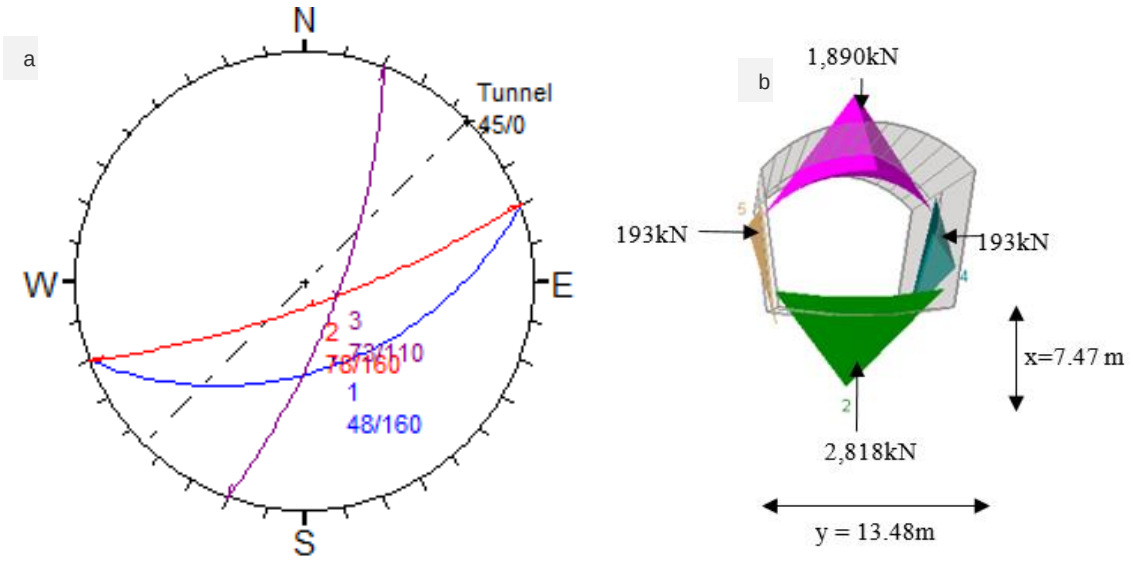

Figure 4-10: (a) Stereonet and (b) isolated unstable wedges based on joint sets

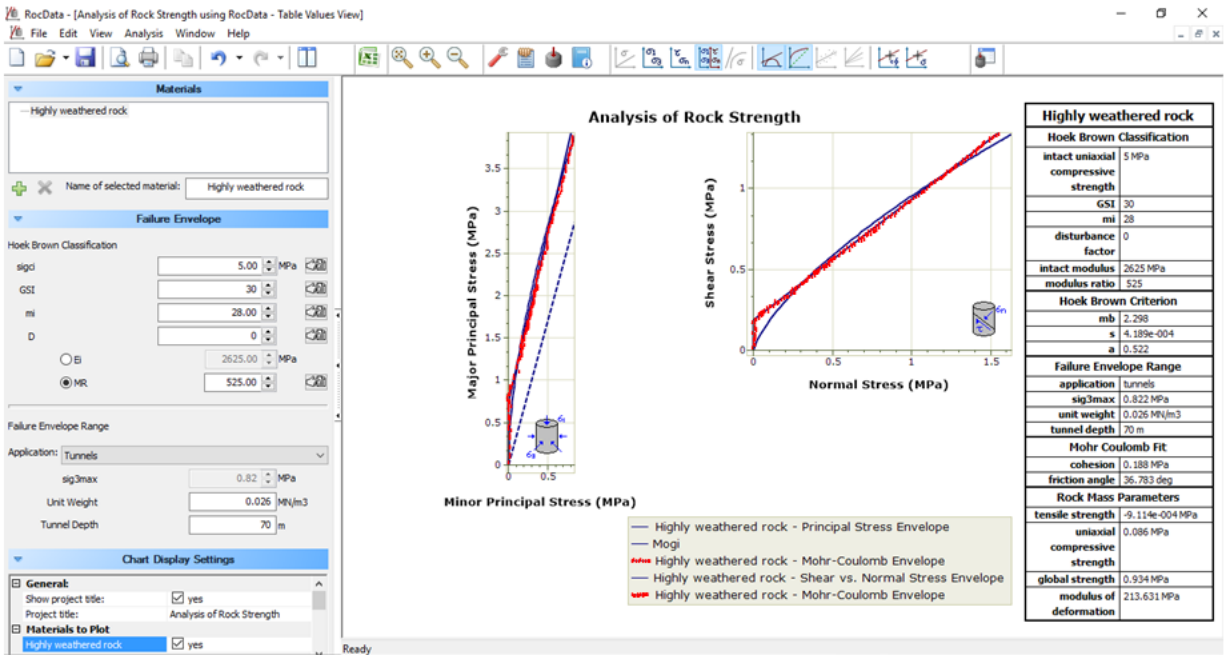

Figure 4-11: Shear strength curves for granite gneiss

Initially the software model was calibrated before the tunnel support system was designed. The purpose of calibration was to develop a model which replicates the actual field situation by either parameter fitting of measured or historic data or reliance on expert estimations (Shull, 2007). In this study, the recommended calibration method involved adjusting the mesh set up using 4 and 10 noded tetrahedron uniformly graded meshes (Carl et al., 2006). Eventually, expert estimations had to be relied on because of the RS^{3}software limitations to support parameter fitting. Development of the 3D RS^3 tunnel support system model involved the following generic steps (representative screenshots are included in Appendix D.4).

1. The project settings were adjusted to metric units, cartesian plane orientation of the plunge was horizontal, stress analysis as 500 iterations and groundwater conditions as none because no groundwater table was encountered.
2. External and excavation boundary conditions were specified by geometry selection.
3. Material properties and excavation sequence were defined. Slices were used to differentiate the rock materials and excavation was modelled using three sequential stages.

For conservative design, the weakest highly weathered granite gneiss rock material was analysed.

4. Support bolts and liner properties were defined.

Support capacities were selected based on four criteria 1) software suggested parameters, 2) published theory and experiences, 3) convergence of stresses and 4) iterative trial computations.

5. In-situ stress conditions were defined and boundary extents fixed by auto restrain underground so that the model performed as a rigid body during the analysis.

Caution was taken to ensure that the distance between boundary extents and the excavation was at least four times the tunnel diameter following TLDG (2004) recommendation.

6. Rock wedges were simulated by customizing a 4 noded tetrahedron graded mesh. The study model developed has 1,091,895 tetrahedron elements and 1,496,473 nodes in total.
7. Analysis was by computation of the model. Model instability was evaluated by considering field stresses, stress redistribution, displacement and associated unstable wedges.
8. Support parameters which limited deformation, stresses and failure of the surrounding rock mass were then selected. In this study, pattern rock bolting, wire mesh reinforced shotcrete and reinforced concrete linings were selected in order to ensure robust support of the excavation.
9. Finally, the results of the analysis were viewed.

The tunnel deformation which comprised stress redistribution (Figure 4-12), displacement (Figure 4-13), extent of failure zone (Figure 4-14) and loose wedges (Figure 4-15) were identified and evaluated. The red arrows showed the extent of tunnel deformation and the maximum value was read off the interpret window. The extent of unstable wedges was measured using a linear dimension tool and the longest dimension was approximately 3 m beyond the excavated face.

Results were assessed and the sequence of re-adjustment, re-meshing and re-computation of the model were repeated until eventually support which counteracted the deformation was achieved (Figure 4-16) and the model converged. The FEM analysis and support design are summarized in Table 4-4.

Table 4-4: Karuma tunnel support design

Rock class	Material description	Maximum mean effective stress (MPa)	Maximum total displacement (mm)	Extent of failure zone beyond excavation (m)	Support system
IV	Blocky soft rock mass with a high degree of weathering and discontinuities	51	36	3	Rock bolts, wire mesh reinforced shotcrete lining and reinforced concrete lining.
Description of the support (details of support properties are included in Appendix D-4)					
Rock bolts	19mm diameter ten-meter-long fully grouted steel bolts of 102 kN capacity spaced at 1.5 m apart on a 3 m x 3 m grid extending 3m beyond the tunnel roof and sidewalls. The bolts should be installed at the centre of steel face plates and trimmed to flash with the excavation.				
Shotcrete	200 mm x 200 mm grid of 4 mm diameter wire welded mesh. 200 mm thick layer reinforced shotcrete support ring installed on excavation.				
Concrete	Flexible final 400 mm thick class 25 concrete support ring overlying the shotcrete. Concrete's Young's modulus, E_s of 30000 hence the modulus ratio, (E_g / E_s) for the tunnel segment is 5000 / 30000 = 0.17				
Note: Initial modelling considers shotcrete of low modulus until it has hardened after 28-day strength (RTM, 2009)					

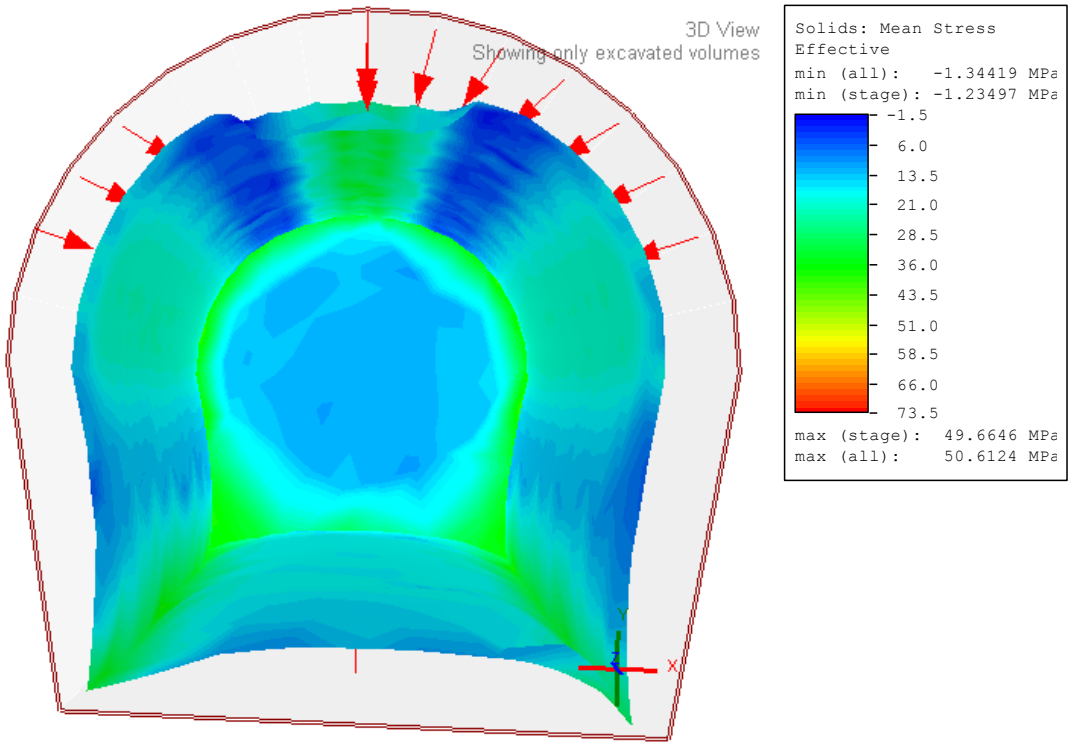

Figure 4-12: Deformed contours showing extent of caving in from stress redistribution

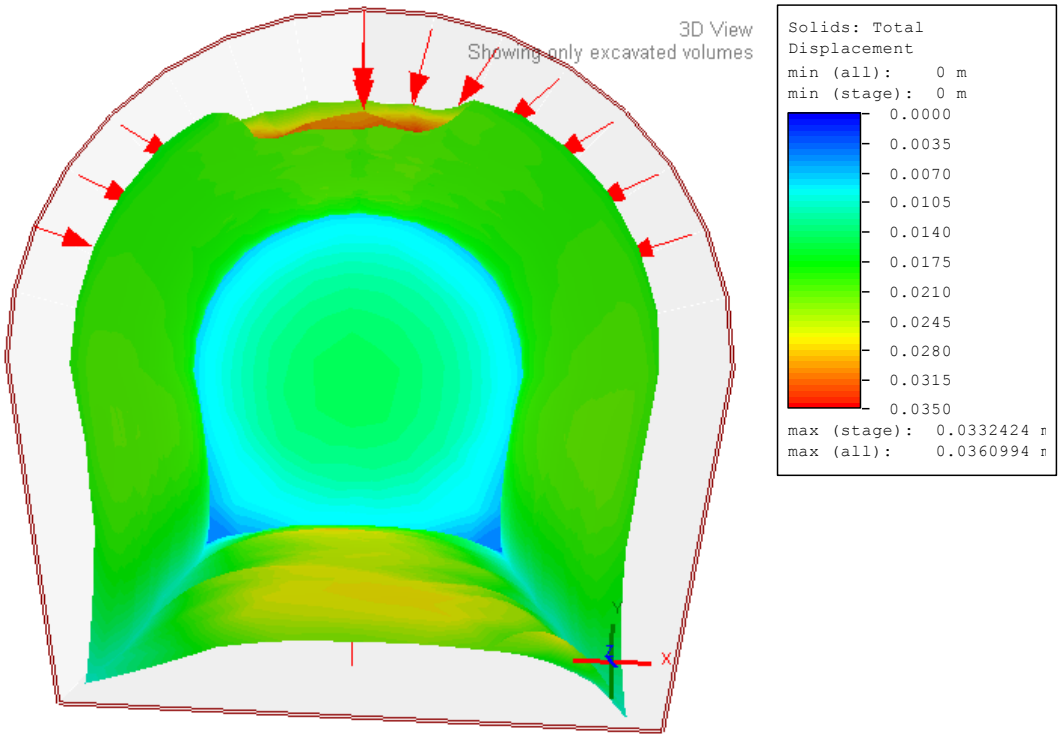

Figure 4-13: Deformed contours showing extent of caving in

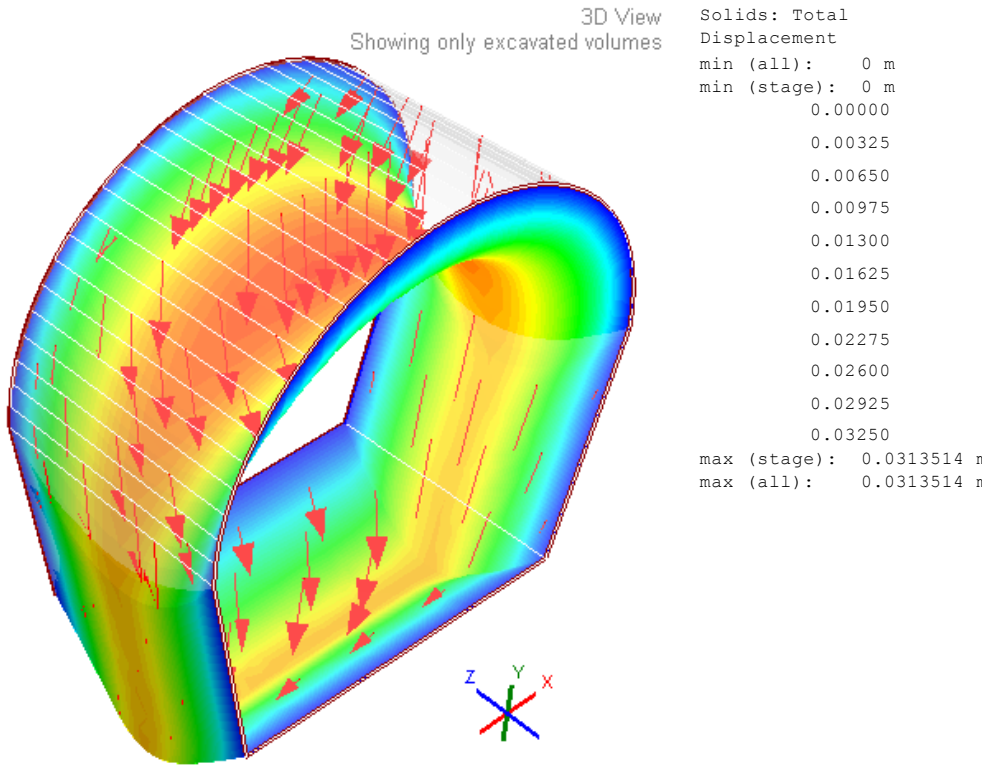

Figure 4-14: Perspective view of surrounding rock mass displacement vectors

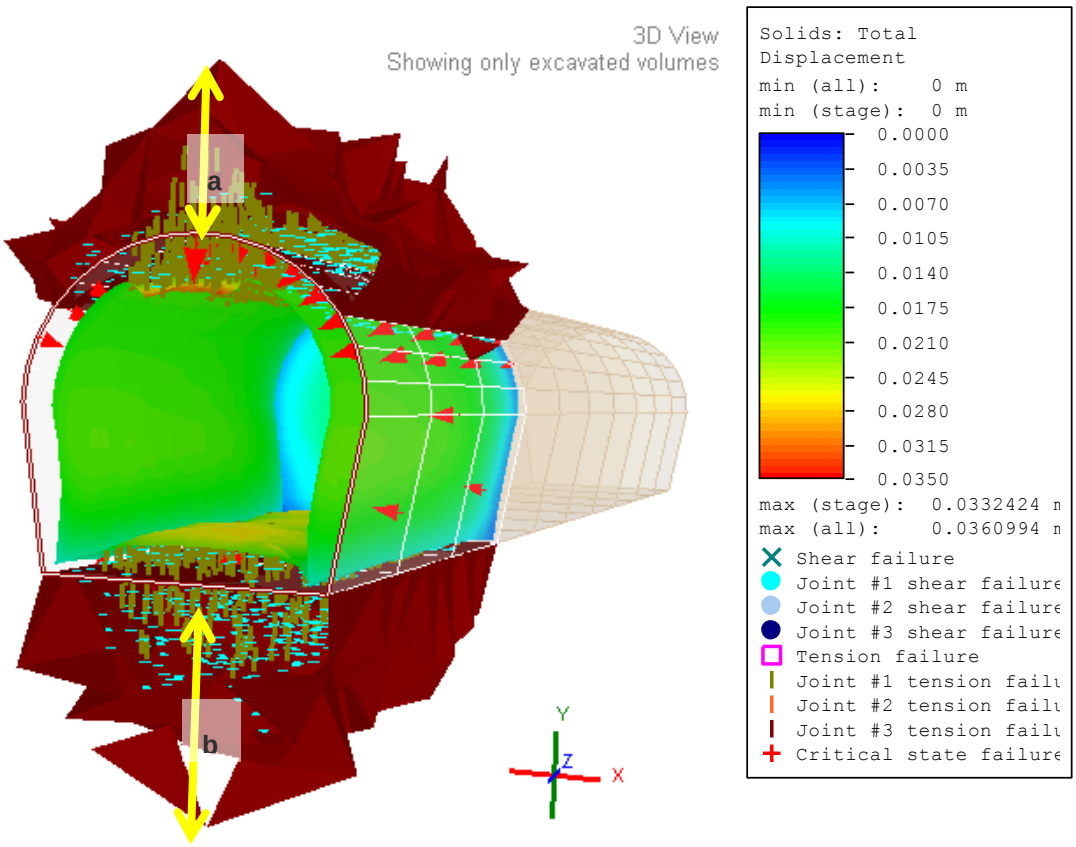

Figure 4-15: Extent of failure zone surrounding tunnel segment

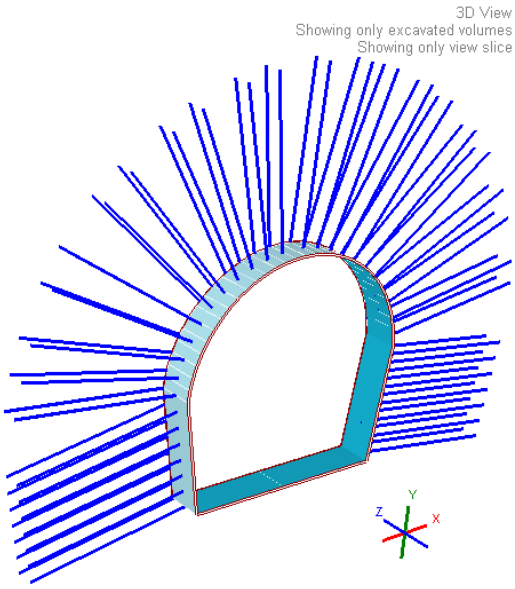

Figure 4-16: RS^3 Model of Karuma tunnel support system

4.2.5 Conventional method

Traditional methods to design tunnel supports are predominantly geological classification - using charts, commercial engineering software, observations and handy (pocket) tools. The exposed

rock type, features and discontinuities are evaluated by observation and by use of handy tools. The geological campus and hammer are common handy tools which are used to measure the angle of dip or strike of major discontinuities and to estimate rock strength when a mechanical force is applied onto the excavated surface by knocking it with both head and tip, respectively. Figure 4-17 shows both tools. Charts are used to quickly estimate suitable tunnel support requirements for site specific characteristics. Nonetheless, most geological methods are useful throughout the project lifecycle for both early approximations and final design.

Figure 4-17: (a) Geological compass and (b) Hammer
Source: Commons (2011)

During the site visit, along with an experienced geologist, the excavated surface was scratched, broken and peeled with a relatively hard blow of the tip of the hammer indicating weak rock (see Figure 4-18). Additionally, from the field observations, geological descriptions, structure and surface conditions of the rock, a GSI value of around 30 was selected from the inbuilt RocData GSI chart shown in Figure 4-19.

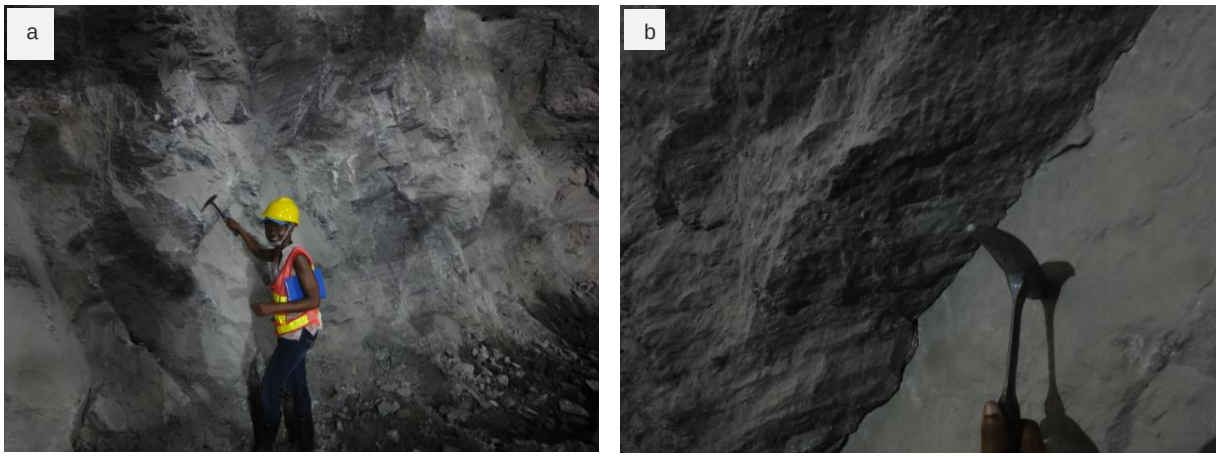

Figure 4-18: Assessing rock strength with a) tip and b) head of the geological hammer

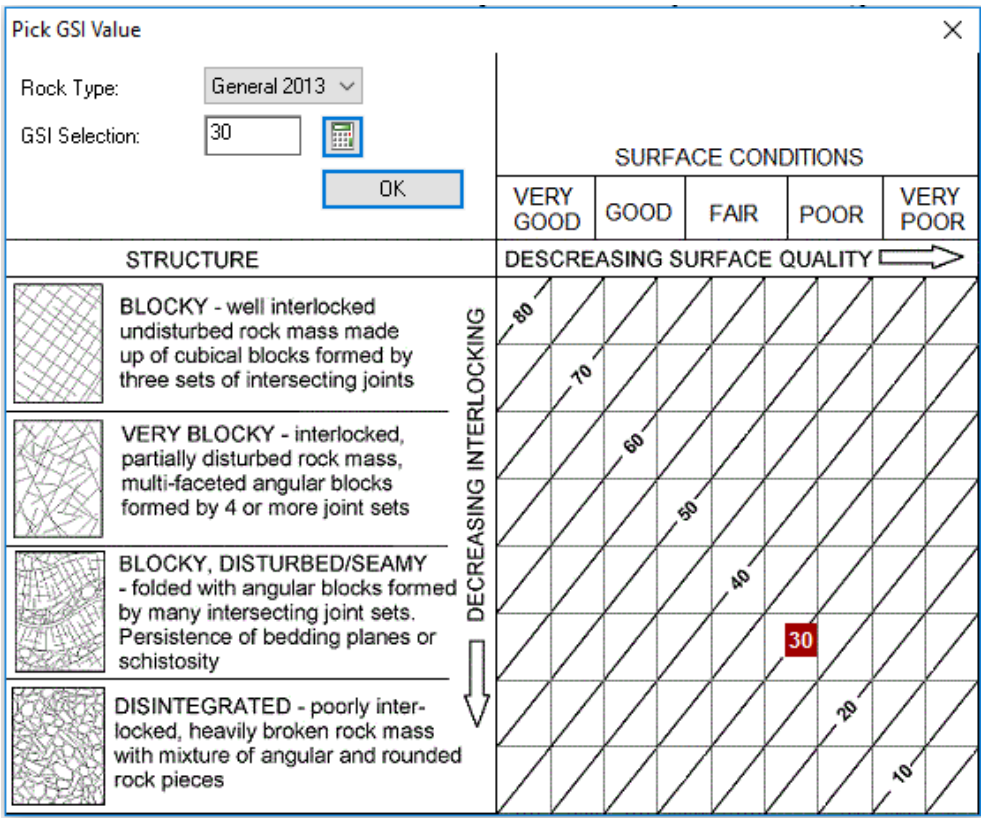

Figure 4-19: GSI estimation
Source: RocData (2016)

From the GIs, a Q value of 0.4 was obtained and recorded as indicative of very poor ground conditions. Conventional estimation of the tunnel support involved the following steps.

1. Using the Q value, the support capacity selected ranged between 30 to 60 tonnes per square meter as shown in Figure 4-20. In meteric units, the support is equivalent to 294.2 - 588.4kPa.
2. A more comprehensive estimation of support parameters was assessed using Figure 4-21.

The chart was used to estimate bolt length, spacing and shotcrete thickness by relating the Q-value, Excavation Support Ratio (ESR) and tunnel dimensions. The span and height relate to the sidewall and roof support, respectively.

3. The Span/ESR and Height/ESR ratio were computed and their intersections with the Q-value gave the suitable reinforcement category for the sidewalls and roof, respectively.
4. Corresponding details of support requirements were then read off at the bottom of the chart.
5. The bolt length for a unit ESR was read off at the right-hand vertical axis.
6. Suitable length of the rock bolt was then calculated as a product of the respective reading and the ESR value of 1.6.

Table 4-5 summarizes support requirements based on the conventional method. However, a 5 m bolt length and 200 mm thick shotcrete lining were considered for practical and safety reasons

instead of bolt lengths of 4.4 m and 120 mm and shotcrete thicknesses of 3.8 m and 90 mm for the sidewalls and roof, respectively.

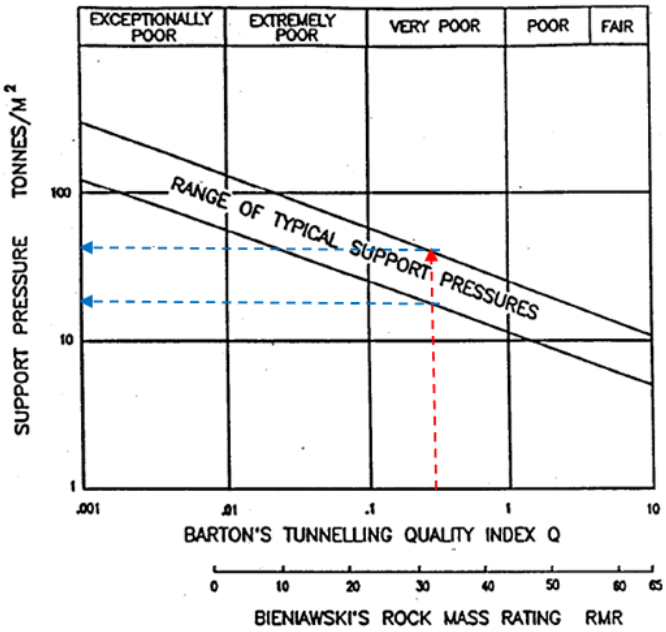

Figure 4-20: Estimated support capacity range
Adapted from Hoek (1999)

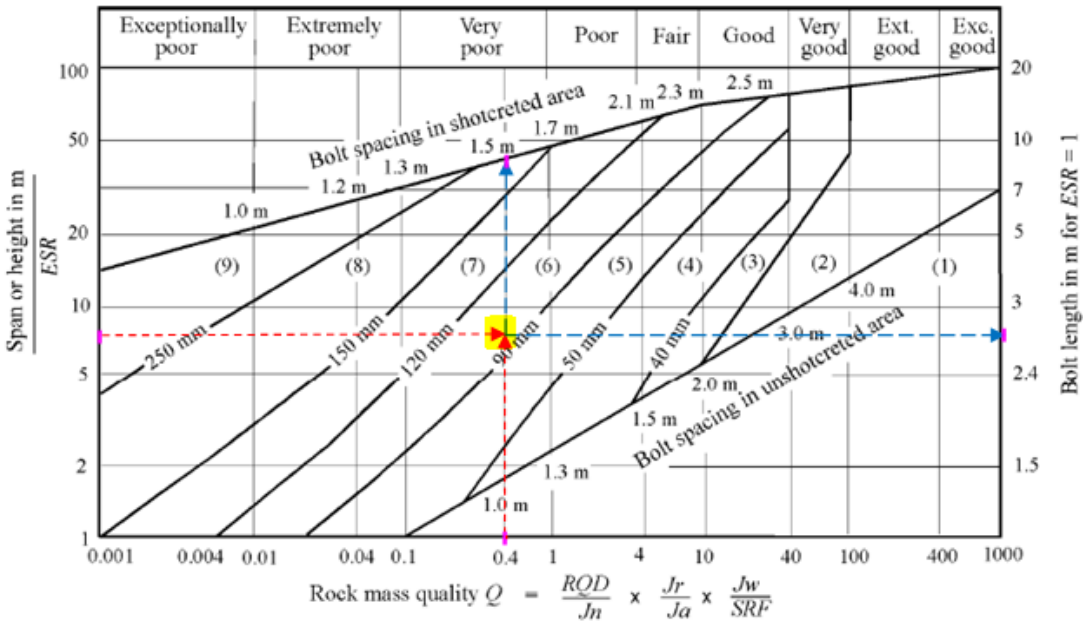

REINFORCEMENT CATEGORIES

1) Unsupported
2) Spot bolting
3) Systematic bolting
4) Systematic bolting with 40-100 mm unreinforced shotcrete
5) Fibre reinforced shotcrete, 50 - 90 mm, and bolting
6) Fibre reinforced shotcrete, 90 - 120 mm, and bolting
7) Fibre reinforced shotcrete, 120 - 150 mm, and bolting
8) Fibre reinforced shotcrete, > 150 mm, with reinforced ribs of shotcrete and bolting
9) Cast concrete lining

Figure 4-21: Comprehensive estimation of tunnel support
Adapted from Hoek et al. (1995)

Table 4-5: Karuma support requirements from charts

Parameter description	Sidewall	Roof
Support capacity (kPa)	294.2 - 588.4	294.2 - 588.4
Span/ESR	13 /1.6 = 8.125	9/1.6 = 5.625
Reinforcement category	6	5
Bolt length for ESR = 1 (m)	2.75	2.4
*Fibre reinforced shotcrete thickness (mm) from table 3-10	120	90
Fibre reinforced shotcrete thickness (mm) recommended by RTM (2009)	**200**	**200**
**Rock bolts [length (m) @ spacing (m)]	**5 @1.5**	**5 @1.5**
Notes: * For conservative design, upper limits of the ranges were considered ** Fully grouted bolts are recommended because of encountered perched water sources.		

From the second graph, the tunnel support was necessary but no actual capacities of the support could be determined using the second chart. Clearly, neither chart can be used independently to fully design tunnel support. Both methods are simplistic and incidental in nature because most important considerations such as hydrogeology, strain, in-situ stresses, Young's modulus and the Poisson's ratio are not catered for. The chart methods are fixed and constructability issues such as relaxation, stress redistribution and deformation which influence rock loads and support capacities are overlooked. Furthermore, there is no indication of concrete lining requirements.

4.3 Summary

This chapter presented three independent approaches to designing a tunnel support system. Geological conditions of a Karuma tunnel segment were considered. The support was designed by the analytical method, finite element method and conventional method. The analytical design of tunnel support gave the most conservative values of the rock loads, thereby support capacities. FEM analysis gave the least conservative capacities but significantly longer rock bolts. The traditional method estimated a range of support pressures. However, the methods were independent of each other and neither approach fed into another in any of the three methods thereby giving different outputs for the same instability problem. Therefore, the output results were dissimilar and not directly comparable. Table 4-6 summarizes the different results and the tunnel support system is illustrated in Figure 4-22 and Figure 4-23 below.

Considering the uniqueness of each method, it is recommended that the design of tunnel support systems assesses geotechnical engineering instability problems using each of the methods independently. The most conservative design, which represents the highest factor of safety, should then be considered as the required adequate parameter for stability of the underground excavated civil structure.

Table 4-6: Evaluation of Karuma tunnel support from the different methods

Item description	Analytical method	Finite Element Method (FEM)	Conventional method
Main basis and theme	Earth pressures	Geological and finite element analysis	Geological material characteristics
Rock loads to be resisted	P_v = 799.17 kN P_h = 591.47 kN P_{invert} = 399.59 kN	Compressive stress = 15 MPa	Unknown
Tunnel support system	Rock bolts, shotcrete and concrete	Rock bolts, shotcrete and concrete	Rock bolts, shotcrete and concrete
Support capacity	111 kN	102 kN	294.2 – 588.4 kPa
*Rock bolts [length (m) @ spacing (m)] (usually steel)	**Unspecified (usually available in 6m lengths)	10 @ 1.5	5 @ 1.5
Bolt diameter (mm)	16	19	**Unspecified
Fibre reinforced shotcrete thickness (mm)	200	200	200
Reinforced concrete lining (mm)	400 mm thick class 25	400 mm thick class 25	Unspecified

Notes:

1. For practical reasons, uniform supports are recommended for the tunnel roof, sidewall and invert.
2. Support installation is subject to practicability on site with regards to field geological conditions, construction method, contractor expertise, market availability and cost. However, a registered geotechnical engineer with underground experience must be consulted to ensure overall stability and safety of the excavation.
3. Field stresses, deformation and stress relaxation should be investigated continually.
4. * Fully grouted rock bolts with face plates are recommended.
5. **Bolt dimensions are according to manufacturer production lengths.
6. A minimum spacing of 1 m is usually recommended; although spacing generally depends on the rock quality and geological conditions encountered during tunnel excavation.

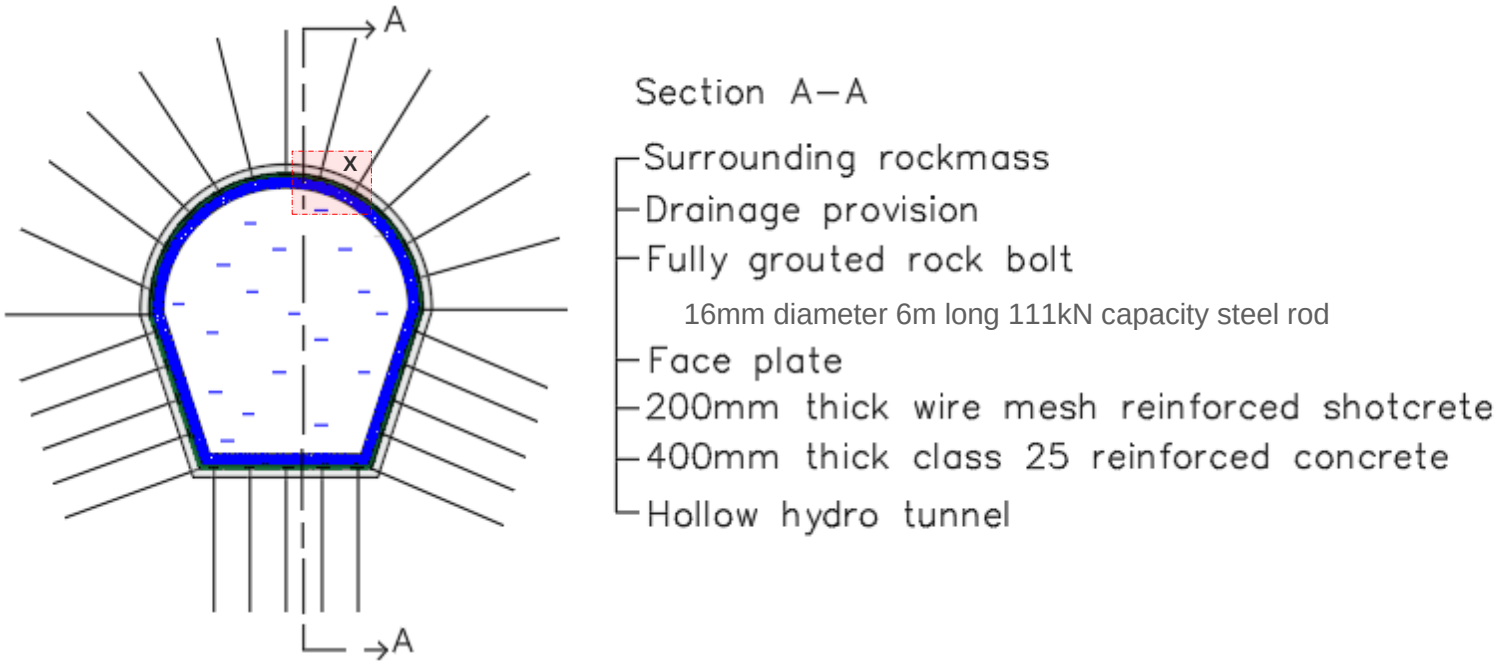

Figure 4-22: Tunnel support system for Karuma

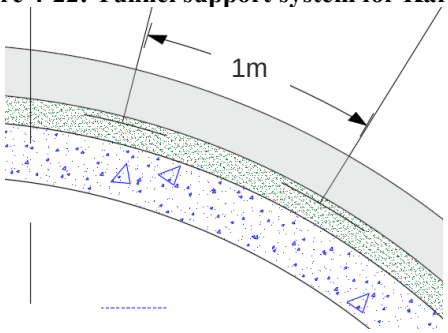

Figure 4-23: Detail X

5 CONCLUSION AND RECOMMENDATIONS

5.0 Introduction

This study, investigated the geological and geotechnical factors influencing the stability of tunnel support and design systems for safe and stable underground tunnels. The stability of the tunnel was checked by evaluating the peak loads causing instability at the tunnel roof, sidewall and invert. This was done in order to establish the minimum required resistance for stability of a tunnel.

Geological conditions and parameters of the proposed Karuma project in Uganda were used in this study to evaluate the loads causing instability. Geotechnical engineering design of the adequate tunnel support system was explored using the analytical, FEM and conventional methods. Conclusions and recommendations drawn from the study are presented in the following sections.

5.1 Conclusion

The study explored the design of a support system for a 9 m high 13 m wide span underground horseshoe-shaped tunnel excavated approximately 70 m below the ground surface. Karuma's typical geological conditions which formed the input for three approaches comprised highly weathered class IV rock with a unit weight, γ of 27.5kN/m^3, cohesion, c of 13.11kPa, angle of internal friction, ϕ of 32°, Young's modulus, E_m = 5000MPa, Poisson's ratio, ν of 0.25 and rock mass quality, Q of 0.72.

The following observations were made from the study;

1. The solution of an instability problem varies depending on the method used to analyze it.
2. The analytical, FEM and conventional methods are independent with no correlations.
3. Design of tunnel support systems by the analytical method was most conservative. In this study, an ultimate load of 799.17 kN was calculated for Karuma rock and the corresponding minimum principal support recommended was a pattern of 16 mm diameter fully grouted rock bolts, each of capacity 111kN spaced a meter apart.

Overall this study found that a comprehensive design of an adequate tunnel support system cannot be accomplished using only one approach. The required support selected should be the most conservative result of the different independent solutions. The highest capacity of the support represents the highest factor of safety, a universal engineering design concept. Through rigorous designs, underground geotechnical engineering instability problems causing tunnel catastrophes may consequently be minimized thereby addressing the societal outcries.

5.2 Recommendations

The following recommendations were made for further study to improve geotechnical engineering design of support systems for tunnel structures:

1. Undertake further research and studies to improve geotechnical engineering and rock mechanics equations for computation of rock loads, including possible determination of bolt spacing based on an equivalent uniformly distributed load.
2. Streamlining the analytical, FEM and convetional methods for the design of tunnel support systems in order to give correlated results to an instability problem.
3. Conducting a hollistic study which involves assesing the effect of each assumption independently and behavior of the excavation alongside real-time field testing and monitoring. Instrumentation can be embeded to record real time rock mass deformation and stress characteristics so as to develop a reliable mathematical tool based on actual field data.
4. Collation of tunnel information and data in order to model the behaviour of surrounding rock mass so as to assess actual field conditions and check practicality of the models.
5. Investigating the external prolonged pore water pressure build-up resulting from hydrogeological ground processes and internal water loads experiencing operational tunnels.

References

Adhikary, D.P. & Dyskin, A.V. 1997. *Modelling_the_Deformation_of_Underground Excavations in Layered Rock Masses.* International Journal of Rock Mechanics & Mineral Science Volume 34:3-4, ISSN 0148-9062 Paper 005 © Elsevier Science Ltd

Amadei, B. Stephansson. O. 1997. *Rock Stress and its Measurement*. Chapman and Hall, London

Amann, F. Ündül, Ö. & Kaiser, P.K. 2014. *Crack Initiation and Crack Propagation in Heterogeneous Sulfate-Rich Clay Rocks* Rock Mechanics and Rock Engineering Volume 47, Issue 5, pp. 1849–1865

American Federation of Mineralogical Societies. 2014. *Mohs Scale of Mineral Hardness*. Retrieved on 2016 October 3 from http://www.amfed.org/t_mohs.htm

Archanjo, J. C. Hollanda, M. H. B.M., Rodrigues, W.O. S., Neves, B. B.B. & Armstrong, R. 2008. *Fabrics of Pre- and Syntectonic Granite Plutons and Chronology of Shear Zones in the Eastern Borborema Province, NE Brazil.* Journal of Structural Geology 30 (2008) pp. 310-326

Badenhorst, W. Theron, E. & Stott, P. 2015. *Duplicate Testing Conducted on the Input Parameters for the Estimation of Potential Expansiveness of Clay.* Innovative Geotechnics for Africa © ISBN: 978-9938-12-936-6 pp. 605-610

Balmer, G. 1952. *A General Analytical Solution for Mohr's Envelope*. American Society for Testing aand Materials (ASTM) 52, pp. 1260-1271.

Barla, G. 1974. *Rock Anisotropy: Theory and Laboratory Testing*. Rock Mechanics. Udine, Italy: L. Muller. 131

Barton, N., Lien, R. & Lunde, J. 1974. *Engineering Classification of Rock Masses for the Design of Tunnel Support.* Journal of Rock Mechanics Volume 6 pp. 189-236 © Springer-Verlag

Barton, N. & Grimstad, E. 2014. *Forty Years with the Q-system in Norway and Abroad.*

Beaver, P. 1972. *A History of Tunnels* The Citadel Press. Secaucus New Jersey

Bertuzzi, R. & Pells, P.J. 2002. *Design of Rock Bolt and Shotcrete Support of Tunnel Roofs in Sydney Sandstone.* Australian Geomechanics: Journal and News of the Australian Geomechanics Society, 37(3), pp. 81-90

Bickel, J. O., Kuesel, T.R. & King, E. H. 1996. *Tunnel Engineering Handbook*. e-ISBN-13: 978-1-4613-0449-4 Second Edition. Chapman & Hall

Bieniawski, Z.T. 1973. *Engineering Classification of Jointed Rock Masses*. Trans-South African Institution of Civil Engineers. Volume 15, pp. 335-344.

Bieniawski, Z.T. 1992. *Design Methodology in Rock Engineering*. Balkema, Rotterdam

Blake, L. S. 1989. *Civil Engineers Reference Book*. Fourth Edition. © Elsevier Ltd ISBN-13: 978-0750619646

Bond, A. & Harris. A. 2008. *Decoding Eurocode 7*. Taylor and Francis Group ISBN 0-203-93772-4

Bondarchuk, A. Ask, M. V. S., Dahlström, L. O. & Nordlund, E. 2012. *Rock Mass Behavior Under Hydropower Embankment Dams: A Two-Dimensional Numerical Study*. Rock Mechanics and Rock Engineering. doi:10.1007/s00603-011-0173-2

Boniwell, M. 2015. Retrieved on 2016 August 15 from http://www.chockstone.org/chockstone.asp

Brown, E. T., Bray. J. W., Ladanyi. B. & Hoek. E., 1983. *Ground Response Curves for Rock Tunnels.* Journal of Geotechnical Engineering, Volume 109, No. 1. ©ASCE, ISSN 0733-9410/83/0001-0015

Carl. J., Müller-Hoeppe. D. & Meadows. M. 2006. *Comparison of Tetrahedral and Brick Elements for Linear Elastic Analysis.* Term Project AFEM Spring 2006. Retrieved on 2016 June 20 from www.colorado.edu/engineering/cas/courses.../CarlMullerMeadows.report.pdf

CEDD, 2015. *Catalogue of Notable Tunnel Failures - Case Histories (up to April 2015).* Civil Engineering and Development Department (CEDD) HongKong. Retrieved on 2016 July 12 from http://www.cedd.gov.hk/eng/publications/geo/doc/HK%20NotableTunnel%20Cat.pdf

Chatzivasileiadis, S., Ernst. D. & Andersson. G. 2013. *The Global Grid*. Renewable Energy 57 pp. 372-383 Elsevier Ltd.

CIRIA C683, 2006. *The Rock Manual*. The Use of Rock in Hydraulic Engineering. ISBN: 0-86017-683-1. London

CNN, 2012. Retrieved on 2016 September 5 from http://edition.cnn.com/2012/12/03/world/asia/japan-tunnel/

Commons, 2011. Retrieved on 2016 July 01 from https://en.wikipedia.org/wiki/Geologic_map#/media/File:Brunton.JPG

Craig, R. F. 2004. *Craig's Soil Mechanics*. Spon Press ISBN 0-203-57441-9

Crouch S. L. & Starfield A. M. 1984. *Boundary Element Methods in Solid Mechanics* Quarterly Journal of Engineering Geology and Hydrogeology v.17:399-400, doi:10.1144/GSL.QJEG.1984.017.04.18

de Wit, J.C.W.M. & van Putten, E. 2012. *Immersed Tunnels*. Competitive tunnel technique for long (sea) crossings.

Deree, U. D. & Deree, W. D. 1989. *Rock Quality Designation (RQD) After Twenty Years*

Dunning, J. 2005. *Earth Materials and Processes: Minerals and Earth Chemistry*. G-103 Module Two Lecture Notes. Indiana University Bloomington. Retrieved on 2016 July 18 from http://www.indiana.edu/~g103/theinteractiveearth/2-minerals/module2.html

Durrheim, R.J., Roberts, M.K.C. Haile, A.T., Hagan, T.O., Jager, A.J., Handley, M.F. Spottiswoode, S.M. & Ortlepp W.D. 1998. *Factors Influencing the Severity of Rockburst Damage in South African Gold Mines.* The Journal of the South African Institute of Mining and Metallurgy pp.53-58

DSI, 2012. Dywidag Systems International (DSI). *DSI ALWAG Systems Mechanical Anchors and Rebar Rock Bolts en* Retrieved on 2016 October 2 from http://www.dywidag-systems.com/uploads/media/DSI-ALWAG-Systems_Mechanical-Anchors-and-Rebar-Rock-Bolts_en.pdf

Eberhardt, E. 2012. *The Hoek–Brown Failure Criterion*. Geological Engineering, EOAS, University of British Columbia, Vancouver, Canada. DOI 10.1007/s00603-012-0276-4 © Springer-Verlag

Elam, M. L. 2009. *Great Naval Shipworm Teredo navalis*. Pacific Northwest Aquatic Invasive Species Profile Retrieved on 2016 July 7 from http://depts.washington.edu/oldenlab/wordpress/wp-content/uploads/2013/03/Teredo-navalis_Elam.pdf

Marshall, C. & Fairbridge, R. 1999. *Encyclopedia of Geochemistry*. Encyclopedia of Earth Sciences Series. Springer Netherlands. Series ISSN 1388-4360

FHA, 1991. *Rock and Mineral Identification for Engineers* U.S. Department of Transportation Federal Highway Administration (FHA). Retrieved on 2016 July 18 from https://www.fhwa.dot.gov/pavement/pccp/fhwahi91205.pdf

Franki, 2008. *A Guide to Practical Geotechnical Engineering in Southern Africa* - Fourth Edition

Gargaud, M. 2011. *Encyclopedia of Astrobiology*. Volume 3 Springer Science & Business Media. ISBN 9783642112713

Gemstone.com, 2016. *Mohs Scale of Mineral Hardness*. Retrieved on 2016 October 3 from http://www.gemstoneuniverse.com/media/articles/images/m/o/mohs_scale_of_mineral_hardness_chart.jpg

Geology.com, 2015. *Granite* Retrieved on 2016 August 12 from http://geology.com/rocks/granite.shtml © 2005-2016

Ghimire, N. S. B. & Reddy. M. J. 2013. *Optimal Reservoir Operation for Hydropower Production using Particle Swarm Optimization and Sustainability Analysis of Hydropower*. ISH Journal of Hydraulic Engineering, 2013 Volume 19, No. 3, 196–210, http://dx.doi.org/10.1080/09715010.2013.796691

Ghobadi, M. H. Firuzi, M. & Asghari-Kaljahi, E. 2016. *Relationships Between Geological Formations and Groundwater Chemistry and Their Effects on the Concrete Lining of Tunnels* (Case Study: Tabriz Metro line 2) Environmental Earth Sciences doi:10.1007/s12665-016-5785-0 © 2016 Springer International Publishing.

Greer, A. J. 2012. *Finite Element Modeling and Stress Analysis of Underground Rock Caverns.* University of California, Irvine, ProQuest Dissertations Publishing, 2012. 3512688.

Guidelines for Soils and Rock Logging in South Africa. 2001. Second Impression, edited by A.B.A. Brink and R.M.H. Bruin, Proceedings of Geoterminology Workshop organised by AEG,SAICE, and SAIEG, 1990

Hadjigeorgiou, J. 2016. *Rock Support: Degradation and Failure* Proceedings of the Ground Support 2016, Luleå, Sweden. Edited by Nordlund, E., Jones, T. and Eitzenberger, A.

Hapgood, F. 2004. *The Underground Cutting Edge: The Innovators who made Digging Tunnels High-tech.* Invention & Technology Volume 20, #2 Retrieved on 2016 August 5 from http://www.mindfully.org/Technology/2004/Underground-Boring-Machines1sep04.htm

He, M. 2014. *Latest Progress of Soft Rock Mechanics and Engineering in* China. Journal of Rock Mechanics and Geotechnical Engineering, 6(3), pp. 165-179. doi:10.1016/j.jrmge.2014.04.005

Headland, P., Strater, N. & Younis, M. 2008 *Rock Mass Characterization for the WSSC Bi-County Water Tunnel.* North American Tunneling 2008 Proceedings. Ed. Roach. ISBN 9780873352635 pp. 513-521

Heck, P., Nilipour, N. & Seingre, G. 2016. *Lessons Learned from Detailed Design and Construction of Nant-De-Drance Powerhouse*. Proceedings of the Hydro2016 conference, 10-12 October, Montreux, Switzerland

Heidbach, O. Tingay, M. & Wenzel, F. 2010. *World Stress Map Project Newsletter June 2010*. Frontiers in Stress Research. Tectonophysics 482 (2010) pp. v–vi doi:10.1016/j.tecto.2009.11.009 Retrieved on 2016 July 01 from http://mdcampbell.com/WSM_Newsletter_June_2010.pdf

Hemphill, G. B. 2012. *Practical Tunnel Construction* © John Wiley & Sons, 05 Oct 2012 - Technology & EngineeringISBN 9781118330005

Hochella, M. F., Eggleston, C. M., Elings, V. B., Parks, G. A., Brown, G. E., Wu, C. M., & Kjoller, K. 1989. *Mineralogy in two Dimensions: Scanning Tunneling Microscopy of Semiconducting Minerals With Implications for Geochemical Reactivity* American Mineralogist, Volume 74, pp. 1233-1246

Hoek, E. 1977. *Structurally Controlled Instability In Underground Excavations.* American Rock Mechanics Association 18th U.S. Symposium on Rock Mechanics (USRMS), 22-24 June, Golden ARMA-77-0362

Hoek, E. 1993. *Practical Rock Engineering*. Unpublished rock engineering course notes prepared for the University of Toronto.

Hoek, E. 1999. *Rock Engineering Course Notes.* Rotterdam, The Netherlands: A. A. Balkema Publishers.

Hoek, E. 2001. *Big Tunnels in Bad Rock.* Journal of the Geotechnical and Geo-environmental Engineering, Volume 127, No. 9, pp. 726-740.

Hoek, E. 2016. *Hoek's Corner.* Accesed on 2016 September 23 from https://www.rocscience.com/learning/hoek-s-corner

Hoek, E. & Bray, J.W. 1991. *Rock Slope Engineering*. Elsevier Science Publishing: New York.

Hoek, E, Carranza-Torres, C., Diederichs, M. & Corkum, B. 2008. *The 2008 Kersten Lecture. Integration of Geotechnical and Structural Design in Tunneling.* Tutorial 18 Vlachopoulos and Diederichs method_H2008

Hoek, E., Kaiser, P. K. & Bawden, W. F. 1995. *Support of Underground Excavations in Hard Rock.* Rotterdam, Netherlands: A. A. Balkema Publishers. ISBN 89 5410 187 3

Hoek, E. 2014. *Rock-Support Interaction Analysis for Tunnels in Weak Rock Masses.* Retrieved on 2016 October 31 from Geotechpedia.com

Hustrulid, W. A. 2000. *Slope Stability in Surface Mining* SME ISBN: 9780873351942

IEA, 2014. *Key World Energy Statistics*. International Energy Agency (IEA) Report

Iowa, 2014. The Collaboration for NDT Education Resource Center, Iowa State University, www.ndt-ed.org. © 2016 Reference An IAC Publishing Labs Company

Ingerslev, C. 2010. *Immersed and floating tunnels*. Science direct. Procedia Engineering 4 (2010) pp.51-59

Ingerslev, L.C.F. 2003. *Understanding immersed and floating tunnels.* (Re)Claiming the Underground Space, Saveur (ed.) © 2003 Swets & Zeitlinger, Lisse, ISBN 90 5809 542 8 257 Volume 1, pp. 257 – 263 The Netherlands: A.A. Balkema Publishers.

ITA, 2009. *General Report on Conventional Tunneling Method* (No. 002). International Tunneling Association (ITA) ISBN: 978-2-9700624-1-7 No.002

Jauch, F. 2000. *Using Borehole Geophysics for Geotechnical Classifications of Crystalline Rock Masses in Tunneling*. PhD Dissertation. Swiss Federal Institute of Technology, Zurich. Retrieved on 2016 July 23 from http://e-collection.library.ethz.ch/eserv/eth:23677/eth-23677-02.pdf

Jean, P., Amelot. A., Andre. D., Berbet. F., Bousquet-Jacq. F., Curtil. S., Durville. J., Fabre. D., Fleurisson. J., Gaudin. B., Goreych. M.,Homand. F., Parais. G., Peraud. J., Robert. A., Vaskou. P., Vibert. C. & Wojtkowiak. F. 2003. *A.F.T.E.S Guidelines for Caracterisation of Rock Masses Useful For the Design and the Construction of Underground Structures*

Jones, A. P. 1989. *Civil Engineers Reference Book*. Rock Mechanics and Rock Engineering. Edited by L S Blake © Reed Educational and Professional Publishing Ltd. The Bath Press, Bath ISBN O 7506 1964 3 pp.10/3-10/39

Jones. F. 2017. *Electrical Resistivity of Geologic Materials*. University of British Columbia, Department of Earth and Ocean Sciences, Accessed from https://www.eoas.ubc.ca/ubcgif/iag/foundations/properties/resistivity.html

Kalinga, O. J. 2016. *East African Mountains.* Encyclopædia Britannica Online. Retrieved on 2016 July 15 from https://global.britannica.com/place/East-African-mountains

Kang, H. P. & Lu, S. L. 1991. *An Analysis on the Mechanism of Roadway Floor Heave*. China Journal of Rock Mechanics and Engineering 10(4): pp. 362–373

Kanji, M. A. 2014. *Critical Issues in Soft Rocks*. Journal of Rock Mechanics and Geotechnical Engineering, 6(3), 186-195. doi:10.1016/j.jrmge.2014.04.002

Karuma, 2014. Karuma Hydropower Plant. Basic Design Report 2 Engineering Geology

Karuma, 2015. Karuma Hydropower Plant. Technical Design Report (Volume II Engineering Geology)

Kawata, K., Isago, N., Kusaka, A. & Mashimo, H. 2014. *Research on the Effect of Risk Mitigation Measures Against Earthquake for mountain Tunnel Through Static Loading Test*. North American Tunneling 2014 Proceedings. Society for mining, Metallurgy & Exploration Inc. pp. 337-344. Ed. Davidson et al., ISBN 0873354001, 9780873354004

Kent, S. 1860. *Water World* © copyright waterwereld 2002-2025 Retrieved on 2016 July 7 from http://www.waterwereld.nu/shipworm.php

Keyter, G. J. 2016. *Ingula Pumped-Storage Scheme: Design, Construction, Instrumentation and Monioring of the Ingula Power Caverns*. Proceedings of the Hydro2016 conference held in Montreux, Switzerland. October 10-12, 2016.

Kim & Yoo, 2002. *Design Loading for Deeply Buried Box Culverts.* Highway Research Center Auburn University, Alabama

Kimball, D. 2007. *A Scale Model of Marc Brunel's Tunneling Shield in the Brunel Museum at Rotherhithe.* Retrieved on 2016 July 7 from http://www.smithsonianmag.com/history/the-epic-struggle-to-tunnel-under-the-thames-14638810/?no-ist

Konstantis, Konstantis & Spyridis, 2016. *Tunnel Losses: Causes, Impact, Trends and Risk Engineering Management.* World Tunnel Congress (WTC) 2016-Poster-v1-3

Kristjánsson, G. 2014. *Rock Bolting and Pull-out Test on Rebar Bolts*. Thesis Norwegian University of Science and Technology

Lance, G., Anderson. J. & Lamont. D. 2007. *Third Party Safety Issues in International Urban Tunneling.* Underground Space- 4th Dimension of metropolises- Bartak, Hrdina, Romancov & Zlamal (eds) © Taylor & Francis Group, London, ISBN 978-0-415-40807-3

Langer, B. 1994 *Excerpt of Course Notes for University of Alaska Fairbanks*. Retrieved on 2016 August 23 from http://www.uaf.edu/files/olli/Lab2_Final_RockID.pdf

Leveson, D. J. 2005. Geology Course Notes. Brooklyn College. Retrieved on 2016 October 3 from http://academic.brooklyn.cuny.edu/geology/leveson/core/graphics/hardsim/mohs.gif

Li, S. Q., Feng, T. & Wang, C. L. 2005. *Study on Mechanism and Control of Soft Rock Roadway Floor Heave in Gequan Coal Mine*. China Journal of Rock Mechanics and Engineering 24(8): pp.1450–1455

Liu, Q. S. & Zhang, H. 2003. *Study on Stability and Support of Rock Masses Surrounding Deep Coal-Mine Roadway*. China Journal of Rock Mechanics and Engineering 22(S1): pp. 2195–2220

Luwalaga, 2013. Retrieved on 2016 April 22 from https://sites.google.com/site/luwalagahome/2013-work/presentations/8-0-tunneling

Lynn, A. 2006. *Box Jacking- A Useful Construction Tool*. 4th International Engineering and Construction Conference - July 28, 2006. pp. 1-5. Retrieved on 2016 July 10 from http://berkeleyengineering.com/box-jacking-paper.pdf

Marie, J. 1998. *Tunneling: Mechanics and Hazards*. Retrieved on 2016 September 9 from http://www.umich.edu/~gs265/tunnel.html

Marinos, V. 2014. *Tunnel Behaviour and Support Associated with the Weak Rock Masses of Flysch*. Journal of Rock Mechanics and Geotechnical Engineering, 6(3), 227-239. doi:10.1016/j.jrmge.2014.04.003

Marston, A. & Anderson, A. O. 1913. *Theory of Loads on Pipes in Ditches*.

McDonough, W. F. 1995. *The Composition of the Earth*. Chemical Geology

Mokhtari. M., Alqahtani. A. A. & Tutuncu. A.N. 2013. *Failure Behavior of Anisotropic Shales*. 47th United States Rock Mechanics / Geomechanics Symposium, San Francisco, USA.

Mohammed, J. 2015. *Underground Structures Support, Stress & Strain of Tunnel*

Murck, W.B., Skinner, J. B. & Porter, C. S. 1997. *Dangerous Earth*. An Introduction to Geologic Hazards. J. Wiley, ISBN 0471135658, 9780471135654

NEH, 2012. *Engineering Classification of Rock Materials*. Chapter 4, National Engineering Handbook (NEH). Part 631 Geology. United States Department of Agriculture (USDA), Natural Resources Conservation Service (NRCS). Retrieved on 2016 July 18 from http://directives.sc.egov.usda.gov/OpenNonWebContent.aspx?content=31848.wba

NGS, 2015. National Geographic Society (NGS) Produced by Caryl-Sue and edited by Jeannie Evers, Emdash Ed. Retrieved on 2016 July 17 from http://nationalgeographic.org/encyclopedia/crust/

Nielsen,Y. 2009. *Loads on Tunnels*._Course Notes_Tunnel Design & Construction Middle East Technical University (METU)

NTSB, 2007. *Ceiling Collapse in the Interstate 90 Connector Tunnel Boston*, Massachusetts, July 10, 2006. National Transportation Safety Board (NTSB). Highway Accident Report NTSB/HAR-07/02. Washington, DC.

Ongodia, J.E., Kalumba, D. & Mutikanga, H.E. 2016. *An Account of Tunnel Support Systems for Soft Rock Mass Conditions*. Proceedings of the first Southern African Geotechnical Conference held in Sun City, South Africa, March- Jacobsz (Ed.) Taylor & Francis Group, London, ISBN 978-1-138-02971-2 pp. 205-211

Owor, M., Tindimugaya, C., Brown, L., Upton, K. & Ó Dochartaigh, B.É. 2016. *Africa Groundwater Atlas: Hydrogeology of Uganda*. British Geological Survey. Retrieved on 2016 August 8 from http://earthwise.bgs.ac.uk/index.php/Hydrogeology_of_Uganda

Palmström. A. 1995. *Rock Masses as Construction Materials. Chapter Two*: PhD thesis. RMi – a rock mass characterization system for rock engineering purposes. Oslo University, Norway, 1995, 400 p.

Panda, M. K., Mohanty, S., Pingua, B. M. P. & Mishra, A. K. 2014. *Engineering Geological And Geotechnical Investigations along the Head Race Tunnel in Teesta Stage-III Hydroelectric Project, India.* Engineering Geology, 181, pp. 297-308 doi:10.1016/j.enggeo.2014.08.022

Panthi, K. K. 2006. *Analysis of Engineering Geological Uncertainties Related to Tunneling in Himalayan Rock Mass Conditions*. Norwegian University of Science and Technology. ISBN 82-471-7825-7

Patey, D R. 1972. *Bentonite Tunneling Shield Breaks New Ground*. Contract Journal/UK/ Volume 249 Issue: 4855. Retrieved on 2015 September 23 from http://Trid.Trb.Org/View.Aspx?Id=126246 pp.34-35

Perri, G. 2007. *Behavior Category and Design Loads for Conventionally Excavated Tunnels* Retrieved on 2016 October 5 from http://www.gianfrancoperri.com/Documents/90-2007%20Behavior%20category%20and%20design%20loads%20for%20conventionally%20excavated%20tunnels.pdf

Prasad, B. 2015. *Tunnel Design Overview*. Retrieved on 2016 September 20 from https://www.linkedin.com/pulse/tunnel-design-overview-bandula-prasad

PRC, 2008. *Specification for Design of Hydraulic Tunnels.* State Development and Reform Commission, Electric Power Industry Standards. China Electric Power Press. People's Republic of China (PRC) T0017830 ISBN 978-7-5083-6723-1

Prior, S. 2016. *Tunnel Construction*. Retrieved 2016 July 7 from http://www.forgottenrelics.co.uk/tunnels/construction/overview.html#top

Piteau, D.R. 1972. *Engineering Geology Considerations and Approach in Assessing the Stability of rock slopes*. Bulletin of the Association of Engineering Geologists IX, pp. 301–320.

Redd, 2012. *Atomic Structure and Typical Additives.* Retrieved on 2016 July 18 from https://www.reddit.com/r/Elements/comments/vmlyq/glass_part_3_atomic_structure_and_typical/

Rocscience, 2016. *RS3*. 3D *Finite Element Geomechanics Software and Program for Underground Excavations*. http://www.rocscience.com.

Rowley, S.J. 2005. *Teredo navalis Great Shipworm*. In Tyler-Walters H. and Hiscock K. (eds) Marine Life Information Network: Biology and Sensitivity Key Information Reviews, [on-line]. Plymouth: Marine Biological Association of the United Kingdom. Available from: http://www.marlin.ac.uk/species/detail/2117

RTM, 2009. *Technical Manual for Design and Construction of Road Tunnels -Civil Elements* Road Tunnel Manual (RTM) FHWA-NHI-09-010 U.S. Department of Transportation Federal Highway Administration Publication No. FHWA-NHI-10-034

Rudnick, R. L. & Gao, S. 2003. *Composition of the Continental Crust*. Treatise On Geochemistry Volume 3 ISBN 0-08-044338-9 pp. 1–64 © Elsevier Ltd.

Russo, G., Kalamaras, G.S. & Grasso. P. 1998. *A Discussion on the Concepts of Geomechanical Classes, Behavior Categories and Technical Classes for an Underground Project*. Gallerie e Grandi Opere in Sotterraneo n.54: pp 40-51.

Sabatini, P. J., Bachus. R.C., Mayne. P.W., Schneider. J.A. & Zettler. T.E. 2002. *Geotechnical Engineering Circular No. 5 Evaluation of Soil and Rock Properties*. International Society of Rock Mechanics (ISRM) and the American Society for Testing and Materials (ASTM) D5878 Technical Manual, U.S. Department of Transportation

Sepp, S. 2000. *Rock Types & Minerals*. Retrieved on 2016 July 16 from http://www.sandatlas.org/minerals/ Unpublished

Schlüter, T. 1997. *Geology of East Africa.* (With contributions by Craig Hampton) ISBN 978-3-443-11027-7

Sharp, J. M. Jr. 2007. *A Glossary of Hydrogeological Terms* The University of Texas, Austin, Texas

Short. N. M. 1999. *Some Basic Concepts Underlying the Science Of Geology* Retrieved on 2016 August 7 from http://saturniancosmology.org/files/geology/sect2_1a.html

Shull, 2007. Retrieved on 2016 June 18 from https://en.wikipedia.org/wiki/Verification_and_validation_of_computer_simulation_models

Smyth, R. J. & McCormick, C. T. 1995. *Mineralogy: Fundamental Science of Earth Materials* University of Colorado. Geology 3010 Course Notes Retrieved on 2016 August 9 from http://ruby.colorado.edu/~smyth/G30101.html

Soil Manual, 1993. *Soil Survey Mannual* Chapter 3, Glossary of soil Science Terms, Soil Science Society of America. Soil Survey Staff U.S. Dept of Agriclture. Retrieved on 2016 July 13 from http://henrico.us/assets/Soil-Parent-Materials.pdf

Solak, T. & Schubert, W. 2004. *Influence of Block Size and Shape on the Deformation Behavior & Stress Distribution around Tunnels*. International Society for Rock Mechanics (ISRM) Regional Symposium. Proceedings of Eurock 2004 & 53rd Geomechanics Colloquium, October 2004, VGE. Salzburg, Austria, ISBN 3-7739-5995-8, pp.

Sousa, L.R., 2010. *Risk Analysis for Tunneling Projects*_Phd thesis_Massecheutes Institute of Technology

Spackova, O. 2012. *Risk Manageent of Tunnel Construction Projects*. PhD_Dissertation Czech Technical University in Prague

Spang, R. 2004. *Integral Approach to the Design of Rockfall Mitigation Measures*. Korean National Conference on the Rainfall and Slope Stabilization. Korean Geotechnical Society, South Korea.

Stegner, W. 1971. *Angle of Repose*. Penguin Books ISBN 014016930X, 9780140169300

Steiner, W. 2000. *Squeezing Rock in Tunneling:_Identification and Important Factors* Rivisita Italiana Di Geotecnica Volume 1 pp.9-15

Sydney, 2006. *From Segregation, Transport, and Emplacement of Magmas, to the Solid State Deformation of Granitoids: Microstructures, Fabrics, and Finite Strain Fields.*The University of Sydney, School of Geosciences, Division of Geology and Geophysics. Retrieved on 2016 July 19 from http://www.geosci.usyd.edu.au/users/prey/Granite/Granite.html

Terzaghi, K. 1946. *Rock Deffects and Loads on Tunnel Supports.* Reprinted from Rock Tunneling with Steel Supports. The Commercial Shearing & Stamping Co. Soil Mechanics Series No. 25

Thomas-Lepine, C. 2012. *Rock Bolts - Improved Design and Possibilities.* Masters Dissertation of the Civil Engineering school of ENTPE, France in partnership with NTNU, Norway. Retrieved on 2016 October 5 from http://www.diva-portal.org/smash/get/diva2:566190/FULLTEXT01.pdf

Torres, C.A. 2008. *Geometric Characterisation of Rock Mass Discontinuities using Terrestrial Laser Scanner & Ground Penetrating Radar.* Phd Thesis

TRRL, 1973. Transport and Road Research Laboratory (TRRL). United Kingdom.

Tsesarsky, M. & Hatzor, Y. H. 2005. *Tunnel roof deflection in blocky rock masses as a function of joint spacing and friction – A parametric study using discontinuous deformation analysis (DDA).* © 2005 Elsevier Ltd. All rights reserved. doi:10.1016/j.tust.2005.05.001

Tshering, K. 2012. *Stability Assessment of Headrace Tunnel System for Punatsangchhu II Hydropower Project, Bhutan*. Norwegian University of Science and Technology (NTNU), Trondheim.

TLDG, 2004. Specification for Tunneling. *Tunnel Lining Design Guide* (TLDG). The British Tunneling Society and the Institution of Civil Engineers. London: Thomas Telford Publishing, ISBN: 0 7277 2986 1.

UC&T, 2014. *Surface-Groundwater-Tunnel Inflow Modeling* Underground Construction & Tunneling (UC&T) Retrieved on 2016 August 12from http://uct.mines.edu/res_parflow.html

USACE, 1997. *Tunnels and Shafts in Rock* Engineering and Design, United States Army Corps of Engineers (USACE) EM1110-2-2901 Retrieved on 2016 August 23 from http://www.publications.usace.army.mil/USACE-Publications/Engineer-Manuals/udt_43544_param_page/2/

USGS, 2016. *World Geological Map*. United States Geological Survey (USGS), Department of the Interior Retrieved from http://earthquake.usgs.gov/data/crust/maps.php on July 1 2016 at 0900hours.

Varanasi, 2009. Mineral Engineering Rock Slope Course Notes. Retrieved on 2016 August 3 from http://www.iitbhu.ac.in/faculty/min/rajesh-rai/NMEICT-Slope/lecture/c1/l2.html 1

Venkatramaiah, C. 2012. *Geotechnical Engineering* Fourth edition. New Age International (P) Ltd., Publishers ISBN: 81-224-3351-7

Viggiani, G. 2012. *Geotechnical Aspects of Underground Construction in Soft Ground*. Technology and Engineering 7th International Symposium on Geotechnical Aspects of Underground Construction in Soft Ground, Rome, Italy.

Wahlstrom, E. E. 1973. *Tunneling in Rock*. Developments in Geotechnical Engineering 3. Elsevier Scientific Publishing Company, Amsterdam. ISBN 0-444-41064-3

Waldron, J. 2009. *Geologic Structures and Maps: Fabrics and Folds* Course Notes EAS 233 Winter 2009 University of Alberta

Wang, S., Li, C., Liu, Z. & Fang, J. 2014. *Optimization of Construction Scheme and Supporting Technology for HJS Soft Rock Tunnel*. International Journal of Mining Science and Technology, 24(6), 847-852. doi:10.1016/j.ijmst.2014.10.018

Weller, R. 2015a. *Rocks*. Cochise College. Geology Home Page. wellerr@cochise.edu Retrieved on 2016 July 15 from http://skywalker.cochise.edu/wellerr/GLG101/GLG101-igneous-rocks.htm

Weller, R. 2015b. *Rocks*. Cochise College. Geology Home Page. wellerr@cochise.edu Retrieved on 2016 July 15 from http://skywalker.cochise.edu/wellerr/GLG101/GLG101-sedimentary-rocks.htm

Weller, R. 2015c. *Rocks*. Cochise College. Geology Home Page. wellerr@cochise.edu Retrieved on 2016 July 17 from http://skywalker.cochise.edu/wellerr/GLG101/GLG101-metamorphic-rocks.htm

Werme, C., J. Hunt, E. Beller, K. Cayce, M. Klatt, A. Melwani, E. Polson. & Grossinger. R. 2010. *Removal of Creosote-Treated Pilings and Structures from San Francisco Bay*. Prepared for California State Coastal Conservancy. Contribution No. 605. San Francisco Estuary Institute, Oakland, California.

West, G. 2005. *Innovation and the Rise of the Tunneling Industry*. Cambridge University Press. ISBN: 0521673356, 9780521673358

Williams A. A. B., Pidgeon J. T. & Day P. W. 1985. *Problem Soils in South Africa -State*

of the Art. The Civil Engineer in South Africa, Volume 27, No.7, pp. 367-373, 375-377, p. 407

Wood, J. & Guth, A. 2015. *East Africa's Great Rift Valley: A Complex Rift System*. Michigan Technological University Retrieved on 2016 July 15 from http://geology.com/articles/east-africa-rift.shtml

Yavuz, H. 2006. *Support Pressure Estimation for Circular and Non-Circular Openings Based on a Parametric Numerical Modelling Study*. The South African Institute of Mining and Metallurgy SA ISSN 0038–223X/3.00 + 0.00. pp.129-138

Yi, N. T. 2006. Hong Kong Institute of Vocational Education. Retrieved on 2015 September 21 from http://tycnw01.vtc.edu.hk/cbe2024/3-Tunnel.pdf

Yoshinaka & Nishimaki. 1981. *Weak Rock: Soft, Fractured and Weathered Rock*. Proceedings of the International Symposium on Weak Rock held in Tokyo, September 1981. ISBN: 90 6191 209 1

Yu, Z., Kulatilake, P.H.S.W. & Jiang, F. 2012. *Effect of Tunnel Shape and Support System on Stability of a Tunnel in a Deep Coal Mine in China*. Geotechechnical and Geological Engineering 30: 383. doi:10.1007/s10706-011-9475-0

Zhai, E., Qixiang, F., Shengshan, G. & Haibing, X. 2016. *Owner's Design Check During Construction of the Underground Powerhouse Caverns for a Major Chinese Hydro Project*. Proceedings of the Hydro2016 conference, 10-12 October, Montreux, Switzerland

Zhang, C., Wang, Z. & Wang, Q. 2015. *Deformation and Failure Characteristics of the Rock Masses in Tunnels.* Mathematical Problems in Engineering. Research Article © Hindawi Publishing Corporation

Zhao, 2015. *Properties of Rock Discontinuities*_Rock Engineering Course Notes Laussane Retrieved on 2016 August 31 from http://lmr.epfl.ch/webdav/site/lmr/users/172086/public/RockMechanics/Notes%20-%20Chapter%205.pdf

Zhongming, S. U. 2015. *Mechanical Model for Inverted Arch of Highway Tunnel in Weak Surrounding Rock and Dynamic Design*. 5th International Conference on Information Engineering for Mechanics and Materials (ICIMM) pp.844-847. Atlantis Press

Zia, U. 2016. *Tunneling.* Retrieved on 2016 November 18 from http://www.slideshare.net/UsamaZia1/ce3019-a-16-tunneling?next_slideshow=3

Abstract Accepted

Ongodia, J.E., Kalumba, D., Brajesh, K. O., & Mutikanga, H.E. Design *Considerations for Optimum Support System Components of a Hydropower Tunnel- A case study of Karuma (600MW) hydropower dam in Uganda.* Submitted for the International Conference on Soil Mechanics and Geotechnical Engineering (ICSMGE) 2017 to be held in COEX, Seoul, Korea

Appendices

A Tunnel orientations

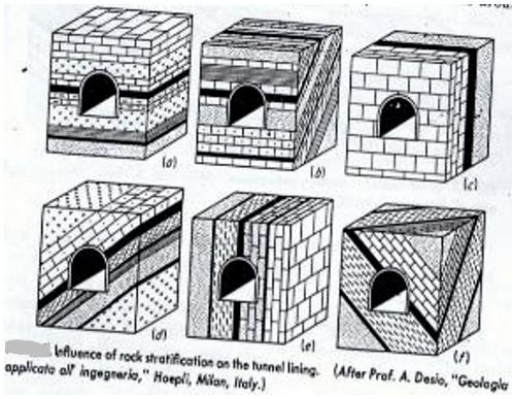

Influence of rock stratification on the tunnel lining. (After Prof. A. Desio, "Geologia applicata all' ingegneria," Hoepli, Milan, Italy.)

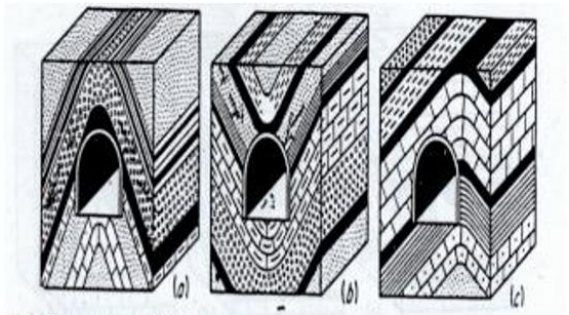

Tunnel located in anticline and syncline. (After Prof. A. Desio, "Geologia applicata all' ingegneria," Hoepli, Milan, Italy.)

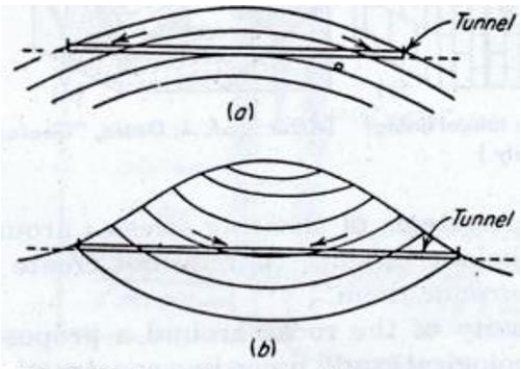

Tunnel crossing (a) an anticline and (b) a syncline.

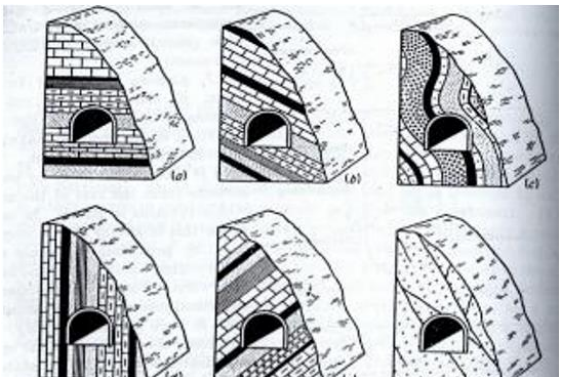

Tunnels close to a steep slope. (After Prof. A. Desio, "Geologia applicata ingegneria," Hoepli, Milan, Italy.)

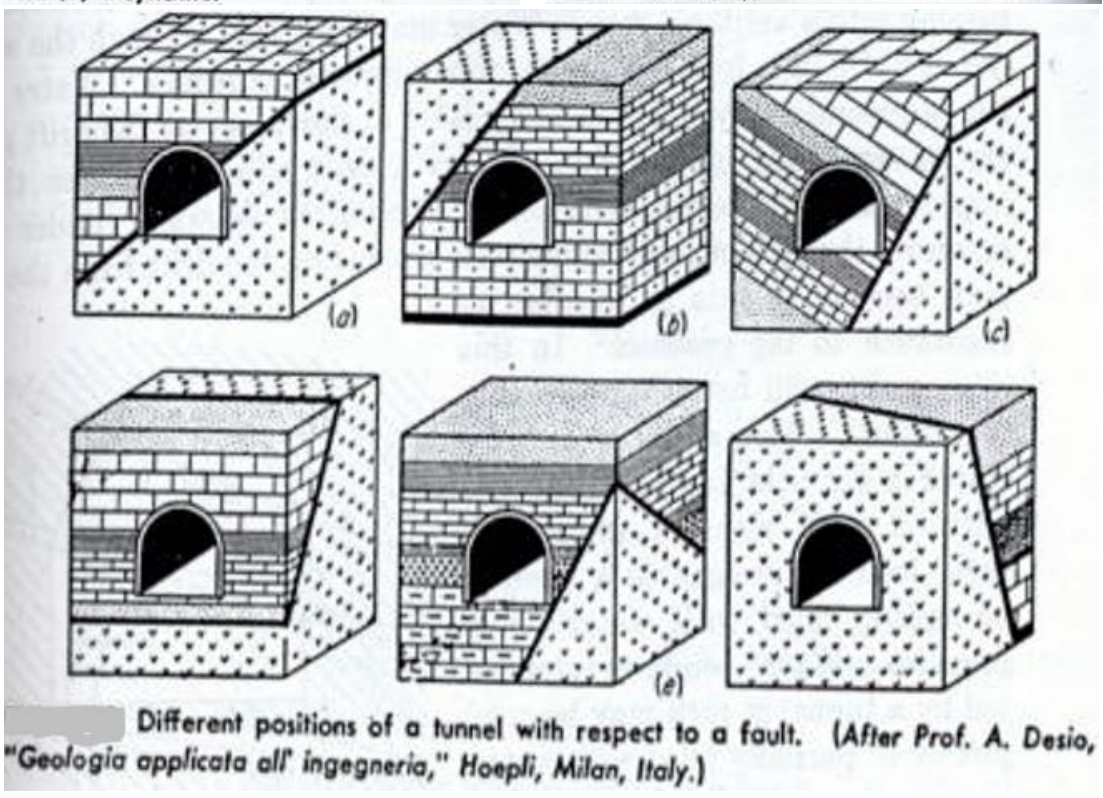

Different positions of a tunnel with respect to a fault. (After Prof. A. Desio, "Geologia applicata all' ingegneria," Hoepli, Milan, Italy.)

Tunnel orientations with respect to site geology and geological features
Source: Zia (2016)

B Aids for physical identification of rocks and minerals

B.1 Hardness scales: Give relative hardness of minerals on Moh's scale and other methods.

Rock hardness compared with minerals

Hardness	Mineral / *other
>10	Lonsdaleite (Hexagonal diamond) *
>10	Wurtzite boron nitride*
10	Diamond
9	Corundum
8	Topaz
7+	Hardened Steel file*
7	Quartz
6-7	Glass*
6.5	Iron pyrite*
6	Orthoclase feldspar
5.5	Knife blade*
5	Apatite
4.5	Iron*
4-4.5	Platinum*
4	Fluorite
3	Calcite or copper penny*
2.5-3	Gold* or Silver *
2.5	Finger nail*
2	Gypsum
1	Talc

Source: Adapted from American Federation of Mineralogical Societies (2014) and Gemstone.com (2016)

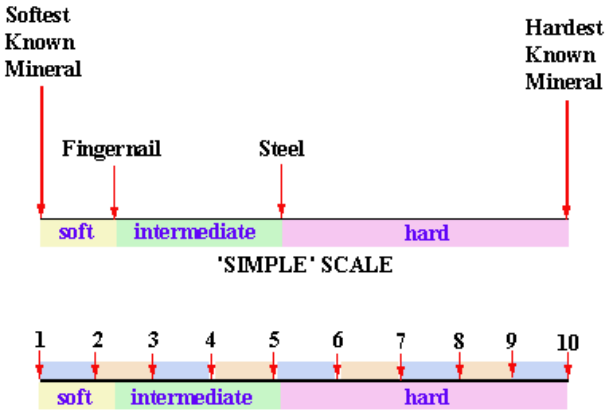

Rock hardness scales
Source: Leveson (2005)

Description	Compressive strength (MPa)	Test method
Very strong	100-250	Requires many blows of a geological hammer to break intact rock specimens
Strong rock	50-100	Hand held specimens broken by a single blow of a hammer
Moderately strong	25-50	Firm blow with geological pick indents rock to 5mm, knife just scrapes surface
weak	5-25	Knife may cut material but too hard to shape
soap	1- 5	Material crumbles under firm blow of geological pick, can be scraped with knife

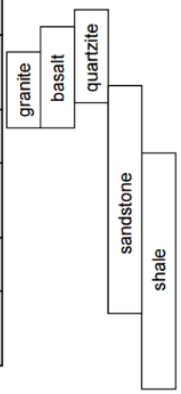

Rough field test for compressive strength
Source: Boniwell (2015)

B.2 Mineral identification flow charts

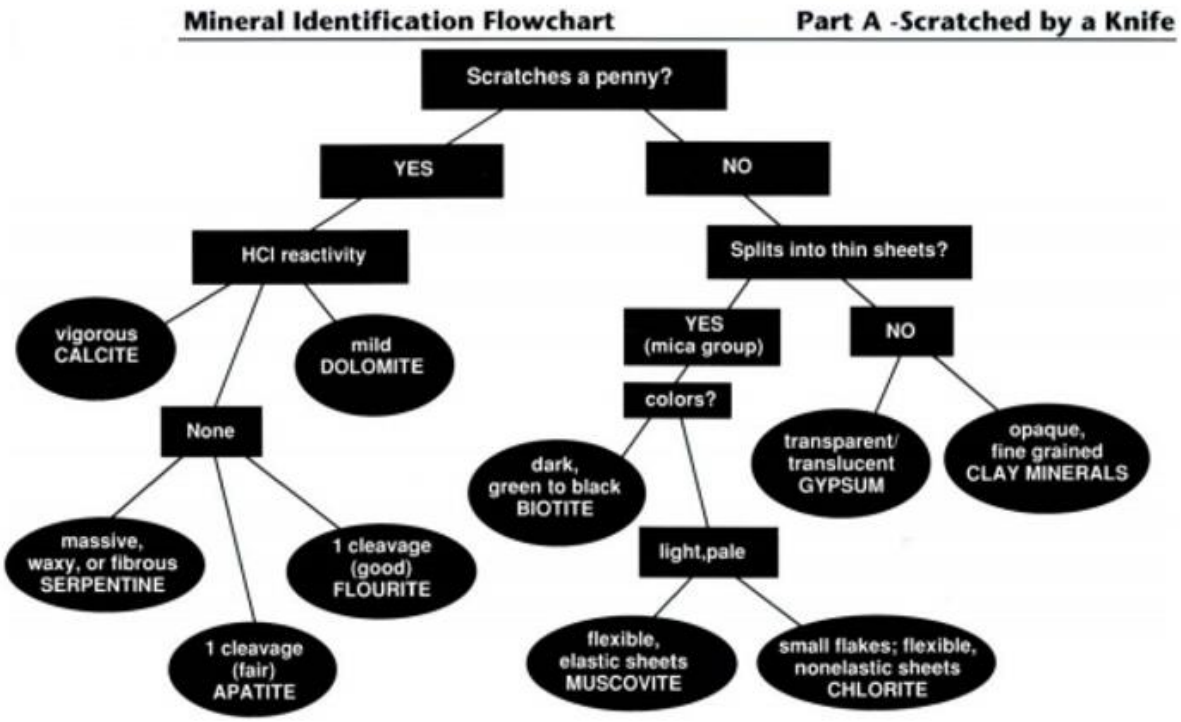

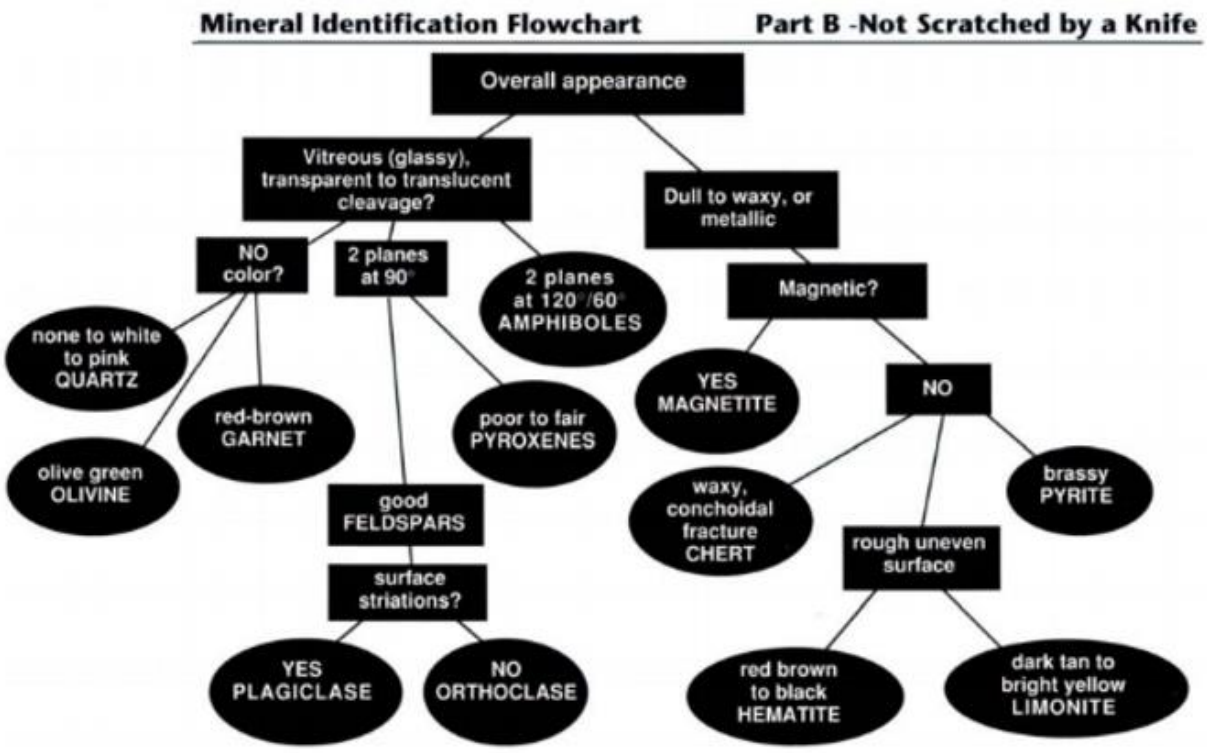

Rock Identification Flowchart **Part-A**
Rocks with Mineral Grains/Crystals Easily Visible to the Naked Eye

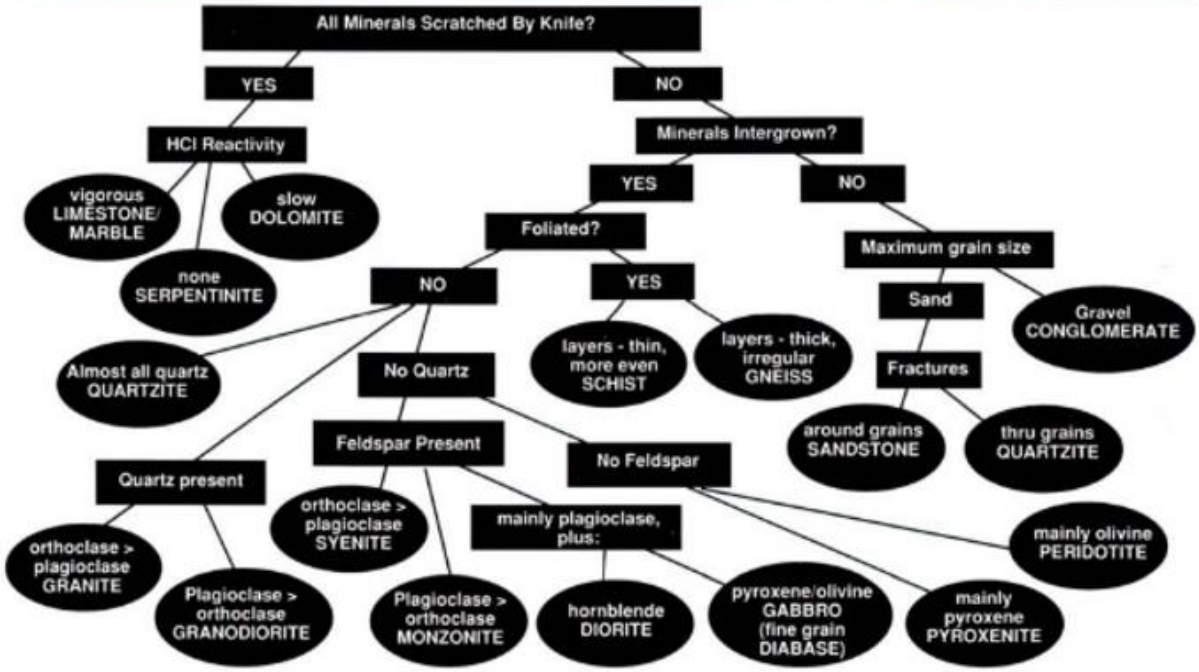

Rock Identification Flowchart **Part-B**
Rocks With Very Fine Mineral Grains/Crystals
Not Easily Visible to the Naked Eye

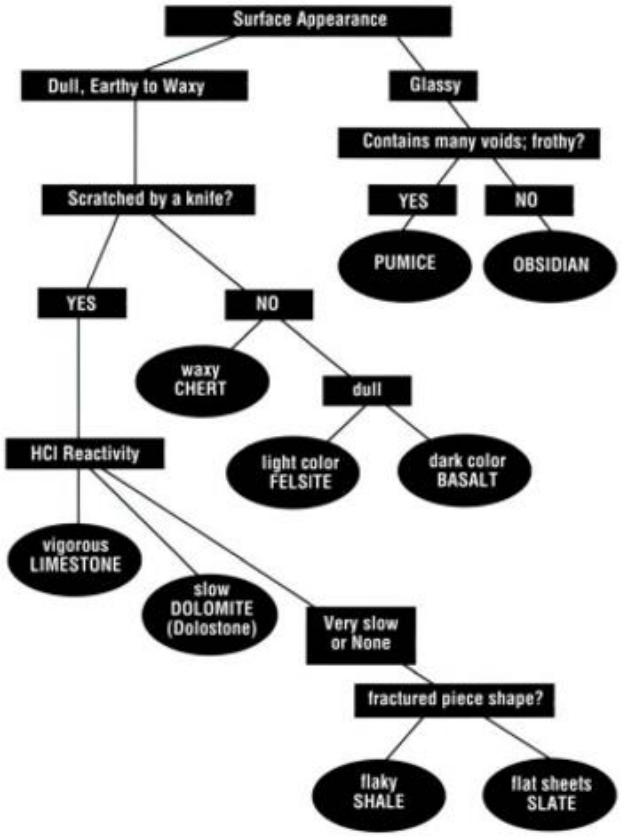

B.3 Identification of the rock type

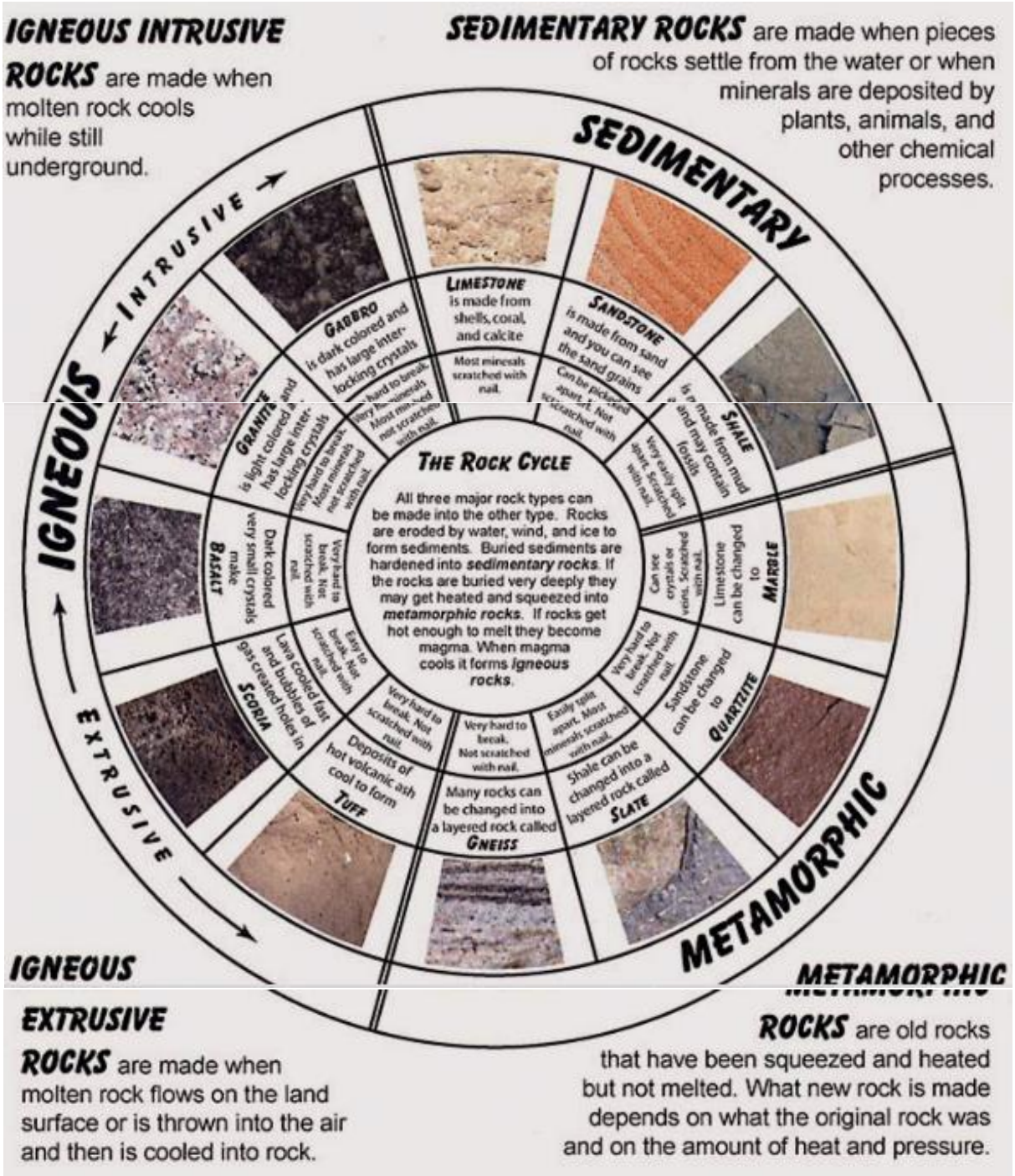

Source: Langer (1994)

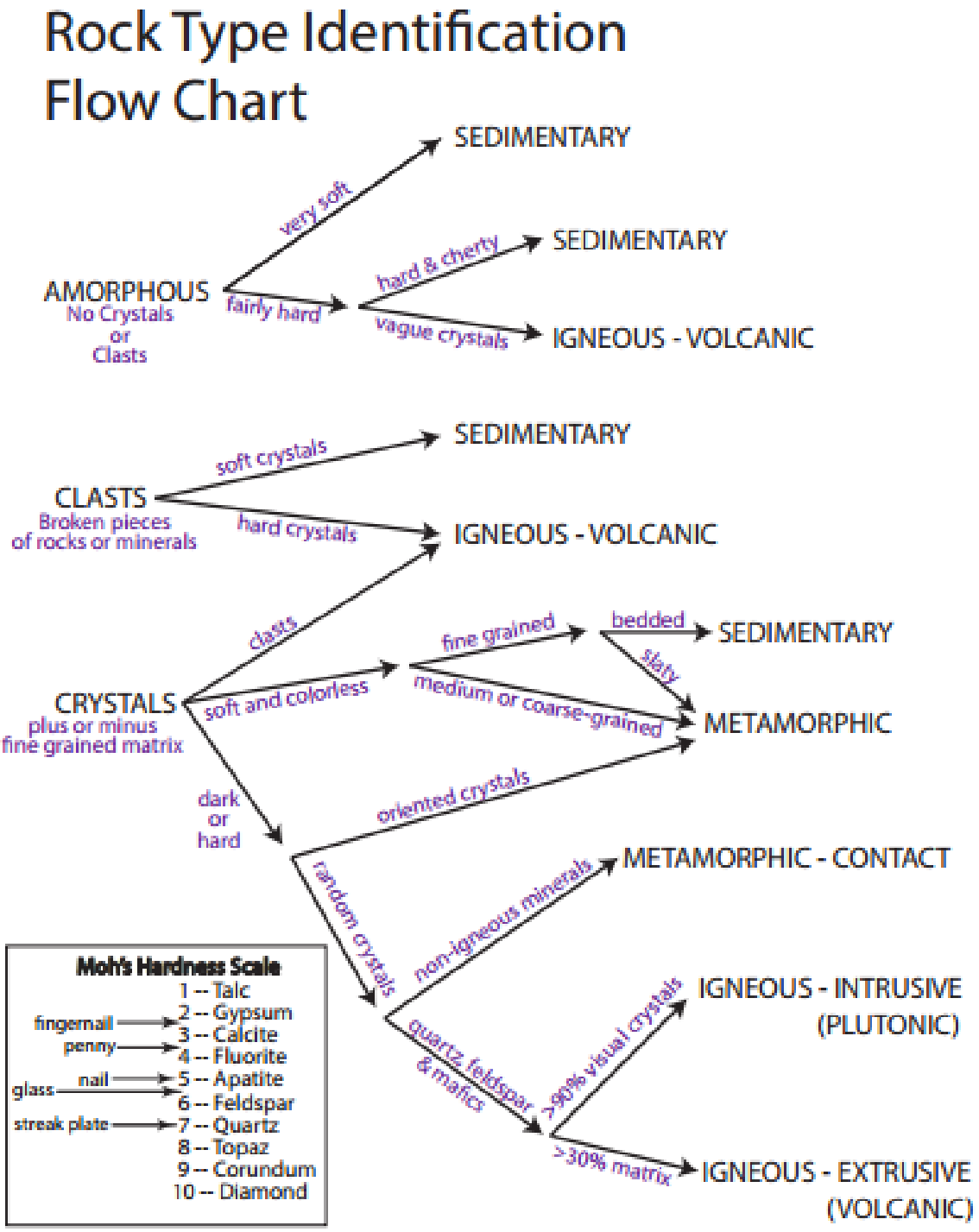

Source: Rock identification algorithm (FHA, 1991)

Properties of common rock minerals (Adapted from NEH, 2012)

Mineral	Hardness	Cleavage	Other
Pyrite	6 - 6½	None	Brassy, fool's gold, weathers easily to give iron stain, common accessory mineral in many rock types.
Hematite	5½ - 6½	None (in massive form)	Red-brown, common accessory in many rocks, cement in many sandstones
Magnetite	6	None (in granular form)	Black, magnetic, common accessory mineral in many rock types
Limonite	5 - 5½	None	Yellow-brown, earthy, may appear softer than 5, formed by alteration of other iron minerals
Fluorite	4	1 plane	Common accessory mineral in limestones and dolostones, translucent to transparent.
Calcite	3	3 planes at 75°	Very common, occurs in many rock types, chief mineral in limestone, vigorous reaction with dilute hydrochloric acid (HCl)
Dolomite	3½ - 4	3 planes at 74°	Common, with calcite in dolomitic limestone or dolostone (>50% dolomite), vigorous reaction with dilute HCl only when powdered
Apatite	5	1 poor plane	Common minor accessory
Gypsum	2	4 perfect planes	Common mineral, especially in limestones and shales, may occur in layers
Quartz	7	None	Very common, may occur in many rock types, glassy, translucent to transparent, may be coloured, very resistant to weathering, chief mineral in sandstones
Chert	7	None	Cryptocrystalline (microscopic crystals) variety of quartz, appears massive to naked eye, common in limestones or in complete layers associated with limestones, light tan to light brown. Similar minerals: flint (dark brown to black), jasper (red), chalcedony (waxy look, tan to brown).
Orthoclase	6	2 planes at 90°	A feldspar, very common in many rock types, white to grey to red-pink, translucent to transparent. Cleavage distinguishes it from quartz
Plagioclase	6	2 planes at 94°	A feldspar, very common in many rock types, appears similar to orthoclase. Distinguished by the presence of thin parallel lines on cleavage faces due to crystal structure.
Olivine	6½ - 7	None	Transparent to translucent, olive green, glassy. Common accessory mineral in metamorphic and some igneous rocks, also in sands and sandstones.
zircon	7½	None	Usually colourless to brown; usually translucent; common accessory mineral in igneous rocks and some metamorphic rocks; also in sands and sandstones
Pyroxene (mineral group)	5 - 7	2 planes at 87° and 93°	Most common in the darker igneous rocks. Usually green to black: translucent to transparent. Most common mineral is Augite.
Amphibole (mineral group)	5 - 6	2 planes at 56° and 124°	Most common in metamorphic rocks and the darker igneous rocks. Usually green to brown to black; translucent to transparent. Distinguished from pyroxenes by cleavage. Most common mineral is hornblende.
Clay minerals (a group)	2 -2½	1 plane	Usually fine grained, earthy; often derived from weathering of feldspars. Montmorillonite is the swelling clay that expands with the absorption of water. Illite is the common clay mineral in many shales.
Talc	1	1 plane	Very soft, greasy; cleavage may be hard to see because the particles are very fine. Typically, white to pale green. Usually in metamorphic or altered igneous rocks.
Serpentine	2 – 5 (usually 4)	None	Massive to fibrous; greasy to waxy; various shades of green. Found in altered igneous or metamorphic rocks. Fibrous variety is the source of asbestos.
Muscovite	2 - 2½	1 plane	A mica; perfect cleavage allows splitting into thin clear transparent sheets. Usually light yellow to light brown. Common in light coloured igneous rocks and metamorphic rocks.
Biotite	2½ - 3	1 plane	A mica; perfect cleavage allows splitting into thin smoky transparent sheets. Usually dark green to brown to black. Found in light to medium coloured igneous rocks and metamorphic rocks.
Chlorite	2 - 2½	1 plane	Similar to the micas; usually occurs in small particles so cleavage produces flake. Flakes are flexible but not elastic as are the micas. Usually some shade of green.

C Rock mass classification

C.1 Competency

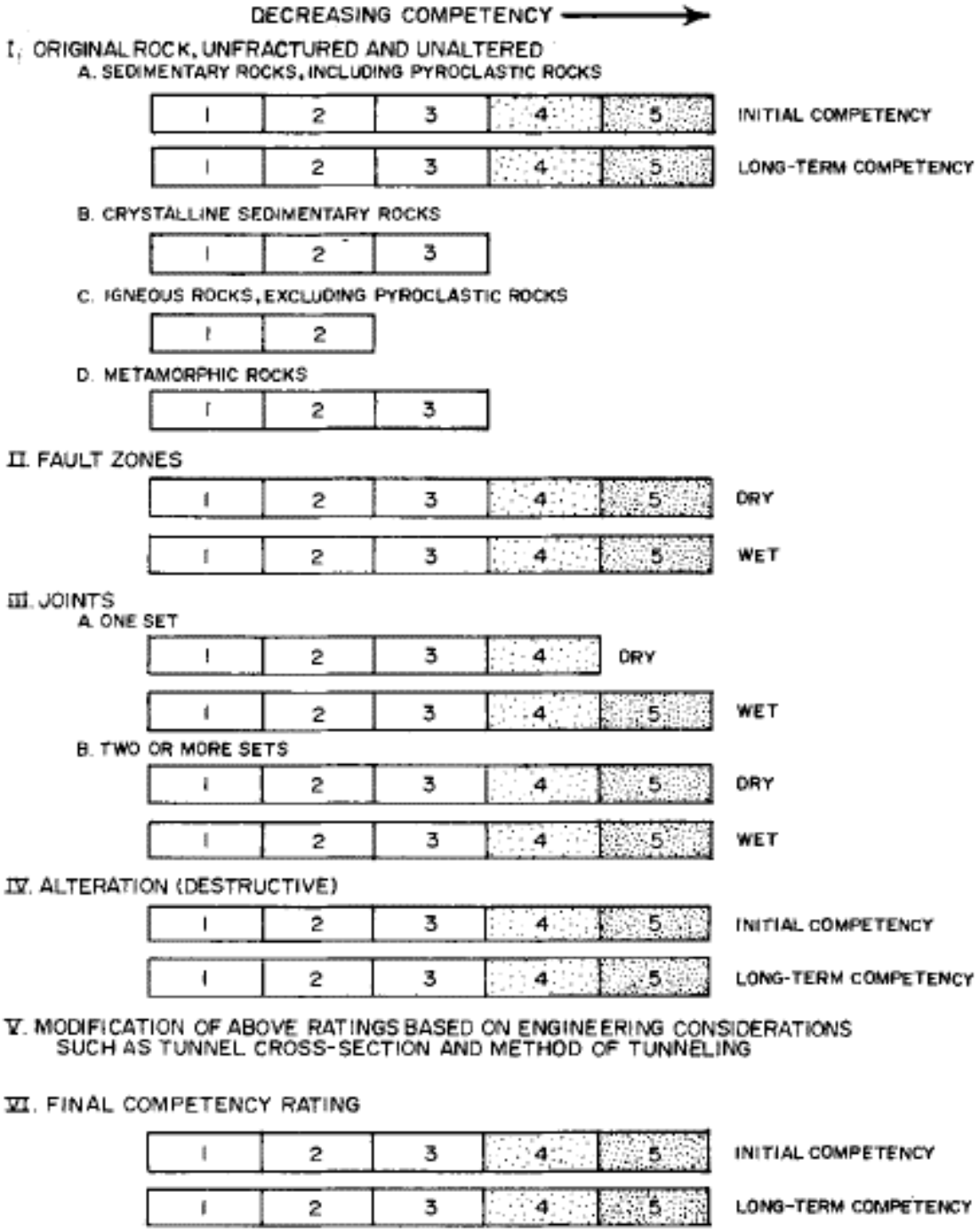

Rating rock competency
Source: Wahlstrom (1973)

A. CLASSIFICATION PARAMETERS AND THEIR RATINGS									
Parameter			**Range of values**						
1	Strength of intact rock material	Point-load strength index	>10MPa	4 – 10MPa	2 – 4MPa	1 – 2MPa	For this low range, uniaxial compressive strength is preferred		
		Uniaxial compressive strength	>250MPa	100 – 250MPa	50 – 100MPa	25 -50 MPa	5.25MPa	<1.5MPa	<1MPa
	Rating		15	12	7	4	2	1	0
2	Drill core quality, RQD (%)		90 - 100	75 - 90	50 - 75	25-50	<25		
	Rating		20	17	13	8	3		
3	Spacing of discontinuities		>2m	0.6 – 2m	200 – 600mm	60 – 200mm	<60mm		
	Rating		20	15	10	8	5		
4	Condition of discontinuities (see E)		Very rough surfaces Not continuous No separation Unweathered wall rock	Slighylt rough surfaces Separation <1mm Slightly weathered walls	Slightly rough surfaces Separation < 1mm Highly weathered walls	Slickensided surfaces or Gouge < 5mm thick or Separation 1.5mm Continuous	Soft gouge > 5mm thick or Separation > 5mm Continuous		
	Rating		30	25	20	10	0		
5	Groundwater	Inflow per 10m tunnel length (µm)	None	<10	10 - 25	25 - 125	>125		
		(Joint water pressure) (Major principal σ)	0	<0.1	0.1 – 0.2	0.2 – 0.5	>0.5		
		General conditions	Completely dry	Damp	Wet	Dripping	Flowing		
	Rating		15	10	7	4	0		

B. RATING ADJUSTMENT FOR DISCONTINUITY ORIENTATIONS						
Strike and dip orientations		Very favourable	Favourable	Fair	Unfavourable	Very unfavourable
Ratings	Tunnels and mines	0	-2	-5	-10	-12
	Foundations	0	-2	-7	-15	-25
	slopes	0	-5	-25	-50	-

C. ROCK MASS CLASSES DETERMINED FROM TOTAL RATINGS					
Rating	100 - 81	80 - 61	60 - 41	40 - 21	<21
Class number	I	II	III	IV	V
Description	Very good rock	Good rock	Fair rock	Poor rock	Very poor rock

D. MEANING OF ROCK CLASSES					
Class number	I	II	III	IV	V
Average stand-up time	20years for 15m span	1year for 10m span	1 week for 5m span	10hours for 2.5m span	30min for 1m span
Cohesion of rock mass (kPa)	>400	300 - 400	200 - 300	100 – 200	<100
Friction angle of rock mass (°)	>45	35 - 45	25 - 35	15 - 25	<15

E. GUIDELINES FOR CLASSIFICATION OF DISCONTINUITY CONDITIONS					
Discontinuity length (persistence) (m)	<1	1 – 3	3 – 10	10 – 20	>20
Rating	6	4	2	1	0
Separation (aperture) (mm)	None	<0.1	0.1 – 1.0	1 – 5	>5
Rating	6	5	4	1	0
Rougness	Very rough	Rough	Slightly rough	Smooth	Slickensided
Rating	6	5	3	1	0
Infilling (gouge) (mm)	None	Hard filling <5	Hard filling >5	Soft filling <5 2	Hard filling >5
Rating	6	4	2		0
Weathering	Unweathered	Slightly weathered	Moderately weathered	Highly weathered	Decomposed
Ratings	6	5	3	1	0

F. EFFECT OF DISCONTINUITY STRIKE AND DIP ORIENTATION IN TUNNELING			
Strike perpendicular to tunnel axis		Strike parallel to tunnel axis	
Drive with dip-Dip 45 - 90°	Drive with dip-Dip 20 - 45°	Dip 45 - 90°	Dip 20 - 45°
Very favourable	Favourable	Very favourable	Fair
Drive against dip-Dip 45 - 90°	Drive against dip-Dip 20 - 45°	Dip 0 – 20° irrespective of strike degree	
Fair	Unfavourable	Fair	

Note:
- Some conditions are mutually exclusive. For instance, if filling is present, the roughness of the surface will be overshadowed by the influence of the gouge. In such cases use A.4 directly.
- Modified after Wickham et al. (1972)

Bieniawski's rock mass rating system

Source: Adapted after RTM (2009)

C.2 Individual parameter classification to calculate Q

DESCRIPTION	VALUE	NOTES
1. ROCK QUALITY DESIGNATION	*RQD*	
A. Very poor	0 - 25	1. Where *RQD* is reported or measured as ≤ 10 (including 0), a nominal value of 10 is used to evaluate *Q*.
B. Poor	25 - 50	
C. Fair	50 - 75	
D. Good	75 - 90	2. *RQD* intervals of 5, i.e. 100, 95, 90 etc. are sufficiently accurate.
E. Excellent	90 - 100	
2. JOINT SET NUMBER	J_n	
A. Massive, no or few joints	0.5 - 1.0	
B. One joint set	2	
C. One joint set plus random	3	
D. Two joint sets	4	
E. Two joint sets plus random	6	
F. Three joint sets	9	1. For intersections use ($3.0 \times J_n$)
G. Three joint sets plus random	12	
H. Four or more joint sets, random, heavily jointed, 'sugar cube', etc.	15	2. For portals use ($2.0 \times J_n$)
J. Crushed rock, earthlike	20	
3. JOINT ROUGHNESS NUMBER	J_r	
a. Rock wall contact		
b. Rock wall contact before 10 cm shear		
A. Discontinuous joints	4	
B. Rough and irregular, undulating	3	
C. Smooth undulating	2	
D. Slickensided undulating	1.5	1. Add 1.0 if the mean spacing of the relevant joint set is greater than 3 m.
E. Rough or irregular, planar	1.5	
F. Smooth, planar	1.0	
G. Slickensided, planar	0.5	2. J_r = 0.5 can be used for planar, slickensided joints having lineations, provided that the lineations are oriented for minimum strength.
c. No rock wall contact when sheared		
H. Zones containing clay minerals thick enough to prevent rock wall contact	1.0 (nominal)	
J. Sandy, gravely or crushed zone thick enough to prevent rock wall contact	1.0 (nominal)	
4. JOINT ALTERATION NUMBER	J_a	ϕr degrees (approx.)
a. Rock wall contact		
A. Tightly healed, hard, non-softening, impermeable filling	0.75	1. Values of ϕr, the residual friction angle, are intended as an approximate guide to the mineralogical properties of the alteration products, if present.
B. Unaltered joint walls, surface staining only	1.0	25 - 35
C. Slightly altered joint walls, non-softening mineral coatings, sandy particles, clay-free disintegrated rock, etc.	2.0	25 - 30
D. Silty-, or sandy-clay coatings, small clay-fraction (non-softening)	3.0	20 - 25
E. Softening or low-friction clay mineral coatings, i.e. kaolinite, mica. Also chlorite, talc, gypsum and graphite etc., and small quantities of swelling clays. (Discontinuous coatings, 1 - 2 mm or less)	4.0	8 - 16

ADDITIONAL NOTES ON THE USE OF THESE TABLES

When making estimates of the rock mass Quality (*Q*), the following guidelines should be followed in addition to the notes listed in the tables:

1. When borehole core is unavailable, *RQD* can be estimated from the number of joints per unit volume, in which the number of joints per metre for each joint set are added. A simple relationship can be used to convert this number to *RQD* for the case of clay free rock masses: $RQD = 115 - 3.3\,J_v$ (approx.), where J_v = total number of joints per m^3 ($0 < RQD < 100$ for $35 > J_v > 4.5$).
2. The parameter J_n representing the number of joint sets will often be affected by foliation, schistosity, slaty cleavage or bedding etc. If strongly developed, these parallel 'joints' should obviously be counted as a complete joint set. However, if there are few 'joints' visible, or if only occasional breaks in the core are due to these features, then it will be more appropriate to count them as 'random' joints when evaluating J_n.
3. The parameters J_r and J_a (representing shear strength) should be relevant to the weakest significant joint set or clay filled discontinuity in the given zone. However, if the joint set or discontinuity with the minimum value of J_r/J_a is favourably oriented for stability, then a second, less favourably oriented joint set or discontinuity may sometimes be more significant, and its higher value of J_r/J_a should be used when evaluating *Q*. The value of J_r/J_a should in fact relate to the surface most likely to allow failure to initiate.
4. When a rock mass contains clay, the factor *SRF* appropriate to loosening loads should be evaluated. In such cases the strength of the intact rock is of little interest. However, when jointing is minimal and clay is completely absent, the strength of the intact rock may become the weakest link, and the stability will then depend on the ratio rock-stress/rock-strength. A strongly anisotropic stress field is unfavourable for stability and is roughly accounted for as in note 2 in the table for stress reduction factor evaluation.
5. The compressive and tensile strengths (σ_c and σ_t) of the intact rock should be evaluated in the saturated condition if this is appropriate to the present and future in situ conditions. A very conservative estimate of the strength should be made for those rocks that deteriorate when exposed to moist or saturated conditions.

6. STRESS REDUCTION FACTOR			***SRF***	
a. Weakness zones intersecting excavation, which may cause loosening of rock mass when tunnel is excavated				
A. Multiple occurrences of weakness zones containing clay or chemically disintegrated rock, very loose surrounding rock any depth)			10.0	1. Reduce these values of *SRF* by 25 - 50% but only if the relevant shear zones influence do not intersect the excavation
B. Single weakness zones containing clay, or chemically disintegrated rock (excavation depth < 50 m)			5.0	
C. Single weakness zones containing clay, or chemically disintegrated rock (excavation depth > 50 m)			2.5	
D. Multiple shear zones in competent rock (clay free), loose surrounding rock (any depth)			7.5	
E. Single shear zone in competent rock (clay free). (depth of excavation < 50 m)			5.0	
F. Single shear zone in competent rock (clay free). (depth of excavation > 50 m)			2.5	
G. Loose open joints, heavily jointed or 'sugar cube', (any depth)			5.0	
b. Competent rock, rock stress problems				
	σ_c/σ_1	σ_t/σ_1		2. For strongly anisotropic virgin stress field (if measured): when $5 \le \sigma_1/\sigma_3 \le 10$, reduce σ_c to $0.8\sigma_c$ and σ_t to $0.8\sigma_t$. When $\sigma_1/\sigma_3 > 10$, reduce σ_c and σ_t to $0.6\sigma_c$ and $0.6\sigma_t$, where σ_c = unconfined compressive strength, and σ_t = tensile strength (point load) and σ_1 and σ_3 are the major and minor principal stresses.
H. Low stress, near surface	> 200	> 13	2.5	
J. Medium stress	200 - 10	13 - 0.66	1.0	
K. High stress, very tight structure (usually favourable to stability, may be unfavourable to wall stability)	10 - 5	0.66 - 0.33	0.5 - 2	
L. Mild rockburst (massive rock)	5 - 2.5	0.33 - 0.16	5 - 10	
M. Heavy rockburst (massive rock)	< 2.5	< 0.16	10 - 20	3. Few case records available where depth of crown below surface is less than span width. Suggest *SRF* increase from 2.5 to 5 for such cases (see H).
c. Squeezing rock, plastic flow of incompetent rock under influence of high rock pressure				
N. Mild squeezing rock pressure			5 - 10	
O. Heavy squeezing rock pressure			10 - 20	
d. Swelling rock, chemical swelling activity depending on presence of water				
P. Mild swelling rock pressure			5 - 10	
R. Heavy swelling rock pressure			10 - 15	

Source: Hoek et al. (1995)

C.3 Rock GSI ratings and their shear strength envelopes

a

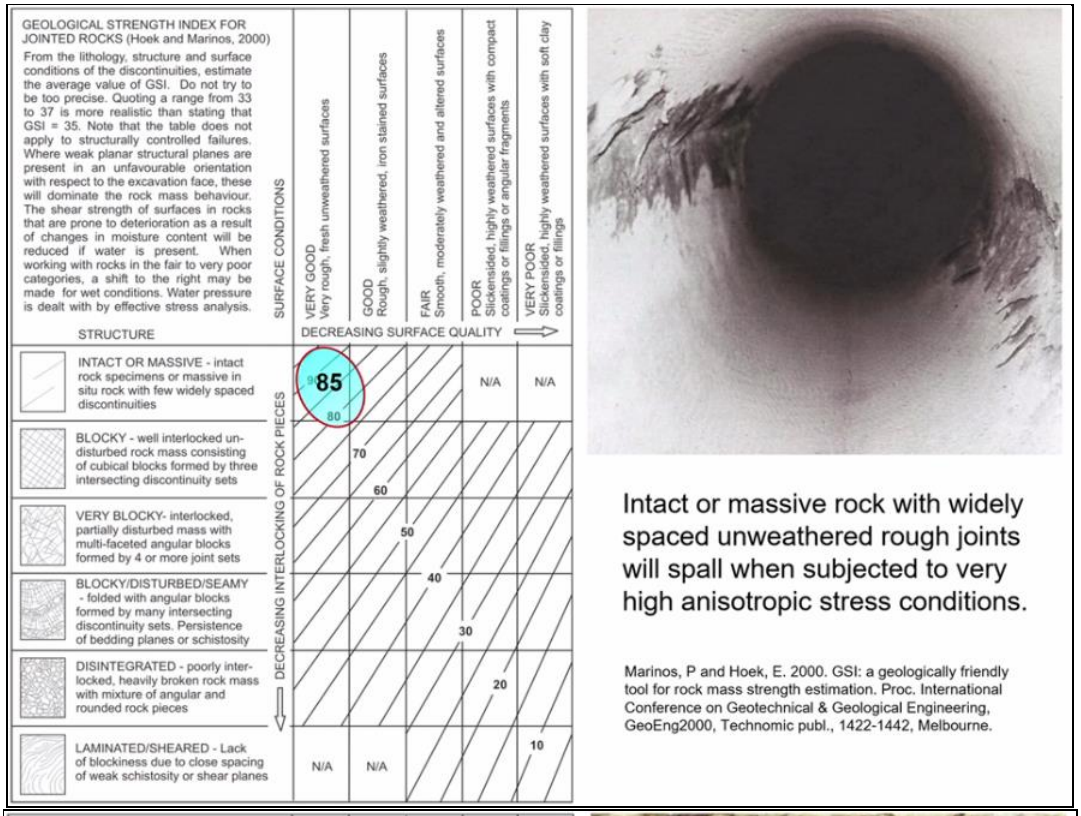

b

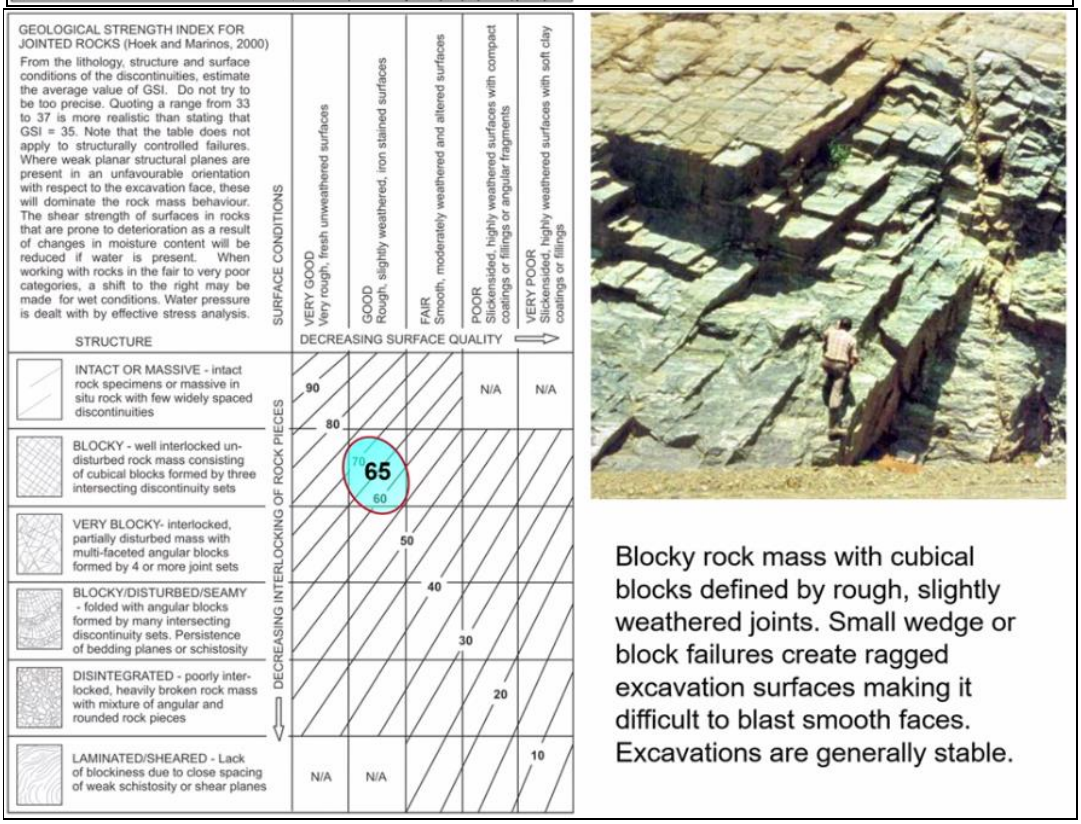

c

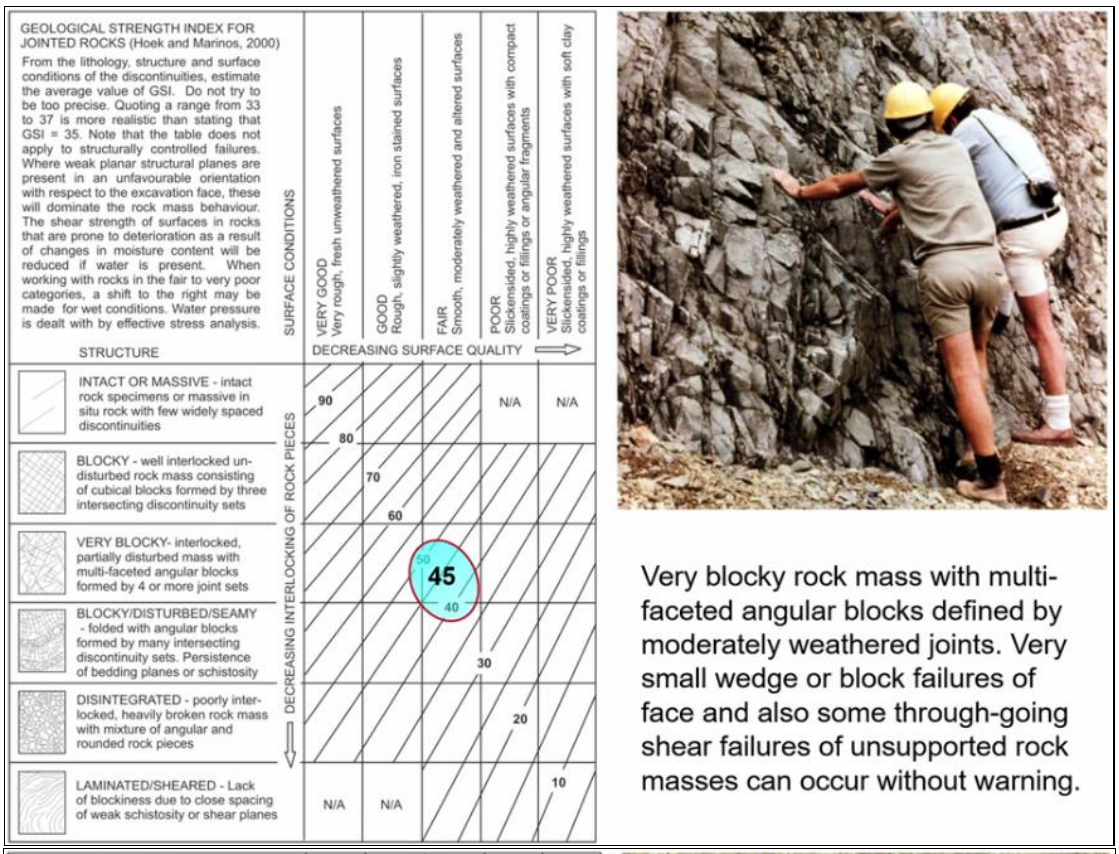

Very blocky rock mass with multi-faceted angular blocks defined by moderately weathered joints. Very small wedge or block failures of face and also some through-going shear failures of unsupported rock masses can occur without warning.

d

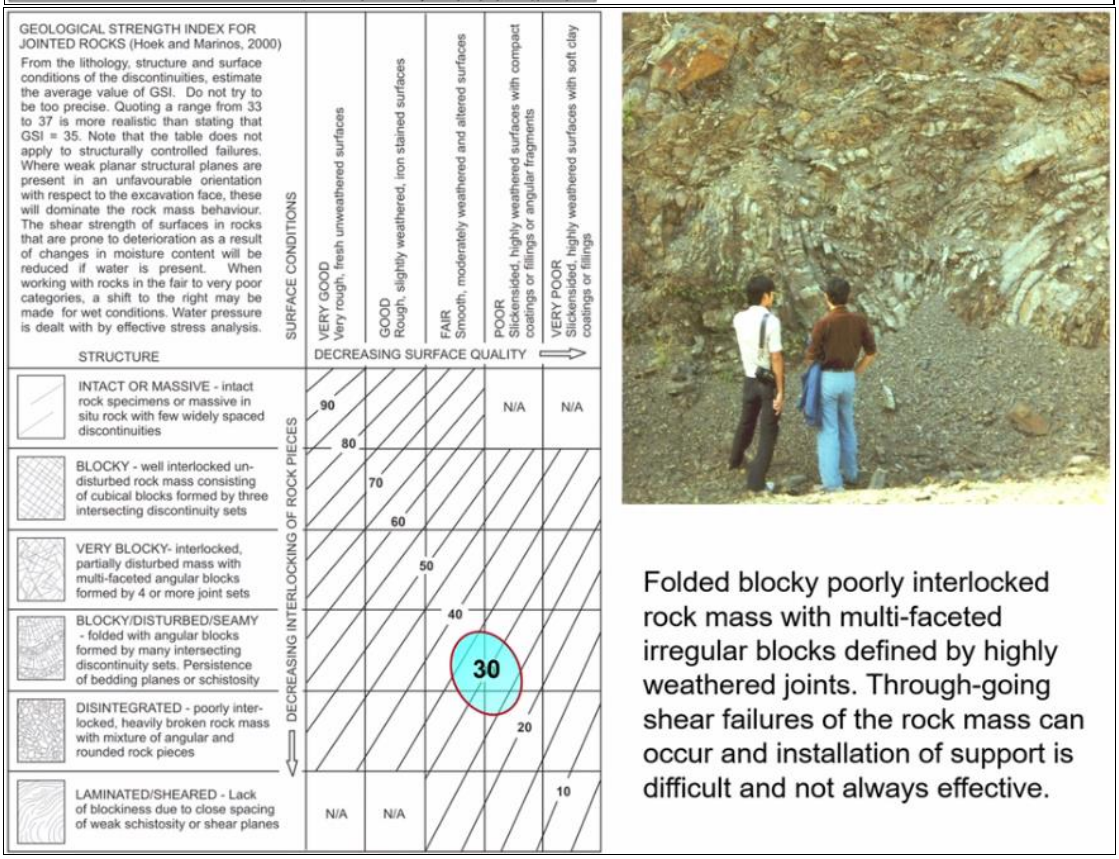

Folded blocky poorly interlocked rock mass with multi-faceted irregular blocks defined by highly weathered joints. Through-going shear failures of the rock mass can occur and installation of support is difficult and not always effective.

e

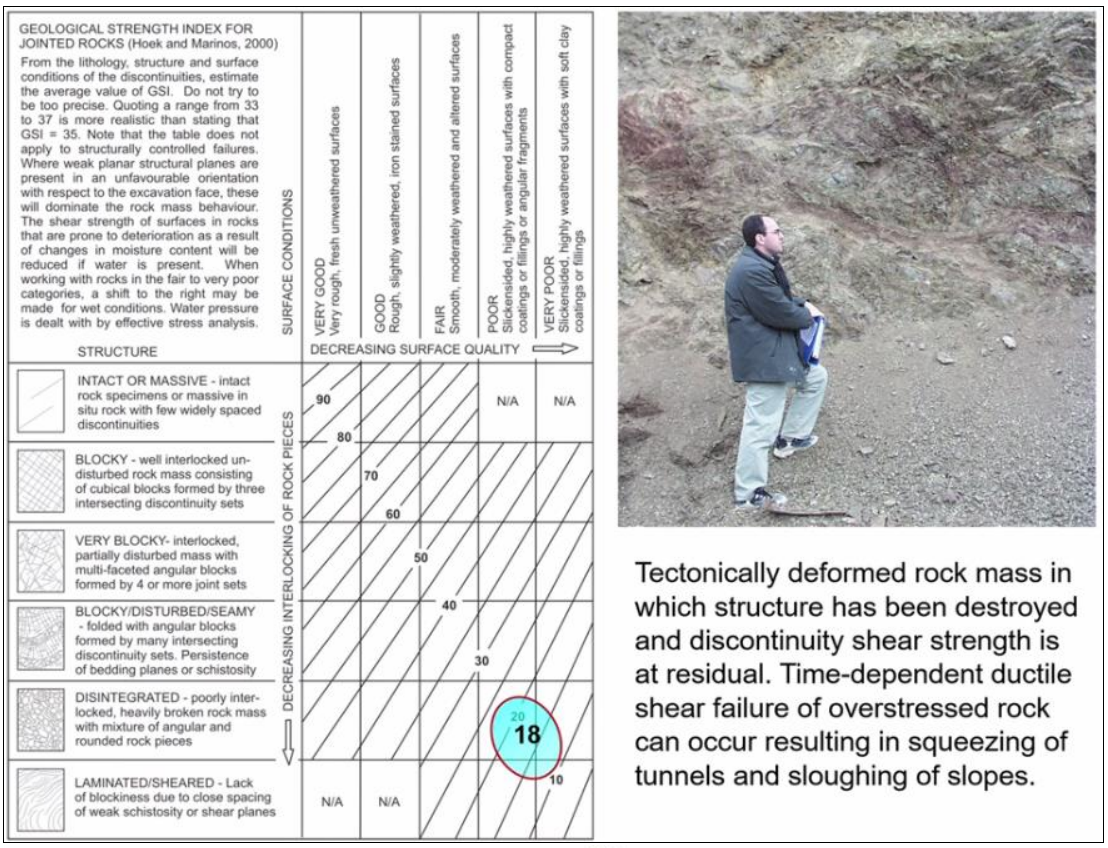

f

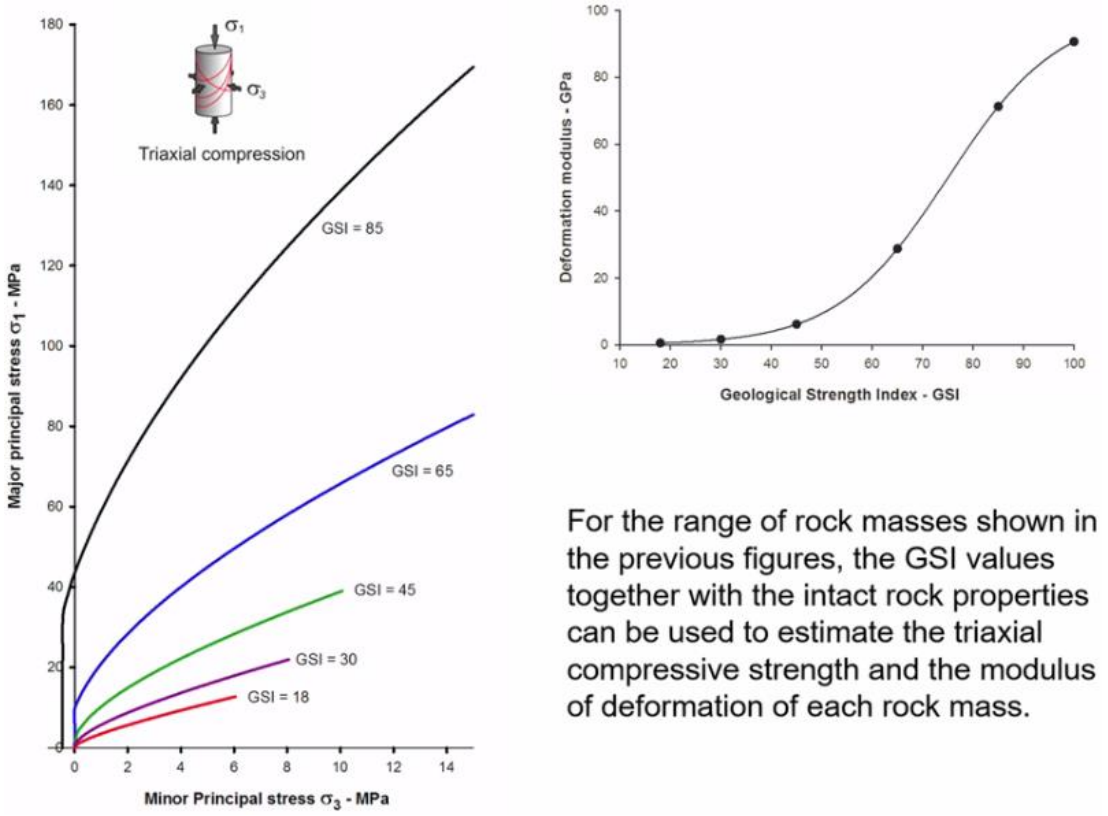

Source: Hoek (2016)

D Karuma

D.1 Geotechnical investigation data

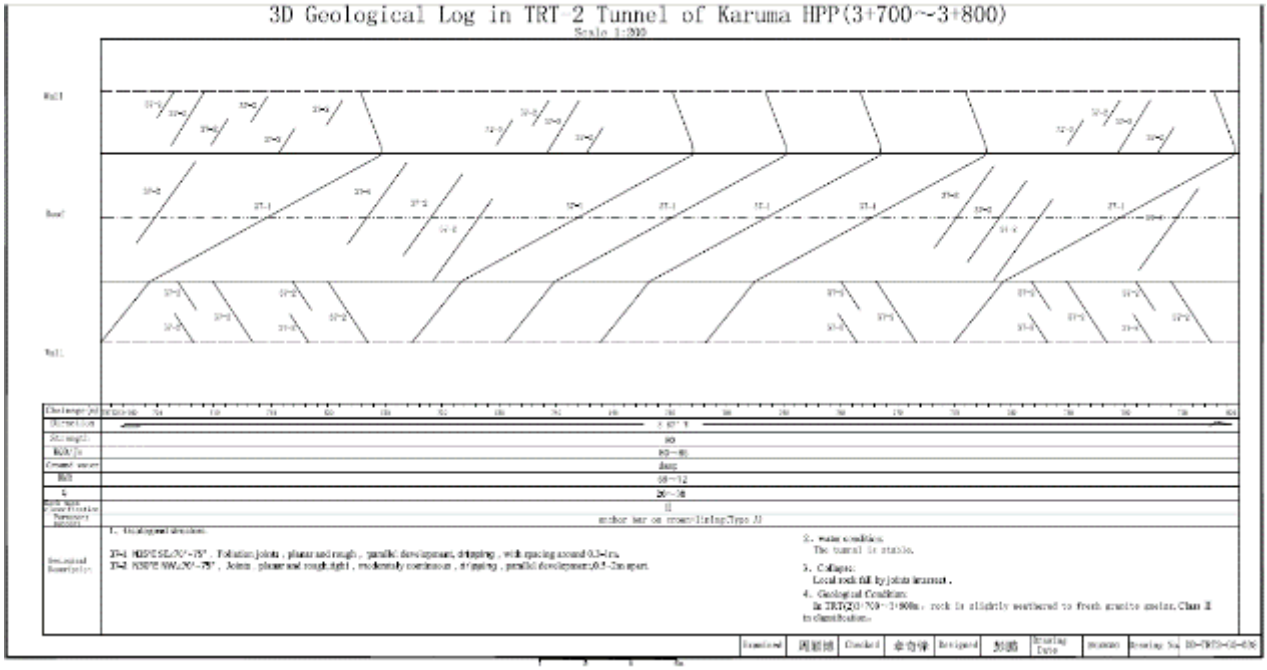

Source: Karuma (2014)

In-situ and Laboratory Tests

Method	Scope of Investigation
Geological mapping	17.9 km^2 covered
Topographical surveys	16.4 km^2 covered
Borehole drilling	4.3 km / 33 boreholes
Exploration trenches / pits	1,577 m^3 / 60 trenches
Geophysical exploration seismic	42 km / 54 profiles
In-situ testing	68 boreholes / 599 sections Permeability Lugeon and water injection tests, SPT and ground stress measurements
Laboratory testing	193 sets (Rock, Soil parameters, Water, Permeability, 20 sets of UCS)

	ɣ kN/m^3	φ' °	c' kPa
Alluvium	17	20	10
Eluvium	15	14	0
Completely weathered	20	22	20

Source: Karuma (2014)

D.2 Local geology

Standard names of the formations are given based on the native names of the areas where they are geographically located. The period of their formation is defined in geological terms. The table is a useful tool for data collection and gathering geological information. Also, both the geological structures and lithology of each formation are presented in the table.

Uganda's geological provinces

Main formation	Geological period	Lithology and structure	Geographical location
IGNEOUS			
Elgon complex	Neogene	Pyroclastic and lahar-type alkaline/sodic volcanic rocks and associated carbonatite plugs and fenites deposited in the linear Elgon depression	Eastern Uganda
Albertine group	Pleistocene-Holocene	Ultrapotassic and carbonatite volcanic rocks deposited in the Albertine Rift	Northern segment of the Western Rift
PRECAMBRIAN CRATON			
Lake Victoria terrane[15]	Neoarchean	Forms part of the Tanzania Craton and is a predominantly granite-greenstone terrane with nepheline syenite and gabbro intrusions.	Southwestern Uganda
West Tanzania terrane	Neoarchean	Also, forms part of the Tanzania Craton comprising granitoid-gneissic-migmatic rocks.	Along the border between Uganda and Tanzania
PRECAMBRIAN METASEDIMENTARY			
Rwenzori fold belt	Palaeoproterozoic	Gneissose-granitoid basement formed during the Eburnian Orogenic Cycle. The fold belt wraps around the Tanzania Craton with a predominantly ENE-WSW structural trend in the east, curving into a N-S trend in the south-west.	Southern Uganda

[15] A terrane is a fault-bounded area or region with a distinctive stratigraphy, structure and geological history. It is also a shorthand term in geology for a "tectonostratigraphic terrane".

Uganda's geological provinces

Buganda Group	Palaeoproterozoic	Metasediments and mafic, partly pillow-textured volcanics overlying the Rwenzori fold belt. The Buganda group is intruded by syn- and post-tectonic granitoids of the Sembabule and Mubende-Singo suites.	Central Uganda
Kagera-Buhweju Supergroup	Palaeoproterozoic	Platform deposits comprising post-tectonic molasse-type sediments, including quartzite, pelite, conglomerate, shale and phyllite. Deposited following the Eburnian Orogenic Cycle. These rocks have been subjected to complex tectonic processes and are mildly deformed.	Western Uganda
North Kibaran Belt/Trough	Palaeoproterozoic	It is a younger belt compared to the Kagera-Buhweju Supergroup. It includes metasediments of the Akanyaru-Ankole Supergroup and the North Kibaran Igneous Province. The North Kibaran Igneous Province consists of an alignment of mafic and ultramafic layered complexes and mafic dykes and sills, including the Lake Victoria Arcuate Dyke Swarm.	Southwest Uganda Its centre is in central Rwanda (9-14.5 km thick) and it extends to North-western Tanzania
Mityana Group	Palaeoproterozoic	Mityana Group consists of platform sediments including conglomerate, sandstone, siltstone and gritstone. It is not intruded by dykes of the Lake Victoria Arcuate Dyke Swarm hence it is younger than the metasediments of the North Kibaran Belt.	Central Uganda (Overlying the Buganda Group)
Bunyoro Group	Palaeoproterozoic	It is a younger belt compared to the Mityana Group. It comprises rocks of glacial and periglacial origin related to the Sturtian glaciation.	Western Uganda
PRECAMBRIAN MOBILE/OROGENIC BELT			
West Nile Block	Archean	This forms the Ugandan section of the Bomu-Kibalian Shield of northeastern Congo. It is predominantly composed of Mesoarchean granulite, gneiss, granitoid and charnokite, and is intruded by younger (Neoarchean) mafic volcanics.	Along the border between Uganda and the Democratic Republic of the Congo (DRC)

Uganda's geological provinces

North Uganda Terrane	Archean	This unit is mainly composed of Neoarchean gneissose-migmatic rocks and is separated from the western Nile Block by the Madi-Igisi Belt.	West Nile region
Madi Igisi Belt	Archean-Proterozoic	This is composed of reworked rocks of the West Nile Block (WNB) and North Uganda Terrane (NUT) and younger Proterozoic meta-volcanics, metasediments and ultramafics. It is a narrow thrust and shear belt trending north-south	Between the WNB and NUT.
Karamoja Belt	Proterozoic	This comprises a west to north-west trending thrust belt of amphibolite-grade supracrustals, granitoids and ophiolites. It contains the Aswa Shear Zone, which is a brittle-ductile, north-west trending, mega strike-slip shear zone, with complex, anastomosing fault planes. The belt is a representation of the East African Orogen.	Along the border between Uganda and Kenya
Midigo-Adjumani Suite	Proterozoic	This is a suite of granitoids found in the WNB and North Uganda Terrane.	West Nile and northern Uganda
SEDIMENTARY – CRETACEOUS-TERTIARY			
Albertine Graben	Late Eocene-Neogene	This is a hydrocarbon-bearing sequence of terrigenous sediments, alkaline/sodic volcanics and ultra-potassic and carbonatitic volcanics. It is a 4 km thick sequence which was laid down in the Albertine Rift, a part of the Western Rift	Western Uganda
SEDIMENTARY – MESOZOIC-PALAEOZOIC			
Karoo Basins	Mesozoic-Palaeozoic	Karoo deposits are restricted to a few small occurrences and comprise clays, minor arenaceous and carbonaceous beds, siltstone, diamictites and dropstones.	Southern Uganda
UNCONSOLIDATED SEDIMENTARY			
Lake Victoria strandline deposits, Lake Kyoga raised beach deposits, and Albertine Nile deposits	Pleistocene-Holocene	Discontinuous deposits, predominantly beach sands and gravels, with finer silts and clays.	Central and Western Uganda

Source: Adapted from Owor et al. (2016)

D.3 Additional information for analytical design

Other important information which is useful to design tunnel support systems			
Parameter	**Description**	**Reference**	**Remark**
	When tunnel wall rock is stable Vertical stress, σ_v $\sigma_v = \frac{\alpha\gamma - c}{\lambda \tan\phi_f}[1 - \exp(-\lambda_n \tan\phi_f)] + p\exp(-\lambda_n \tan\phi_f)$ $where\ \lambda = \tan^2(45° - 0.5\phi)\ and\ \lambda_n = z/a$ a is a coefficient of relative depth and when z = H σ_v is the pressure acting on the tunnel roof whereas p = surcharge pressure 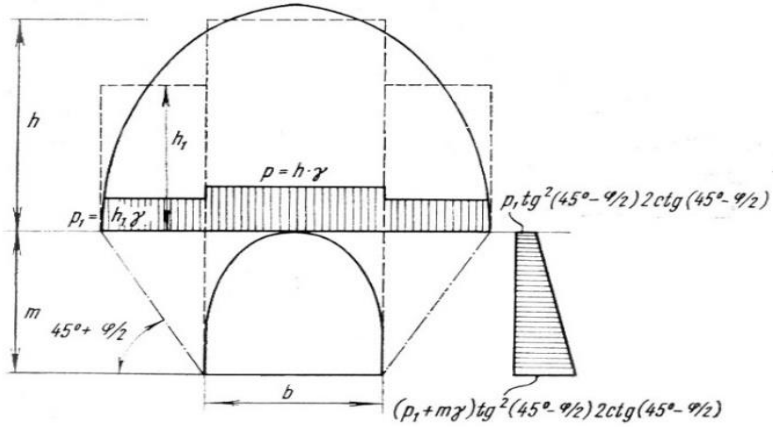 The peak lateral earth pressure is assumed to correspond to the roof pressure, such that the lateral pressure intensity e_1 and e_2 at the tunnel roof and invert, respectively will be $e_1 = P_h \tan^2(45° - 0.5\phi) - 2c\tan(45° - 0.5\phi)$ at invert level the $m\gamma$ component of the wedge is added, thus: $e_2 = (P_h + m\gamma) \tan^2(45° - 0.5\phi) - 2c\tan(45° - 0.5\phi)$		

	Lateral earth pressures aid bending moments therefore cohesion enhances stability by reducing the magnitude of lateral earth pressure (Tsesarsky & Hatzor, 2005).		
Hydrostatic pressure	Hydrostatic pressure load of water, normal to the tunnel surface = load of water / external hydrostatic pressure	RTM (2009)	
Internal loads	Inflow and lining pressure analysis using flow net 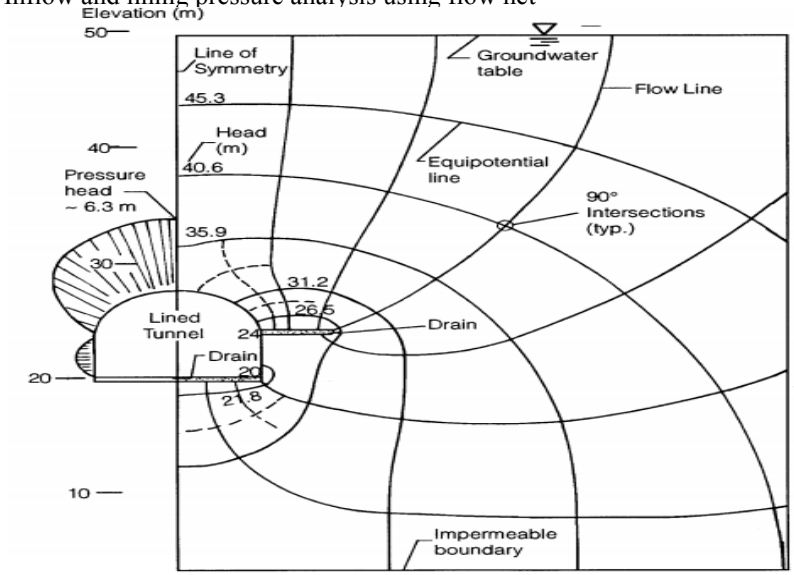	US Army Corps (EM_1110-2-2901)	Data from field-installed piezometers is used to draw the flow net.
Deformation modulus	$\varepsilon_m = \sqrt{\frac{\sigma_c}{100}} 10^{(GSI-\frac{10}{40})}$	Yavuz (2006)	Field measured parameters are preferred where available
Rock mass strength	$\sigma_m = \frac{2c\cos\phi}{1-\sin\phi}$		
Forces on inclined strata	Pressure of loose strata above roof ≈ 0.25B for steep strata and 0.5B for gently inclined strata	Terzaghi (1946)	Gives extent of disturbance at top and sides in inclined strata.

	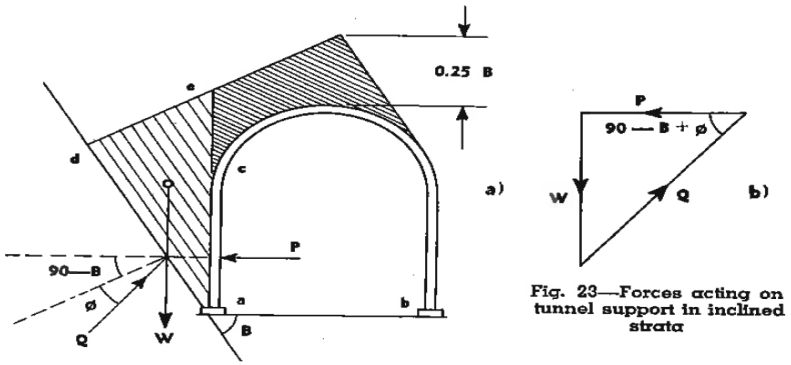 Fig. 23—Forces acting on tunnel support in inclined strata <u>Change in load magnitude after inclusion of support</u> $H_{ult} = 1.15C(B_{width}+H_{tunnel}) = 1.15\ (13+9) = 25.3$ where C = constant depending on degree of compactness, B_{width}= tunnel width and H_{tunnel} = height of tunnel Rock load increases by 15% <u>Lateral loads on sides</u> * Unit pressure, $P_h = 0.30w(0.5H_t+H_p)$ where w = weight/ft^3 of sand		This is not applied in the study because the orientation of Karuma strata is not known. Change in load of 25.3MPa, for c = 1is insignificant *developed for sand therefore requires improvement to adapt for rock mechanics applications
	$P_{roof} = \left(\frac{2}{J_r}\right) Q^{-⅓}$ *where* P_{roof} = permanent roof support pressure in kg/cm^2, J_r = joint roughness number and Q = rock mass quality $P_{roof} = \frac{2J_n^{½}(Q)^{-⅓}}{3J_r}$ Support members: a) Roof bolt length, L_b = 2+0.15B/ESR and anchor length, L_a = 0.40B/ESR b) Sidewalls bolt length, L_b = 2+0.15h/ESR and anchor length, L_a = 0.35h/ESR	Barton, Lien & Lund (1974)	The equations are similar to the ones referenced in the geological charts for estimation of support parameters.

	where L = length (m), B = span (m), h = height of excavation (m) and ESR is the Excavation Support Ratio wall thickness for equilibrium (cm), t is given by $t = \frac{PR}{\sigma}$ where P = externally applied pressure (kg/cm^2), R = internal radius of lining (cm) and σ = compressive stress in lining (kg/cm^2)		
	Surrounding circumferential stresses on the cavern wall (σ_θ) can be obtained from $\sigma_\theta = \gamma(\alpha + \beta\lambda)(H' + kr_o)$ where α and β are calculation coefficients.		
	Rock strength is considered insignificant for conservative design of rock loads and support capacities. However, rock strength for non-conservative design is given by F(kN) = L × (12 × RMR × RQD5 - 505) where Lis the bolt length (m) in rock, RMR is the rock mass rating and RQD_5 is the sum of the bits longer than 5cm over the total length of the core Or F(kN) = 0.557GSI2 - 46.6GSI + 1114 with GSI = 9ln(Q′) + 40 and Q′ = Q with Jw = SRF = 1 where GSI is geological strength index, Q is the tunneling index, Jw is the joint water-reduction factor and SRF is the stress reduction factor.	Thomas-Lepine (2012)	

D.4 Screen shots showing an overview of the FEM design

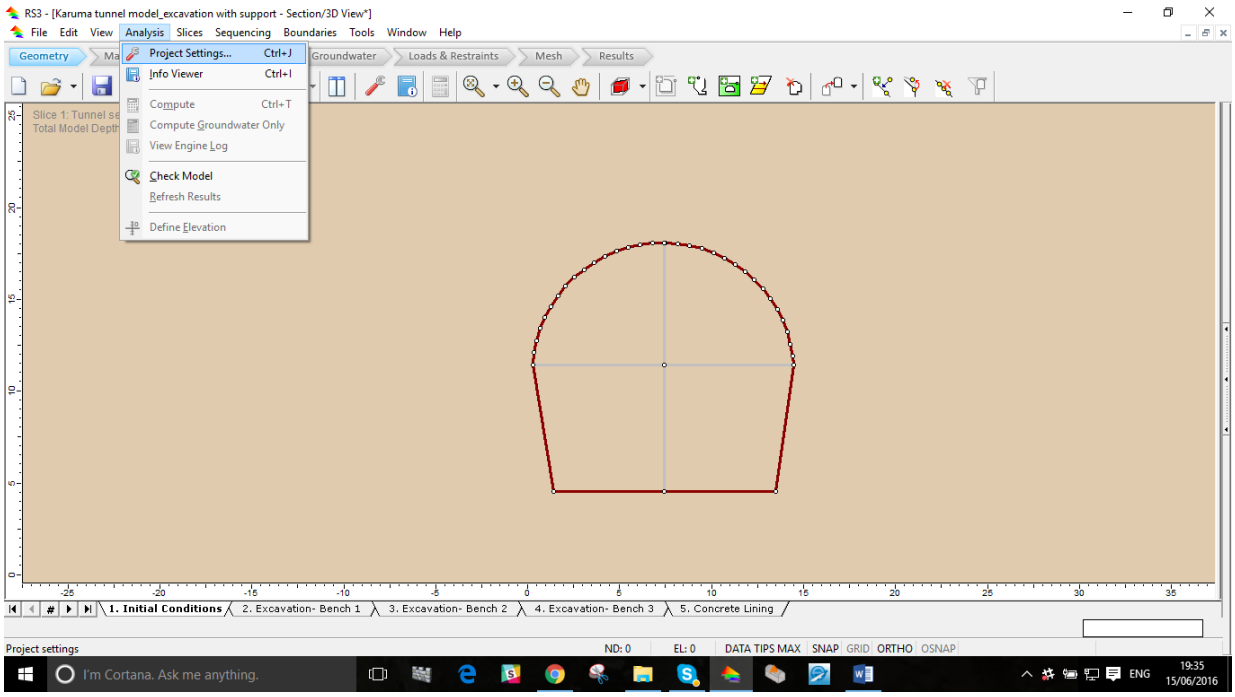

Project settings under Analysis menu

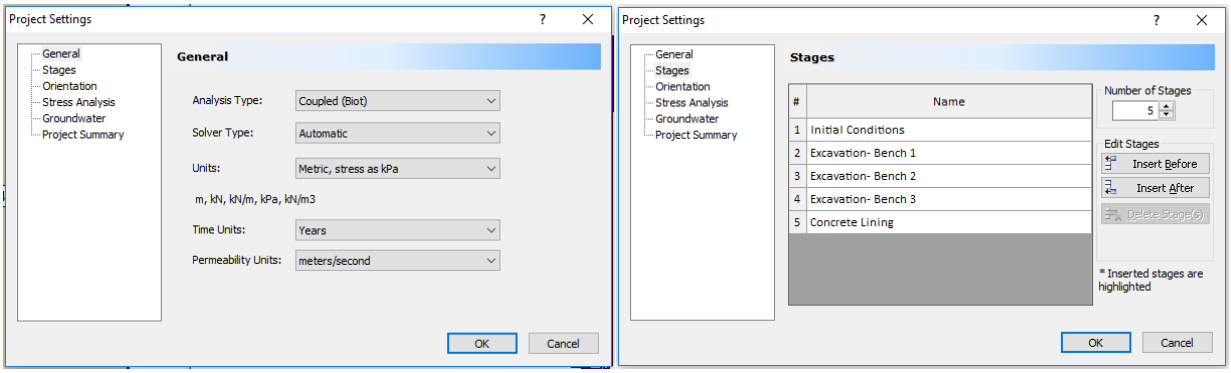

General and Stage settings

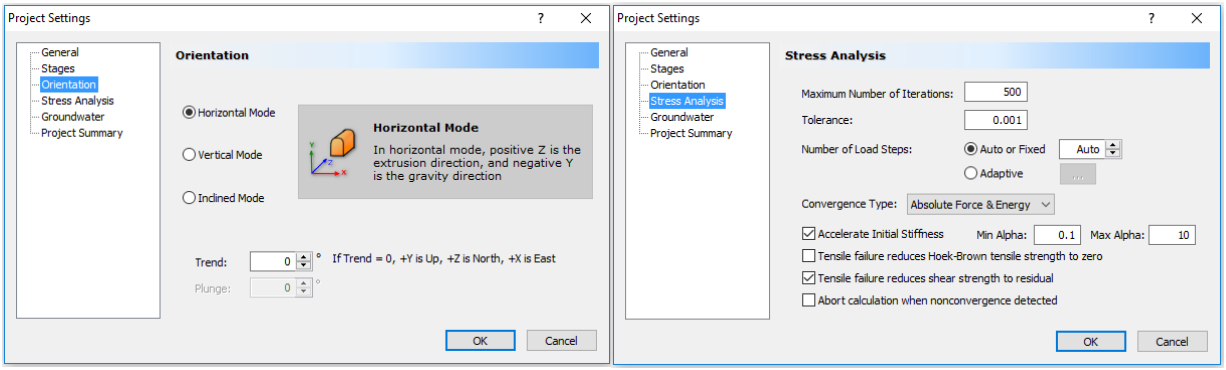

Orientation and Stress Analysis settings

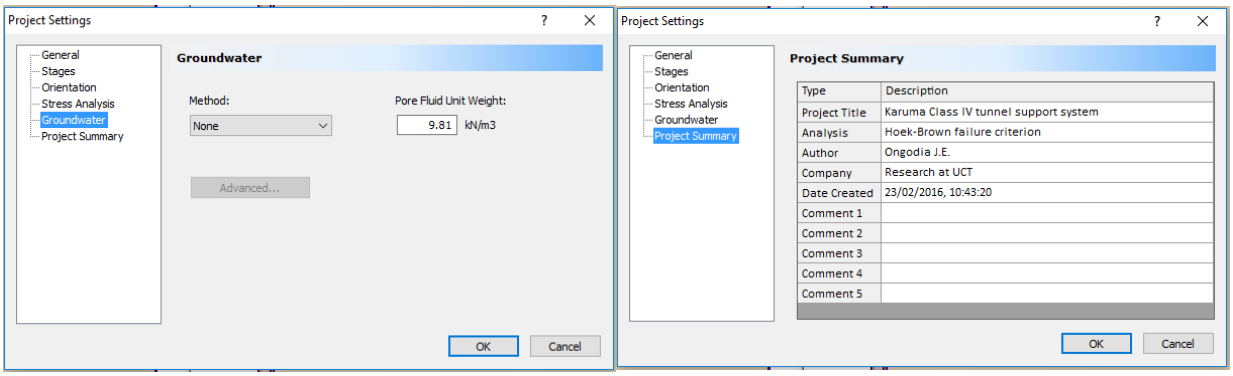

Groundwater and project summary

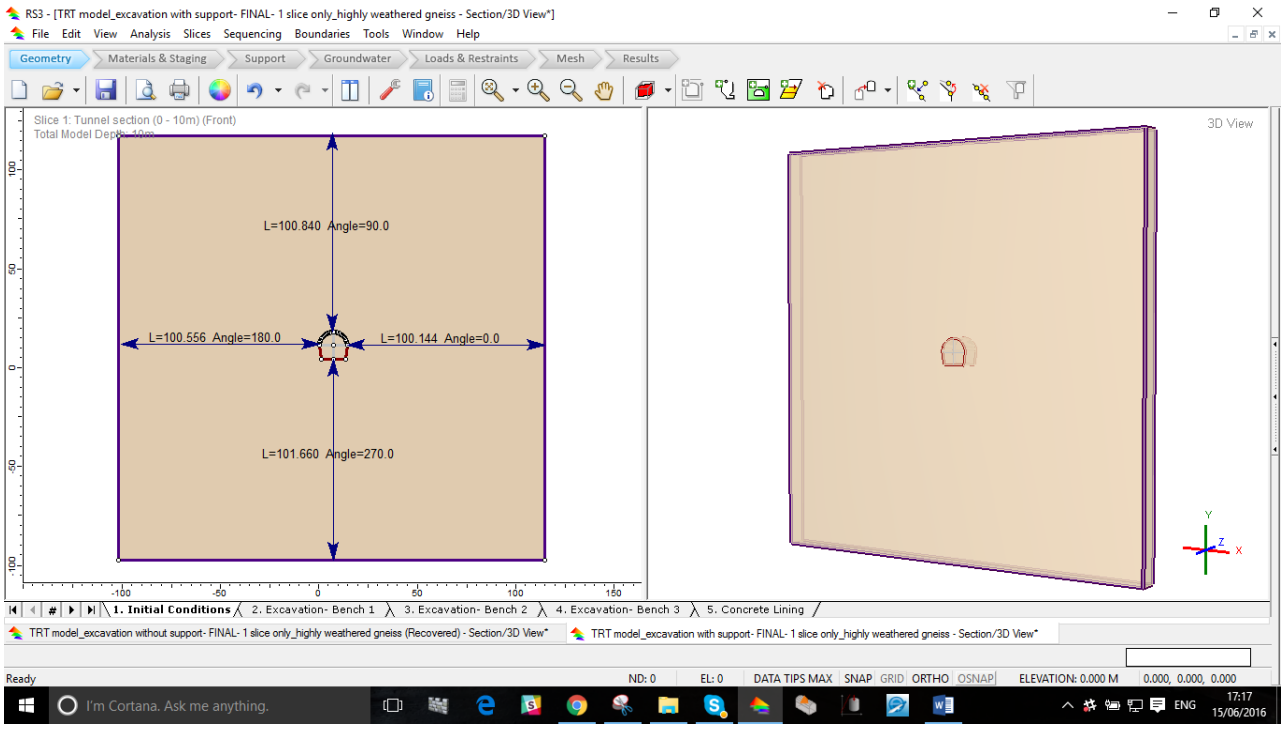

Geometry of the model

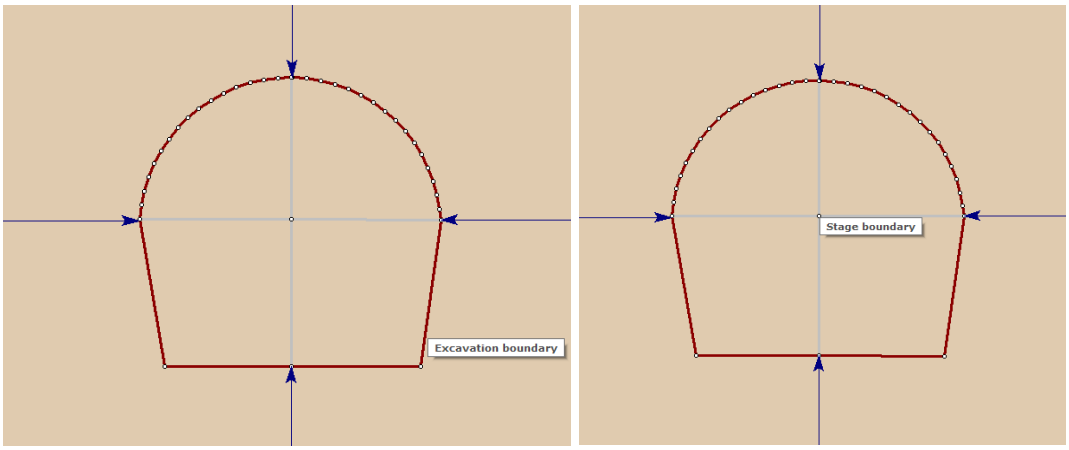

Excavation and stage boundaries

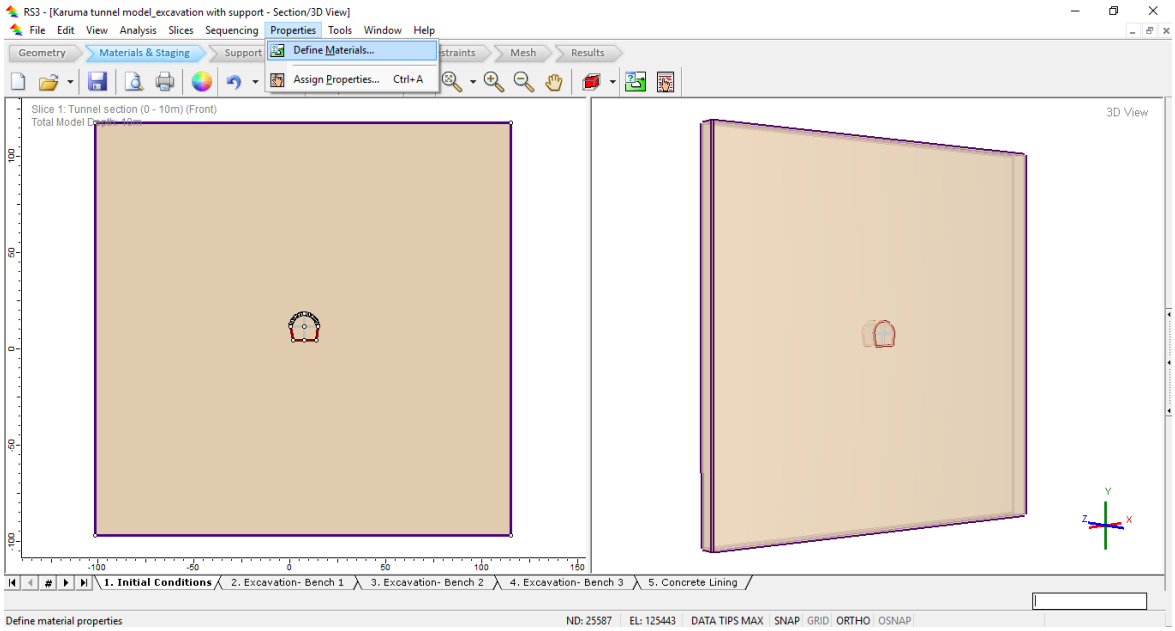

Material and staging tab and properties menu

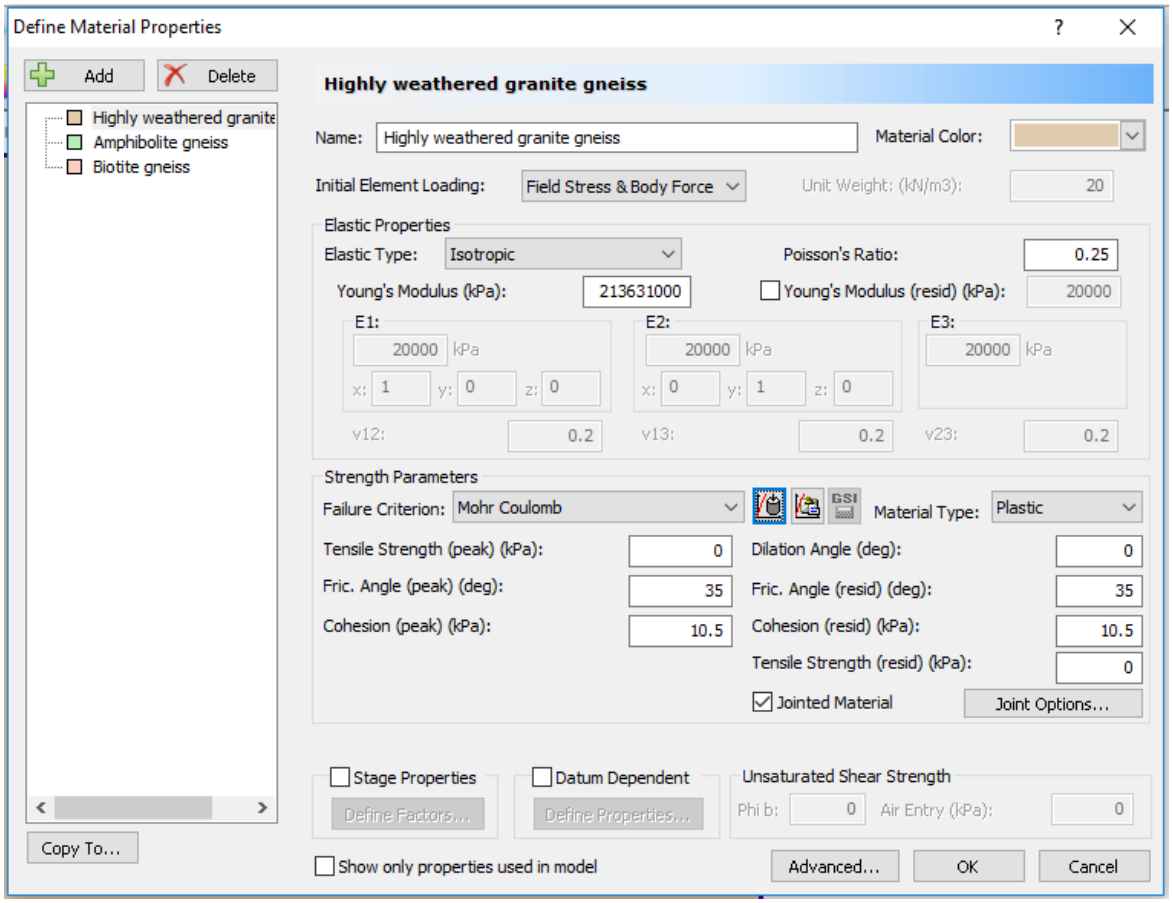

Material properties

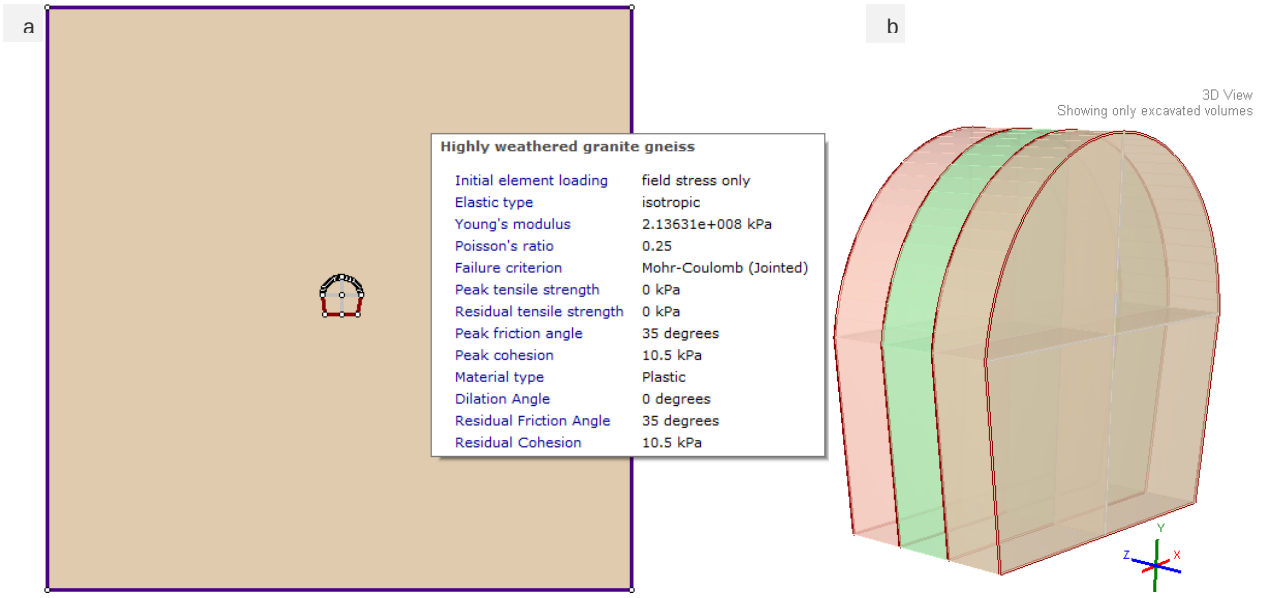

(a) Properties assigned to model and (b) Slices representing different rock materials at the segment

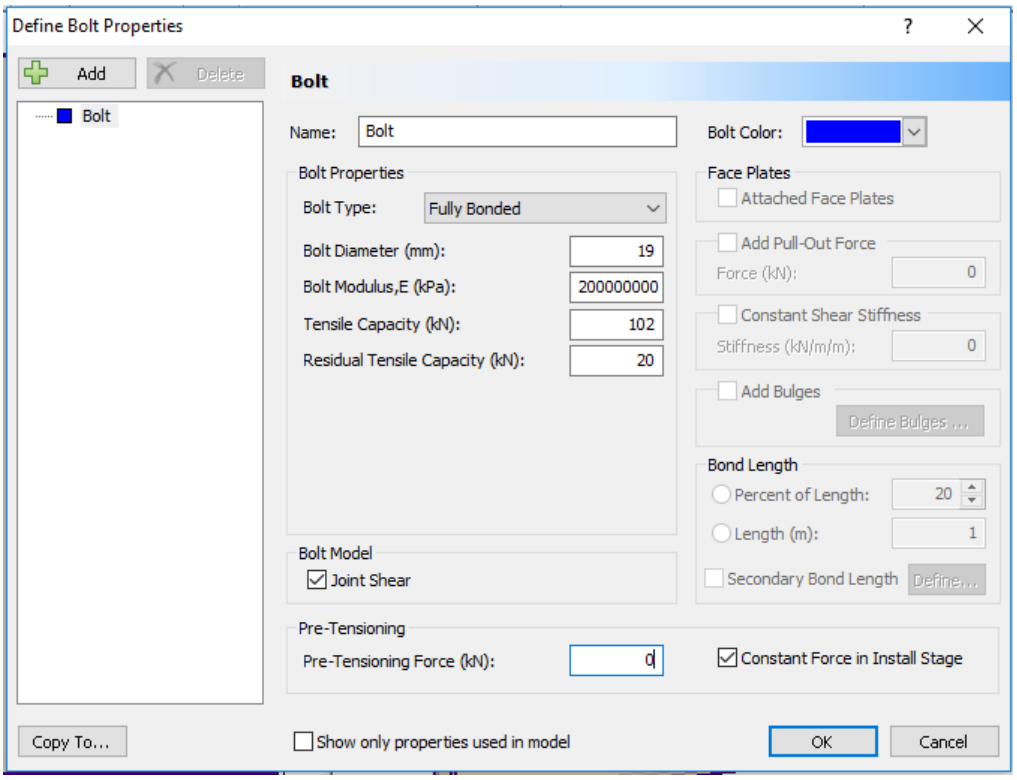

Bolt properties

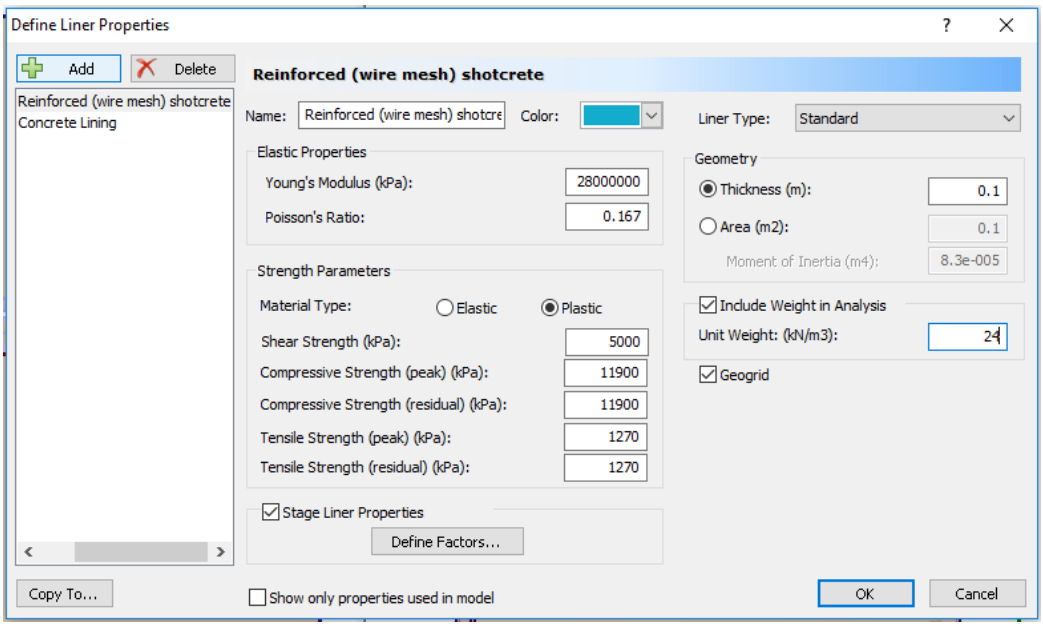

Wire mesh reinforced shotcrete properties

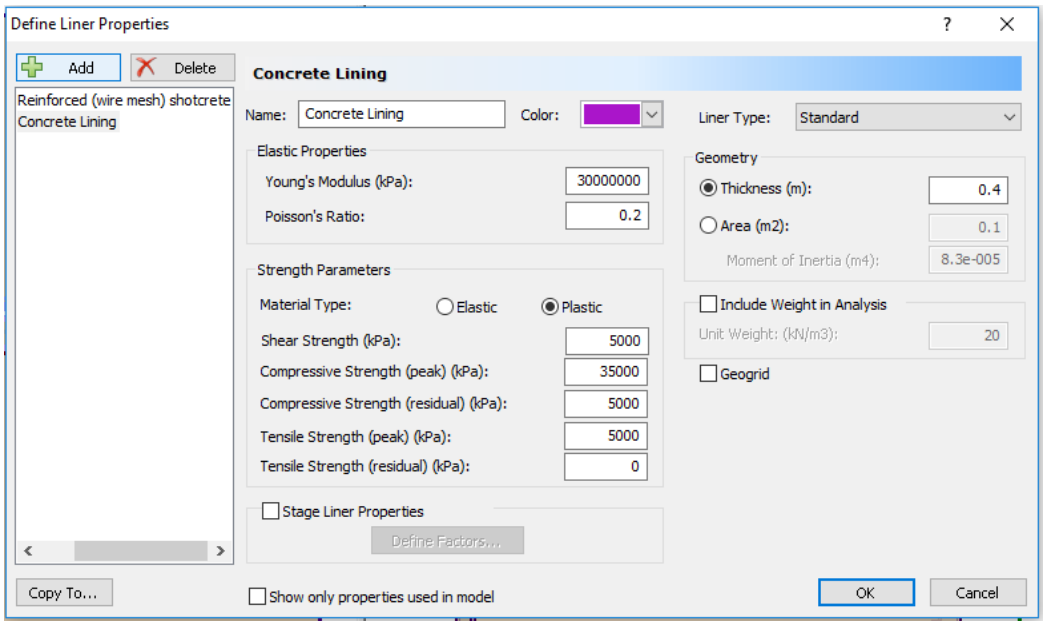

Concrete lining properties

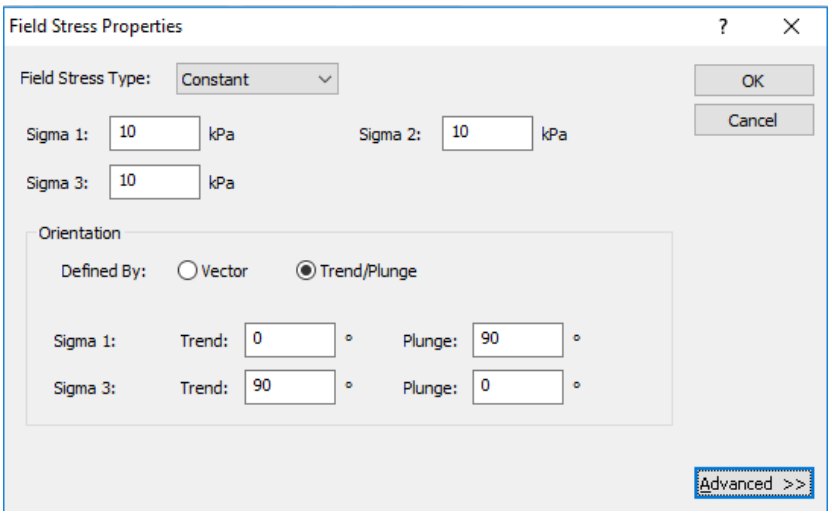

Loads from surrounding rock

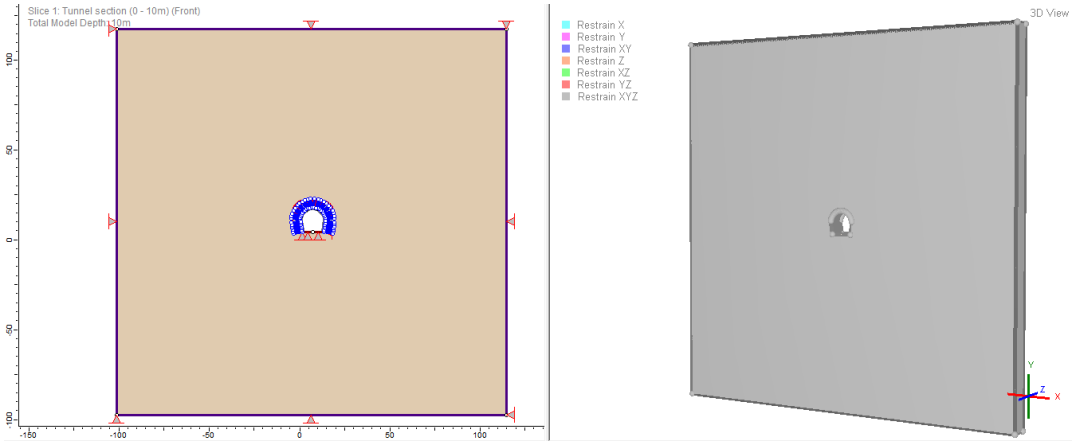

Underground restraints

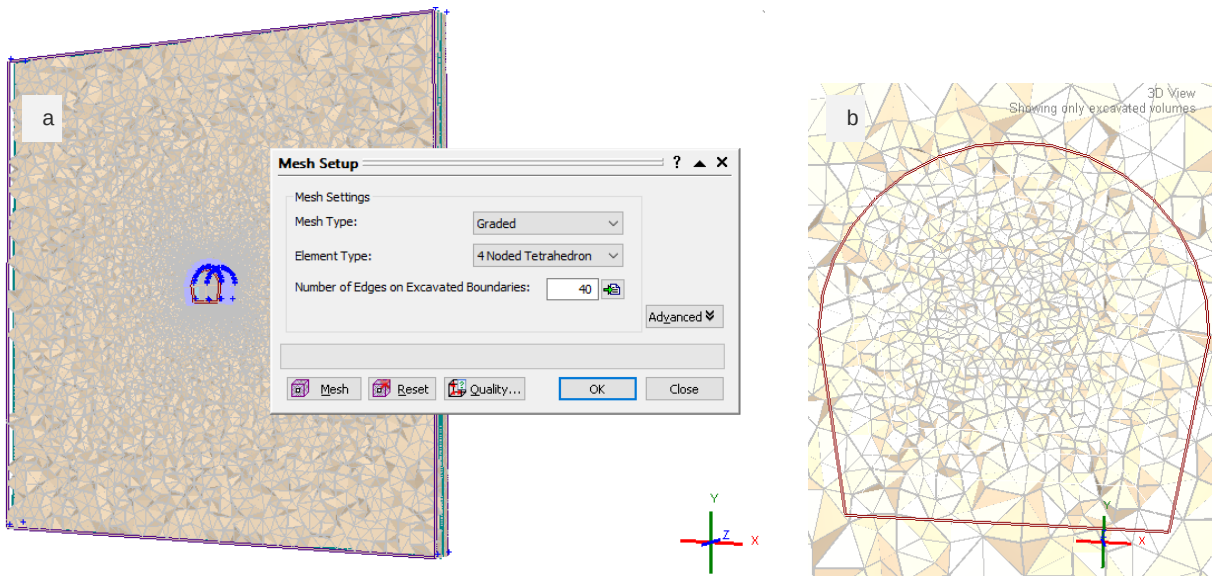

a) Mesh customization and b) Discretized mesh

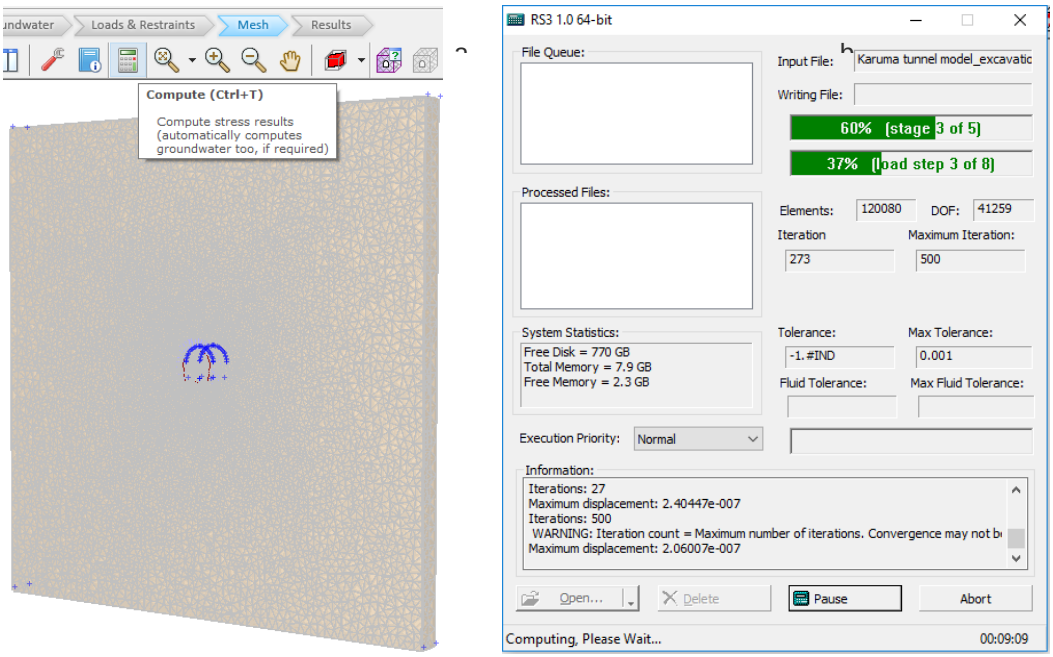

Model computation window

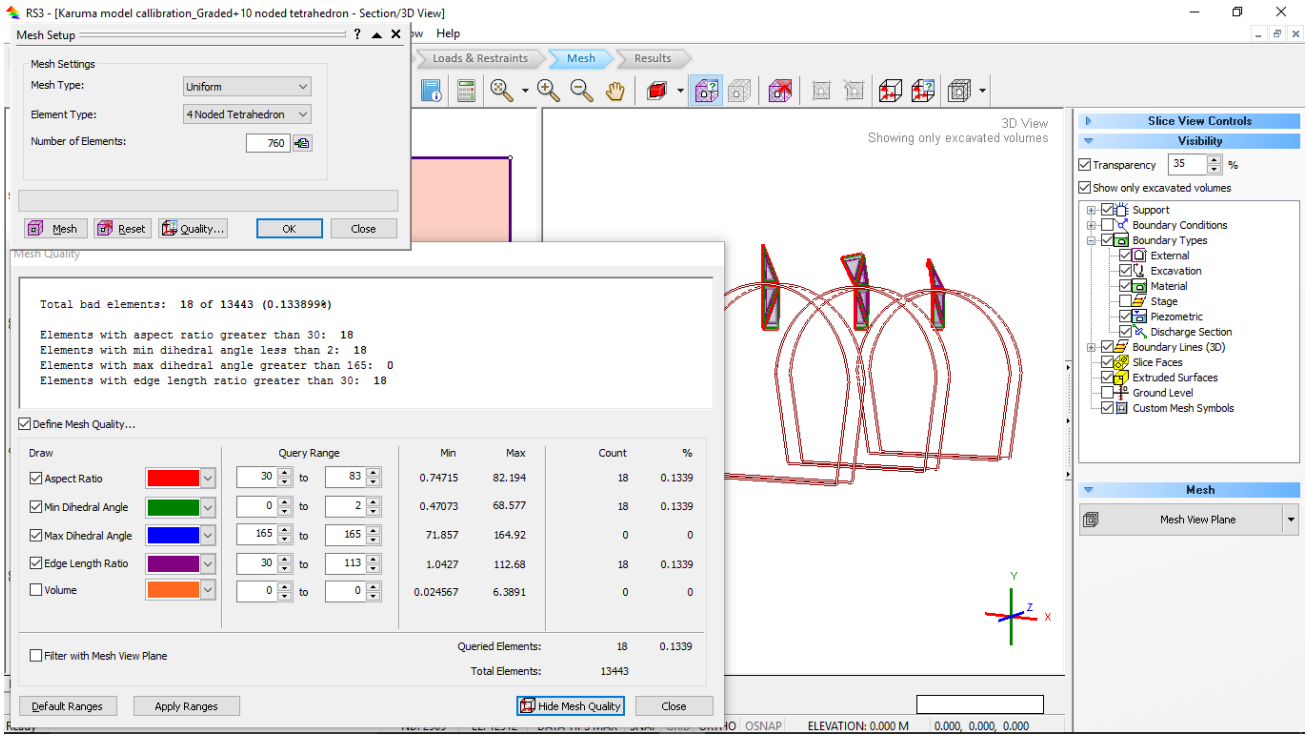

Calibration of the uniform mesh

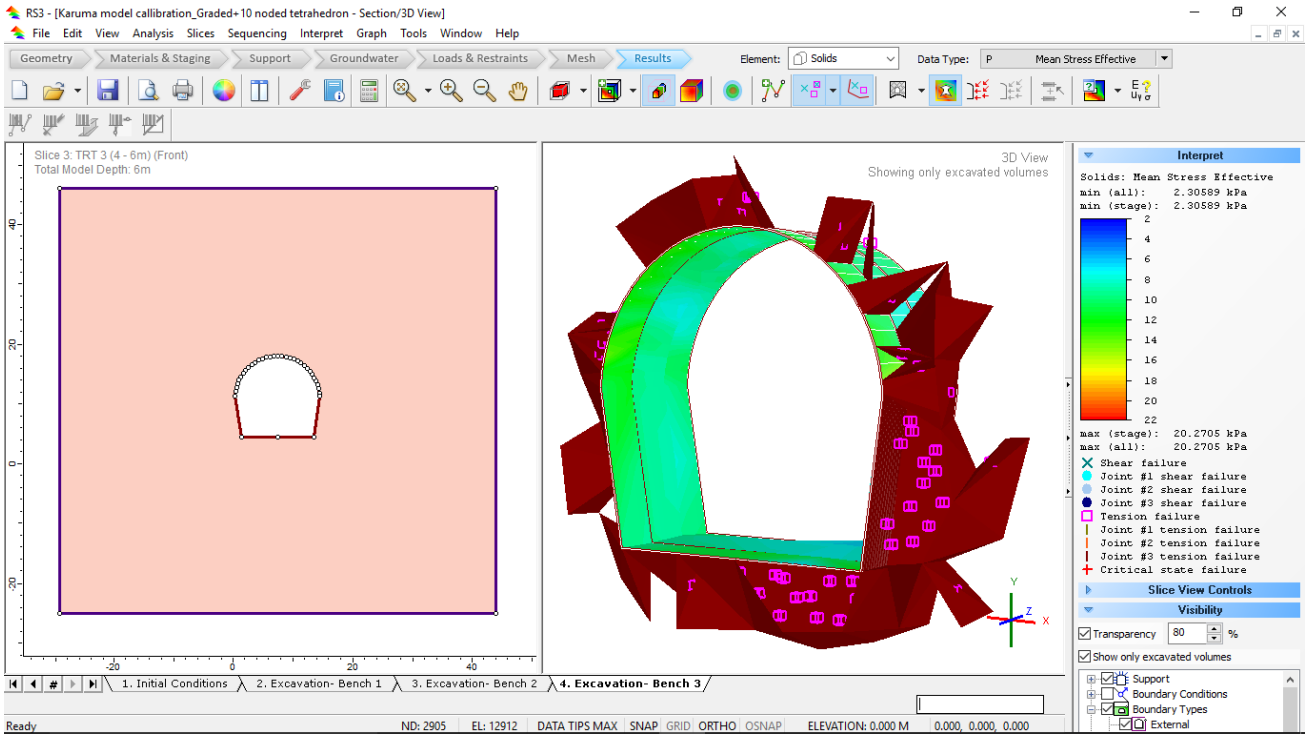

Uniform mesh calibration results and extent of failure zone

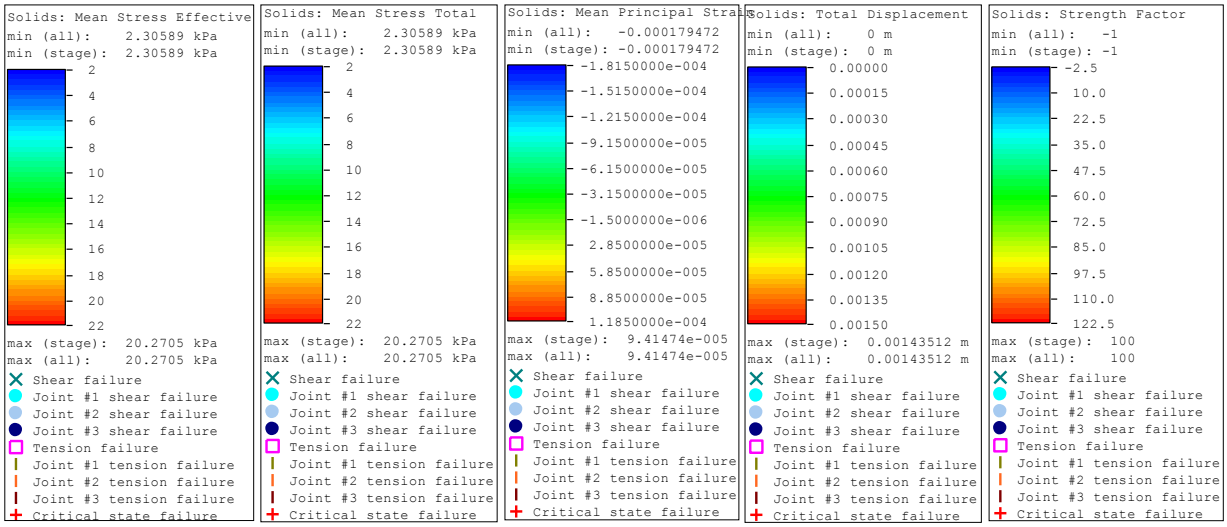

Uniform mesh calibration results of stress, strain, displacement and strength factor

Note: From the calibration, effective parameters were equal to the total parameters as expected from theory since the ground water table was not encountered.

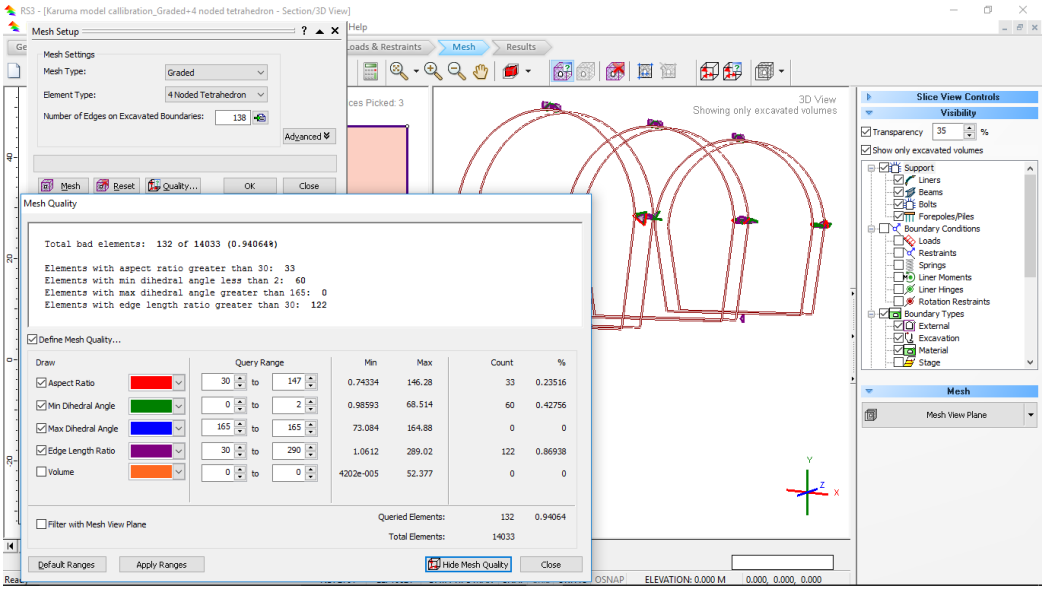

4 noded tetrahedron mesh calibration

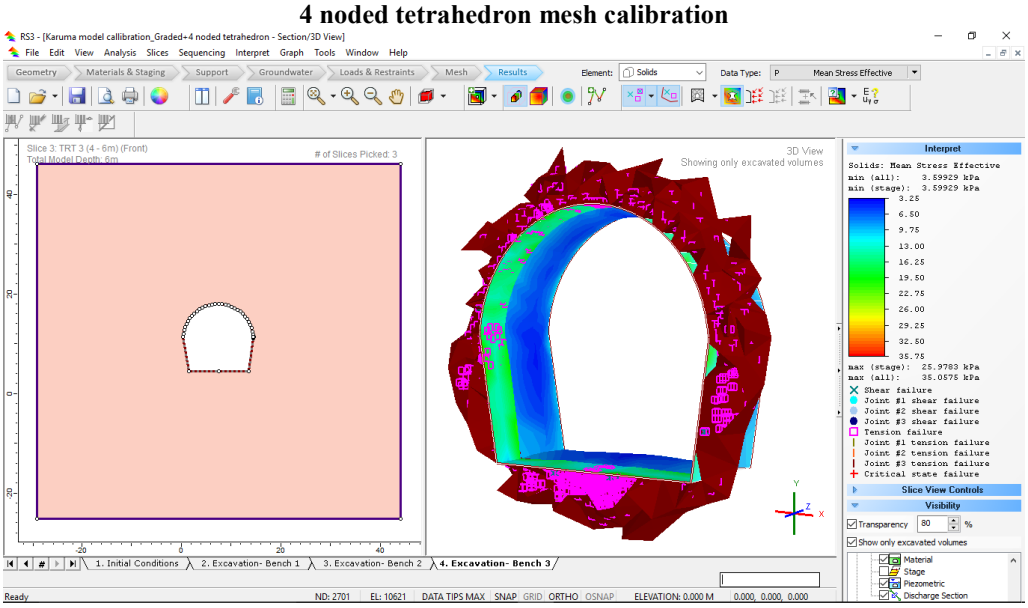

4 noded tetrahedron wedges and the extent of failure zone

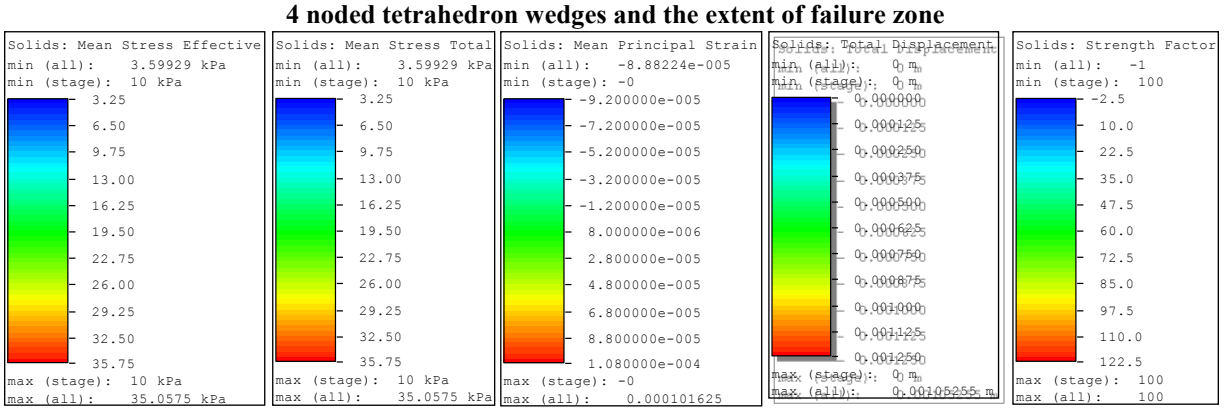

4 noded element results of stress, strain, displacement and strength factor

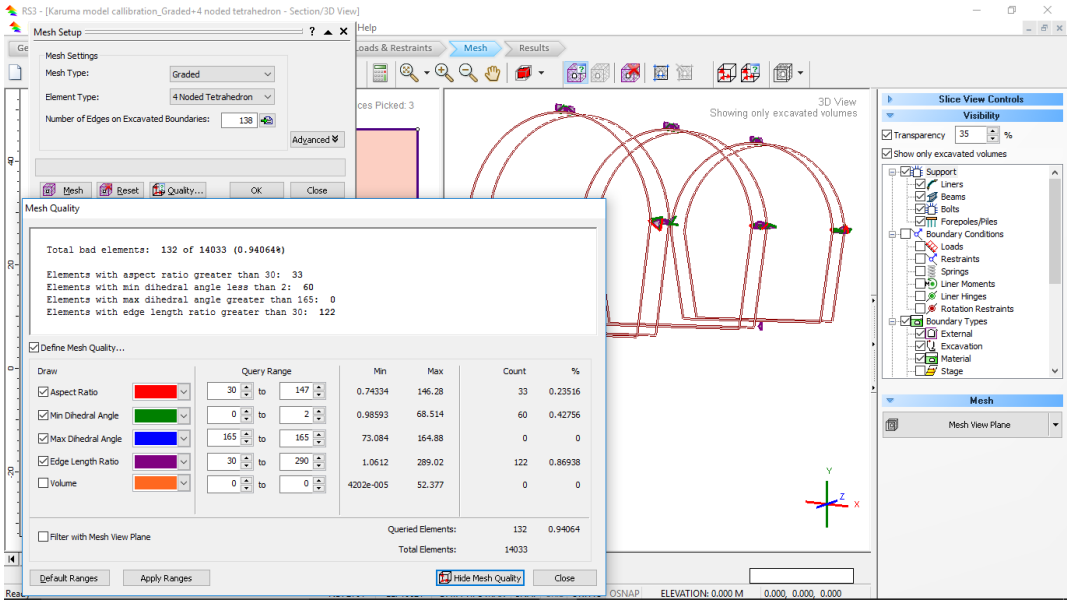

10 noded tetrahedron mesh calibration

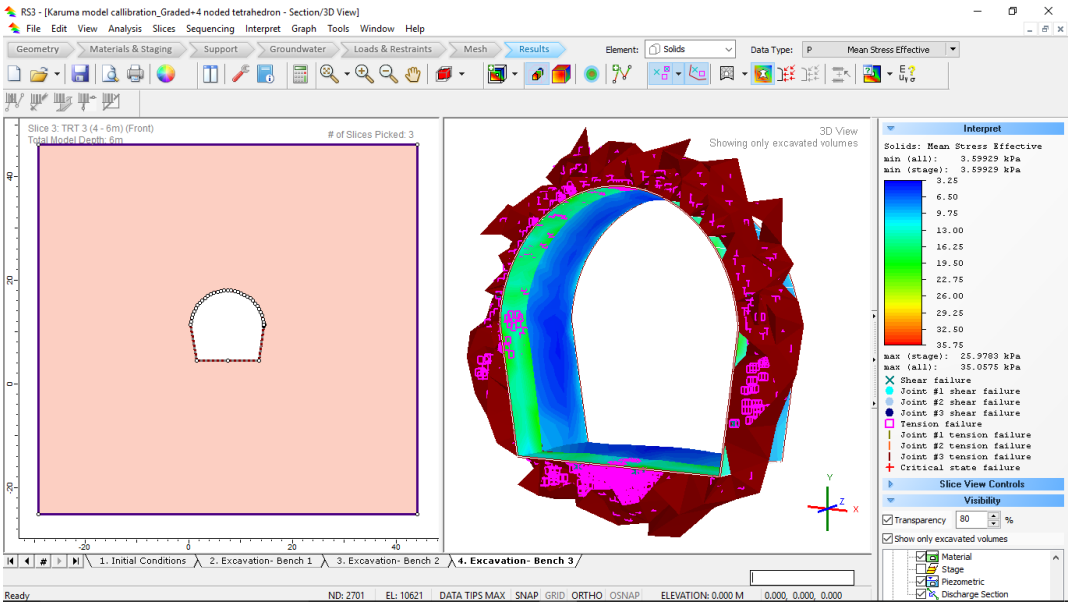

10 noded tetrahedron wedges and the extent of failure zone

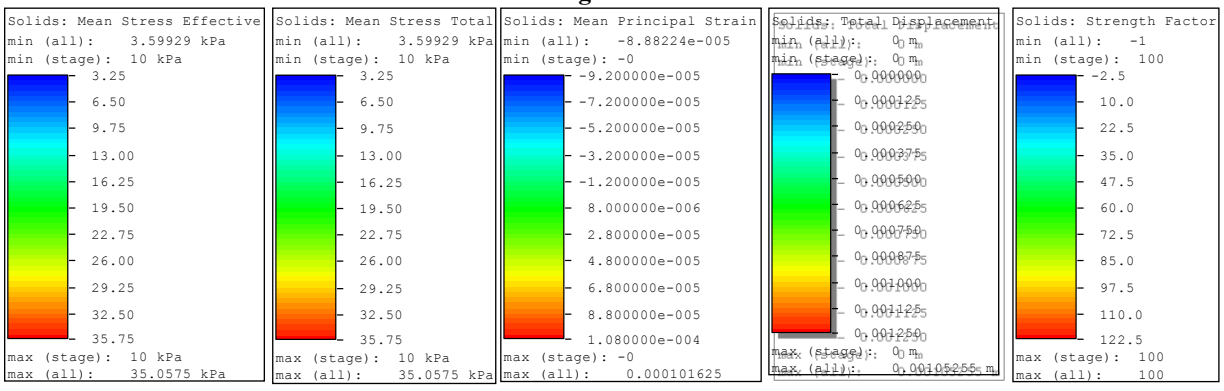

10 noded element results of stress, strain, displacement and strength factor

D.5 Ethics Clearance Form for Research